



The  
University  
Of  
Sheffield.

Molecular  
Biology &  
Biotechnology.

# Mechanistic understanding of $\beta$ -lactam resistance in *Staphylococcus aureus*.

By

Callum J Portman Ross, BSc (Hons)

(University of Essex)

A thesis submitted for the degree of Doctor of Philosophy

Thursday 23<sup>rd</sup> May 2024

The University of Sheffield  
Faculty of Science  
Department of Molecular Biology and Biotechnology

## Summary

Antibiotic resistance is a definitive crisis of the 21<sup>st</sup> century and diseases caused by such organisms are responsible for considerable morbidity and mortality worldwide. *Staphylococcus aureus* is an opportunistic pathogen capable of colonising a range of niches within the human host. It is more commonly known as its antibiotic resistant derivative, Methicillin Resistant *S. aureus* (MRSA). MRSA occurs upon acquisition of the ability to express a novel penicillin binding protein PBP2A (*mecA*), that participates in cell wall biosynthesis and demonstrates a low affinity for  $\beta$ -lactams, allowing the cells to survive in the presence of antibiotics. Other, chromosomal mutations in genes, called potentiators (*pot*) are known to be involved in the development of high-level resistant MRSA strains.

My study aimed to characterise the mechanism by which PBP2A confers antibiotic resistance. The bacterial two hybrid system was used to identify PBP2A protein partners that may influence its activity. Random libraries of protein expression constructs did not identify novel interactions for PBP2A. Neither did further directed screening of PBP2A with a range of other proteins involved in cell morphogenesis during growth and division. Importantly my study highlighted the interaction of PBP2A with the endogenous PBP2, whereby the non-native PBP2A may piggyback onto the wide range of PBP2 partners.

High-level resistant MRSA strains that both make PBP2A, and harbour *pot* mutations can be re-sensitised to the effects of  $\beta$ -lactams using compounds such as (-)-epicatechin gallate (ECg). I used a directed evolution approach to identify genes involved in the mode of action of ECg. The genes were all functionally associated with nucleotide signalling pathways, highlighting the link between high-level MRSA development and basic cellular physiology. My work has provided novel understanding of the mechanism underpinning MRSA and new avenues to develop adjunct approaches to rationally develop new control regimes, to beat MRSA.

# Acknowledgements

Professor Simon Foster for being an amazing supervisor and his confidence in me throughout the process, I am very lucky to have done a PhD in such an amazing lab with both your guidance and that of the wider team, past and present.

A massive thank you to Dr's Bartek, Kasia, Josh and Lucia for being amazing scientists, coolest lab mates and lovely friends and for not minding when I decided to spontaneously defrost freezers. It was a crazy time to do a PhD, and it was lovely sharing it with you both Dr's Katie and Tom. Thank you to Dr Mariana Tinajero-Trejo for sharing a bay with me (& the sheer number of agar plates I seemed to generate throughout the PhD) and for looking out for me.

I am grateful to the MRC's DiMeN Doctoral training partnership for the opportunity to carry out this project, especially Dr Emily Goodall for building the best DTP, and the DiMeN gang Naz, Laura, Becky, Becky and Sarah, everyone who's been part of the DTP over the years.

Thanks to Helen Shaw for her patience, encouragement and support throughout a range of challenges, and for teaching me things I didn't know I needed to learn as part of this journey, you're a pleasure to work with.

Sheffield gang/Bio bois/A's for the much needed drinks/coffees/swims/corridor chats/fondues/waterfall climbing and generally for being the most amazing community of PhD students you could ask for.

My Mum, Dad, Sabrina and Alexander for their support, help and encouragement in this and everything I do.

Grandad, John Ross, I reckon you'd've loved a printed copy of this...

To Ro. This might have been a long chapter, but it's been an awesome one, and I cannot wait for our next adventures (esp. if the last four years are anything to go by). Thanks for putting up with the plants and everything else that comes with living with me (PhD Student Verison). I am proud of us both for persevering and thankful for everything you do day in and day out. I couldn't do very much without your support and appreciate how we challenge each other to be the best we can 🐉

## **Publications to which this study has contributed.**

Adedeji-Olulana, A. F., Wacnik, K., Lafage, L., Pasquina-Lemonche, L., Tinajero-Trejo, M., Sutton, J. A. F., Bilyk, B., Irving, S. E., **Portman Ross, C. J.**, Meacock, O. J., Randerson, S. A., Beattie, E., Owen, D. S., Florence, J., Durham, W. M., Hornby, D. P., Corrigan, R. M., Green, J., Hobbs, J. K., & Foster, S. J. (2024). **Two codependent routes lead to high-level MRSA.** *Science*, 386(6721), 573–580. <https://doi.org/10.1126/SCIENCE.ADN1369>

Sutton, J. A. F., Cooke, M., Tinajero-Trejo, M., Wacnik, K., Salamaga, B., **Portman Ross, C.**, Lund, V. A., Hobbs, J. K., & Foster, S. J. (2023). **The roles of GpsB and DivIVA in Staphylococcus aureus growth and division.** *Frontiers in Microbiology*, 14, 1241249. <https://doi.org/10.3389/FMICB.2023.1241249>

# Table of Contents

<b>SUMMARY</b> .....	<b>II</b>
<b>ACKNOWLEDGEMENTS</b> .....	<b>III</b>
<b>PUBLICATIONS TO WHICH THIS STUDY HAS CONTRIBUTED.</b> .....	<b>IV</b>
<b>TABLE OF CONTENTS</b> .....	<b>V</b>
<b>LIST OF TABLES</b> .....	<b>XII</b>
<b>LIST OF FIGURES</b> .....	<b>XIV</b>
<b>CHAPTER 1 INTRODUCTION</b> .....	<b>1</b>
<b>1.1 <i>Staphylococcus aureus</i></b> .....	<b>1</b>
1.1.1 Infections and Epidemiology.....	1
<b>1.2 <i>Staphylococcus aureus</i> cell wall Structure and Dynamics</b> .....	<b>2</b>
1.2.1 Cell wall ultrastructure .....	2
1.2.2 Staphylococcal Peptidoglycan .....	3
1.2.3 Peptidoglycan Synthesis .....	6
1.2.3.1 Cytoplasmic reactions .....	6
1.2.3.2 Translocation and lipid II incorporation.....	6
1.2.3.3 Action of PG synthetases.....	6
1.2.3.3.1 Transglycosylation and Transpeptidation.....	6
1.2.4 Penicillin Binding Proteins.....	7
1.2.5 Cell wall Hydrolysis .....	10
1.2.6 Cell wall dynamics during growth and division.....	13
1.2.7 The divisome and septal placement.....	15
<b>1.3 Antibiotics</b> .....	<b>17</b>
1.3.1 Metabolism targeting.....	17
1.3.2 DNA & Protein Synthesis targeting.....	17
1.3.3 Membrane targeting.....	18
1.3.4 Cell Wall targeting.....	18
<b>1.4 Antibiotic resistance in <i>S. aureus</i>.</b> .....	<b>21</b>
<b>1.5 Mechanisms of resistance</b> .....	<b>23</b>
1.5.1 Vancomycin and glycopeptides .....	23
1.5.2 Fluroquinolones .....	23
1.5.3 Mupirocin.....	23
<b>1.6 Staphylococcal <math>\beta</math>-lactam resistance</b> .....	<b>24</b>
1.6.1 The <i>SCCmec</i> complex.....	24
1.6.1.1 Genetic organisation of <i>SCCmec</i> .....	26

1.6.2 PBP2A and associated $\beta$ -lactam resistance.....	26
<b>1.7 The mechanism of high-level resistance to <math>\beta</math>-lactams .....</b>	<b>31</b>
1.7.1 Auxiliary Factors.....	31
1.7.1.1 Cell wall homeostasis.....	31
1.7.1.2 Cell wall Stress stimulon.....	32
1.7.2 Heterogenous and Homogenous Resistance.....	34
1.7.3 Potentiators of methicillin resistance .....	34
1.7.3.1 Protein turnover.....	34
1.7.3.2 Nucleotide signalling.....	35
1.7.3.3 RNA polymerase.....	35
1.7.3.4 Quorum Sensing.....	36
1.7.3.5 Cell wall homeostasis .....	36
1.7.3.6 Development of high-level MRSA.....	37
<b>1.8 Aims.....</b>	<b>37</b>
<b>CHAPTER 2 MATERIALS AND METHODS.....</b>	<b>40</b>
<b>2.1 Growth Media.....</b>	<b>40</b>
2.1.1 Luria-Bertani (LB).....	40
2.1.2 Minimal Media.....	40
2.1.3 Tryptone soya.....	40
2.1.4 Baird-Parker agar .....	40
2.1.5 LK .....	41
<b>2.2 Antibiotics.....</b>	<b>41</b>
<b>2.3 Bacterial Strains and Plasmids .....</b>	<b>41</b>
2.3.1 <i>Staphylococcus aureus</i> strains.....	41
2.3.2 <i>Escherichia coli</i> strains.....	41
2.3.3 Plasmids.....	41
<b>2.4 Buffers and Solutions .....</b>	<b>46</b>
2.4.1 Phosphate buffered saline (PBS).....	46
2.4.2 Tris-Acetate buffer (TAE) (50X).....	46
2.4.3 TBSI .....	46
2.4.4 SDS-PAGE Solutions.....	46
2.4.4.1 SDS-PAGE reservoir buffer.....	46
2.4.4.2 SDS-PAGE loading Buffer .....	46
2.4.5 Western Blotting Solutions.....	47
2.4.5.1 Transfer buffer.....	47
2.4.5.2 TBST (wash solution) .....	47

2.4.5.3 Blocking Buffer .....	47
2.4.6 $\beta$ - galactosidase liquid assay solutions.....	47
2.4.6.1 ABT .....	47
2.4.6.2 Stopping Solution .....	47
2.4.6.3 ABTN.....	47
2.4.7 Co-immunoprecipitation solutions and buffers.....	47
2.4.7.1 Lysis buffer.....	47
2.4.7.2 Membrane extraction buffer .....	48
2.4.7.3 No salt wash buffer.....	48
2.4.7.4 Dilution buffer .....	48
2.4.7.5 Wash buffer .....	48
<b>2.5 Enzymes and chemicals .....</b>	<b>48</b>
<b>2.6 Centrifugation .....</b>	<b>48</b>
2.6.1 Ultra centrifugation .....	49
<b>2.7 Determination of bacterial cell density.....</b>	<b>49</b>
2.7.1 Spectrophotometric measurement.....	49
<b>2.8 Determination of minimum inhibitory concentration.....</b>	<b>49</b>
2.8.1 Determination of minimum inhibitory concentration by microdilution.....	49
<b>2.9 Antibiotic methods.....</b>	<b>50</b>
2.9.1 Antibiotic MIC by ETest.....	50
2.9.2 Antibiotic Gradient plate for directed evolution.....	50
<b>2.10 DNA Purification techniques.....</b>	<b>50</b>
2.10.1 Genomic DNA extraction .....	50
2.10.2 Plasmid purification .....	50
2.10.3 Gel extraction of DNA.....	51
2.10.4 Purification of PCR products .....	51
<b>2.11 <i>In vitro</i> manipulation of DNA .....</b>	<b>51</b>
2.11.1 Primer Design.....	51
2.11.2 PCR amplification.....	51
2.11.2.1 Phusion DNA polymerase .....	51
2.11.2.2 Colony PCR Screening of <i>S. aureus</i> .....	51
2.11.2.2.1 Lysostaphin solution .....	57
2.11.2.2.2 Proteinase K solution.....	57
2.11.3 Restriction endonuclease digestion .....	57
2.11.4 Gibson Assembly .....	57
2.11.5 Agarose gel electrophoresis.....	57

2.11.6 DNA sequencing.....	57
2.11.7 Determining DNA concentration.....	57
<b>2.12 Protein Analysis.....</b>	<b>58</b>
2.12.1 Preparation of whole cell lysate .....	58
2.12.2 SDS PAGE .....	58
2.12.3 Coomassie Staining.....	58
2.12.4 Western Blotting.....	58
2.12.4.1 Transfer.....	58
2.12.4.2 Antibody binding and washing.....	59
2.12.4.3 Detection.....	59
2.12.5 Co-Immunoprecipitation .....	59
2.12.5.1 Growth of Strains for Co-immunoprecipitation .....	59
2.12.5.2 Preparing membrane fractions for immunoprecipitation .....	59
2.12.5.3 Co-immunoprecipitation.....	60
2.12.5.3.1 Bead equilibration.....	60
2.12.5.3.2 Protein binding.....	60
2.12.5.3.3 Washing.....	60
2.12.5.3.4 Elution.....	60
<b>2.13 Transformation Techniques .....</b>	<b>61</b>
2.13.1 Transformation of <i>E. coli</i> .....	61
2.13.1.1 Preparation of <i>E. coli</i> chemically competent cells .....	61
2.13.1.2 Transforming chemically competent <i>E. coli</i> .....	61
2.13.2 Transformation of <i>S. aureus</i> .....	61
2.13.2.1 Preparation of electrocompetent <i>S. aureus</i> .....	61
2.13.2.2 Transformation of electrocompetent <i>S. aureus</i> .....	62
2.13.3 Bacterial two hybrid screening.....	62
2.13.4 Library Transformation and screening.....	62
2.13.5 Directed bacterial two hybrid screening.....	62
2.13.6 Solid Media Assays.....	62
2.13.7 Liquid media assays.....	68
<b>2.14 Phage Techniques.....</b>	<b>68</b>
2.14.1 Preparation of Phage Lysate.....	68
2.14.2 Phage Transduction .....	69
<b>2.15 Microscopy Techniques .....</b>	<b>69</b>
2.15.1 Fixing of Cells for imaging.....	69
2.15.2 Microscopy .....	70
2.15.3 Image processing.....	70



<b>2.16 DNA Sequencing</b> .....	<b>70</b>
2.16.1 Sanger Sequencing .....	70
2.16.2 Whole Genome Sequencing.....	70
2.16.3 Data Analysis .....	70
<b>CHAPTER 3 PENICILLIN BINDING PROTEIN INTERACTION MAPPING USING THE BACTERIAL TWO HYBRID SYSTEM</b> .....	<b>71</b>
<b>3.1 Introduction</b> .....	<b>71</b>
3.1.1 Aims of this chapter.....	73
<b>3.2 Results</b> .....	<b>76</b>
3.2.1 Screen of bacterial two-hybrid libraries.....	76
3.2.2 Establishing the two hybrid library screening protocol .....	78
3.2.3 Screening bacterial two hybrid libraries for PBP interactions.....	80
3.2.3.1 C terminal T18 fusion library screening .....	82
3.2.3.2 N terminal T18 fusion library screening.....	84
3.2.3.3 Identifying interacting protein partners .....	86
3.2.3.4 Bioinformatics analysis of putative hits .....	90
3.2.4 Confirmation of novel interactions using full length gene constructs of identified proteins .....	91
3.2.4.1 Gibson Assemblies.....	91
3.2.4.2 Commercial Gene synthesis .....	91
3.2.4.3 Solid media assay .....	97
3.2.5 Preliminary liquid assay investigation of interacting protein partners .....	97
<b>3.3 Discussion</b> .....	<b>101</b>
<b>CHAPTER 4 DIRECTED ANALYSIS OF PROTEIN-PROTEIN INTERACTIONS</b> .....	<b>105</b>
<b>4.1 Introduction</b> .....	<b>105</b>
4.1.1 Aims of this Chapter.....	109
<b>4.2 Results</b> .....	<b>109</b>
4.2.1 Directed B2H screening .....	109
4.2.1.1 Cell wall morphogenesis factor: GpsB.....	110
4.2.1.2 Cell wall hydrolases.....	114
4.2.1.2.1 LytH.....	114
4.2.1.2.2 LytN .....	118
4.2.1.3 Investigating Antibiotic resistance determinant: PBP2A.....	121
4.2.2 Liquid Media Assays.....	124
4.2.3 Protein interaction mapping .....	126
4.2.4 Investigating protein interactions using co-immunoprecipitation .....	130
4.2.4.1 CO-IP experimental design .....	130
4.2.4.2 Design of PBP2A fluorescent fusions.....	131

4.2.4.3 Strain construction and method development for CO-IP .....	134
4.2.4.4 Strain validation.....	134
4.2.4.5 Verification of strains using $\alpha$ -GFP antibodies .....	134
4.2.4.6 Verification of SpA strains for CO-IP.....	134
4.2.4.7 Microscopy of strains for Co-immunoprecipitation .....	135
<b>4.3 Discussion.....</b>	<b>140</b>
<b>CHAPTER 5 ANALYSIS OF THE MECHANISM OF ACTION OF RESENSITISING AGENTS THAT MODULATE <math>\beta</math>-LACTAM RESISTANCE IN MRSA. ....</b>	<b>142</b>
<b>5.1 Introduction .....</b>	<b>142</b>
5.1.1 Aims.....	145
<b>5.2 Results .....</b>	<b>146</b>
5.2.1 (-)-epicatechin gallate sensitises MRSA. ....	146
5.2.2 Isolation of ECg insensitive derivatives of MRSA.....	148
5.2.2.1 Identification of chromosomal mutations in sensitiser resistant strains .....	151
5.2.2.2 A common theme for mutated genes .....	157
5.2.3 Construction of sensitiser resistant, transposon insertion MRSA strains.....	160
5.2.3.1 Effects of sensitising compounds on transposon insertion strains .....	163
5.2.4 Investigating the effect of other compounds that sensitise MRSA to $\beta$ -lactams.....	165
5.2.4.1 Oxacillin resistance in the presence of sensitising compounds.....	165
5.2.5 The stringent response as a modulator of high-level resistance in MRSA.....	168
5.2.5.1 Characterising resistance in the presence of a stringent response inducer.....	170
5.2.5.2 Induction of the stringent response decreases antimicrobial susceptibility.....	172
5.2.5.3 Rescuing MRSA from the effects of sensitising compounds via induction of the stringent response.....	174
<b>5.3 Discussion.....</b>	<b>177</b>
<b>CHAPTER 6 GENERAL DISCUSSION .....</b>	<b>181</b>
<b>6.1 The danger of antimicrobial resistance.....</b>	<b>181</b>
<b>6.2 Insights into PBP2A protein-protein interactions.....</b>	<b>181</b>
<b>6.3 The basis of high-level resistance in MRSA .....</b>	<b>183</b>
<b>6.4 Future Perspectives .....</b>	<b>186</b>
<b>REFERENCES .....</b>	<b>187</b>
<b>APPENDICES .....</b>	<b>224</b>
Appendix 1 Loci nearest T18 Reporter Gene .....	224
Appendix 2 Summary of in frame fusions of proteins identified by bacterial two hybrid library screen.....	226

Appendix 3 B2H Constructs; Genewiz order reference 40-541290844 .....	232
Appendix 4 LytN and LytH Constructs; Genewiz order reference 40-541290844.....	236
Appendix 5 PBP2A GFP Constructs; Genewiz order reference 40-760878046.....	238
Appendix 6 Table of Variant Calling.....	241
Appendix 7 PCR analysis of transposon insertions.....	242

## List of Tables

Table 1.1. Overview of Staphylococcal penicillin binding proteins and their molecular roles.	9
Table 1.2 Putative PG hydrolases of <i>S.aureus</i> COL identified by an <i>in silico</i> screen	11
Table 2.1 Antibiotics and Resensitising Agents	42
Table 2.2 <i>S. aureus</i> Strains	43
Table 2.3 <i>E. coli</i> strains used in this study.	45
Table 2.4 Primers used in this study	53
Table 2.5 T25 Bacterial Two Hybrid Constructs	64
Table 2.6 T18 Bacterial two hybrid Constructs	66
Table 3.1. Methods used to characterise Protein-Protein interactions.	74
Table 3.2 Total colonies screened for each combination of Bacterial two hybrid libraries and PBP expressing constructs.	81
Table 3.3 Summary of bacterial two hybrid screening of C terminal T18 fusion libraries of 0.5-1 kbp and 1-3 kbp sized fragments	83
Table 3.4. Summary of bacterial two hybrid screening of N terminal T18 fusion libraries of 0.5-1 kbp and 1-3 kbp sized fragments	85
Table 3.5 Summary of in frame fusions by library from bacterial two hybrid screening.	92
Table 3.6. Sub-contracted BACTH constructs	96
Table 4.1 Minimum inhibitory concentrations of strains designed for co-immunoprecipitation using GFP tagged PBP2A by Etest.	136
Table 5.1 Table of Resensitising agents	143
Table 5.2. Minimum inhibitory concentration (MIC) by Etest Oxacillin ( $\mu\text{g}/\text{mL}$ ) on TSA and in the presence of (-)-epicatechin gallate (50 $\mu\text{g}/\text{mL}$ )	147
Table 5.3. List of ECg insensitive methicillin resistant strains generated by directed evolution in the presence of (-)-epicatechin gallate on a gradient of methicillin.	150
Table 5.4 Summary of Variant Calling for (-)-epicatechin gallate (ECg) resistant strains.	154
Table 5.5 Antibiogram of parental strains in the presence of (-)-epicatechin gallate	161
Table 5.6 Antibiogram of transposon insertion mutants in the presence of (-)-epicatechin gallate	164
Table 5.7 Minimum inhibitory concentrations (MIC) for sensitising compounds by broth microdilution in tryptone soya broth ( $\mu\text{g}/\text{mL}$ )	166
Table 5.8 Oxacillin resistance of characteristic laboratory strains in the presence of sensitising compounds	167

Table 5.9 Antibigram of transposon insertion mutants in the presence of sensitising compounds

169

## List of Figures

Figure 1.1 Gram positive cell wall ultrastructure.	4
Figure 1.2 <i>S. aureus</i> peptidoglycan building blocks.	5
Figure 1.3 Peptidoglycan biosynthesis in <i>S. aureus</i> .	8
Figure 1.4 The targets of peptidoglycan hydrolases	12
Figure 1.5 Cell wall synthesis and architecture.	14
Figure 1.6 The divisome and septum formation in <i>S. aureus</i> .	16
Figure 1.7 Antimicrobial modes of action within the cell.	19
Figure 1.8. <i>S. aureus</i> antibiotic targets in peptidoglycan and cell wall active antibiotics.	20
Figure 1.9 Timeline of introduction of antibiotics and the emergence of antibiotic resistance in <i>S. aureus</i> .	22
Figure 1.10 SCC <i>mec</i> integration and excision in <i>S. aureus</i> .	25
Figure 1.11 Comparison of the staphylococcal chromosomal cassette types SCC <i>mec</i> I-V	28
Figure 1.12 Molecular Structure of <i>S. aureus</i> PBP2A.	30
Figure 1.13 Schematic of auxiliary factors involved in $\beta$ -lactam resistance in MRSA.	33
Figure 1.14 Schematic of Potentiators involved in $\beta$ -lactam resistance in MRSA.	38
Figure 1.15 Levels of antibiotic resistance in <i>S. aureus</i> .	39
Figure 3.1 Principle of the bacterial two hybrid (BACTH) assay for determining protein-protein interactions <i>in vivo</i> .	75
Figure 3.2. Diagrammatical scale representation of the penicillin binding proteins fused to bacterial two hybrid T25 reporter proteins used in this study.	77
Figure 3.3 Progression of a sample through the bacterial two hybrid screening workflow	79
Figure 3.4 Plasmid maps of bacterial two hybrid vectors pUT18(N) and pUT18(C) with a gDNA fragment ligated into the BamHI restriction site	87
Figure 3.5 Example analysis of in frame negative (A) and positive (B) fusions from bacterial two hybrid screen.	89
Figure 3.6 Schematic of Gibson assembly to create in frame fusion of gene of interest (goi) fusions to BACTH reporter (T18) in pUT18 vectors.	93
Figure 3.7 Plasmid maps and restriction digests of B2H constructs.	94
Figure 3.8 Plasmid maps and restriction digests of B2H constructs.	95
Figure 3.9 Summary of solid media assay of full-length gene constructs of proteins identified in bacterial two hybrid library screen.	99
Figure 3.10 Preliminary $\beta$ -Galactosidase activity of bacterial two hybrid interacting partners identified in library screening.	100

Figure 4.1 Peptidoglycan hydrolases.	107
Figure 4.2 Diagram of GpsB in frame fusions with B2H T25 and T18	111
Figure 4.3. Solid media assay of T25 array of B2H constructs screened against GpsB T18	112
Figure 4.4. Solid media assay of T18 array of B2H constructs screened against GpsB T25	113
Figure 4.5 Diagrammatical representation of cell wall hydrolases LytH and LytN with T25 and T18 B2H reporters.	115
Figure 4.6 Solid media assay of T25 array of B2H constructs screened against LytH T18	116
Figure 4.7 Solid media assay of T18 array of B2H constructs screened against LytH T25	117
Figure 4.8 Solid media assay of T25 array of B2H constructs screened against LytN T18	119
Figure 4.9 Solid media assay of T18 array of B2H constructs screened against LytN T25	120
Figure 4.10 Solid media assay of T18 constructs of Staphylococcal proteins screened against PBP2A	122
Figure 4.11 Solid media assay of T25 constructs of Staphylococcal proteins screened against PBP2A	123
Figure 4.12 Identification of B2H interacting partners of LytH and LytN determined by liquid $\beta$ -galactosidase assay.	125
Figure 4.13 Identification of B2H interacting partners of T25~GpsB determined by $\beta$ -galactosidase liquid assay.	127
Figure 4.14 Identification of B2H interacting partners of T18 GpsB determined by $\beta$ -galactosidase liquid assay.	128
Figure 4.15 Protein interaction mapping of <i>S. aureus</i> as determined by two hybrid analysis in the context of the literature.	129
Figure 4.16 Location of key GFP tagged proteins in a representative cell	132
Figure 4.17 Construction of chromosomal <i>mecA</i> GFP fusions in <i>S. aureus</i>	133
Figure 4.18 Western blots to verify control strains for co-immunoprecipitation using $\alpha$ -GFP (A) and $\alpha$ -PBP2 (B)	137
Figure 4.19 DNA electrophoresis of PCR products confirming <i>spa</i> inactivation in strains for Co-immunoprecipitation.	138
Figure 4.20 Structured illumination microscopy (SIM) of strains expressing fluorescently tagged proteins of interest for co-immunoprecipitation and investigation of cellular localisation.	139
Figure 5.1. Generation of (-)-epicatechin gallate (ECg) insensitive strains of MRSA	149
Figure 5.2 Lineage of parental strains and ECg insensitive strains generated by the directed evolution of high-level resistant strains.	152

Figure 5.3 Strains generated by directed evolution and location of mutations in proteins represented diagrammatically.	156
Figure 5.4 Mapping SNP changes on Rel proteins.	158
Mutations found in (A) <i>relA</i> and (B) <i>relQ</i> , during directed evolution screen. Parental <i>rpoB</i> <sup>H929Q</sup> strains shown in grey and mutations found in <i>rpoC</i> <sup>G740R</sup> strains shown in black. <b>Figure 5.5 Purine and ppGpp biosynthesis pathways.</b>	158
Figure 5.6 Diagram of transposon mutagenesis of <i>relA</i> in <i>S. aureus</i> .	162
Figure 5.7 Determination of the minimum inhibitory concentration of Serine hydroxamate for representative <i>Staphylococcus aureus</i> strains.	171
Figure 5.8. Evaluation by Etest of the effects of serine hydroxamate on oxacillin resistance	173
Figure 5.9 Filter disk assay using SHX rescues growth of MRSA from a combination of methicillin and ECg.	175
Figure 5.10. Use of DL-serine hydroxamate to rescue MRSA from the effects of sensitising compounds.	176
Figure 5.11 The stringent response modulates MRSA resistance to oxacillin in the presence of sensitising compounds.	180
Figure 6.1 Development of resistance in MRSA	185



# Chapter 1 Introduction

## 1.1 *Staphylococcus aureus*

*Staphylococcus aureus* is a Gram-positive coccus (Lowy, 1998) which colonises the anterior nares of approximately 12–30% of individuals persistently and 16–70% intermittently as a commensal (Wertheim et al., 2005). *S. aureus* is also capable of colonizing diverse ecological niches within its human host. As a pathogen *S. aureus* causes significant morbidity and mortality worldwide.

*S. aureus* infections show three general types: (i) superficial lesions such as soft tissue and wound infections (Le Loir et al., 2003); (ii) systemic and life-threatening conditions such as endocarditis, osteomyelitis, pneumonia, brain abscesses, meningitis, and bacteraemia; and (iii) toxinoses such as gastroenteritis scalded skin syndrome and toxic shock syndrome, as a result of staphylococcal enterotoxins (Aires de Sousa and Lencastre, 2004). *S. aureus* infections can result in metastatic foci of infection, present beyond the initial boundaries of infection, and are found in many high-risk patients being treated for Gram-positive bacteraemia (Vos et al., 2012).

### 1.1.1 Infections and Epidemiology

As a result of biofilm formation on biotic and abiotic surfaces many staphylococcal infections are associated with medical devices including indwelling catheters (Tong et al., 2015). After initial attachment of organisms present in a niche, changes in gene regulation allows the growth of a biofilm as a community and in response to quorum sensing as opposed to individual cells (Al-Mebairik et al., 2016; Le and Otto, 2015).

*S. aureus* strains have spread globally, becoming one of the most prevalent nosocomial diseases where there are no clinical signs of an infection on admission and positive blood cultures 48 hours after hospital admission (Pinho et al., 2001). More recently *S. aureus* has been evidenced to be responsible for increasing morbidity, driven by an epidemic of community acquired infections of strains resistant to  $\beta$ -lactams and expressing certain virulence factors (Tong et al., 2015). French et al., (1990) highlighted four independent risk factors for mortality from *S. aureus* infections: underlying disease, length of hospitalisation before bacteraemia, previous antibiotic therapy, and inadequate anti-staphylococcal therapy. *S. aureus* is armed with an extensive repertoire of virulence factors enabling toxicity, invasiveness, and immune evasion. Specific and controlled mechanisms regulate the virulence

of *S. aureus* throughout its different growth phases and in response to environmental conditions. Regulation of virulence involves two component regulatory systems including *agr*, *saeRS* and *srrAB* (Bronner et al., 2004).

## **1.2 *Staphylococcus aureus* cell wall Structure and Dynamics**

### **1.2.1 Cell wall ultrastructure**

The cell wall maintains the cytoplasmic turgor pressure (Xiong et al., 2005). The structure of the cell wall is shown diagrammatically in Figure 1.1. The cell membrane and cell wall are separated by an exoplasmic space (Matias and Beveridge, 2007). The perturbation of the cell membrane lipid palisade by antimicrobial compounds has allowed their function to be interrogated through measurement of their fatty acid and phospholipid content, membrane fluidity, and transmembrane potential ( $\Delta\psi$ ) (Bayer et al., 2000; Koo et al., 1996; Yeaman et al., 1998; Yeaman and Yount, 2003). Carotenoid compounds such as Staphyloxanthin are membrane bound giving staphylococcal strains their characteristic golden colouration and have been proposed as having a comparative function to the eukaryotic steroids which regulate and maintain membrane fluidity (Rohmer et al., 1979).

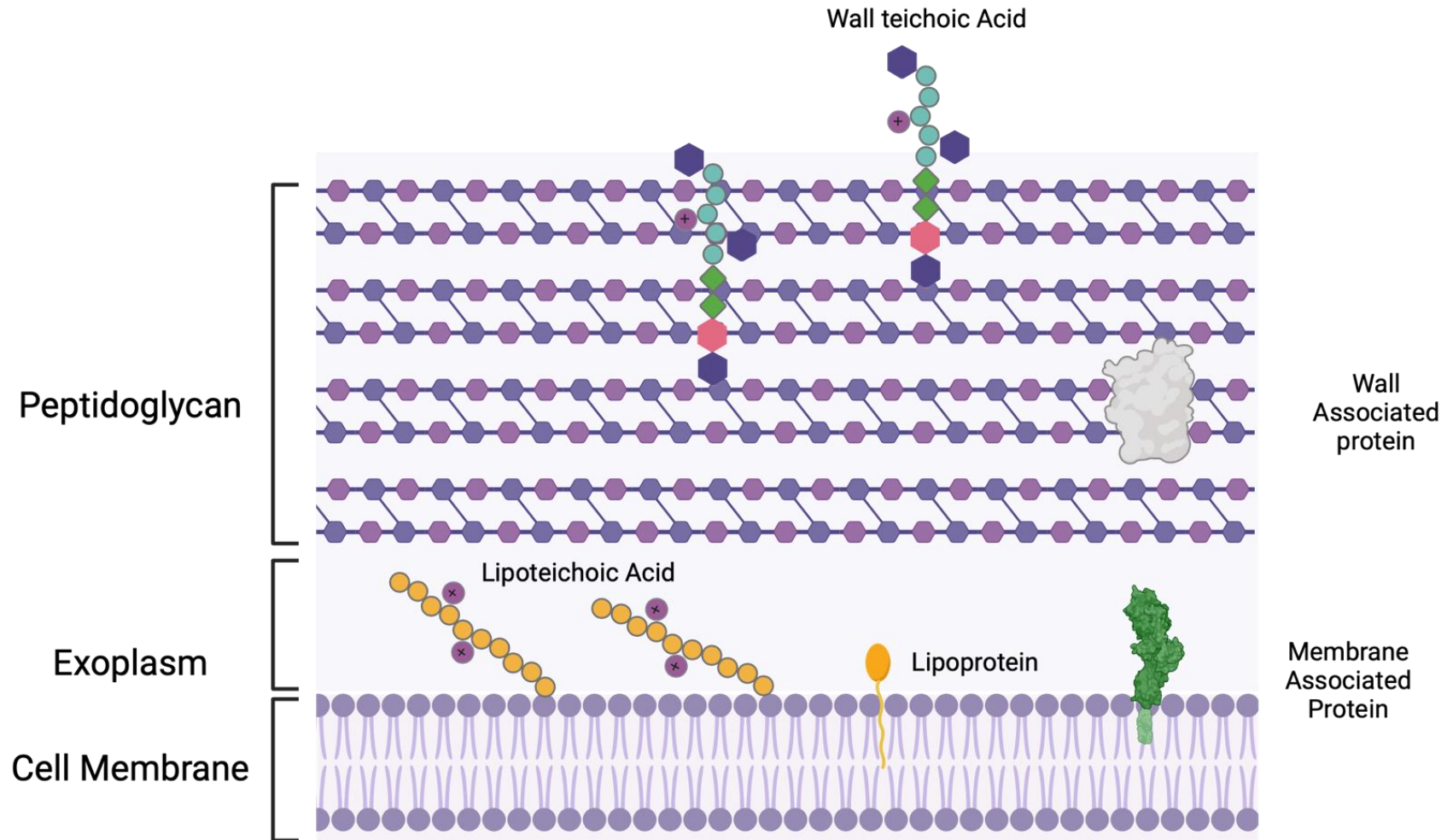
The staphylococcal cell wall consists of a thick layer of peptidoglycan (PG) (30- 100nm thick (Vollmer et al., 2008), which provides cells the ability to withstand turgor pressure, maintain cell shape and support pathogenicity and virulence (Sauvage et al., 2008). PG crosslinks also allow covalent attachment of proteins to the cell wall by sortase A (Schneewind and Missiakas, 2019, 2012). Other polymers are also present in the staphylococcal cell envelope whereby wall and lipoteichoic acids (WTA and LTA), are associated with the cell wall and membrane respectively (Section 1.2.1).

LTA play a key role in the regulation of the cell shape and cell size of *S. aureus*. LTA are single unbranched polymers of 1,3-linked glycerol subunits attached to Glc<sub>2</sub>- diacylglycerol (Fischer et al., 2011). LTA are integral to the cell membrane of the Gram-positive cell and are conditionally essential for growth of *S. aureus* (Reichmann et al., 2014). Controlling the length of LTA promotes survival under stressful conditions (Hesser et al., 2020) and those cells expressing long LTA are sensitised to cell wall hydrolases and  $\beta$ -lactam antibiotics (Hesser et al., 2020). Interestingly, survival in the absence of LTAs has also been shown in strains where the monofunctional PG glycosyltransferase SgtB is deactivated (Karinou et al., 2019). Other compensatory mutations in genes such as *vraT*, *mazE*, *clpX* (Karinou et al., 2019) or *gdpP* (Corrigan et al., 2011) also support the survival of LTA negative strains.

WTA of *S. aureus* consist of a polyribitol-phosphate backbone being partially substituted with variations of sugars/amino sugars (Endl et al., 1983). As an important secondary glycopolymer in the cell wall WTA have an integral role in pathogenesis and evasion of the host immune system (Keinhörster et al., 2019). Their production and export to the cell envelope is tightly regulated by transcription factor MgrA and the two component systems: Agr, GraRS and ArlRS (Keinhörster et al., 2019). These systems link the specific phenotypes of pathogenic clinically acquired MRSA strains are linked by high-levels of WTA in the cell wall (Wanner et al., 2017). The synthesis machinery and thus presence of WTA has also been shown to be important for the release of cytolytic toxins (Brignoli et al., 2022). WTA expression is also required for high-level  $\beta$ -lactam resistance (Campbell et al., 2011).

## 1.2.2 Staphylococcal Peptidoglycan

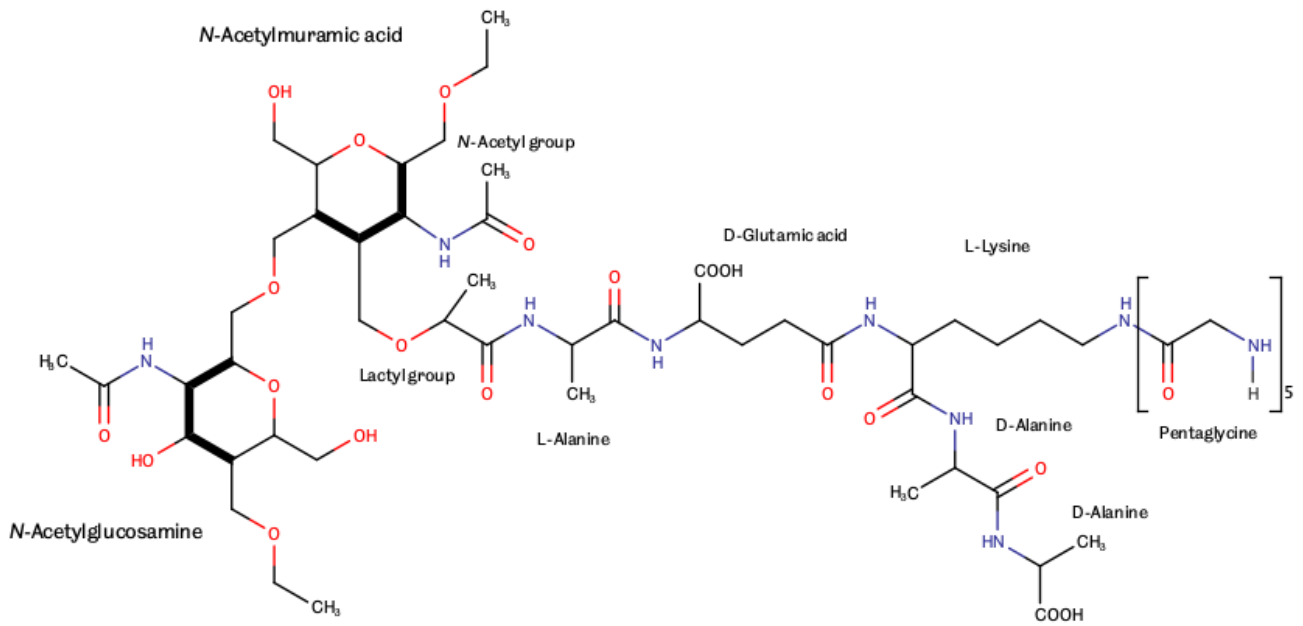
The major structural polymer in the cell wall is PG which is essential for viability and shape determination (Sauvage et al., 2008). *S. aureus* PG is made of glycan strands of alternating disaccharides, *N*-acetylmuramic acid (MurNAc) and *N*-acetylglucosamine (GlcNAc), crosslinked by peptide side chains attached to MurNAc (Figure 1.2) (Ghuysen, 1968; Vollmer et al., 2008). The individual GlcNAc-MurNAc units are linked by  $\beta$ -1,4 glycosidic bonds by transglycosylation (TGase) reactions (Vollmer et al., 2008). *S. aureus* has peptide sidechains linked to the MurNAc residues formed of pentapeptide building blocks, consisting of L-alanine, D-glutamine, L- lysine and D-alanyl-D-alanine (Pinho et al., 2013; Vollmer et al., 2008). Crosslinks are formed between side chains through Penicillin Binding Protein-mediated transpeptidation (TPase) reactions. These occur between D-alanine at the 4<sup>th</sup> residue in one side chain and L-lysine at the position 3 on the adjacent side chain via a pentaglycine bridge (Figure 1.2) (Pinho et al., 2013; Vollmer et al., 2008). In *S. aureus*, between 72-93% of available PG side chains participate in crosslinks (Vollmer et al., 2008).



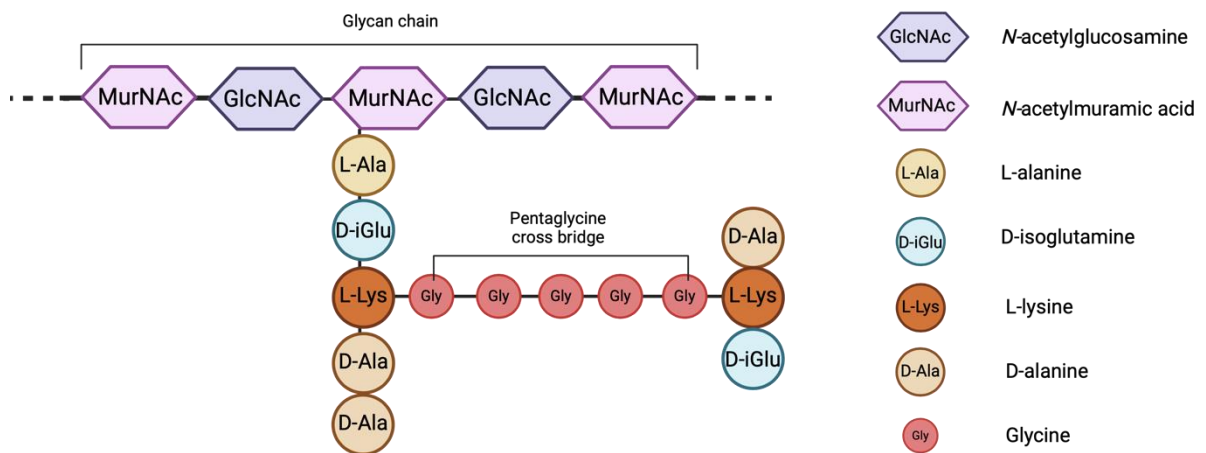
**Figure 1.1 Gram positive cell wall ultrastructure.**

Diagram representing the ultrastructure of the Gram-positive cell wall showing cell membrane, exoplasm, peptidoglycan, associated proteins and lipoteichoic and wall teichoic acids. (Adapted from Brock et al., 2003; Porfirio et al., 2019)

A



B



**Figure 1.2 *S. aureus* peptidoglycan building blocks.**

Skeletal chemical structural formula of *S. aureus* building blocks (A) and diagrammatical representation of a PG. (Adapted from (Egan et al., 2017; Vollmer et al., 2008). Created with BioRender.com.

### 1.2.3 Peptidoglycan Synthesis

The process of *S. aureus* peptidoglycan (PG) biosynthesis is shown in Figure 1.3.

#### 1.2.3.1 Cytoplasmic reactions

Firstly, in the cytoplasm, nucleotide sugar-linked precursors UDP-N-acetylglucosamine (UDP-GlcNAc) and UDP-N-acetylmuramic acid (UDP-MurNAc) are synthesised from fructose-6-phosphate (Macheboeuf et al., 2006). Mur ligases MurC, MurD, MurE and MurF decorate UDP-MurNAc with amino acids to form the UDP-MurNAc pentapeptide (Kouidmi et al., 2014; Typas et al., 2012).

#### 1.2.3.2 Translocation and lipid II incorporation

The second stage of PG synthesis occurs associated at the cytoplasmic membrane, the UDP-MurNAc pentapeptide precursor is linked to the transport lipid bactoprenol, forming lipid I. Subsequently, GlcNAc is added from UDP-GlcNAc to lipid I, forming lipid II. The subsequent addition of a pentaglycine bridge to the 3<sup>rd</sup> position at L-lysine, results in Lipid II-Gly<sup>5</sup>. (Macheboeuf et al., 2006; Pinho et al., 2013; Typas et al., 2012). This is then flipped across the cell membrane by MurJ for PG assembly (Ruiz, 2008; Sham et al., 2014).

#### 1.2.3.3 Action of PG synthetases

*S. aureus* has a high degree of crosslinking between muropeptides giving the three-dimensional mesh its strength and rigidity compared to other organisms (Snowden and Perkins, 1990). In *S. aureus* multiple proteins contribute to the exoplasmic synthesis of PG, it is hypothesised that *S. aureus* synthetases function as a complex to facilitate assembly (Reed et al., 2011).

##### 1.2.3.3.1 Transglycosylation and Transpeptidation

The synthesis of PG requires transglycosylation to polymerise glycan chains and transpeptidation for peptide crosslinking, which are the final stages of PG biosynthesis (Typas et al., 2012). There are three types of these PG synthetases: bifunctional TGase-TPases (the class A PBPs), mono-functional TPases (the class B PBPs) and monofunctional TGases (Vollmer et al., 2008). These collectively result in the respective polymerisation of lipid II, and cross-linking of the flexible peptide stems into the newly synthesised PG (Macheboeuf et al., 2006; Pinho et al., 2013; Typas et al., 2012).

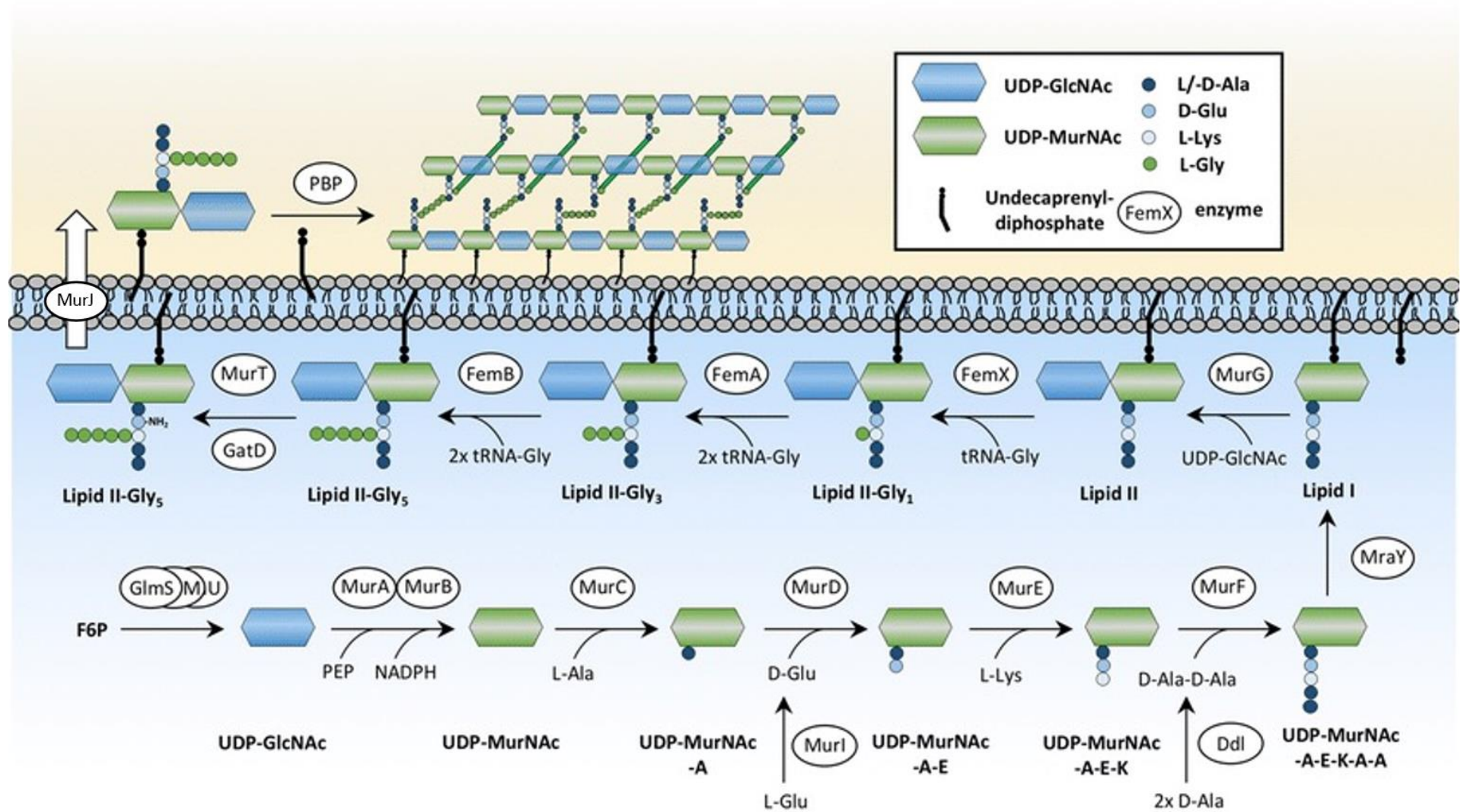
In *S. aureus* multiple proteins, including four penicillin binding proteins (PBPs) (1.2.4) and two monofunctional transglycosylases (MGT and SgtA), all contribute to the exoplasmic synthesis

of PG (Reed et al., 2011). Interactions between proteins play a vital role in PG synthesis, which highlights the function of the highly conserved proteins FtsW and RodA (Taguchi et al., 2019). FtsW is a transglycosylase (linking the subunits), which acts with its cognate pair PBP1 (Reichmann et al., 2019). Similarly, RodA (transglycosylase) works with the transpeptidase PBP3 required for the correct localisation of PG at peripheral synthesis sites (Reichmann et al., 2019).

## 1.2.4 Penicillin Binding Proteins

Penicillin-binding proteins (PBPs) catalyse the final stages of PG metabolism by performing crosslinking using transglycosylase (TG) and transpeptidase (TP) reactions (Fishovitz et al., 2014). PBPs are divided into low (LMW) and high (HMW) molecular weight PBPs. They consist of a cytoplasmic N-terminal tail, a transmembrane anchor and two functional C terminal extracellular domains joined by a linker (Goffin and Ghuysen, 1998; Lovering et al., 2007; Macheboeuf et al., 2006). HMW PBPs are divided into Class A or Class B depending on the activity of the N terminal domain, whereby both have TP activity. Class A PBPs also have a TG domain which elongates glycan chains (Goffin and Ghuysen, 1998; Sauvage et al., 2008). Class B PBPs have an interacting partner which provides TG activity (Zapun et al., 2008). *S. aureus* has only four PBPs (*E. coli* has 12 (Sauvage et al., 2008)), of which two are essential, PBP1 (class B with only TP activity) and PBP2 (class A, bifunctional with both TG and TP activities) (Wacnik et al., 2022). The essential role of PBPs in cellular growth and division makes them a target for antibiotics which compete for the active site and result in cell death due to inhibition of PG synthesis (Salamaga et al., 2021).

PBP1 acts with FtsW with essential roles in cell division both as an enzyme and as a regulator of septal plate formation (Reichmann et al., 2019; Wacnik et al., 2022). The HMW Class A PBP2 has a collaborative role with PBP4 (Łęski and Tomasz, 2005). PBP3 is a HMW Class B which is non-essential for cell viability and is involved in *S. aureus* attaining a spheroid morphology where it uses the TG activity of RodA with which it forms a cognate pair (Reichmann et al., 2019). The LMW PBPs have endopeptidase or carboxypeptidase activity, cleaving peptide side chains on PG to regulate crosslinking. The LMW PBP4 has transpeptidase activity which results in higher levels of PG cross linking (da Costa et al., 2018; Łęski and Tomasz, 2005; Loskill et al., 2014; Maya-Martinez et al., 2019). The non-native PBP2A involved in antibiotic resistance is discussed in chapter 1.6.2, Table 1.1 provides an overview of the staphylococcal PBPs and their molecular functions.



**Figure 1.3 Peptidoglycan biosynthesis in *S. aureus*.**

PG precursors are synthesised and assembled in the cytoplasm through a series of steps. They are subsequently linked to transport lipid forming lipid I and lipid II. Lipid II is translocated across the cell membrane via MurJ activity. On the exterior of the cell membrane, PBPs and other enzymes catalyse transpeptidation and transglycosylation reactions to incorporate substrate (lipid II) into nascent peptidoglycan. ( Jarick *et al.*, 2018).



**Table 1.1. Overview of Staphylococcal penicillin binding proteins and their molecular roles.**  
Adapted from (Panchal, 2018). \*PBP2A is only found in MRSA

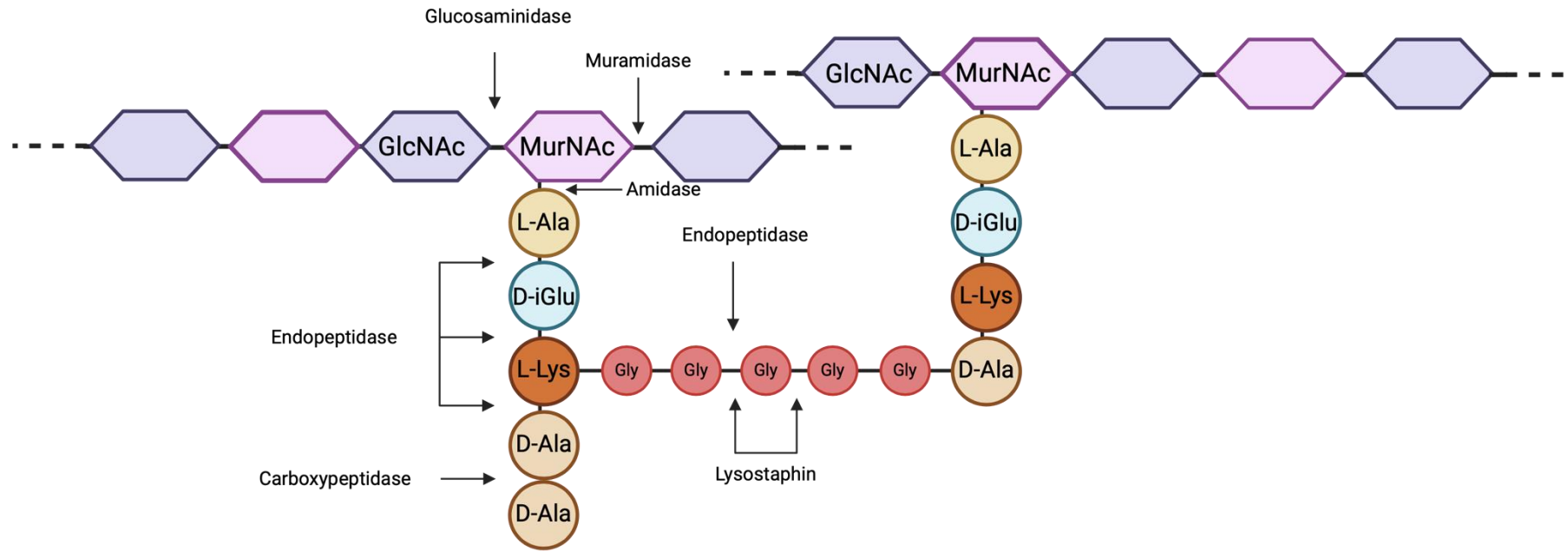
<b>PBP (gene)</b>	<b>Classification</b>	<b>Molecular function</b>	<b>References</b>
PBP2 ( <i>pbp2</i> )	HMW Class A	Essential for cell division	(Pinho et al., 2001)
PBP2A*( <i>mecA</i> )	HMW Class B	Non-native PBP, required for peptidoglycan biosynthesis and $\beta$ -lactam resistance	(Mariana G. Pinho et al., 2001)
PBP1 ( <i>pbp1</i> )	HMW Class B	Essential for cell growth and division.	(Sandro F. F. Pereira et al., 2009)
PBP3 ( <i>pbp3</i> )	HMW Class B	Interacts with RodA for off septal PG synthesis	(Reichmann et al., 2019)
PBP4 ( <i>pbp4</i> )	LMW	Required for high-level peptidoglycan crosslinking	(Memmi et al., 2008; WYKE et al., 1981)

### 1.2.5 Cell wall Hydrolysis

As well as PG synthesis, hydrolysis is required to allow cell growth and division (Salamaga et al., 2021). PG hydrolases regulate and control cell wall development, division, and synthesis (Uehara and Bernhardt, 2011). Inhibition of PG cell wall hydrolases result in cell death and in the presence of antibiotics in deregulation of PG hydrolases also lead to death (Salamaga et al., 2021). *S. aureus* has multiple putative PG hydrolases (Table 1.2) (Wheeler, 2012). PG hydrolases can be categorised according to their bond specificity (Figure 1.4). N-acetylmuramyl-L-alanine amidases (amidases) cleave the amide bond between the L-alanine of the stem peptide and N-acetylmuramic acid of the glycan (Vermassen et al., 2019; Vollmer et al., 2008). Endopeptidases cleave the peptide side chain at any position that can result in dissolution of the PG macromolecule. Glycosidases catalyse hydrolysis of the glycosidic linkages in the glycan backbone of PG. Glycosidases can be further categorised as N-acetyl-B-D-muramidases (muramidases) that cleave after the N-acetylmuramic acid residues, and N-acetyl-B-D-acetylglucosaminidases (glucosaminidases) that cleave after N-acetylglucosamines (Vermassen et al., 2019).

**Table 1.2 Putative PG hydrolases of *S.aureus* COL identified by an *in silico* screen**  
Adapted from (Wheeler, 2012).

<b>Protein</b>	<b>Activity</b>	<b>Locus (<i>Sa</i>COL)</b>	<b>Reference</b>
Atl	Amidase/Glucosaminidase	1062	(Oshida <i>et al.</i> , 1995)
SagA	Putative glucosaminidase	2298	(Murray, 2001)
SagB	Putative Glucosaminidase	1825	(Mohamad, 2007)
ScaA (Sle1/Aaa)	Amidase	0507	(Heilmann <i>et al.</i> , 2005) (Pourmand <i>et al.</i> , 2006)
ScaB	Unknown	0723	(Pourmand <i>et al.</i> , 2006)
ScaC	Unknown	2581	(Pourmand <i>et al.</i> , 2006)
ScaD	Unknown	2291	(Pourmand <i>et al.</i> , 2006)
ScaE	Unknown	0820	(Pourmand <i>et al.</i> , 2006)
ScaF	Unknown	0270	(Pourmand <i>et al.</i> , 2006)
ScaG	Unknown	2557	(Pourmand <i>et al.</i> , 2006)
ScaH	Putative glucosaminidase	2666	(Pourmand <i>et al.</i> , 2006; Mohamad, 2007)
Scal	Unknown	1576	(Pourmand <i>et al.</i> , 2006)
ScaJ	Unknown	2295	(Pourmand <i>et al.</i> , 2006)
IsaA	Putative lytic transglycosylase	2584	(Stapleton <i>et al.</i> , 2007)
LytM	Lysostaphin like	0263	(Ramadurai and Jayaswal, 1997)
LytN	Amidase/Endopeptidase	1264	(Sugai <i>et al.</i> , 1998; Frankel <i>et al.</i> , 2011)
SceD	Putative lytic transglycosylase	2088	(Stapleton <i>et al.</i> , 2007)
SA0191	Putative lysostaphin LytM	0191	(Wheeler, 2012)
SA1687	Putative amidase LytC	1687	(Wheeler, 2012)
SA2195	Putative lysostaphin LytM	2195	(Wheeler, 2012)



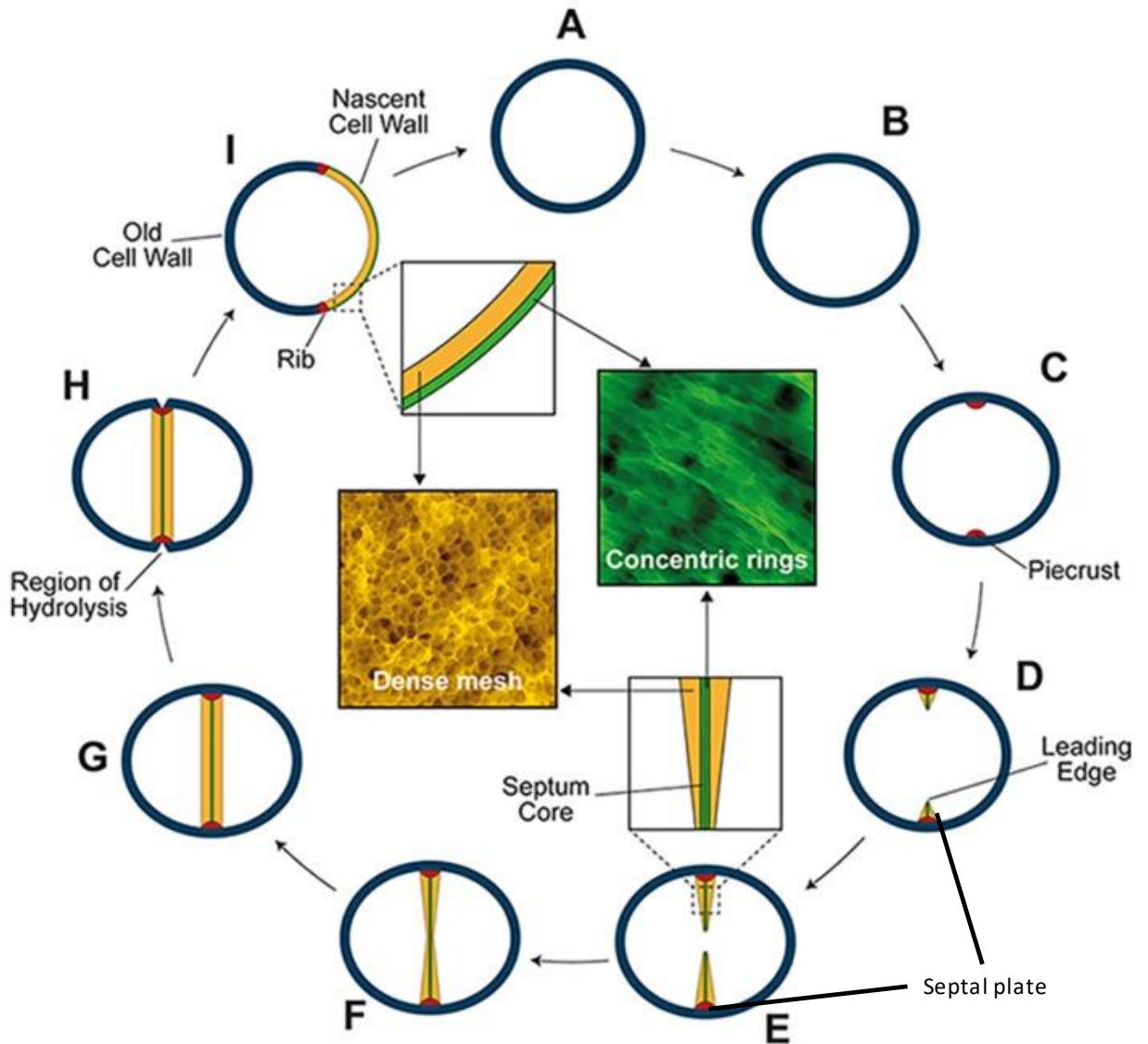
**Figure 1.4 The targets of peptidoglycan hydrolases**

The action of hydrolases (Arrows) on peptidoglycan backbones and sidechains of *S. aureus* peptidoglycan (Vollmer et al., 2008). (D-Iglu, D-Iso-glutamine, GlcNAc *N*-acetylglucosamine, MurNAc, *N*-acetylmuramic acid).

### 1.2.6 Cell wall dynamics during growth and division

Figure 1.5 shows the staphylococcal cell cycle, with associated major cell wall architectural features and the location of key cell wall synthesis. Between division events the cell size increases and aspect ratio changes (Figure 1.5 A, B) (Monteiro et al., 2015). Septum formation begins with the addition of the PG piecrust (Figure 1.5 C) (Turner et al., 2010). The piecrust acts as a foundation for septal plate formation, which is then initiated. The septum is thinner at the leading edge as it develops (Figure 1.5 D) (Lund et al., 2018; Matias and Beveridge, 2007). New PG is synthesised and incorporated (Figure 1.5 E) until annulus fusion occurs (Figure 1.5 F). PG incorporation continues at the septum until a uniform thickness is achieved (Figure 1.5 G) (Lund et al., 2018). PG hydrolase activity at the outer surface of the cell (Figure 1.5 H) in the plane of septation (Komatsuzawa et al., 1997) result in cracks or splits allowing rapid separation of the daughter cells (Zhou et al., 2015). Ribs remain marking the site of cell division and delineating those sectors of cell wall from different generations (Figure 1.5 I) (Turner et al., 2010).

The architecture of the PG is determined by both synthesis and hydrolysis during the cell cycle (Pasquina-Lemonche et al., 2020). The inner face of the septum during synthesis has a concentric ring architecture, which is revealed on the outside of the new daughter cells (Figure 1.5, shown in green) (Pasquina-Lemonche et al., 2020). The bulk of the septum internal to the rings is synthesised as a fine mesh (Figure 1.5, shown in yellow), that forms the inside of the cell wall after scission. The cell periphery also has a fine mesh at the internal face of the wall that matures into a more open structure at the outside (Figure 1.5 shown in blue) (Pasquina-Lemonche et al., 2020).

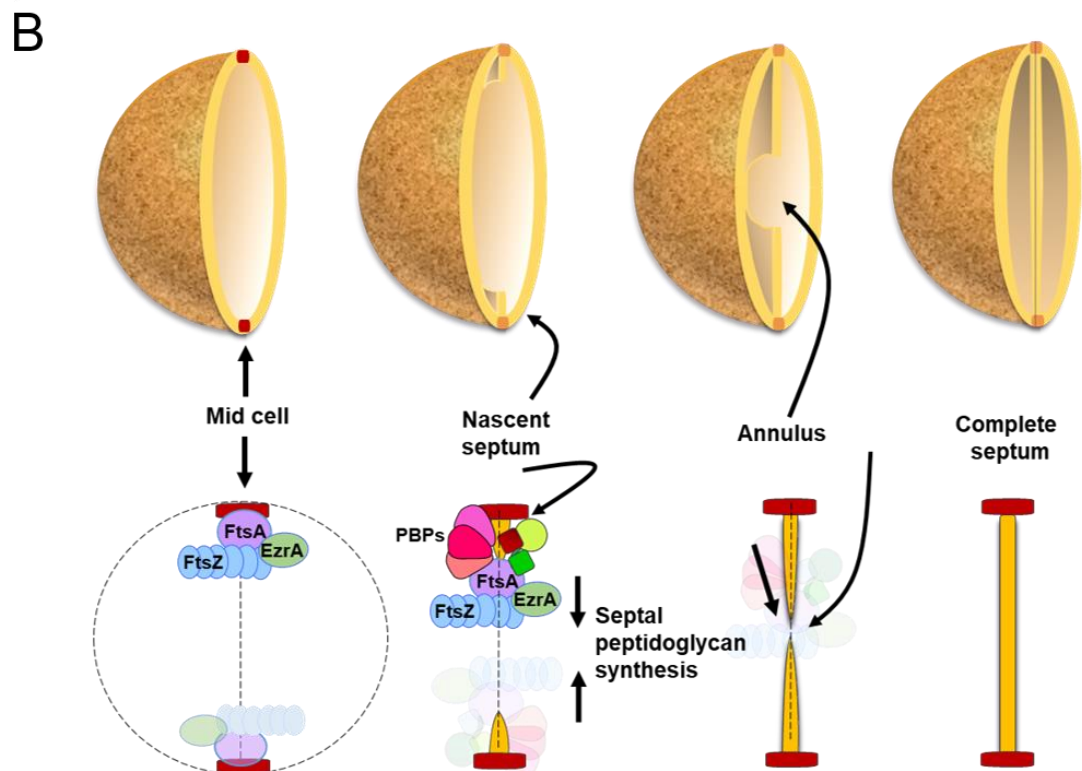
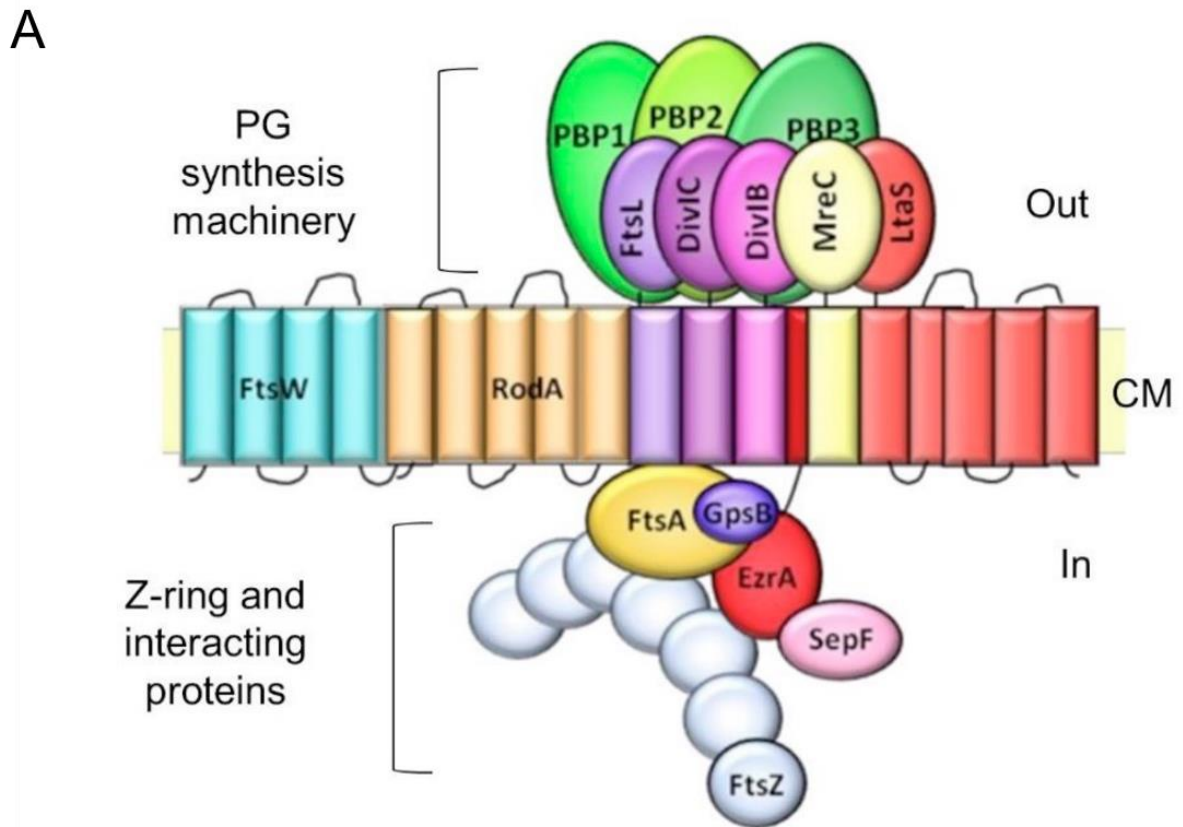


**Figure 1.5 Cell wall synthesis and architecture.**

Conceptual model of the *S. aureus* mode of PG synthesis during the cell cycle, demonstrating regions of synthesis and hydrolysis. The ultrastructure of PG demonstrated by atomic force microscopy is also shown. Adapted from (Lund et al., 2018; Pasquina-Lemonche et al., 2020; Wacnik et al., 2022).

### 1.2.7 The divisome and septal placement

Cell division allows *S. aureus* to proliferate and requires both spatial and temporal control of morphogenesis to result in two daughter cells. These processes utilize a protein complex called the divisome (Lund et al., 2018; Pereira, 2018). The divisome is a molecular machine allowing coordination of activities across the cell membrane, exoplasm and cell wall (Figure 1.6). One of the most important divisome components is the tubulin homologue FtsZ, which recruits other division proteins such as FtsA and GpsB to the division site (Bi and Lutkenhaus, 1991; Bisson-Filho et al., 2017; Eswara et al., 2018; McCausland et al., 2019; Sacco et al., 2022). EzrA, ZapA and SepF facilitate divisome assembly by acting as a scaffold between the cytoplasmic and exoplasmic regions, providing an interface between the cytoplasmic scaffold and PG synthesis machinery (Chaudhuri et al., 2009; Steele et al., 2011). Late-stage cell division proteins, such as the integral trimeric complex of DivIB, DivIC and FtsL interact with the cell wall regulating its synthesis facilitating the recruitment of PBPs (Bottomley et al., 2017; Tinajero-Trejo et al., 2022). DivIC is an essential regulator of the spatial and temporal synthesis of PG, by recruiting PBP2 (Tinajero-Trejo et al., 2022). The splitting of the cell into two hemispherical daughter cells (Above, Figure 1.5 H) is facilitated by the “nicking” action of cell wall hydrolases including autolysins in the cell wall along the plane of septation (Komatsuzawa et al., 1997; Turner et al., 2010) resulting in rapid separation of daughter cells (Zhou et al., 2015).



**Figure 1.6 The divisome and septum formation in *S. aureus*.**

Multiple proteins interact to form the z- ring and to act as PG synthesis machinery (A) PG formation requires a dynamic complex of division components (B) (Adapted from Bottomley, 2011; Bottomley et al., 2017; Steele et al., 2011; Sutton et al., 2023; Tinajero-Trejo et al., 2022).



## 1.3 Antibiotics

The discovery of penicillin's antibacterial potential in 1929 (Fleming, 1929) and its' clinical implementation heralded an age where infectious diseases could be combatted with relative ease (D'Costa et al., 2007). Since then, multiple antibiotics have been used in the clinic, targeting a range of essential biological functions (Figure 1.7).

### 1.3.1 Metabolism targeting

Metabolic pathways in *S. aureus* are prime targets for antibiotics as they allow chemicals of similar structures to be used to inhibit metabolic synthesis of essential compounds such as folic acid (Lade and Kim, 2021). Sulfonamides are competitive antagonists and analogues of *p*-aminobenzoic acid (PABA) (Ovung and Bhattacharyya, 2021) which is required for the subsequent DNA synthesis in bacteria (Zessel et al., 2014), Sulfonamides competitively inhibit the enzyme dihydropteroate synthetase inhibiting the production of dihydrofolate DHF (Pareek et al., 2013). Trimethoprim blocks the subsequent reduction of DHF to the active form of folic acid: tetrahydrofolate (THF) (Gleckman et al., 1981). The combination of these agents results in the inhibition of the essential metabolism of folic acid within the cell which results in their bactericidal activity due to inhibition of cell division (Nemeth et al., 2015; Wood and Austrian, 1942). They act effectively as combined agents to eradicate methicillin resistant *S. aureus* (MRSA) from patients (Frei et al., 2010; Harbarth et al., 2015).

### 1.3.2 DNA & Protein Synthesis targeting

Fluoroquinolones including ciprofloxacin, delafloxacin and ofloxacin have potent activity against staphylococcal infections. They primarily target topoisomerase IV (Hooper, 2000), and resistance has been documented as a consequence of antibiotic efflux (Acar and Goldstein, 1997; Hooper, 2000; Kaatz et al., 1993; Trucksis et al., 1991; Weber et al., 2003). In cases of fluoroquinolone resistance, ciprofloxacin has been used in tandem with the targeted RNA polymerase inhibitor, rifampicin. Rifampicin has potent action and a low minimum inhibitory concentration against *S. aureus* (Campbell et al., 2001). While *rpoB* mutations can confer resistance, rifampicin's effectiveness is often enhanced by synergistic combinations with other antibiotics (Chambers, 1997). Mupirocin, produced by *Pseudomonas fluorescens* was described in 1971 as pseudomonic acid A (Fuller et al., 1971). Reversibly inhibiting isoleucyl-transfer RNA, its restricted systemic use due to rapid breakdown necessitates localized application for treating superficial skin infections (Morton et al., 1995; Parenti et al., 1987).

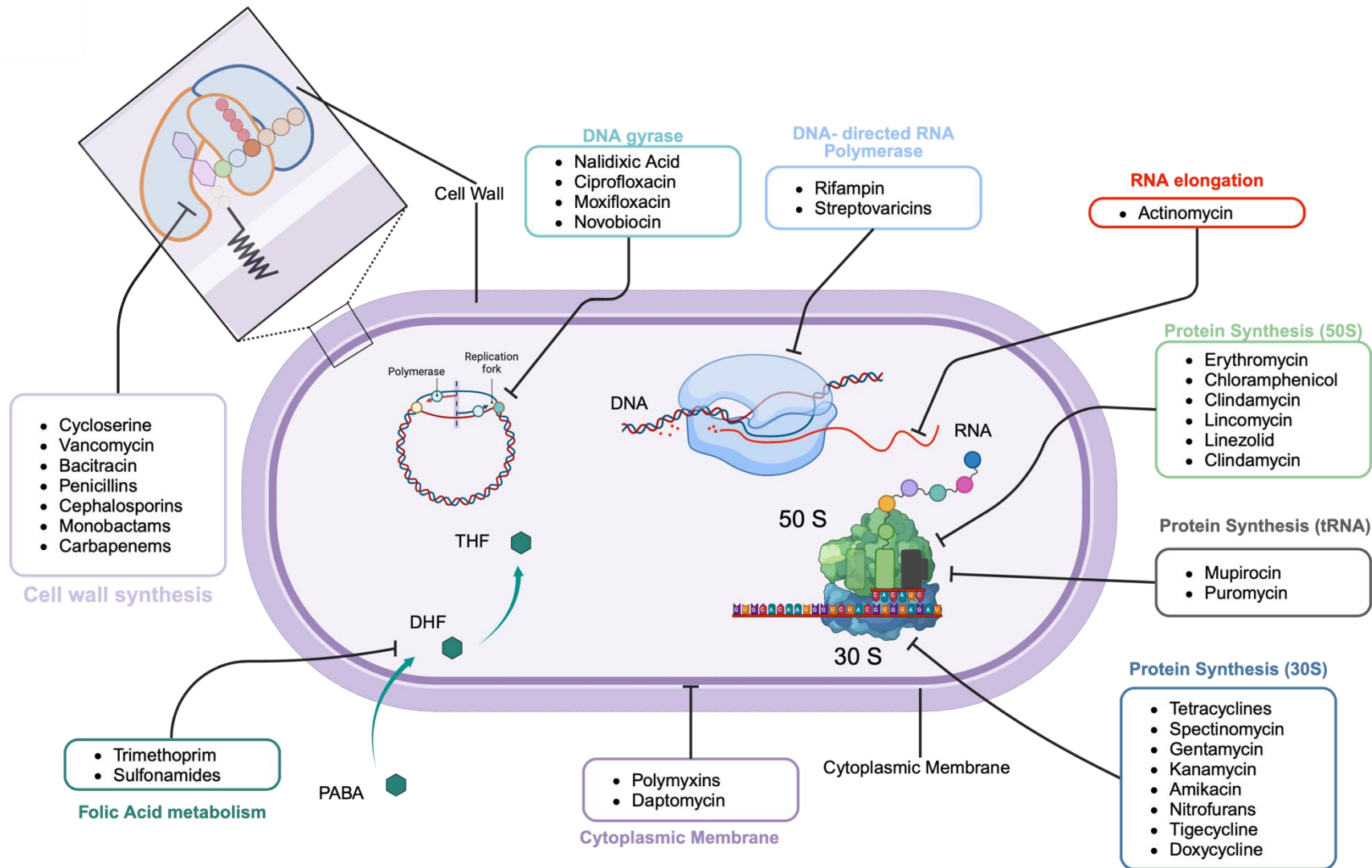
Protein synthesis inhibiting antibiotics including aminoglycosides, tetracyclines, oxazolidinones and macrolides, all inhibit protein synthesis by targeting different ribosomal subunits (Carter et al., 2000; Magnet and Blanchard, 2005). For instance, tetracyclines prevent binding of aminoacyl-RNA to the A site of the 30S ribosomal subunit (Geigenmuller et al., 1986; Ross et al., 1998), the aminoglycoside Arbekacin, a derivative of kanamycin, inhibits the action of the decoding centre of the 30S subunit. The 50S subunit is targeted by both macrolides like azithromycin and oxazolidinones including tedizolid interacting with 23s rRNA to block the peptide exit tunnel and preventing the formation of the 70s complex respectively (Champney and Burdine, 1995; Kisgen et al., 2014; Zhanel et al., 2015).

### **1.3.3 Membrane targeting**

The integrity of the cell membrane is essential for survival and antibiotics which target the lipid palisade show effective bactericidal effect against *S. aureus* (Huang, 2020). Polymyxin and lipopeptide antibiotics are often used as drugs of last resort for the treatment of bacterial infections (Ledger et al., 2022). Novel synthetic polymyxins and lipopeptides exhibit activity against Gram-positive bacteria including *S. aureus*, but only daptomycin is approved for clinical use (Eisenstein et al., 2010; Rudilla et al., 2018). Daptomycin, a cyclic anionic lipopeptide, results in membrane depolarisation (Alborn et al., 1991; Silverman et al., 2003) and inhibits cell envelope synthesis by interfering with membrane fluid microdynamics (Müller et al., 2016). This reorganisation of the architecture of the cell membrane also mislocates essential cell division proteins (Pogliano et al., 2012).

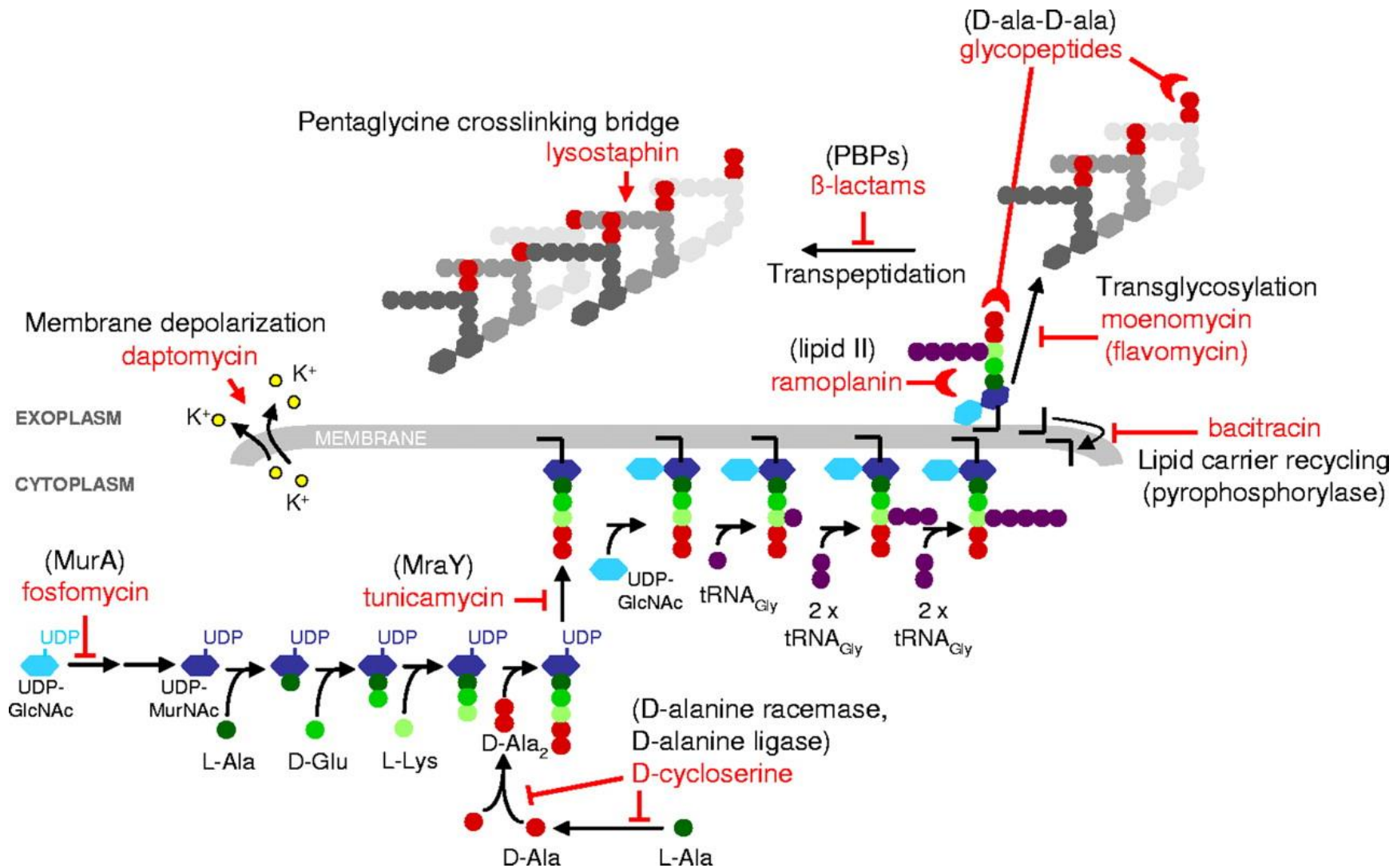
### **1.3.4 Cell Wall targeting**

The complex mesh of cross-linked PG protects the bacterial cell, as well as contributing to resistance and virulence, making the cell wall and its synthesis a target for antibiotics (McCallum et al., 2010). Cell wall targeting antibiotics mainly fall into two classes, glycopeptides and  $\beta$ -lactams. The glycopeptide vancomycin, isolated from soil bacteria, targets cell wall synthesis by competitively binding the peptidoglycan precursor *N*-acetylmuramylpentapeptide stopping the extension of side chains thus preventing the transpeptidase from completing the cross-linking reactions in PG (Barna and Williams, 1984). Teicoplanin is another glycopeptide antibiotic with anti-staphylococcal efficacy and can be administered intramuscularly due to its longer half-life (Chambers, 1997). Whereas  $\beta$ -lactams such as methicillin inhibit the transpeptidase activity of the native *S. aureus* PBPs required in late state extra cellular PG biosynthesis (Goffin and Ghuyssen, 1998b). Figure 1.8 details the cell wall active antibiotics in *S. aureus*.



**Figure 1.7 Antimicrobial modes of action within the cell.**

A diagram of a representative bacterial cell showing the targets of antibiotics within the cell including DNA transcription and translation. Created with BioRender.com Adapted from Lade and Kim (2021).



**Figure 1.8. *S. aureus* antibiotic targets in peptidoglycan and cell wall active antibiotics.**

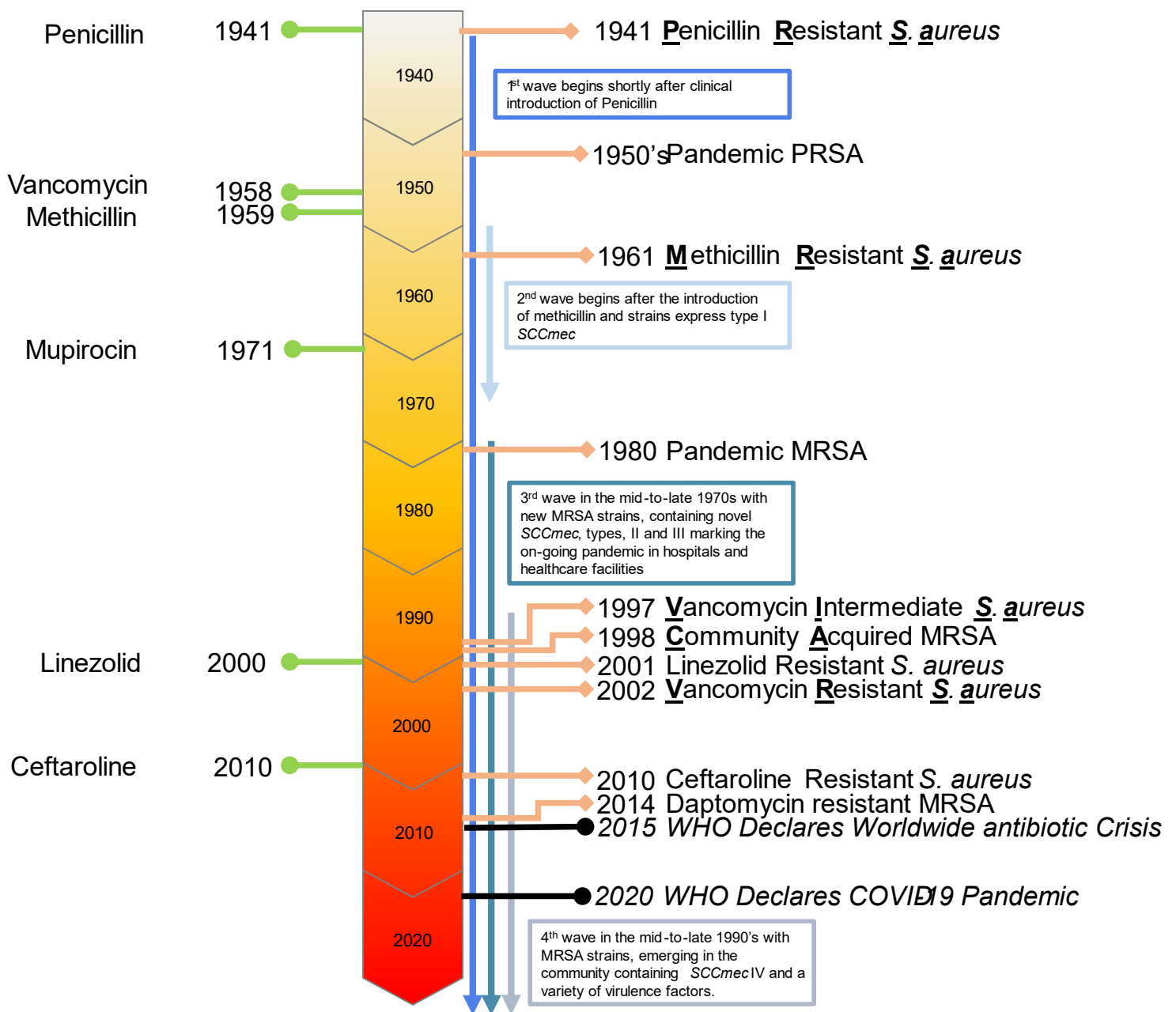
Red blocked arrows indicate inhibition of enzymatic reactions; red half-moon arrows indicate inhibition of cell wall synthesis; red arrows indicate pentaglycine bridge cleavage and membrane disruption. Taken from (McCallum et al., 2011, 2010).

## 1.4 Antibiotic resistance in *S. aureus*.

The unrestricted use of antimicrobial therapy in the last eight decades has resulted in antimicrobial resistance (AMR) being a definitive global crisis of the 21<sup>st</sup> century. Governments, clinicians, and researchers alike, recognise that the treatment of infectious diseases remains a significant challenge in clinical settings today. Exerting health and economic burdens on society the global annual cost of AMR could increase to 10 million deaths and US\$100 trillion by 2050 (O'Neill, 2018).

A few pathogens with significant clinical importance have escaped the action of antibiotics, dubbed the ESKAPE pathogens: *Enterococcus faecium*, *Staphylococcus aureus*, *Klebsiella pneumoniae*, *Acinetobacter baumannii*, *Pseudomonas aeruginosa*, and *Enterobacter spp.* (Rice, 2008). Together it has been highlighted how this group of pathogens poses a threat to healthcare worldwide. Understanding their potential danger will help determine how we manage the AMR crisis (Pendleton et al., 2013). These pathogens rapidly develop resistance to newly developed antibiotics and a representative timeline for *S. aureus* is shown in Figure 1.9. Methicillin resistant *Staphylococcus aureus* (MRSA) infections often occur in patients demonstrating multiple co-morbidities; highlighted in increasing numbers of clinical cases where infections arise in vulnerable patients with diabetes and small cell lung cancer (Horiuchi et al., 2019). Patients with cancer, diabetes and undergoing dialysis are all at risk of life-threatening MRSA infections. Perhaps this occurs as they are subjected to longer hospital stays, repeated hospitalisation, surgery, and intravenous catheters which are identified as co-morbidities (Graffunder, 2002).

Internationally there is a recognised need for research and development of antibiotics essential for the prevention, treatment, and clinical management of infectious diseases in modern healthcare (WHO, 2015).



**Figure 1.9 Timeline of introduction of antibiotics and the emergence of antibiotic resistance in *S. aureus*.**

Introduction of new antibiotics in green, 4 waves of resistant *Staphylococcus aureus* shown as vertical arrows.

Figure collated from: Anantabotla et al., 2014; Chambers and DeLeo, 2009; Fuller et al., 1971; Ghahremani et al., 2018; Herold et al., 1998; Hiramatsu et al., 1997; Rammelkamp and Maxon, 1942; Ventola, 2015; WHO, 2015.

## 1.5 Mechanisms of resistance

There are four major modes of antibiotic resistance: limiting uptake of a drug, modification of drug targets, inactivation of a drug, and active efflux (Reygaert, 2018; Sabath, 1982). These mechanisms are represented in the manner by which resistance is determined to antibiotics used to combat staphylococcal infections.

### 1.5.1 Vancomycin and glycopeptides

Isolates of vancomycin intermediate-resistant *S. aureus* (VISA) with MIC= 4.8 µg/mL have a polygenic basis due to mutations in genes including *clpP* (resulting in cell wall thickening, slow growth and reduced autolysis), *agr* and *rpoB* which also attenuates virulence and reduces susceptibility (McGuinness et al., 2017). Vancomycin resistance, with a MIC of  $\geq 16$  µg/mL, in *S. aureus* is plasmid mediated and conferred by the *vanA* gene (Levine, 2006; Shajari et al., 2017). Resistance is maintained by retention of the enterococcal plasmid pAM830 or transposition of the *van* operon into a staphylococcal plasmid (Łęski and Tomasz, 2005). The newly identified glycopeptide antibiotic corbomycin have been shown to reduce the bacterial burden in *in vivo* models of skin infections (Culp et al., 2020).

Teicoplanin resistance has arisen during therapy for endocarditis and can be generated *in vitro* (Kaatz et al., 1990). Mutations in the *tcaRAB* operon have been shown to be the main driver that gives rise to teicoplanin resistance (Bischoff and Berger-BÄCHI, 2001).

### 1.5.2 Fluroquinolones

Clinically significant mutations have been documented in the *grlA* gene which encodes the A subunit of topoisomerase IV (Ferrero et al., 1995) Therapeutic failures associated with isolation of fluoroquinolone-resistant strains of staphylococci have been increasingly described since 1991 (Trucksis et al., 1991). As a broad-spectrum group of antibiotics, they leave an open niche after treatment making patients vulnerable to clinically acquired infections such as MRSA which exhibit higher levels of resistance (Acar and Goldstein, 1997; Weber et al., 2003)

### 1.5.3 Mupirocin

Two levels of resistance to mupirocin exist, in one study of clinical *S. aureus* and coagulase-negative staphylococci isolates from skin and soft-tissue infections, high-level mupirocin resistance was found in 8.2% and 15.6% of coagulase negative staphylococci, while low-level mupirocin resistance was found in 17% *S. aureus* and 8.9% coagulase negative staphylococci (Rudresh et al., 2015). Low to intermediate level resistance is caused by mutations in the target isoleucyl-tRNA synthetase enzyme (Morton et al., 1995b).

## 1.6 Staphylococcal $\beta$ -lactam resistance

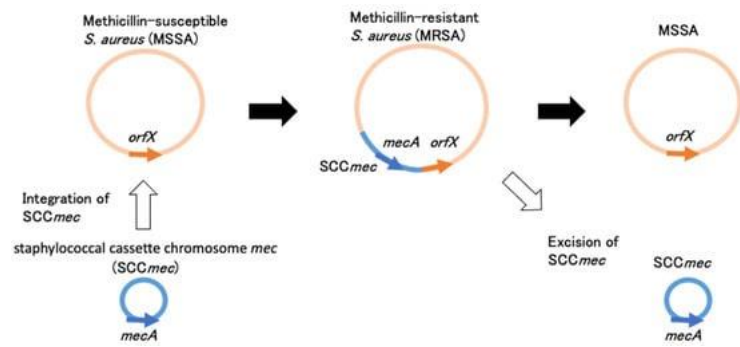
Staphylococci have two primary mechanisms for resistance to  $\beta$ -lactam antibiotics: the expression of an enzyme capable of hydrolysing the  $\beta$ -lactam ring, thus rendering the antibiotic inactive, and the acquisition of a gene encoding a modified penicillin-binding protein (PBP), known as PBP2A, found in MRSA and coagulase-negative staphylococci (Llarrull et al., 2009).

Shortly after the introduction of penicillin as a frontline treatment for *S. aureus* infections, penicillin resistant *S. aureus* were isolated (Figure 1.9). An enzyme later identified as a  $\beta$ -lactamase which, on incubation with penicillin rendered it unable to inhibit growth of *S. aureus* was identified in the 1940's by Abraham and Chain (Abraham and Chain, 1940). *S. aureus* can produce four types of  $\beta$ -lactamases A, B, C, and D (Neu, 1985a; Sabath, 1982; Zygmunt et al., 1992).  $\beta$ -lactamases are plasmid encoded which allow rapid spread and results in extremely high MICs (Livermore, 1995; Neu, 1985b)).  $\beta$ -lactamases are regulated in response to the presence of antibiotic, mediated by the *BlaR1* system (Wang et al., 1991).

### 1.6.1 The *SCCmec* complex

MRSA developed from methicillin susceptible strains of *S. aureus* due to the acquisition of the staphylococcal cassette chromosome (*SCCmec*). The 52 kb DNA cassette results in the expression of methicillin resistance via PBP2A (*mecA*) and the regulatory network responsible for its control (Ito et al., 2001, 1999; Katayama et al., 2000). The *SCCmec* inserts into a specific locus in the *S. aureus* chromosome (Figure 1.10) (Chambers and DeLeo, 2009) and is present as a number of different types. The emergence of these is shown in Figure 1.9. It has been hypothesised that *mecA* originated initially from *Staphylococcus sciuri* which provided the mobile element into which the *SCCmec* was incorporated with *S. vitulinus* and *S. fleurettii* contributing to the assembly of the complex (Rolo et al., 2017; Tsubakishita et al., 2010). However, the independent emergence of *mec* has been identified during the pre-antibiotic era in hedgehogs harbouring MRSA with *mecC*, due to a commensal fungus which produces  $\beta$ -lactams resulting in a selective advantage of strains containing the *mec* cassette (Larsen et al., 2022).





**Figure 1.10 SCC*mec* integration and excision in *S. aureus*.**

SCC*mec* of extra cellular origin is incorporated into the staphylococcal genome, at *orfX* resulting in Methicillin resistance, its excision reverts strains to being methicillin susceptible. (Katayama et al., 2000)

### 1.6.1.1 Genetic organisation of *SCCmec*

*SCCmec* contain distinct genetic elements required for resistance which share similar structural backbones (Lakhundi and Zhang, 2018). Each type contains *mec*, the region containing the *mecA* gene, its regulators, surrounded by open reading frames (ORFs) and insertion sequences, the cassette chromosomal recombinase (*ccr*) gene complex, ensuring *SCCmec* mobility and the joining regions J1-3 (Ito et al., 2009). The *ccr* gene complex encodes DNA recombinases which ensure precise site and orientation specific integration into the staphylococcal chromosome (Katayama et al., 2000). The *mec* gene complex contains not only the *mecA* gene but also insertion sequences and a hyper variable region (HVR), these regions allow its classification into five main groups (Ito et al., 2009). Figure 1.11 shows the different *SCCmec* types.

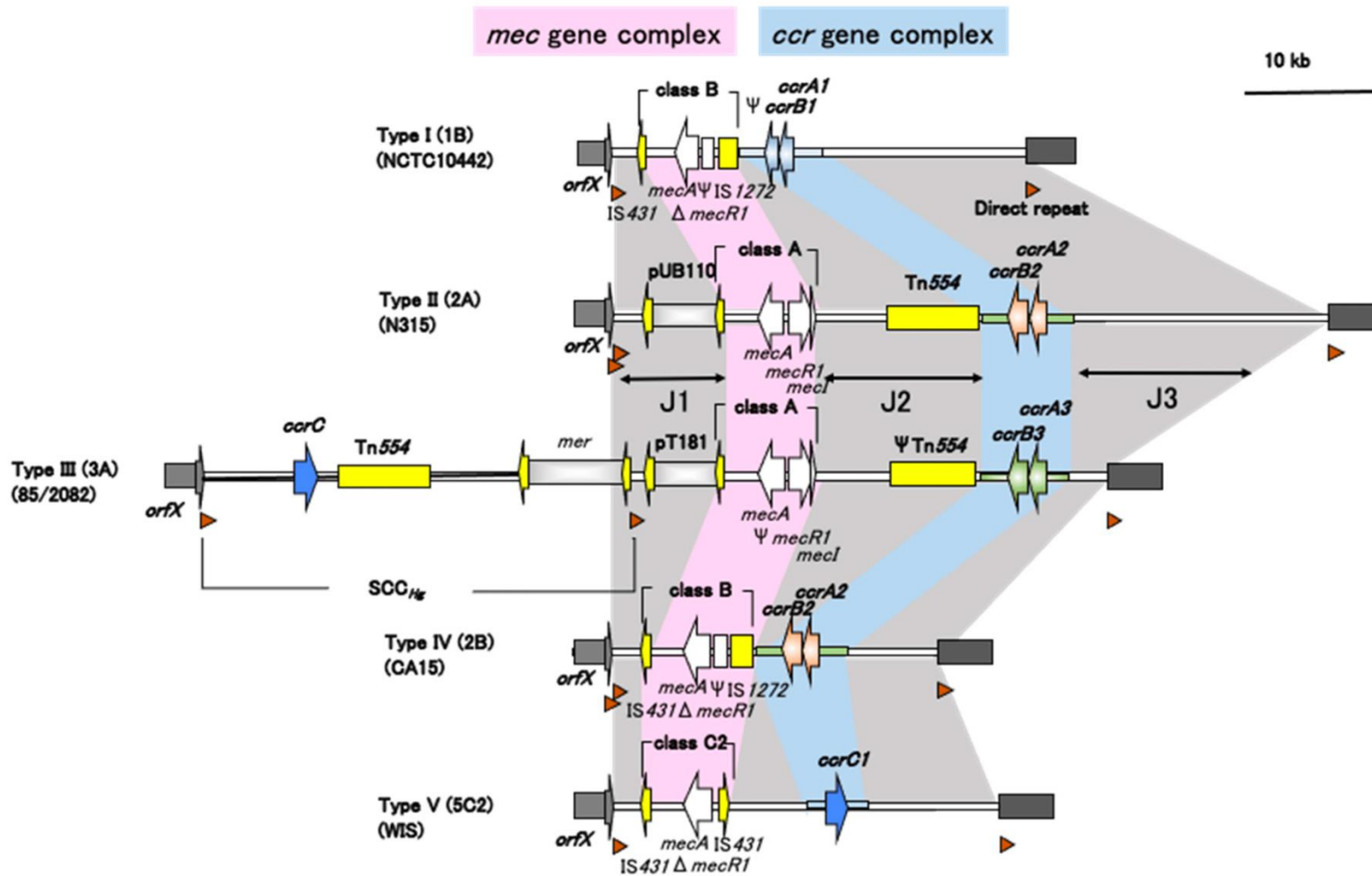
As part of *SCCmec* the *mecA* gene is carried in the *mec* gene complex of four main classes. The class A (Type II) *mec* gene complex contains intact *mecR1* and *mecl* regulatory genes upstream of *mecA*, insertion sequence IS431 downstream of *mecA* and hyper variable region (HVR) (Ito et al., 2009). In class B (Type I) *SCCmec* IS1272 is inserted upstream of *mecA* resulting in truncated *mecR1* and IS431 downstream of the *mecA* and HVR (Ito et al., 2009) The class C *mec* gene complex is divided into two classes based on the orientation of IS431: class C1 and C2. Each class contains truncated *mecR1* due to IS431 being both up and down stream of *mecA*. IS431 of class C1 has the same orientation upstream and downstream of *mecA* while class C2 carries IS431 flanking *mecA* and regulatory components is in the opposite orientation to class C1 (Ito et al., 2009). Class D *mec* gene complex comprises of a partly deleted *mecR1* with no IS431 downstream of *mec* complex (Ito et al., 2009, 2001; Katayama et al., 2000). Recently the class E *mec* gene complex was identified from a livestock MRSA isolate which contains *blaz*, *mecA*, *mecR1* and *mecl* (J. Liu et al., 2016; Turlej et al., 2011). The joining regions J1, J2 and J3 are classified by location; J1 is located at the right side of the cassette; J2 is between the *mec* and *ccr* gene complexes; and J3 is between the chromosomal junction between *orfX* and the *SCCmec* complex (Ito et al., 2009; J. Liu et al., 2016; Turlej et al., 2011).

### 1.6.2 PBP2A and associated $\beta$ -lactam resistance.

*S. aureus* demonstrates decreased sensitivity to  $\beta$ -lactam antibiotics through the expression of a non-native PBP (Sabath, 1982). Found in MRSA and coagulase-negative staphylococci, the *mecA* gene encodes a modified penicillin-binding protein, known as PBP2A, which is intrinsically resistant to inhibition by  $\beta$ -lactams (Llarrull et al., 2009).

PBP2A was first identified in about 80% of methicillin- and cefazolin-resistant strains of *S. aureus* isolated clinically in Japan in 1982 (Utsui and Yokota, 1985). The strains retained their resistance even after elimination of penicillinase-encoding plasmids. A new PBP fraction (PBP2') having a molecular weight of 78 kDa and low binding affinities for various  $\beta$ -lactam antibiotics was found in MRSA exclusively (Utsui and Yokota, 1985). The sequence of the *mecA* gene contains structural motifs characteristic of cell wall synthetic transpeptidases (De Lencastre et al., 1994a).

It is generally assumed that the *mecA* gene product (PBP2A) acts as a surrogate enzyme which takes over the task of cell wall synthesis from the normal complement of staphylococcal PBPs, since the latter are inhibited by relatively low (e.g. methicillin) concentrations of  $\beta$ -lactam antibiotics. While direct biochemical evidence for a transpeptidase activity in PBP2A is still missing, the essentiality of an intact *mecA* gene for the expression of high-level methicillin resistance has been clearly established by transposon inactivation experiments (Katayama et al., 2001; Kuwahara-Arai et al., 1996; Miragaia, 2018). On the other hand, PBP2A alone cannot be fully in control of the resistant phenotype, since all MRSA isolates, irrespective of their MIC values (from as low as 3 mg/L or as high as 1600 mg/L), were found to contain comparable amounts of PBP2A (Bæk et al., 2014; Parvez et al., 2008).

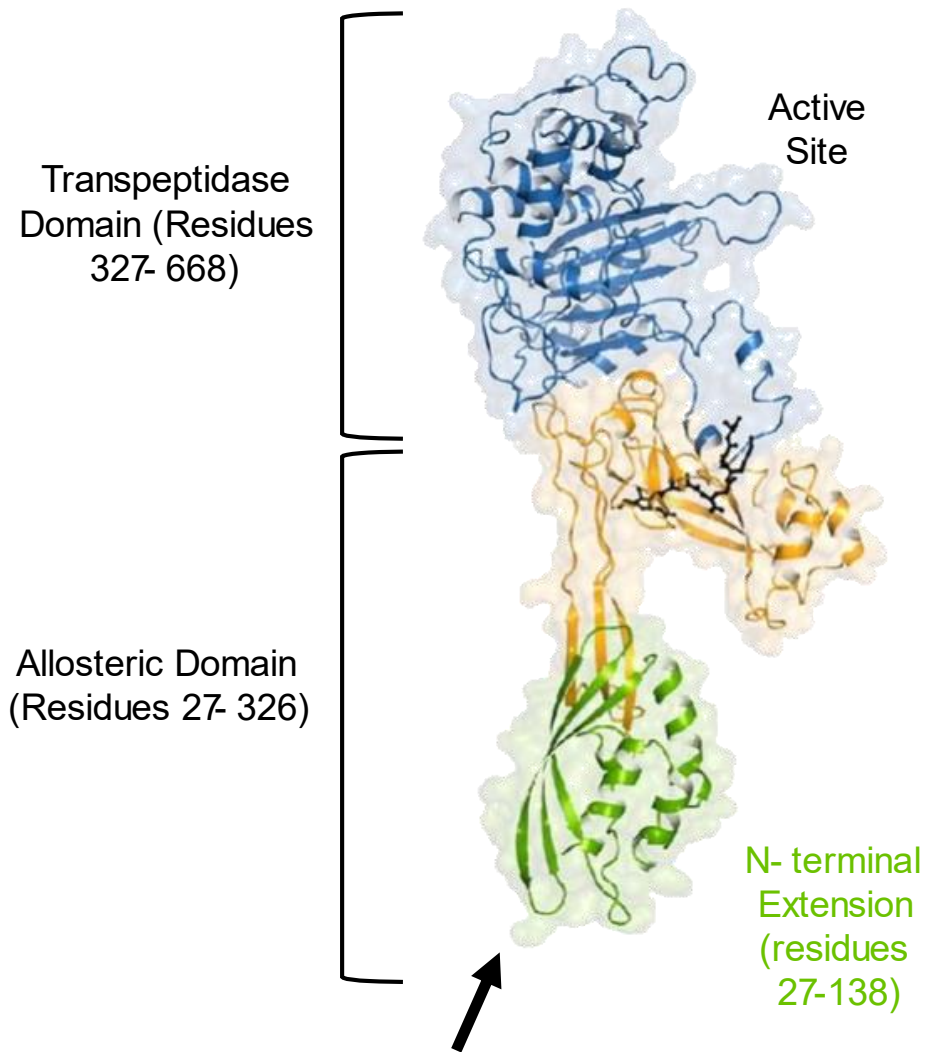


**Figure 1.11 Comparison of the staphylococcal chromosomal cassette types *SCCmecI-V***  
 Integration site sequences and direct repeats are at each end. *mec* gene complex (pink) contextualised by the cassette chromosomal recombinase (*ccr*) gene complex (blue) and the joining regions (J1-3) with joining regions shown in grey. From Uehara (2022).

In newer classes of bactericidal  $\beta$ -lactam antibiotics like cephalosporins, including ceftaroline and ceftobiprole, resistance in MRSA has already been demonstrated (Otero et al., 2013). Recently, novel synergistic combinations of  $\beta$ -lactams have been shown to have bactericidal effects on MRSA both *in vitro* and *vivo* (Bush, 2015). A combination of meropenem, piperacillin and tazobactam stopped cell wall synthesis through combined inhibition of resistance mechanism and allosteric binding allowing  $\beta$ -lactams to once again access the active site of their target enzymes (Bush, 2015).

PBP2A contains an extended N-terminal and a transmembrane anchor and a C-terminal transpeptidase domain which crosslinks neighbouring glycans in the extracellular stage of PG synthesis (Lim and Strynadka, 2002). The activity of PBP2A is localised within functional membrane microdomains which resemble lipid rafts in eukaryotic cells and disruption has been shown to disable PBP2A oligomerization and antibiotic resistance (García-Fernández et al., 2017). PBP2A function is regulated 60Å from the active site, Figure 1.12, (Lim and Strynadka, 2002), whereby the allosteric modulation at the non-penicillin binding domain enables the active site to open to accommodate two adjacent peptide stems for transpeptidation in the presence of  $\beta$ -lactams (Fishovitz et al., 2014). The distant catalytic domain of PBP2A has been shown to be reliant on allosteric activation of the catalytic loop (Mahasenan et al., 2017).

Continual cell wall synthesis in the presence of antibiotics requires cooperative function of the copper dependent transglycosylase domain in PBP2 and the transpeptidase domain of PBP2A alongside a large membrane complex of proteins and perhaps a membrane microdomain involving other, non PBP factors in order to express high-level resistance (Chambers, 2001; García-Fernández et al., 2017; Pinho et al., 2001).



**Figure 1.12 Molecular Structure of *S. aureus* PBP2A.**

Structure and domains of PBP2A. N-terminal coloured in green, the remaining allosteric domain in orange, and the transpeptidase (TP) domain is coloured in blue. Black sticks represent a NAG-NAM pentapeptide. The arrow indicates the point of attachment of the membrane anchor. Taken from Otero et al. (2013)

Previously in a study aiming to separate the divisome from the cell wall of clinical isolates, PBP2A was found to be a constituent of a complex of PBP2 and FtsZ (Paulin *et al.*, 2014) which is indicative of PBP2A having interactions with or proximity to the cell division machinery. PBP2A activity also requires correct folding using chaperones such as PrsA and HtrA which represent an attractive strategy to combat antibiotic resistance (Roch *et al.*, 2019).

## **1.7 The mechanism of high-level resistance to $\beta$ -lactams**

The molecular mechanisms which allow variable levels of strain dependent antimicrobial resistance are not fully understood (Thalsø-Madsen *et al.*, 2019). This is further supported by major disparities between cellular amounts of PBP2A and the antibiotic MIC values. Hence a factor or factors of unknown nature other than the *mecA* gene product must also play an essential role in the phenotypic expression of resistance (De Lencastre *et al.*, 1994).

### **1.7.1 Auxiliary Factors**

The action of PBP2A taking over the transpeptidation of PG from the native PBPs inhibited by  $\beta$ -lactams has a significant impact on cellular physiology and cell wall homeostasis (Panchal *et al.*, 2020; Salamaga *et al.*, 2021). This complexity of compensatory adaptations results in the essentiality of auxiliary factors to maintain high-levels of  $\beta$ -lactam resistance (Roemer *et al.*, 2013). PBP2A is therefore not the only factor associated with  $\beta$ -lactam resistance. As such combination agents can be used to exploit the weakness of the high-level resistant organism (Brown *et al.*, 2012; Wang *et al.*, 2013). Auxiliary factors have previously been identified by transposon mutagenesis screening of chromosomal genes essential to the maintenance of methicillin resistance. Figure 1.13 shows auxiliary factors required for the expression of high-level  $\beta$ -lactam resistance.

#### **1.7.1.1 Cell wall homeostasis**

The PG ultrastructure (See 1.2.6) of the cell wall is essential for the integrity of the cell wall. It's synthesis (See 1.2.4) is the target for  $\beta$ -lactam antibiotics (as shown in Figure 1.8). Many auxiliary factors provide precursors of PG constituents (Maki *et al.*, 1994). During PG biosynthesis proteins GlmU, GlmS, and GlmM are involved in the cytoplasmic synthesis of the UDP-*N*-acetylglucosamine from the PG precursor fructose-6-phosphate, which is then in turn converted into UDP-*N*-acetylmuramate through the activity of auxiliary factors MurA and MurB (Heijenoort, 2001; van Heijenoort, 2007). PG ligases and MurCDEF add a pentapeptide side chain (Heijenoort, 2001). Impairing amino acid transport or D-cycloserine exposure at this

stage leads to  $\beta$ -lactam sensitivity (Gallagher et al., 2020). Genes crucial for divisome formation such as *ftsZ* and *ftsA* have also been described as *aux* factors (Tan et al., 2012).

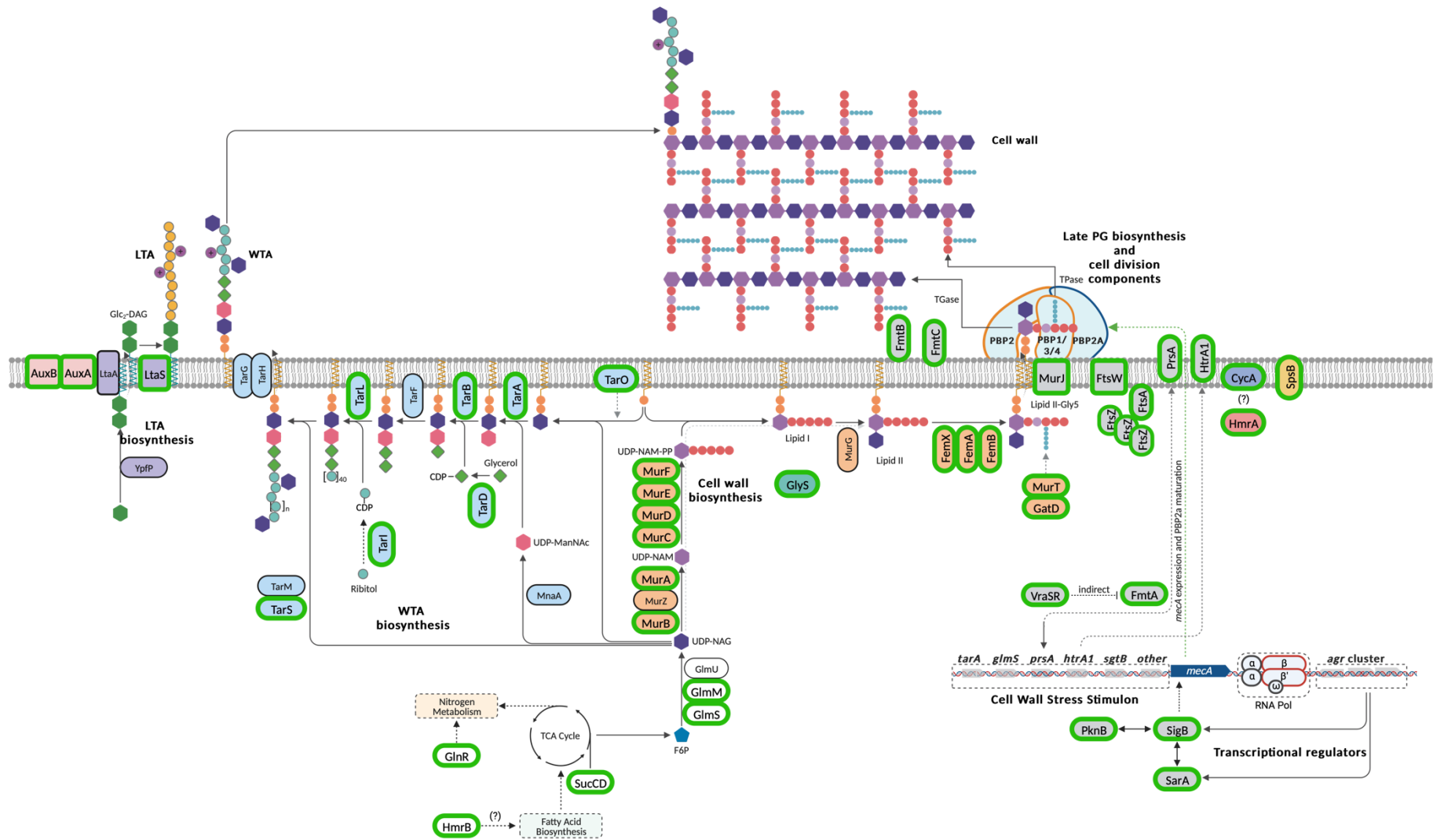
Translocation of lipid II-Gly<sub>5</sub> across the membrane recruits PBP2 and PBP2A in MRSA and the extracellular step of PG biosynthesis then begins, PBP1 catalyses transpeptidation and PBP2 has both transpeptidase and transglycosylase activity. PBP4 provides additional polymerisation of the PG layer, all important processes so it is perhaps unsurprising they are auxiliary factors (Pereira et al., 2009; Reed et al., 2015). In fact, PBP2 remains essential during antibiotic resistance despite its catalytic activity having been inhibited by  $\beta$ -lactams, as PBP2A can only perform transpeptidase cross linking (Pinho et al., 2001; Pinho et al., 2009). This inhibition of normal function also means the activity of PBP4 is important in MRSA to compensate for the unsatisfactory crosslinking in PG synthesised in the presence of antibiotics (Łęski and Tomasz, 2005; Memmi et al., 2008).

PG is not the only polymer in the cell wall. Both WTA and LTA play important roles in the growth, morphology, biofilm formation and virulence of *S. aureus* (Jensen et al., 2019; Jenul and Horswill, 2018; Wanner et al., 2017). Transposon mutagenesis has shown *auxA* and *auxB* are auxiliary genes due to their role in LTA stability (Mikkelsen et al., 2021), TarO is required for WTA synthesis and loss of function either genetically or due to inhibition by tarocin result in reduced resistance to  $\beta$ -lactams (Farha et al., 2013; Jensen et al., 2019).

### 1.7.1.2 Cell wall Stress stimulon

Auxiliary factors include genes involved in physiological processes spanning regulation and cell signalling, including the transcription factor SigB (Wu et al., 1996) and the two-component sensor of cell wall stress VraSR (Kuroda et al., 2003). Regulating and responding to breaches of the integrity of the cell wall activates genes required for cell wall repair when damaged by cell wall targeting antibiotics. The VraSR system consists of histidine kinase VraS, which auto-phosphorylates, which then activates its cognate response regulator VraR. VraR is a regulator of transcription, modulating expression of more than 40 individual genes (Kuroda et al., 2003). Of these 40 genes, termed the cell wall stress stimulon, some are auxiliary factors: *tarA*, *glmS*, *pbp2*, *sgtB* and the *vraSR* operon itself (Boyle-Vavra et al., 2013; Kuroda et al., 2003). The *vraSR* regulon also includes the chaperone *prsA* which ensures correct protein folding and maturation of PBP2A (Jousselin et al., 2016), and metabolic components such as glutamine amidotransferase, GatD (Figueiredo et al., 2012).





**Figure 1.13 Schematic of auxiliary factors involved in  $\beta$ -lactam resistance in MRSA.**

Auxiliary factors (green outline) involved in  $\beta$ -lactam resistance in MRSA, common colours indicated shared biological pathways, factors with no demonstrable impact have a black outline. (Adapted from Bilyk et al., 2022) Created with BioRender.com.

## 1.7.2 Heterogenous and Homogenous Resistance

The levels of methicillin resistance exhibited by strains of *S. aureus* can vary depending on the  $\beta$ -lactam, culture conditions used and are split into heterogenous and homogenous resistance whereby a population consists of a mixed population with sensitivities of  $\geq 5 \mu\text{g/mL}$  or  $\geq 50 \mu\text{g/mL}$  methicillin (De Lencastre et al., 1994b; Hartman and Tomasz, 1986). The mechanism of conversion from a heterogenous population to homogenous high-level resistance is intriguing as it arises from heterogenous populations upon exposure to  $\beta$ -lactam antibiotics (Hartman and Tomasz, 1986). Interestingly the majority of clinically acquired MRSA exhibit heterogenous resistance whereas healthcare acquired MRSA strains like COL have a homogenous high-level resistance phenotype (CA- and HA-MRSA respectively). This conversion is promoted by mutations in the *rpoB* gene encoding the RNA polymerase  $\beta$ -subunit (Aiba et al., 2013) and is associated with an increase in cellular levels of PBP2A (Finan et al., 2002). The conversion from heterogeneous low-level resistance to homogenous high-level resistance is potentiated by mutations in so called *Pot* genes (Bilyk et al., 2022).

## 1.7.3 Potentiators of methicillin resistance

Mutations present in *Pot* genes result in a multi-fold change to levels of resistance, higher than are supported by PBP2A alone. They allow effective accommodation of PBP2A within the cell (Bilyk et al., 2022). They span a significant range of pathways and are a more diverse group than those acting as auxiliary factors. Figure 1.14 shows potentiators of methicillin resistance in MRSA.

### 1.7.3.1 Protein turnover

While it is itself non-essential, (Stahlhut et al., 2017) the complex modulation of  $\beta$ -lactam resistance in MRSA requires ClpXP activity (Bæk et al., 2014; Gardete et al., 2006). The ClpXP system is responsible for targeted protein degradation during the cell cycle (Baker and Sauer, 2012), consisting of two distinct subunits, the ATPase ClpX (recognition, unfolding and translocation of proteins for degradation) and the peptidase ClpP (degrading tagged proteins in its proteolytic chamber) (Baker and Sauer, 2012). Both proteins also have separate independent functionality, ClpX as a molecular chaperone of protein folding and ClpP which can degrade small peptides (Bæk et al., 2014; Feng et al., 2013). The loss of ClpP functionality has a more profound impact on levels of  $\beta$  lactam resistance than ClpX (Feng et al., 2013). The loss of ATPase subunits with different recognition specificities such as ClpC have no effect suggesting that  $\beta$ -lactam resistance associated with the ClpXP system is entirely mediated by ClpP (Bæk et al., 2014). Studies using inactive ClpXP have shown that some Aux factors are

direct targets of ClpXP and therefore their stabilisation may facilitate the observed rise in resistance (Feng et al., 2013).

### 1.7.3.2 Nucleotide signalling

Nucleotide signalling has been identified as having a significant role in methicillin resistance in numerous studies (Dengler et al., 2013; Mwangi et al., 2013; Panchal et al., 2020). The discovery of *S. aureus* cyclic-di-adenosine monophosphate (c-di-AMP) has highlighted its role as a regulatory factor of cellular nucleotide signalling during environmental changes (Corrigan and Gründling, 2013). The enzyme c-di-AMP phosphodiesterase (GdpP) hydrolyses c-di-AMP (Corrigan et al., 2011; Corrigan and Gründling, 2013). GdpP contains two N-terminal transmembrane domains, a sensory domain, a C terminal DHH family motif, named after the conserved Asp-His-His motif in the active site, characteristic of phosphodiesterase's (Corrigan et al., 2011; Griffiths and O'Neill, 2012). Studies have demonstrated that elevated levels of cellular c-di-AMP due to the disruption of *gdpP* lead to increased resistance to  $\beta$ -lactam antibiotics (Banerjee et al., 2010; Corrigan et al., 2016; Griffiths and O'Neill, 2012; Panchal et al., 2020). GdpP is a membrane bound phosphodiesterase (PDE) its cytoplasmic equivalent encoded by *pde2*, which hydrolyses pApA into AMP was recently characterised and leads to decreased susceptibility to  $\beta$ -lactams as an effect of the reduced hydrolysis (Bowman et al., 2016; Panchal et al., 2020). The essential gene *relA*, encoding a (p)ppGpp synthetase which triggers the stringent response was shown to, when point mutations are present, be a potentiator of methicillin resistance (Kim et al., 2013). RelA tightly controls (p)pppGpp turnover as high-levels in the cell, slow translation of gene products for biosynthesis of macromolecules (Corrigan et al., 2016; Gentry et al., 2000; Traxler et al., 2008). The stringent response is usually a response to nutrient starvation, but it plays a vital role in the heterogeneity of resistance in *S. aureus* (Kim et al., 2013). Cross talk between the different nucleotide signalling pathways may demonstrate how these pathways might overlap to prepare the cell to withstand the effects of antibiotics. High-levels of intracellular c-di-AMP are associated with increased levels of PG crosslinking and upregulation of *pbp4* in a *gdpP* mutant (Corrigan et al., 2015).

### 1.7.3.3 RNA polymerase

The *rpoB* and *rpoC* genes encode the two largest RNA polymerase subunits ( $\beta$  and  $\beta'$ ) and are well documented factors that regulate antibiotic resistance in *Bacillus* (Lee et al., 2013). In *S. aureus*, *rpo* mutants have been characterised as a significant factor in the conversion from heterogeneous to homogeneous  $\beta$ -lactam resistance (Panchal, 2018).

RNA polymerase interacts with the essential regulatory protein Spx in *S. aureus* (Zuber, 2004). Spx responds to oxidative stress as it has a CxxC motif (Reyes and Zuber, 2008; Zuber, 2004). Panchal (2018) proposed a model where Spx redox dependent transcriptional regulation is integral to maintenance of the high-level MRSA phenotype. The model demonstrates how mutations in *rpoB* and *rpoC* stabilise transcription and increase PBP2A expression. Strains of *S. aureus* with *rpoB* or *rpoC* mutations highlight the need for finely regulated adaptation to allow high-level methicillin resistance and demonstrate the possible interaction with respiratory components which acts to reduce the stress induced by expression of PBP2A and high-level antimicrobial resistance (Panchal et al., 2020).

RNA polymerase and the ClpXP complex have a feedback loop with the stress regulator Spx, whereby the expression of the Spx regulon is self-regulated through its interactions with the  $\alpha$  subunit of RNA polymerase (Villanueva et al., 2016). ClpXP proteolysis in the cell itself regulates Spx concentration (Stahlhut et al., 2017).

#### **1.7.3.4 Quorum Sensing**

The accessory gene regulator (*agr*) governs quorum sensing and virulence in *S. aureus*. Its inactivation leads to an increase to homogenous high-level resistance in MRSA (Cuirolo et al., 2009; Plata et al., 2011). Expression of the *agr* gene cluster results in the proteins AgrA-D which produce and respond to the build-up of autoinducing peptide, in the environment as a quorum sensing mechanism (Paulander et al., 2018; Riedel et al., 2009). As a global gene regulator, Agr modulates a range of other regulators within the cell including: SarA, SrrAB, SarX, CodY and SigB directly or indirectly (Vuong et al., 2000). A repressed *agr* cluster is associated with high-levels of *mecA* expression, reduced toxin production and generally correlates with HA-MRSA strains, whereas CA-MRSA strains have lower PBP2A levels but increased *agr* expression perhaps related to the structural changes in PG caused by PBP2A (Pozzi et al., 2012; Rudkin et al., 2012). Mutation of *agr* results in a higher proportion of long chain fatty acids being present in the cytoplasmic membrane, contributing to membrane stability and affecting resistance to  $\beta$ -lactams (Rosado et al., 2015; Song et al., 2020).

#### **1.7.3.5 Cell wall homeostasis**

In contrast to the role of many proteins involved cell wall homeostasis and PG homeostasis acting to reduce  $\beta$ -lactam tolerance as auxiliary factors, *lyt* and *dlt* mutations have roles as potentiators of also antimicrobial resistance (Fujimura and Murakami, 2008; Nakao et al., 2000). *lyth* mutations have been shown in both clinical isolates and laboratory strain to result in an increase in methicillin resistance (Fujimura and Murakami, 2008, 1997a). Mutations in

genes in the *dltABCDX* operon are potentiators of  $\beta$ -lactam resistance (Neuhaus and Baddiley, 2003), as the gene products catalyse LTA and WTA decoration with D-alanine residues resulting in changes to the ultrastructure of the cell wall, reducing susceptibility to  $\beta$ -lactam antibiotics (Nakao et al., 2000).

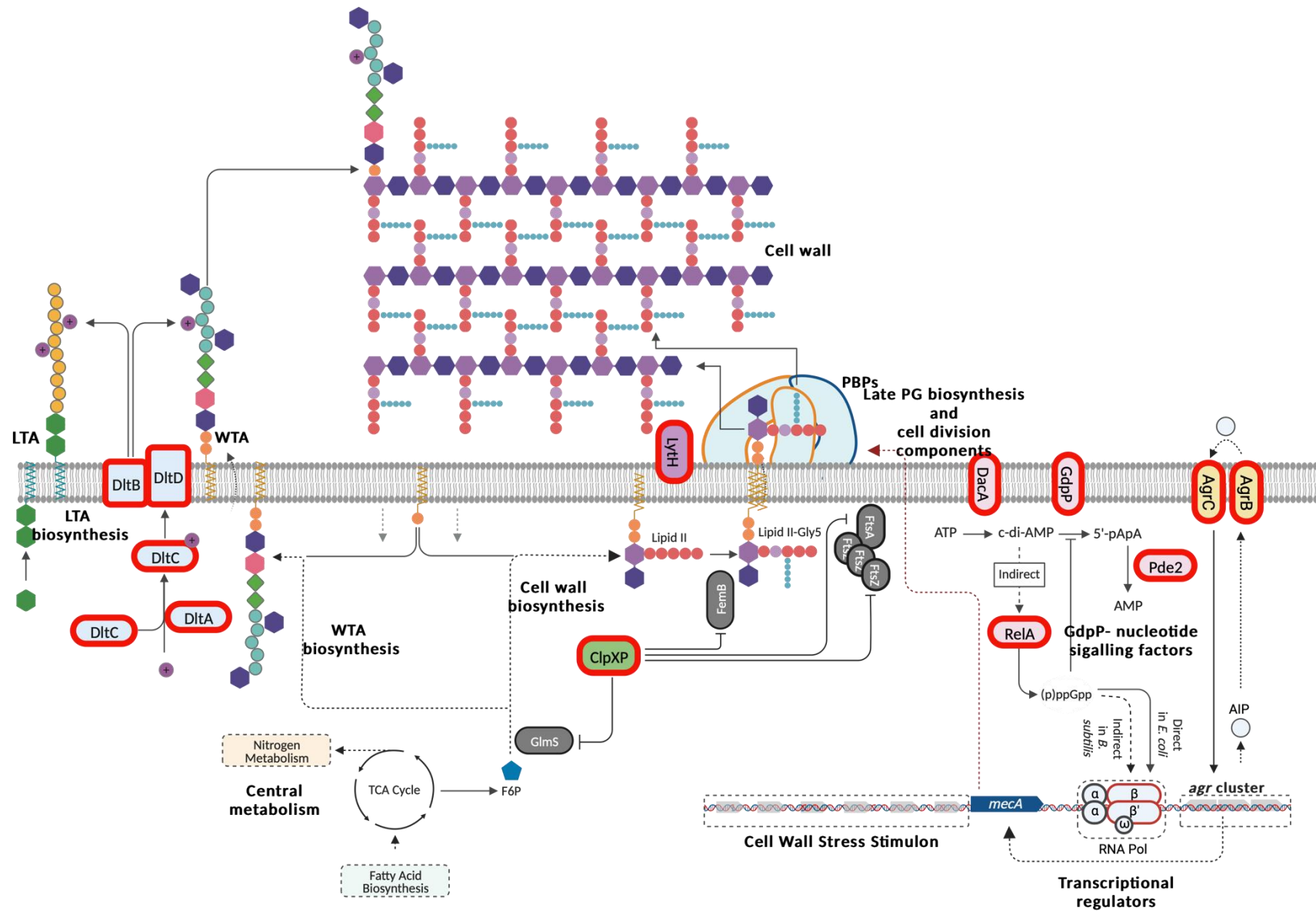
### **1.7.3.6 Development of high-level MRSA**

The *mecA* gene gives rise to increased MIC levels in cells (2- 4  $\mu\text{g}/\text{mL}$  methicillin) but this alone is not responsible for high-level  $\beta$ -lactam resistance and requires potentiators for high-level resistance ( $\geq 256 \mu\text{g}/\text{mL}$ ) and auxiliary factors to maintain low- or high-level resistance (Bilyk et al., 2022; Panchal et al., 2020). This mechanism is represented diagrammatically in Figure 1.15. Developing understanding of the molecular mechanisms underpinning high-level antimicrobial resistance aims to develop either novel targets for new antibiotics or the repurposing of existing antibiotics to treat staphylococcal infections.

## **1.8 Aims**

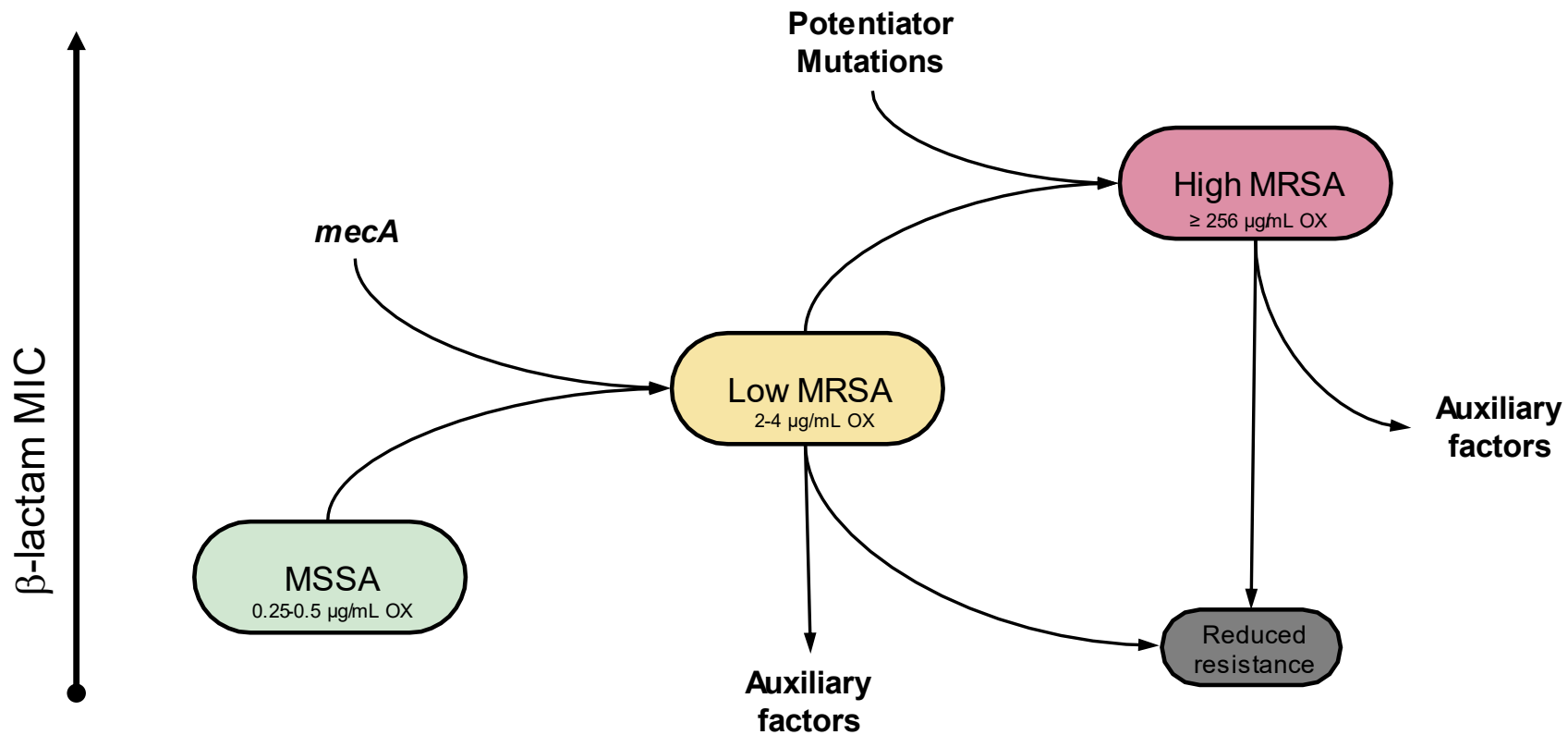
The exact mechanisms by which PBP2A confers high-level antibiotic resistance are not fully understood and my study aimed to investigate how this is manifested. The study used Bacterial Two Hybrid library screening of staphylococcal protein interactions and directed screening of staphylococcal protein constructs to investigate the mechanisms of PBP2A interactions, our study tests whether unknown interactions of PBP2A might support its function. We performed a directed evolution of MRSA, hypothesising that this could provide insight to how this is maintained and whole genome sequencing was then implemented to further determine underlying principles of MRSA. The specific aims were to:

- i. Investigate protein-protein interactions using a random bacterial two hybrid library.
- ii. Perform directed screening of protein-protein interactions.
- iii. Analyse the mechanism of action of agents that modulate  $\beta$ -lactam resistance in MRSA.



**Figure 1.14 Schematic of Potentiators involved in  $\beta$ -lactam resistance in MRSA.**

Potentiators (red outline) of  $\beta$ -lactam resistance in MRSA, common colours indicated shared biological pathways, factors with no demonstrable impact have a black outline. (Adapted from Bilyk et al., 2022) Created with BioRender.com.



**Figure 1.15 Levels of antibiotic resistance in *S. aureus*.**

Methicillin sensitive *S. aureus* (MSSA), which acquires PBP2A or the *SCCmec* demonstrates resistance to low concentrations of β-lactams, to become low MRSA. Point mutations in potentiator genes results in high-level MRSA resistant to concentrations of  $\geq 256 \mu\text{g/mL}$ . Mutations in auxiliary genes in low- and high-level MRSA result in reduced resistance, OX, Oxacillin. Adapted from Bilyk et al. (2022).

## Chapter 2 Materials and Methods

### 2.1 Growth Media

All growth media was prepared using dH<sub>2</sub>O, and autoclaved at 121 °C for 15 min.

#### 2.1.1 Luria-Bertani (LB)

Tryptone (Oxoid)	10 g / L
Yeast extract (Oxoid)	5 g / L
NaCl	5 g / L

1.5 % w/v Sigma Bacteriological agar was added to make LB agar.

#### 2.1.2 Minimal Media

Minimal media used in the bacterial two hybrid analysis (Karimova et al., 2000) was adapted as described in Daniel et al. (2006).

NH <sub>4</sub> Cl	10 mM
NH <sub>4</sub> NO <sub>3</sub>	1.2 mM
MgSO <sub>4</sub>	1 mM
Na <sub>2</sub> SO <sub>3</sub>	0.75 mM
KH <sub>2</sub> PO <sub>4</sub>	0.5 mM
MnCl <sub>2</sub>	0.1 mM
FeCl <sub>3</sub>	4 μM

The pH was adjusted to 7 using sodium hydroxide and the following filter sterilised components added after autoclaving.

Glucose	0.8 % (w/v)
Casamino acids	0.4 % (w/v)
Thiamine	3 μM

#### 2.1.3 Tryptone soya

TSB	30 g / L
-----	----------

1.5 % w/v Sigma Bacteriological agar was added to make TSB agar

#### 2.1.4 Baird-Parker agar

BP agar base (Oxoid)	60 g / L
----------------------	----------



Agar 1.5 % (w/v)

50 mL / L egg yolk emulsion with potassium tellurite (Sigma) was added to cooled agar.

### **2.1.5 LK**

Tryptone (Oxoid) 10 g / L

Yeast extract (Oxoid) 5 g / L

KCl 7 g / L

1.5 % w/v Bacteriological agar (Sigma) was added to make LK agar.

5 % w/v Sodium citrate (NaCit) added to cooled agar.

## **2.2 Antibiotics**

Antibiotics and resensitising agents used in this study are shown in Table 2.1. Stock solutions were filter sterilised using 0.2 µm pore size filter and stored at -20 °C until needed. Media was cooled to 55 °C before antibiotic stock solutions were added to agar plates prior to use. Antibiotic stock solutions were defrosted and then added to liquid media immediately before use.

## **2.3 Bacterial Strains and Plasmids**

### **2.3.1 *Staphylococcus aureus* strains**

*S. aureus* strains used in this study are detailed in Table 2.2 (Below). Strains were stored in Biobank tubes and maintained on TSA, and where necessary verified using Baird-parker agar. Liquid cultures were incubated overnight at 37 °C in either TSA or LB in sterile universal tubes at 250 rpm.

### **2.3.2 *Escherichia coli* strains**

All *E. coli* strains used in this study were stored at - 80 °C in Biobank tubes. Strains were grown on LB agar with appropriate antibiotics to maintain selection. Liquid cultures were incubated overnight in Luria-Bertani medium (Sambrook et al., 1989) at 37 °C in sterile universal tubes on a shaker at 250 rpm. Strains used in this study are shown in Table 2.3.

### **2.3.3 Plasmids**

Plasmids listed were purified using GeneJET Plasmid Miniprep kit according to manufacturer's instructions unless otherwise stated (Thermo Fisher Scientific).

For directed bacterial two hybrid, screening constructs are listed in Section 2.13.5.

**Table 2.1 Antibiotics and Resensitising Agents**

Antibiotic/Resensitising agent	Stock Concentration	Solvent	Storage
Methicillin (Meth)	100 mg/mL	dH <sub>2</sub> O	-20 °C
Erythromycin (Ery)	5 mg/mL	100% (v/v) ethanol	-20 °C
Lincomycin (Lin)	5 mg/mL	100% (v/v) ethanol	-20 °C
Kanamycin (Kan)	50 mg/mL	dH <sub>2</sub> O	-20 °C
Tetracycline (Tet)	5 mg/mL	50% (v/v) ethanol	-20 °C
Ampicillin (Amp)	100 mg/mL	dH <sub>2</sub> O	-20 °C
Epicatechin gallate (ECg)	50 mg/mL	dH <sub>2</sub> O	-20 °C
Serine hydroxamate (SHX)	25 mg/mL	dH <sub>2</sub> O	-20 °C
Norgestimate (NRG)	10 mg/mL	dH <sub>2</sub> O	4 °C
Diclofenac (DSS)	31.25 mg/mL	100% (v/v) ethanol	4 °C
Clomiphene citrate (CC)	4 mg/mL	100% (v/v) ethanol	4 °C

**Table 2.2 *S. aureus* Strains**

SJF ID	Characteristics	Reference
682 SH1000	Functional <i>rsbU</i> <sup>+</sup> derivative of 8325-4.	(Horsburgh et al., 2002)
684 RN4220	Restriction deficient transformation recipient <i>rsbU</i> <sup>+</sup> .	(Kreiswirth et al., 1983)
2103	SH1000 <i>PsecY::secY-gfp+</i> , Ery <sup>R</sup> Lin <sup>R</sup> . Green under fluorescence microscopy.	Laboratory Stock
4618	SH1000 pKASBAR (Kan <sup>R</sup> ) expressing GFP under Pma1M promoter at <i>geh</i> locus.	Laboratory Stock
4772	IPTG-inducible expression of <i>plsY</i> -GFP, Ery <sup>R</sup> Lin <sup>R</sup> .	(Weihs et al., 2018)
4996	<i>lysA::pmecA</i> , Ery <sup>R</sup> Lin <sup>R</sup> . Single copy expression of <i>mecA</i> under its own promoter from <i>lysA</i> locus. Low level resistant to oxacillin (1 µg/mL).	(Panchal et al., 2020)
5003	<i>lysA::pmecA rpoB<sup>H929Q</sup></i> Ery <sup>R</sup> Lin <sup>R</sup> . Trained High level resistant to oxacillin (≥256 µg/mL).	(Panchal et al., 2020)
5010	<i>pmecA</i> removed from <i>lysA::Kan<sup>R</sup> rpoB<sup>H929Q</sup></i> . Low level resistant to oxacillin (0.5 µg/mL).	(Panchal et al., 2020)
5034	<i>lysA::pmecA rpoC<sup>G731R</sup></i> Ery <sup>R</sup> Lin <sup>R</sup> . Trained High level resistant to oxacillin (≥256 µg/mL).	(Panchal et al., 2020)
5320	<i>lysA::tet<sup>R</sup> rpoB<sup>H929Q</sup></i> Low level resistant to oxacillin (0.5 µg/mL).	(Panchal et al., 2020)
5323	<i>geh::pmecA- Kan<sup>R</sup> lysA::tet rpoB<sup>H929Q</sup></i> . Trained High level resistant to oxacillin (≥256 µg/mL).	(Panchal et al., 2020)
5324	<i>geh::pmecA Kan<sup>R</sup></i> Single copy expression of <i>mecA</i> under its own promoter from <i>lysA</i> locus. Low level resistant to oxacillin (1 µg/mL).	(Panchal et al., 2020)
5457	<i>relA::TnNE1714</i> Ery <sup>R</sup> Lin <sup>R</sup> .	This Study/Bohdan Bilyk
5463	<i>relA::TnNE1714</i> Ery <sup>R</sup> Lin <sup>R</sup> . Transduced into <i>geh::mecA, Kan<sup>R</sup></i> .	This Study /Bohdan Bilyk
5659	<i>pLOW-Ppcn-gfp-PBP2</i> Ery <sup>R</sup> Lin <sup>R</sup> .	This Study
6111	<i>alaS::TnNE1575</i> Ery <sup>R</sup> Lin <sup>R</sup> . <i>pmecA(Kan<sup>R</sup>)</i> (SJF 5324).	This Study
6112	<i>alaS::TnNE1575</i> Ery <sup>R</sup> Lin <sup>R</sup> . Transduced into <i>pmecA(Kan<sup>R</sup>) rpoC<sup>G731R</sup></i> (SJF 5673).	This Study
6113	<i>alaS::TnNE1575</i> Ery <sup>R</sup> Lin <sup>R</sup> . Transduced into <i>lysA::tet rpoB<sup>H929Q</sup></i> (SJF 5320).	This Study
6114	<i>alaS::TnNE1575</i> Ery <sup>R</sup> Lin <sup>R</sup> . <i>rpoC</i> (SJF 5672).	This Study
6115	<i>alaS::TnNE1575</i> Ery <sup>R</sup> Lin <sup>R</sup> . Transduced into SH1000.	This Study
6116	<i>glyA::TnNE213</i> Ery <sup>R</sup> Lin <sup>R</sup> . Transduced into <i>pmecA(Kan<sup>R</sup>) rpoC<sup>G731R</sup></i> (SJF 5673).	This Study
6117	<i>glyA::TnNE213</i> Ery <sup>R</sup> Lin <sup>R</sup> . Transduced into SH1000.	This Study
6118	<i>hprT::TnNE917</i> Ery <sup>R</sup> Lin <sup>R</sup> . Transduced into SH1000.	This Study

6119	<i>hprT::TnNE917</i> Ery <sup>R</sup> Lin <sup>R</sup> . Transduced into SH1000.	This Study
6120	<i>hprT::TnNE917</i> Ery <sup>R</sup> Lin <sup>R</sup> . Transduced into <i>pmecA(Kan<sup>R</sup>) rpoB</i> (SJF 5323).	This Study
6121	<i>hprT::TnNE917</i> Ery <sup>R</sup> Lin <sup>R</sup> . Transduced into <i>pmecA(Kan<sup>R</sup>) rpoC<sup>G731R</sup></i> (SJF 5673).	This Study
6122	<i>hprT::TnNE917</i> Ery <sup>R</sup> Lin <sup>R</sup> . Transduced into <i>lysA::tet rpoB<sup>H929Q</sup></i> (SJF 5320).	This Study
6123	<i>relA::TnNE1714</i> Ery <sup>R</sup> Lin <sup>R</sup> . Transduced into <i>pmecA(Kan<sup>R</sup>) rpoC<sup>G731R</sup></i> (SJF 5673).	This Study
6124	<i>relA::TnNE1714</i> Ery <sup>R</sup> Lin <sup>R</sup> . <i>geh::pmecA(Kan<sup>R</sup>)</i> , Transduced into <i>lysA::tet rpoB<sup>H929Q</sup></i> (SJF 5320).	This Study
6125	<i>SAOUHSC_00598::TnNE1093</i> Ery <sup>R</sup> Lin <sup>R</sup> . Transduced into <i>pmecA(Kan<sup>R</sup>) rpoC<sup>G731R</sup></i> (SJF 5673).	This Study
6126	<i>SAOUHSC_00598::TnNE1093</i> Ery <sup>R</sup> Lin <sup>R</sup> . Transduced into SH1000.	This Study
6127	<i>SAOUHSC_00654::TnNE1468</i> Ery <sup>R</sup> Lin <sup>R</sup> . <i>pmecA(Kan<sup>R</sup>)</i> (SJF 5324).	This Study
6128	<i>SAOUHSC_00654::TnNE1468</i> Ery <sup>R</sup> Lin <sup>R</sup> . Transduced into SH1000.	This Study
6129	<i>Tn1093</i> Ery <sup>R</sup> Lin <sup>R</sup> . Transduced into <i>geh::pmecA(Kan<sup>R</sup>)</i> , <i>lysA::tet rpoB<sup>H929Q</sup></i> (SJF 5320).	This Study
6130	<i>Tn1468</i> Ery <sup>R</sup> Lin <sup>R</sup> . Transduced into <i>geh::pmecA(Kan<sup>R</sup>)</i> , <i>lysA::tet rpoB<sup>H929Q</sup></i> (SJF 5320).	This Study
6131	<i>Tn1575</i> Ery <sup>R</sup> Lin <sup>R</sup> . Transduced into <i>geh::pmecA(Kan<sup>R</sup>)</i> , <i>lysA::tet rpoB<sup>H929Q</sup></i> (SJF 5320).	This Study
6132	<i>Pspac PBP2A~GFP</i> C terminal <i>Pspac PBP2A~GFP</i> in pGM068 15, See Genewiz 20220912 order.	This Study
6133	C terminal <i>Pspac PBP2A~GFP</i> in pLOW Transduced into SH1000. See Genewiz 20220912 order.	This Study
6134	N terminal <i>Pspac GFP~PBP2A</i> in pGM068 Ery <sup>R</sup> Lin <sup>R</sup> . Transduced into SH1000. See Genewiz 20220912 order.	This Study
6135	N terminal <i>Pspac GFP~PBP2A</i> in pLOW Ery <sup>R</sup> Lin <sup>R</sup> . Transduced into SH1000. See Genewiz 20220912 order.	This Study
6136	C terminal <i>pspac PBP2A~GFP</i> in pLOW Ery <sup>R</sup> Lin <sup>R</sup> . Transduced into 5010.	This Study
6137	N terminal <i>Pspac GFP~PBP2A</i> in pLOW Ery <sup>R</sup> Lin <sup>R</sup> .	This Study
6138	C terminal <i>Pspac PBP2A~GFP</i> in pLOW Ery <sup>R</sup> Lin <sup>R</sup> .	This Study
6139	N terminal <i>Pspac GFP~PBP2A</i> in pLOW Ery <sup>R</sup> Lin <sup>R</sup> .	This Study
6140	<i>Δspa Pspac PBP2A ~GFP</i> C terminal <i>Pspac PBP2A~GFP</i> in pGM068 Ery <sup>R</sup> Lin <sup>R</sup> .	This Study
6141	<i>Δspa Pspac GFP~PBP2A</i> N terminal <i>GFP~PBP2A</i> in pGM068 Ery <sup>R</sup> Lin <sup>R</sup> .	This Study
6142	<i>Δspa</i> pLOW Ery <sup>R</sup> Lin <sup>R</sup> . <i>Ppcn ftsW ~GFP</i> .	This Study

**Table 2.3 *E. coli* strains used in this study.**

<b>SJF Number</b>	<b>Strain</b>	<b>Genotype</b>	<b>Source</b>
1953	BTH101	<i>F-</i> , <i>cya-99</i> , <i>araD139</i> , <i>galE15</i> , <i>galk16</i> , <i>rpsL1 (Strr)</i> , <i>hsdR2</i> , <i>mcrA1</i> , <i>McrB4</i>	Karimova et al. (1998)
N/A	DH5 Alpha	<i>fhuA2Δ(argF-lacZ)U169 phoA glnV44</i> <i>Φ80Δ(lacZ)M15 gyrA96 recA1 relA1</i> <i>endA1 thi-1 hsdR17</i>	New England Biolabs

## 2.4 Buffers and Solutions

All buffers and solutions were prepared using dH<sub>2</sub>O and stored at room temperature. Solutions were sterilised by either autoclaving or filtration sterilisation where appropriate.

### 2.4.1 Phosphate buffered saline (PBS)

PBS tablets (Thermo Fisher) were dissolved in 500 mL of dH<sub>2</sub>O for 1x and autoclaved at 121 °C for 15 min.

### 2.4.2 Tris-Acetate buffer (TAE) (50X)

Tris base	242 g/L
Glacial acetic acid	5.7 % (v/v)
Na <sub>2</sub> EDTA pH 8.0	0.05 M

1x TAE working solution was made by diluting 50x stock solution with dH<sub>2</sub>O.

### 2.4.3 TBSI

Tris-HCl pH 7.5	50 mM
NaCl	0.1 M

EDTA-free protease cocktail inhibitor (Roche) was dissolved in buffer prior to use.

### 2.4.4 SDS-PAGE Solutions

#### 2.4.4.1 SDS-PAGE reservoir buffer

Tris-HCl	30.3 g / L
Glycine	144 g / L
SDS	10 g / L

#### 2.4.4.2 SDS-PAGE loading Buffer

Glycerol	50 % (v/v)
Tris-HCl pH 6.8	20 mM
SDS	10 % (w/v)
DTT	0.5 mM
Bromophenol blue	0.5 % (v/v)

## 2.4.5 Western Blotting Solutions

### 2.4.5.1 Transfer buffer

Tris-HCl	12 mM
Glycine	96 mM
Ethanol	20% (v/v)

pH adjusted to 8.3 and stored at 4 °C

### 2.4.5.2 TBST (wash solution)

Tris-HCl	20 mM
NaCl	150 mM
Tween 20	0.1% (v/v)

pH adjusted to 7.2-7.4 and stored at 4 °C

### 2.4.5.3 Blocking Buffer

5% (w/v) semi skimmed milk powder (Sigma) was added to TBST buffer prior to use.

## 2.4.6 $\beta$ -galactosidase liquid assay solutions

### 2.4.6.1 ABT

NaCl	5.88 g / L
K <sub>2</sub> HPO <sub>4</sub>	10.5 g / L
KH <sub>2</sub> PO <sub>4</sub>	5.44 g / L
Triton X-100	0.1% (v/v)

### 2.4.6.2 Stopping Solution

Na <sub>2</sub> CO <sub>3</sub>	42.39 g / L
---------------------------------	-------------

### 2.4.6.3 ABTN

ABT	500 mL
Stopping Solution	500 mL

## 2.4.7 Co-immunoprecipitation solutions and buffers

### 2.4.7.1 Lysis buffer

TrisCl	10 mM
NaCl	150 mM
MgCl <sub>2</sub>	5 mM

Adjusted to pH 7.5

Immediately before use, the following were added:

Lysostaphin (Biosynexus) 200 µg/mL

EDTA-free Protease inhibitor tablet (Roche)

#### **2.4.7.2 Membrane extraction buffer**

PBS (Sigma) 1x

NaCl 500 mM

Adjust to pH 7.5

Filter and add:

Triton X-100 1%

#### **2.4.7.3 No salt wash buffer**

PBS 10x

The pH was adjusted to 7.5

Triton X-100 1% (v/v)

#### **2.4.7.4 Dilution buffer**

Tris/Cl 10 mM

NaCl 150 mM

EDTA 0.5 mM

The pH was adjusted to 7.5

As specified by manufacturer (ProteinTech, UK)

#### **2.4.7.5 Wash buffer**

Tris/Cl 10 mM

NaCl 150 mM

EDTA 0.5 mM

The pH was adjusted to 7.5 As specified by manufacturer (ProteinTech, UK).

### **2.5 Enzymes and chemicals**

All chemicals and enzymes were of analytical grade quality and were purchased from Thermo Fisher Scientific, unless otherwise stated. All restriction enzymes, ligases, DNA polymerases, Gibson master mix and appropriate buffers were purchased from New England Biolabs.

### **2.6 Centrifugation**

The following centrifuges were used to harvest samples:



- Eppendorf microcentrifuge 5424, capacity to 24 x 1.5-2 mL microfuges, maximum speed of 21,130 x g (14,800 rpm).
- Fisherbrand™ Microcentrifuges, Micro 17R Capacity: 48mL (24 x 1.5/2mL tubes), Maximum speed/RCF: 13300 rpm/17000 x g.
- Fisher Scientific MegaFuge 40 R Capacity 4 x 1000 mL, Max. RCF 25,314 x g, Max. Speed 15,200 rpm with Thermo Scientific 4700 rpm TX-750 4x 750 mL bucket rotor or fixed angle Fiberlite F14-6x250 LE 6x 250 mL max capacity, 11000 rpm, 8533 x g.

Centrifugation was conducted at room temperature unless otherwise stated.

### **2.6.1 Ultra centrifugation**

The following ultracentrifuge and rotor were used:

- Thermo scientific wX+ ultra series centrifuge with Beckman Type 45 Ti 45,000 rpm rotor.

Rotors and centrifuges were pre chilled to 4 °C

## **2.7 Determination of bacterial cell density**

### **2.7.1 Spectrophotometric measurement**

Spectrophotometric measurements were taken at 600nm (OD 600nm) to determine the bacterial yield of a culture using a Biochrom WPA Biowave DNA spectrophotometer.

## **2.8 Determination of minimum inhibitory concentration**

### **2.8.1 Determination of minimum inhibitory concentration by microdilution**

Compounds of interest were diluted in fresh growth media at double the required highest concentration and serially diluted in a 96-well plate, overnight cultures were diluted in fresh media to OD<sub>600nm</sub> of 0.01 and diluted 10-fold into appropriate wells of 96 well plates. After overnight growth plates were agitated with 300 rpm double orbital shaking and optical density was recorded using a HIDEX sense plated reader. All strains were performed in biological triplicate.

## **2.9 Antibiotic methods**

### **2.9.1 Antibiotic MIC by ETest**

As methicillin Etest strips are not commercially available, oxacillin test strips were used to evaluate  $\beta$ -lactam resistance on agar plates. An overnight culture was diluted to an OD<sub>600nm</sub> of ~2 using fresh culture media. The diluted bacterial culture was inoculated onto TSA agar appropriately substituted with compounds of interest using a cotton swab. An antibiotic Etest strip was then added using tweezers. Etest strips were stored at 4 ° C. Plates were incubated overnight at 37 ° C, a zone of growth inhibition around the strip following incubation allows the MIC to be determined. The antibiotic Etest strip used in this study was oxacillin (bioMérieux).

### **2.9.2 Antibiotic Gradient plate for directed evolution.**

A modified gradient plate technique was used (Bryson and Szybalski, 1952). Two layers of agar were poured into square petri dishes (Thermo Fisher). The bottom layer (slanted) consists of TSA containing 50  $\mu$ g/mL ECg (Sigma) and the top flat layer contains 50  $\mu$ g/mL ECg and 512  $\mu$ g/mL methicillin (Sigma). In parallel, MRSA strains containing mutations in *rpoB* (SJF5003) or *rpoC* (SJF5034) were grown to OD<sub>600</sub> of ~0.8 and 200  $\mu$ L of each was spread over the entire area of an agar plate containing the methicillin gradient in the presence of 50  $\mu$ g/mL ECg and incubated for 24-48 hrs at an appropriate temperature.

## **2.10 DNA Purification techniques**

### **2.10.1 Genomic DNA extraction**

*S. aureus* genomic DNA was extracted and purified using the Qiagen DNeasy blood and tissue kit. 1- 2 mL of an overnight culture was centrifuged at 14,000 rpm for 10 min. The cell pellet was resuspended in 180  $\mu$ L of dH<sub>2</sub>O and 10  $\mu$ L of lysostaphin solution was added (5 mg/mL). The suspension was incubated for 1 hour at 37 °C. Genomic DNA was isolated according to manufacturer's instructions.

### **2.10.2 Plasmid purification**

The GeneJet Plasmid Miniprep kit (Thermo Fisher) was used to purify the plasmids from cultures according to manufacturer's instructions. Warm molecular grade water was used for elution.

### 2.10.3 Gel extraction of DNA

DNA was separated using TAE agarose gel (1% w/v) stained with Midori green (BioRad) and visualised on a UV transilluminator (Sigma). Required bands were excised using a scalpel. The GeneJET gel extraction kit (Thermo Fisher) was used to purify DNA from agarose gels according to manufacturer's instructions.

### 2.10.4 Purification of PCR products

PCR products were purified using the GeneJET PCR purification kit (Thermo Fisher)

## 2.11 *In vitro* manipulation of DNA

### 2.11.1 Primer Design

Primers were designed using Primer3 (<https://primer3.ut.ee>) and primers used in this study are shown in Table 2.4.

### 2.11.2 PCR amplification

PCR amplification was performed in Veriti Thermal Cycler (Applied Biosystems). Thermocycler lids were always pre heated to 105 °C. PCR Products were analysed by gel electrophoresis, see 2.11.5 and where necessary gel extractions (section 2.10.3) or PCR clean-ups (section 2.10.4) were performed.

#### 2.11.2.1 Phusion DNA polymerase

Phusion HF DNA polymerase (Thermo Fisher) was used for all PCRs where proofreading of the DNA sequence is required for the highest quality insert, overhang generation and DNA for sequencing. The following thermocycler programme was used:

Initial Denaturation	98 °C	30 seconds
35 Cycles:		
Denaturation	98 °C	5–10 seconds
Annealing	62 °C	10–30 seconds
Extension	72 °C	15-30 seconds per kB
Final Extension	72 °C	10 minutes
Hold	4 – 10 °C	∞

#### 2.11.2.2 Colony PCR Screening of *S. aureus*

A small amount of *S. aureus* colony (1/4 overnight colony) were resuspended in 20 µL of lysostaphin solution (5 µg/mL), and remaining colony streaked for storage at – 80 ° C. The resuspension was incubated for 10 mins at 37 ° C. 80 µL of the proteinase K (Sigma) solution

was added to lysed cells, vortexed and incubated in a thermocycler according to the following programme:

10 minutes 70 ° C

10 minutes 98 ° C

5 minutes 4 ° C

1 µL of prepared sample was used in PCR as DNA template.

**Table 2.4 Primers used in this study**

F/ For denotes a forward and R/Rev denotes a reverse primer.

#_Primer	Sequence (5' - 3')	Use	Source
1_B2hFNter	tttatgcttccggctcgtatg tt	Sequencing N Terminal T18 Library Fusions	This Study (Sigma)
2_B2hRNter	gcgagcgcgattttccacaaca	Sequencing N Terminal T18 Library Fusions	This Study (Sigma)
3_BACTH For	cgccggatgtactggaaacgg	Sequencing C Terminal T18 Library Fusions	This Study (Sigma)
4_BACTH Rev	cggggctggcttaactatgcg gc	Sequencing C Terminal T18 Library Fusions	This Study (Sigma)
7_pepVGibFor	ctatgaccatgattacgcca tgtggaaagaaaagtcaac	Amplification of <i>pepV</i> , Forward.	This Study (Sigma)
8_pepVGIBRev	tcctctagagtcgacctgcat tcctccacgcataatgaataa attg	Amplification of <i>pepV</i> , Reverse.	This Study (Sigma)
11_Nitroreductase_ gib_F	actgcaggtcgactctagaga tggaattacaacaagcaatag	Amplification and Gibson assembly of nitroreductase	This Study (Sigma)
12_Nitroreductase_ gib_R	attacttagttatatcgatgt taatataatgtaattaagt ctatttttacg	Amplification and Gibson assembly of nitroreductase	This Study (Sigma)
13_NosoGibF	ctatgaccatgattacgcca tgttatttaagaggctcaag	Amplification and Gibson assembly of Nitrogen synthase oxygenase	This Study (Sigma)
14_NosoGibR	tcctctagagtcgacctgcaa tgatggaaagggcactg	Amplification and Gibson assembly of Nitrogen synthase oxygenase	This Study (Sigma)
19_ArsRedGibF	ctatgaccatgattacgcca tgattaaattttaccaatata agaattgtac	Amplification and Gibson assembly of Arsenate reductase	This Study (Sigma)
20_ArsRedGibR	tcctctagagtcgacctgcac gctaaccaagtctctttatat tg	Amplification and Gibson assembly of Arsenate reductase	This Study (Sigma)
21_HisZGibFor	ctatgaccatgattacgcca tgaataattcagaacaattaa ttg	Amplification and Gibson assembly of <i>hisZ</i>	This Study (Sigma)
22_HisZGibRev	tcctctagagtcgacctgcaa agtgttaatcctaataccaac	Amplification and Gibson assembly of <i>hisZ</i>	This Study (Sigma)
23_AminohydrdoGib For	ctatgaccatgattacgcca tgtagattggttccaac	Amplification and Gibson assembly of Aminohydrolase	This Study (Sigma)
24_AminohydrdoGib rev	tcctctagagtcgacctgcaa ttgttttaataacttgctct aatc	Amplification and Gibson assembly of Aminohydrolase	This Study (Sigma)
27_pepVintF	tgttgacggttcttctgctg	Sequencing <i>pepV</i> gene	This Study (Sigma)
28_pepVintR	tgtagttgtcagctcacc	Sequencing <i>pepV</i> gene	This Study (Sigma)

29_NitRedIntF	tgtgcatgttccgaaagacag	Sequencing Nitroreductase gene	This Study (Sigma)
30_NitRedIntR	ccaacatgtacctattcccgc	Sequencing Nitroreductase gene	This Study (Sigma)
35_ArsRedIntF	tacacacggcgcgaaatatic	Sequencing Arsenate Reductase gene	This Study (Sigma)
36_ArsRedIntR	tcgcccattactgctagagg	Sequencing Arsenate Reductase gene	This Study (Sigma)
37_HisZIntF	gaggatttgcagcagatggg	Sequencing <i>hisZ</i> gene	This Study (Sigma)
38_HisZIntR	ccaaacccttcgatgcttcc	Sequencing <i>hisZ</i> gene	This Study (Sigma)
39_AminoHydroIntF	ctattcattcacgtgcgggg	Sequencing aminohydrolase gene	This Study (Sigma)
40_AminoHydroIntR	ctatctgtggtgctgcttg	Sequencing aminohydrolase gene	This Study (Sigma)
51_LytHIntF	gcatcgcctttgatatcacg	Sequencing <i>lytH</i> gene	This Study (Sigma)
52_LytHIntR	gtgcttgatcctggatcatgg	Sequencing <i>lytH</i> gene	This Study (Sigma)
53_LytNIntF	tcgcgaaatcagagttaaatic	Sequencing <i>lytN</i> gene	This Study (Sigma)
54_LytNIntR	actaagtccccaggttcagc	Sequencing <i>lytN</i> gene	This Study (Sigma)
55_LytHGibF	ggtcgactctagagaaaaaaatagaggcatggttatctaaaaagggt	Amplification and Gibson assembly <i>lytH</i> gene	This Study (Sigma)
56_LytHGibR	tagttatatcgatgctacgca gaaaaataaattttaaggcca tcaaca	Amplification and Gibson assembly <i>lytN</i> gene	This Study (Sigma)
57_LytNGibF	aggtcgactctagagaataaa caacaaagtaaagtacgctat tcaattagaaaagt	Amplification and Gibson assembly <i>lytN</i> gene	This Study (Sigma)
58_LytNGibR	ttagttatatcgatgttatgc ttttttaaattggtctaataaa aatcatatcattttcataat	Amplification and Gibson assembly <i>lytN</i> gene	This Study (Sigma)
59_ThioRedGibF	tgaccatgattacgccaatgc aatcaatcaaaagtaatgaat catttaaattctgtaattaata gc	Amplification and Gibson assembly of thioredoxin	This Study (Sigma)
60_ThioRedGibR	ctagagtcgacctgcaaaaag tttctgctaaaaatgattcaa cttgttcag	Amplification and Gibson assembly of thioredoxin	This Study (Sigma)
61_ThioRedIntF	cccagactgtcgtgctatgg	Sequencing thioredoxin	This Study (Sigma)
62_ThioRedIntR	ggtgtgcaattttatcgccg	Sequencing thioredoxin	This Study (Sigma)

116_Tet N INT	tgcttggtgaaaaaagtcttg caa	Internal tet <sup>R</sup> cassette primer	This Study (Sigma)
119_tet C Int	acattcaaggtaaccagccaa c	External tet <sup>R</sup> cassette primer	This Study (Sigma)
120_SPA AMP REV	gcggttttaagccttttactt cc	Amplification of entire <i>spa</i> region	This Study (Sigma)
121_SPA ampl For	ggcgtttcagaagttgtttag a	Amplification of entire <i>spa</i> region	This Study (Sigma)
122_Spa int 1 for	tgctcactgaaggatcgtct	Internal amplification of <i>spa</i>	This Study (Sigma)
123_spa int rev 1	gcgtaacacctgctgcaaat	Internal amplification of <i>spa</i>	This Study (Sigma)
124_SPA INT for 2	tgcagcaattttgtcagcag	Internal amplification of <i>spa</i>	This Study (Sigma)
125_spa int rev 2	caagcaccaaaagaggaagac a	Internal amplification of <i>spa</i>	This Study (Sigma)
130_GlyA_F	gccatcaacataccaacttcg t	<i>glyA</i> gene amplification for Tn insertion validation	This Study (Sigma)
131_GlyA_R	aaaagattggtggcgaacgt	<i>glyA</i> gene amplification for Tn insertion validation	This Study (Sigma)
132_DUF443_F	cgacacaatccttttaagacg c	DUF443 gene amplification for Tn insertion validation	This Study (Sigma)
133_DUF443_R	ccgaacaaaatagtactacct gc	DUF443 gene amplification for Tn insertion validation	This Study (Sigma)
134_reIA_F	acagtaagaccatacgctcgt	<i>relA</i> gene amplification for Tn insertion validation	This Study (Sigma)
135_reIA_R	cggacgtatgattggtgtgg	<i>relA</i> gene amplification for Tn insertion validation	This Study (Sigma)
136_AlaS_F	ggaatatacgcagggtcacc	<i>alaS</i> gene amplification for Tn insertion validation	This Study (Sigma)
137_AlaS_R	acgttcgtcccttttgagga	<i>alaS</i> gene amplification for Tn insertion validation	This Study (Sigma)
138_IsdF_F	tcgctggacaagttgcattt	<i>isdF</i> gene amplification for Tn insertion validation	This Study (Sigma)
139_IsdF_R	ctctgggtgcgcaattaaca	<i>isdF</i> gene amplification for Tn insertion validation	This Study (Sigma)
142_reIANEinsS_F	cagtgcgatgtactttaatac cg	<i>relA</i> gene amplification for Tn insertion validation	This Study (Sigma)
143_reIANEinsS_R	aaaaggccgaatgatggttga	<i>relA</i> gene amplification for Tn insertion validation	This Study (Sigma)
144_NE0213_F	acatgctcaagaggtccacc	NE0213 gene amplification for Tn insertion validation	This Study (Sigma)
145_NE0213_R	taggaatgggcgacacagtt	NE0213 gene amplification for Tn insertion validation	This Study (Sigma)
146_NE1093_F	aagtacgtcaaaatcagcgaa aa	NE0213 gene amplification for Tn insertion validation	This Study (Sigma)

147_NE1093_R	agtaaagaatgaaccaccacc t	NE0213 gene amplification for Tn insertion validation	This Study (Sigma)
150_NE1575_FCterm	gattctgctgcatcaatcgc	NE0213 gene amplification for Tn insertion validation	This Study (Sigma)
151_NE1575_Rcterm	tgttgaacgctctagaaaggc	NE0213 gene amplification for Tn insertion validation	This Study (Sigma)
164_Spa up	aagtcaagcctgaagtcgata tgac	Forward <i>spa</i> primer	Dr Katie Walton
165_Spa down	attgtctttgcttgagtcgcg ttc	Reverse <i>spa</i> primer	Dr Katie Walton
166_Upstream	ctcgattctattaacaaggg	Positive strand amplification of transposon (Transposon end distance 464)	NTML Library
167_Buster	gctttttctaaatgtttttta agtaaatacaagtac	Negative strand amplification of transposon (Transposon end distance 133)	NTML Library

---



### **2.11.2.2.1 Lysostaphin solution**

For 1000  $\mu$ L

Lysostaphin from stock (5 mg/mL) 20  $\mu$ L

Nuclease free water 980  $\mu$ L

### **2.11.2.2.2 Proteinase K solution**

For 1000  $\mu$ L

Proteinase K (Sigma) 50  $\mu$ L

0.5 M Tris-HCl pH 7.5 200  $\mu$ L

Nuclease Free water 750  $\mu$ L

## **2.11.3 Restriction endonuclease digestion**

DNA digests by restriction enzymes were performed using restriction enzymes from New England Biolabs (NEB) according to manufactures instructions using Cutsmart or 3.1 buffers as required (NEB). Reactions were incubated for 1- 6 hours and resulting fragments separated by DNA gel electrophoresis (section 2.11.5) and purified for downstream experiments where required.

## **2.11.4 Gibson Assembly**

For Gibson assemblies of DNA, the NEB High fidelity Gibson assembly kit was used. The manufacturer instructions were followed.

## **2.11.5 Agarose gel electrophoresis**

1% (w/v) Agarose was added to TAE were prepared using agarose (Thermo Fisher) for diagnostic DNA gels or agarose (Sigma) for gel purification and sequencing.

## **2.11.6 DNA sequencing**

Samples were submitted to Source Bioscience UK (<https://www.sourcebioscience.com/home>) for sanger sequencing. Sequencing results were analysed using SnapGene software.

## **2.11.7 Determining DNA concentration**

DNA concentration in purified samples was measured using NanoDrop 3300 spectrophotometer and operating software v.2.9.1. 1  $\mu$ L of DNA elution buffer or molecular

grade dH<sub>2</sub>O was used for blank measurements. 0.5 - 1  $\mu$ L of the sample was used measure DNA concentration at 260 nm.

## **2.12 Protein Analysis**

### **2.12.1 Preparation of whole cell lysate**

To prepare whole cell lysates for Western blotting, overnight cultures with appropriate antibiotics and inducer were sub-cultured into 50 mL of fresh media with supplements in an appropriately sized conical flask to an OD<sub>600nm</sub> of 0.05. Strains were grown with aeration to OD<sub>600nm</sub> 0.5-0.6 and then incubated on ice. A volume equivalent to an OD<sub>600nm</sub> of 0.5 was centrifuged at 4700 rpm for 15 minutes at 4 ° C. Pellets were incubated on ice and cell breakage performed immediately or stored at -20 ° C until required.

1 tablet of EDTA-free protease inhibitor cocktail (ROCHE) was mixed with 50 mL of ice-cold PBS to give PBSI. Pellets were resuspended in 1 mL of PBSI and transferred into Fast Prep tubes on ice. Cell breakage was performed mechanically using 10 cycles of speed 6.5 for 30 s with a two-minute incubation on ice between each run, using a MP Biomedicals FastPrep 24 Homogeniser. Beads were removed from lysis tubes by centrifugation at 2000 rpm for 1 minute at room temperature, supernatant transferred into a fresh Eppendorf tube, centrifugation repeated, and supernatants of the same samples grouped.

### **2.12.2 SDS PAGE**

Samples were mixed with SDS-PAGE Buffer and incubated for 5 minutes at 98 °C. samples were loaded into SDS-PAGE gels (BioRad) in BioRad tanks containing 1X SDS running buffer to separate proteins. Gels were run at 150- 175 V for 45 minutes or until the loading dye reached the end of the gel.

### **2.12.3 Coomassie Staining**

SDS-PAGE gels were submerged in Coomassie Blue (BioRad) following electrophoresis to visualise protein bands. Protein standards (Thermo Fisher) of known molecular mass were used to allow comparison of protein sizes.

### **2.12.4 Western Blotting**

#### **2.12.4.1 Transfer**

Following separation of proteins by SDS-PAGE (Section 2.12.2) the gel was equilibrated in transfer buffer for 10 minutes. Nitrocellulose membrane (Pall BioTrace™) was cut to the same

size as the gel and activated by soaking in methanol (100% v/v). All fibre pads and filter papers were soaked in cold transfer buffer prior to assembly of the sandwich for blotting. The Mini-Protean Tetra cell system (BioRad) was used to transfer proteins to the membrane from the gel by wet transfer in ice-cold transfer buffer. The transfer was run at 100 V for 1 hour.

#### **2.12.4.2 Antibody binding and washing**

After electrophoresis, the membrane was transferred to blocking buffer (2.4.5.3) on a shaker at 4 °C for 60 minutes or overnight. The membrane was then incubated with primary antibody diluted in blocking solution for 1-2 hours at room temperature (RT) or overnight at 4 °C. The membrane was washed three times for 15 minutes in TBST at RT. The membrane was incubated with horseradish peroxidase (HRP) conjugated anti-rabbit IgG secondary antibodies (Sigma) in blocking solution for 60 minutes and was washed three times for 15 minutes in TBST to remove unbound antibodies.

#### **2.12.4.3 Detection**

To detect proteins bound to the membrane, the blot was covered with Clarity Western ECL blotting substrates (BioRad). The blot was scanned using ChemiDoc MP Systems (BioRad) for chemiluminescent detection using GeneSys software (Syngene). Exposure times were altered as necessary to facilitate signal detection.

### **2.12.5 Co-Immunoprecipitation**

#### **2.12.5.1 Growth of Strains for Co-immunoprecipitation**

*S. aureus* strains were grown in 50 mL TSB supplemented with the appropriate antibiotics at 37 °C overnight with aeration, cultures were diluted 1:100 into 1 L TSB supplemented with appropriate antibiotics and IPTG as required. Cultures were grown at 37°C to the logarithmic growth stage of between 0.8 -1 OD<sub>600nm</sub> (approx. up to 3 hrs), with aeration, to allow the expression of the tagged proteins essential in cell division. The entire culture was harvested by centrifugation (8000 rpm, 20 mins, 4 °C).

#### **2.12.5.2 Preparing membrane fractions for immunoprecipitation**

The cell pellet was gently resuspended in 30 mL of lysis buffer and were incubated at 37 °C for 30 mins on an orbital shaking platform to promote cell lysis, cooled on ice, and further lysed using a bath sonicator filled with 50:50 water : ice chips to prevent samples overheating, until clear (approximately 15 mins). The lysate was centrifuged at 4618 x g, 20 min, 4 °C and the supernatant was transferred for ultracentrifugation in pre-chilled ultracentrifugation tubes

and centrifuged at 35000 rpm for 45 minutes at 4 °C. The supernatant was discarded, and the membrane pellet rinsed with lysis buffer (Section 2.4.7.1) to remove cytoplasmic debris. The membrane pellet was resuspended in 1 mL of membrane extraction buffer (Section 2.4.7.2) and homogenized using the bath sonicator for 15 mins, mixed gently by pipetting and sonicated for a further 15 mins. The resulting membrane homogenate was tumbled at 4 °C for 1 hour. A further centrifugation step 10,000 x G, 15 min, 4 ° C was performed to remove the remaining cell debris from the homogenate. The supernatant (1 mL) was added to 1 mL of no salt wash buffer. Separate aliquots (to prevent unnecessary freeze thaw cycles) for CO-IP and SDS-PAGE were snap frozen in liquid nitrogen and stored at - 80 °C until required.

### **2.12.5.3 Co-immunoprecipitation**

For co-immunoprecipitation of protein complexes  $\alpha$ -GFP Nanobodies fused to silicone beads (Proteintech, UK) were chosen.

#### **2.12.5.3.1 Bead equilibration**

As per manufacturer's instructions the  $\alpha$ -GFP Nanobody beads were resuspended by gently inverting the tube. 25  $\mu$ L of bead slurry was transferred into a 1.5 mL reaction tube. 500  $\mu$ L Ice-cold Dilution buffer was added. Beads were sedimented by centrifugation at 2,500 x g for 5 min at 4 °C, the supernatant was discarded.

#### **2.12.5.3.2 Protein binding**

500  $\mu$ L of cell lysate was added to the 25  $\mu$ L equilibrated beads and samples rotated end-over-end for 1 hour at 4 °C.

#### **2.12.5.3.3 Washing**

Beads were sedimented by centrifugation at 2,500 x g for 5 min at 4 °C. If required, the supernatant was saved for further analysis (flow-through/non-bound fraction). Beads were subjected to three washes: resuspended in 500  $\mu$ L wash buffer, and sedimented by centrifugation at 2,500 x g for 5 min at 4 °C. The remaining supernatant was discarded each time and during the last wash step beads were transferred to a new tube.

#### **2.12.5.3.4 Elution**

Any remaining supernatant was removed and the beads were resuspended in 50  $\mu$ L 2x SDS-sample buffer (Laemmli). Beads were boiled for 5 min at 95 °C to dissociate immunocomplexes, beads were removed by centrifuged at 5000 x g for 2 min at 4 °C. The supernatant was analysed by SDS-PAGE / Western Blot.

## **2.13 Transformation Techniques**

### **2.13.1 Transformation of *E. coli***

#### **2.13.1.1 Preparation of *E. coli* chemically competent cells**

Overnight cultures were added to fresh media substituted with antibiotics and grown until they reached exponential growth phase with an OD<sub>600</sub> between 0.3-0.5. Cultures were centrifuged for 10 minutes at 4000 rpm, supernatant discarded and resuspended in ½ volume ice cold CaCl<sub>2</sub> 50 mM. Cells were again collected by centrifugation (10 minutes at 4 °C at 4000 rpm) supernatant discarded and resuspended in 1/10 volume ice cold CaCl<sub>2</sub> (50 mM) 15% (v/v) glycerol and incubated on ice for 20 minutes, before immediate use or aliquoted and stored at -80 °C.

#### **2.13.1.2 Transforming chemically competent *E. coli***

A 100 µL aliquot of previously prepared *E. coli* BTH101 (SJF 1953) chemically competent cells was defrosted on ice. 0.5 µL of library or plasmid DNA, was added to the cells and incubated on ice for 20 minutes. Cells were heat shocked at 42 °C for 1.5 min followed by 1 min on ice. To recover cells, 1 mL of LB was immediately added. Cells were incubated for 1 h at 37 °C on a rotator. 100 µL of appropriately diluted cells were spread onto selective agar plates (LB or MacConkey agar plates containing appropriate media substitutions including antibiotics to maintain resistance markers). The plates were incubated for 24-48 hours at 37°C until colonies appeared.

### **2.13.2 Transformation of *S. aureus***

#### **2.13.2.1 Preparation of electrocompetent *S. aureus***

A fresh single colony of *S. aureus* RN4220 was inoculated into 5 mL of TSB (Section 2.1.3) and grown overnight. Overnight cultures were diluted 1:100 in an appropriately sized flask to facilitate aeration during growth, until OD<sub>600nm</sub> ~ 0.4 to 0.6 was reached. Flasks were then incubated on ice for 20 mins, and cells recovered by centrifugation. (4 °C for 10 minutes) in 50 mL falcon tubes. 10 mL pre-cooled 0.5M autoclaved glycerol buffer was used to gently resuspend cells, and then a further 45 mL added, samples centrifuged (4 °C for 10 minutes), and supernatant removed, the wash step was repeated prior to a resuspension step and incubation on ice for 30 minutes. The supernatant was again removed by centrifugation (4 °C for 10 minutes) and cells resuspended in 1 mL ice cold 0.5 M sucrose buffer. Appropriately

sized aliquots were prepared and snap frozen in liquid nitrogen and stored at - 80 °C until required.

### **2.13.2.2 Transformation of electrocompetent *S. aureus***

200 µL electrocompetent cells were thawed on ice, DNA added and incubated on ice for 20 minutes. Cells were then transferred to an electroporation cuvette (BioRad) pulsed once (25 µF, 1.75 kV and 200 Ω using a GenePulser Xcell Electroporation system). Pre warmed TSB (37°C) was immediately added and samples incubated at 37 ° C for 2 hours. Cells were diluted and plated on pre warmed TSB agar containing appropriate antibiotics.

### **2.13.3 Bacterial two hybrid screening**

#### **2.13.4 Library Transformation and screening**

0.5 µL of library was transformed into chemically competent BTH101 containing PBP1, PBP2 and PBP2A. 0.5 µL of T18 C library was added to an ice-cold tube containing 100 µL of chemically competent cells containing the PBP bait and incubated on ice for 20 minutes. Cells were diluted to 10<sup>-6</sup> in PBS and each dilution was spread onto prewarmed LB agar substituted with 100 µg / mL Ampicillin, 50 µg / mL Kanamycin, 0.5 mM IPTG and 40 µg / mL X-Gal (Thermo Fisher) and incubated at 37 °C for 24 hours. Plates were then incubated at 4 °C allowing further colour generation. Green/blue colonies depicting a positive interaction were sub-cultured for purity. Pure cultures were grown in LB overnight before purification and retransformation of T18 prey by plating transformants onto LB agar containing 100 µg / mL Ampicillin.

#### **2.13.5 Directed bacterial two hybrid screening**

An array of bacterial two hybrid constructs T25 in Table 2.5 and T18 in Table 2.6 were prepared by miniprep and 0.5 µL aliquoted into 96 well plates. For each T18 or T25 bait protein chosen, an array of two hybrid constructs were transformed in a 96 well plate format as per transformation protocol in 2.13.1.2.

#### **2.13.6 Solid Media Assays**

β-Galactosidase activity of bacterial two hybrid strains were evaluated on solid media using X-Gal. The β-galactosidase hydrolysis of X-Gal produces β-D-galactopyranoside and the visual indicator 5-bromo-4-chloro-3-indole which precipitates with a blue/green colour in media. Single colonies of bacterial two hybrid strains were grown in 100 µL of LB or minimal media containing 100 µg / mL ampicillin and 50 µg / mL kanamycin and 0.5 mM IPTG. 5 µL was spotted onto LB agar with 100 µg / mL Ampicillin, 50 µg / mL Kanamycin, 0.5 mM IPTG and 40 µg / mL

X-GAL and incubated at 37 °C overnight or 30 °C for 48 hours. To allow better differentiation between negative controls and positive samples plates were sometimes further incubated at 4 ° C overnight.

**Table 2.5 T25 Bacterial Two Hybrid Constructs**

<b>SJF Number</b>	<b>Construct</b>	<b>Reference</b>
2273	T25-ftsW	(Steele et al., 2011)
2275	T25-divIC	(Steele et al., 2011)
2276	T25-ezrA	(Steele et al., 2011)
2278	T25-yneS	(Steele et al., 2011)
2280	T25-pbp3	(Steele et al., 2011)
2282	T25-ypsB	(Steele et al., 2011)
2284	T25-ypsA	(Steele et al., 2011)
2286	T25-ylmF	(Steele et al., 2011)
2288	T25-yyaA	(Steele et al., 2011)
2289	T25-zapA	(Steele et al., 2011)
2313	T25-divIB	(Steele et al., 2011)
2314	T25-ftsA	(Steele et al., 2011)
2315	T25-ftsA	(Steele et al., 2011)
2316	T25-ftsL	(Steele et al., 2011)
2317	T25-ftsL	(Steele et al., 2011)
2318	T25-pbp2	(Steele et al., 2011)
2327	T25-ezrA	(Steele et al., 2011)
2330	T25-ftsZ	(Steele et al., 2011)
2335	T25-ezrA	(Steele et al., 2011)
2336	T25-yneS	(Steele et al., 2011)
2337	T25-pbp3	(Steele et al., 2011)
2338	T25-ypsB	(Steele et al., 2011)
2339	T25-ypsA	(Steele et al., 2011)
2340	T25-ylmF	(Steele et al., 2011)
2341	T25-yyaA	(Steele et al., 2011)
2342	T25-zapA	(Steele et al., 2011)
2355	T25-ftsA	(Steele et al., 2011)
2356	T25-ftsL	(Steele et al., 2011)
2357	T25-pbp2	(Steele et al., 2011)
2362	T25-ftsZ	(Steele et al., 2011)
2402	parC-T25	(Steele et al., 2011)
2403	parC-T25	(Steele et al., 2011)
2404	parE-T25	(Steele et al., 2011)
2405	parE-T25	(Steele et al., 2011)
2406	pbpA-T25	(Steele et al., 2011)
2413	parC-T25	(Steele et al., 2011)



2414	<i>parC</i> ~T25	(Steele et al., 2011)
2415	<i>parE</i> ~T25	(Steele et al., 2011)
2417	<i>pbpA</i> ~T25	(Steele et al., 2011)
2418	T25~ <i>yneS</i>	(Steele et al., 2011)
2419	T25~ <i>yneS</i>	(Steele et al., 2011)
2937	T25~ <i>mreC</i>	(Steele et al., 2011)
2938	T25~ <i>mreC</i>	(Steele et al., 2011)
3054	T25~ <i>mreD</i>	(Steele et al., 2011)
3055	T25~ <i>mreD</i>	(Steele et al., 2011)
3175	T25~ <i>pbp2</i>	(Steele et al., 2011)
3176	T25~ <i>zapA</i>	(Steele et al., 2011)
3177	T25~ <i>divB</i>	(Steele et al., 2011)
3178	T25~ <i>pbp2</i>	(Steele et al., 2011)
3179	T25~ <i>zapA</i>	(Steele et al., 2011)
3569	<i>cdsA</i> ~T25	(Steele et al., 2011)
3570	<i>cdsA</i> ~T25	(Steele et al., 2011)
3571	<i>cdsA</i> ~T25	(Steele et al., 2011)
3572	<i>cdsA</i> ~T25	(Steele et al., 2011)
3879	T25~ <i>ftsL</i>	(Steele et al., 2011)
3880	T25~ <i>ftsA</i>	(Steele et al., 2011)
3886	T25~ <i>dnaK</i>	(Steele et al., 2011)
3889	<i>dnaK</i> ~T25	(Steele et al., 2011)
3897	T25~ <i>ltaS</i>	(Steele et al., 2011)
3898	T25~ <i>ltaA</i>	(Steele et al., 2011)
3899	<i>ltaA</i> ~T25	(Steele et al., 2011)
3900	T25~ <i>ypfP</i>	(Steele et al., 2011)
3901	<i>ypfP</i> ~T25	(Steele et al., 2011)
3953	T25~ <i>sosA</i>	(Steele et al., 2011)
5139	T25~ <i>pbp1</i> <sup>stop</sup>	(Wacnik et al., 2022)
5140	T25~ <i>pbp1</i> <sup>pastA</sup>	(Wacnik et al., 2022)
5258	T25~ <i>mecA</i>	This Study, Chapter 3
5259	<i>mecA</i> ~T25	This Study, Chapter 3
5614	T25~ <i>lytH</i>	This Study, Chapter 4
5616	T25~ <i>lytN</i>	This Study, Chapter 4

---

**Table 2.6 T18 Bacterial two hybrid Constructs**

<b>SJF Number</b>	<b>Construct</b>	<b>Reference</b>
1966	T18- <i>ysxC</i>	(Steele et al., 2011)
1967	T18- <i>rpsE</i>	(Steele et al., 2011)
1968	T18- <i>rpsJ</i>	(Steele et al., 2011)
1969	T18- <i>rplQ</i>	(Steele et al., 2011)
1970	T18- <i>glpD</i>	(Steele et al., 2011)
1971	T18- <i>tuf</i>	(Steele et al., 2011)
1972	T18- <i>secA</i>	(Steele et al., 2011)
1973	T18- <i>rpsB</i>	(Steele et al., 2011)
2291	T18- <i>ftsW</i>	(Steele et al., 2011)
2293	T18- <i>ftsZ</i>	(Steele et al., 2011)
2295	T18- <i>divC</i>	(Steele et al., 2011)
2297	T18- <i>ezrA</i>	(Steele et al., 2011)
2301	T18- <i>yneS</i>	(Steele et al., 2011)
2303	T18- <i>ypsB</i>	(Steele et al., 2011)
2305	T18- <i>ypsA</i>	(Steele et al., 2011)
2307	T18- <i>ylmF</i>	(Steele et al., 2011)
2308	T18- <i>yyaA</i>	(Steele et al., 2011)
2310	T18- <i>zapA</i>	(Steele et al., 2011)
2319	T18- <i>divB</i>	(Steele et al., 2011)
2320	T18- <i>divC</i>	(Steele et al., 2011)
2322	T18- <i>ftsA</i>	(Steele et al., 2011)
2323	T18- <i>ftsL</i>	(Steele et al., 2011)
2325	T18- <i>pbp2</i>	(Steele et al., 2011)
2328	T18- <i>yneS</i>	(Steele et al., 2011)
2343	T18- <i>ftsW</i>	(Steele et al., 2011)
2344	T18- <i>ftsZ</i>	(Steele et al., 2011)
2345	T18- <i>divC</i>	(Steele et al., 2011)
2346	T18- <i>ezrA</i>	(Steele et al., 2011)
2347	T18- <i>parC</i>	(Steele et al., 2011)
2348	T18- <i>yneS</i>	(Steele et al., 2011)
2349	T18- <i>ypsB</i>	(Steele et al., 2011)
2350	T18- <i>ypsA</i>	(Steele et al., 2011)
2351	T18- <i>ylmF</i>	(Steele et al., 2011)
2352	T18- <i>yyaA</i>	(Steele et al., 2011)
2353	T18- <i>zapA</i>	(Steele et al., 2011)
3007	T18- <i>ezrA</i>	(Steele et al., 2011)

3012	T18-ftsZ	(Steele et al., 2011)
3174	T18C-zapA	
3439	T18-spa <sup>SS2</sup>	(Steele et al., 2011)
3440	spa <sup>SS1</sup> -T18	(Steele et al., 2011)
3441	T18-ltaS	(Steele et al., 2011)
3442	T18-pbp4	(Steele et al., 2011)
3573	cdsA-T18	(Steele et al., 2011)
3574	cdsA-T18	(Steele et al., 2011)
3876	T18-ypsB	(Steele et al., 2011)
3881	T18-ylmF	(Steele et al., 2011)
3887	T18-DNAK	(Steele et al., 2011)
3888	DNAK-T18	(Steele et al., 2011)
3892	T18-ltaS	(Steele et al., 2011)
3893	T18-ltaA	(Steele et al., 2011)
3894	ltaA-T18	(Steele et al., 2011)
3895	T18-yfpP	(Steele et al., 2011)
3896	yfpP-T18	(Steele et al., 2011)
3952	T18-sosA	(Steele et al., 2011)
5137	T18-pbp1 <sup>stop</sup>	(Wacnik et al., 2022)
5138	T18-pbp1 <sup>pasta</sup>	(Wacnik et al., 2022)
5256	mecA-T18	This Study, Chapter 3
5257	T18-mecA	This Study, Chapter 3
5603	SAOUHSC_01868-T18	This Study, Chapter 3
5604	SAOUHSC_00531-T18	This Study, Chapter 3
5605	SAOUHSC_02134-T18	This Study, Chapter 3
5606	SAOUHSC_03015-T18	This Study, Chapter 3
5607	T18-SAOUHSC_00833	This Study, Chapter 3
5608	SAOUHSC_02912-T18	This Study, Chapter 3
5609	SAOUHSC_00835-T18	This Study, Chapter 3
5610	SAOUHSC_02773-T18	This Study, Chapter 3
5611	T18-SAOUHSC_00435	This Study, Chapter 3
5612	B1T38_13765-T18	This Study, Chapter 3
5613	SAOUHSC_00834-T18	This Study, Chapter 3
5615	T18-lytH	This Study, Chapter 4
5617	T18-lytN	This Study, Chapter 4

---

### 2.13.7 Liquid media assays

The method used was based on Youngman (1990) and Battesti and Bouveret (2012). 4-methylumbelliferyl-beta-D-galactopyranoside (MUG) can be hydrolysed to 4-Methylumbelliferone (MU) and known concentrations of MU be used to relate fluorescence to enzymatic activity to allow comparisons between samples.

A single colony of B2H strains was inoculated into 3 mL of LB with appropriate antibiotics for plasmid maintenance (Section 2.1.1) and incubated overnight. 10 mL of fresh minimal media broth containing appropriate antibiotics and IPTG inoculated with 100  $\mu$ L of culture and incubated at 37 ° C, 250 rpm until OD<sub>600nm</sub> reached approximately 0.5. Triplicate samples of 100  $\mu$ L were collected and cells harvested by centrifugation at 14,000 rpm for 5 min. The supernatant was discarded, and the pellets were stored at -70 ° C. The cell pellets were thawed at RT for 5 min and then resuspended in 0.5 mL ABT (Section 2.4.6.1). 50  $\mu$ L of freshly prepared MUG was added, tubes mixed and immediately incubated at 25 ° C for 60 min. The reaction was stopped by addition of 0.5 mL ABTN (Section 2.4.6.3). Aliquots of 250  $\mu$ L of each sample were pipetted into the top well of a black 96-well flat bottom microtiter plate (Greiner BioOne). Samples were serially diluted in 225  $\mu$ L to 1:1000 and 25  $\mu$ L was removed from the 1:1000 dilution to maintain a consistent well volume of 225  $\mu$ L. The fluorescence of each sample was measured at 355/460 nm, 0.1 s using a HIDEX sense plate reader. MUG units were calculated by the following equation:

$$\frac{\text{Amount MU (pmol)} \times \text{reaction volume (mL)}}{\text{Incubation time (min)} \times \text{sample volume (mL)} \times \text{OD}_{600nm} \times \text{Culture volume (mL)}}$$

Where:	Reaction volume	=	1.05 mL
	Incubation time	=	60 min
	Sample volume	=	0.225 mL
	Culture volume	=	0.1 mL

MUG units of activity were normalised by dividing by the negative control of each plate.

## 2.14 Phage Techniques

### 2.14.1 Preparation of Phage Lysate

To prepare phage lysate of *S. aureus*, donor strains were grown overnight in 5 mL LK, with shaking at 250 rpm, 37 °C. 150  $\mu$ L overnight culture was added to 5 mL phage buffer, 5 mL fresh growth medium (TSB) and 200  $\mu$ L phage. Samples were incubated at 25°C without agitation

overnight or until the mixture had totally cleared. Lysates were filter sterilised through a 0.45 µm syringe filter and stored at 4 °C.

### **2.14.2 Phage Transduction**

Strains were grown at 37°C with shaking overnight in 50 mL LK (Section 2.1.5) with appropriate antibiotics for maintenance of plasmids. Cells were harvested by centrifugation at 4600 rpm 4 °C for 10 minutes and re suspended in 3 mL LK. 500 µL recipient strain was added to 1 mL LK, 10 µL 1M CaCl<sub>2</sub> and 500 µL phage lysate. Controls were prepared with 500 µL of recipient cells, 1.5ml LK, 15 µL 1M CaCl<sub>2</sub> (no phage control). Samples were incubated for 25 min at 37 °C without shaking, samples were incubated for a further 15 min with agitation at 250 rpm.

1 mL ice cold 0.02M NaCit was added, and samples incubated for 5 minutes on ice prior to centrifugation at 5000 rpm for 10 min at 4 °C. The supernatant was removed, and cells resuspended in 1 mL ice cold 0.02 M NaCit and incubated on ice for 45 min. 100 µL aliquots were spread onto LK plates with sodium citrate and antibiotics appropriate to select for donor phage material, added prior to cooling. Plates were incubated at 37 °C for at least 24 hours or until colonies developed.

## **2.15 Microscopy Techniques**

### **2.15.1 Fixing of Cells for imaging**

Overnight cultures were grown in appropriate antibiotics and IPTG as required. 100 µL of each overnight was added to 5 mL fresh growth medium and grown to OD<sub>600nm</sub> 0.4 – 0.7, centrifuged at 4500 rpm for 10 minutes and pellets resuspended in 1 mL PBS.

Cells were protected from light throughout the preparation process. Cells were centrifuged and resuspended in 300 µL of PBS and 20 µL of NHS-ester was mixed with 100 µL of 2 mM Alexa Fluor™ 647 NHS Succinimidyl Ester (AF647). Samples were incubated on a rotating platform for 10 minutes and centrifuged (13000 rpm, 5 minutes) with 200 µL PBS. Fixation was performed by adding 1 mL of freshly prepared paraformaldehyde (PFA) (Section 2.5) and samples incubated in the dark at room temperature for 30 minutes. Fixed cells were washed twice with dH<sub>2</sub>O and mounted using compressed air on poly-L-lysine coated slides (Thermo Fisher). Slow fade gold (Invitrogen, S36937) was added to fixed samples prior to addition of coverslips.

## **2.15.2 Microscopy**

Structured illumination microscopy was performed on a DeltaVision deconvolution microscope (Applied, precision, GE Healthcare) and was kindly conducted by Dr. Mariana Tinajero-Trejo and Dr. Lucia Lafage. Appropriate wavelengths for selected stains/fluorophores NHS-ester (355nm) and GFP (488nm) were used.

## **2.15.3 Image processing**

Images were processed using Fiji (ImageJ, 2.9.0/1.53t) (Schindelin et al., 2012), wavelengths assigned visible colours as required and unless otherwise stated micrographs shown are average intensity projections generated using z-stacks. Brightness was adjusted to match that of the negative controls.

## **2.16 DNA Sequencing**

### **2.16.1 Sanger Sequencing**

Samples were submitted to Source Biosciences (<https://sourcebioscience.com>) for Sanger Sequencing.

### **2.16.2 Whole Genome Sequencing**

Samples were submitted to Microbes NG, (<https://microbesng.com>) for whole genome sequencing. Samples were submitted on dry ice as purified genomic DNA or as strains in lysis buffer.

### **2.16.3 Data Analysis**

NCTC8325 whole genome sequence (accension number NC\_007795) was used as a reference for comparison. This pipeline for data analysis was optimised and performed by MicrobesNG (Birmingham UK), this included reporting of discriminatory mutations. The variant calling spreadsheets were transposed and filtered using Microsoft Excel, and for each mutation present in a gene given a score using =COUNTIF([Sample\_data\_range], "<>"), and resulting scores filtered from low (occurring in only one strain) to high (occurring in multiple to all strains).

# Chapter 3 Penicillin binding protein interaction mapping using the bacterial two hybrid system.

## 3.1 Introduction

Building detailed and mechanistic understanding of how *S. aureus* synthesises peptidoglycan, forms the septal plate and coordinates cell division requires characterisation of the complicated network of protein-protein interactions within the cell. The synthesis of peptidoglycan, the main constituent of the cell wall is supported by the staphylococcal penicillin binding proteins. *S. aureus* has 4 PBPs of which two are essential, PBP1 and PBP2 (Pinho et al., 2013). Furthermore, *S. aureus* is an important antibiotic resistant pathogen supported by the acquisition of a novel PBP, PBP2A (Lim and Strynadka, 2002). Thus, understanding how the complex mechanism of cell wall homeostasis is maintained in the presence of cell wall targeting antibiotics makes the study of the protein-protein interactions vitally important.

In *S. aureus*, the high molecular weight monofunctional transpeptidase PBP1 is essential for bacterial cell division (Sandro F. F. Pereira et al., 2009). PBP1 has a transpeptidase domain and two penicillin binding and serine/threonine kinase-associated domains (PASTA) (Wacnik et al., 2022). PBP1 has multiple roles as a regulator of division and linking the peptide side chains of newly synthesised glycan strands, thus contributing to the complex structures of peptidoglycan during septum formation (Wacnik et al., 2022).

PBP1 has a stabilising role during cell division, mediated through interactions with interacting proteins. For instance, FtsW, which has transglycosylase activity, polymerases lipid II into peptidoglycan, acts as a cognate pair with PBP1 allowing normal incorporation of peptidoglycan at the septum (Taguchi et al., 2019, Reichmann et al., 2019). The complexity of cell division and septum formation is mediated by a range of intraprotein interactions. PBP1 has been shown to interact with PBP2, RodA, EzrA, FtsW, DivIB and DivIC by bacterial two hybrid assay (Steele et al., 2011). More recently the mechanism by which PBP1 interacts with other essential proteins has been more closely examined at a protein domain level (Wacnik et al., 2022). Truncation of the peptidoglycan binding, PASTA domains results in reduced interaction with DivIB and FtsW but other known interacting partners are unaffected suggesting they are N terminal interactions (Wacnik et al., 2022).

While PBP1 has transpeptidase activity, it has been shown to interact with PBP2 (Bottomley, 2011; Steele et al., 2011), a high molecular weight, class A PBP involved in the final stages of

peptidoglycan biosynthesis which is the primary transpeptidase involved in cell wall synthesis (Georgopapadakou et al., 1986). In *S. aureus* PBP2 is the only bifunctional enzyme involved in peptidoglycan biosynthesis with both glycosyltransferase and transpeptidase activity (Lovering et al., 2007). PBP2 is recruited to the septal division plate by its pentapeptide substrate, but this is prevented by acylation in the presence of oxacillin (Pinho and Errington, 2004)

In addition to substrate mediated localisation, PBP2 has multiple interactions within the cell division machinery and interacts with PBP1, PBP2A and the staphylococcal monofunctional transferases MGT and SgtA (Reed et al., 2011). PBP2 has also been evidenced as having a cooperative function with PBP4 and PBP2A (Łęski and Tomasz, 2005).

MRSA is mediated via the acquisition of a novel penicillin binding protein called PBP2A with a low affinity for antibiotics (Brown and Reynolds, 1980; Chambers et al., 1985). The PBP2A interactions with PBP2 highlights their cooperation and shared role in the maintenance of resistance to antibiotics. PBP2 transpeptidase activity is essential in MSSA but it is not required in MRSA expressing PBP2A, therefore this functionality of PBP2 is compensated for by PBP2A (Pinho et al., 2001). It was subsequently shown that mutagenesis of PBP2 transpeptidase activity reduces resistance from  $\geq 256 \mu\text{g/mL}$  to  $12 \mu\text{g/mL}$  (Pinho et al., 2009). In the presence of oxacillin, acylated PBP2 can be localised by the presence PBP2A (Pinho and Errington, 2004). PBP2A is responsible for transpeptidation in cell wall synthesis when  $\beta$ -lactams inactivate PBP2 (Lim and Strynadka, 2002).

Despite the presence of PBP2A not affecting doubling times in comparison to the SH1000 parent, it has profound effects on the physiology of the cells, with 193 genes being differentially expressed including upregulation of nitrate reductase regulators (Panchal et al., 2020). Characterising the protein interactions necessary to support the role of PBP2A in resistance are all important for studying the mechanisms of staphylococcal cell division especially in the presence of antibiotics (Salamaga et al., 2021).

The propensity of PBP2A to attain misfolded conformations necessitates the extra cellular folding factors PrsA and HtrI in maintaining antibiotic resistance (Roch et al., 2019). PBP2A has also been shown to interact with FloA in the context of membrane microdomain assembly (García-Fernández et al., 2017). However, the interactions of PBP2A have never been characterised systematically. Therefore, using a library of genetic constructs to probe for previously unknown interactions could further understanding of its specific role in cell growth and division in the presence and absence of antibiotics.



A wide range of methodologies each with their own strengths and caveats can be used to interrogate the complex network of protein interactions that support the growth and pathogenicity of *S. aureus*. Table 3.1 details some of the methods used to characterise protein-protein interactions to support investigation of cellular physiology, metabolism, and drug targets across a range of organisms.

Previous experiments in our laboratory and many other research groups have successfully used the bacterial two hybrid system to interrogate interactions between staphylococcal proteins (Steele et al., 2011; Wacnik et al., 2022; Wood et al., 2019). The bacterial two hybrid system uses *E. coli* allowing the reconstitution of a cAMP signalling pathway. The adenylate cyclase gene is split into two fragments, encoding proteins of 18 kDa and one 25 kDa. These interacting proteins re-constitute the signalling pathway transcriptionally activating a reporter gene: *lac* or *mal* (Karimova et al., 1998). The *E. coli* BTH101 strain (SJF 1953) used has a low frequency of *lac*<sup>+</sup> revertants (Karimova et al., 1998) making it a reliable expression system for the reporting vectors. The bacterial two hybrid system also allows the use of liquid assays to quantify interactions using the hydrolysis of 4-methylumbelliferone (Karimova et al., 1998). The principle of the two-hybrid assay is summarised in Figure 3.1.

In *E. coli* the bacterial two hybrid system was used to identify the multiple interactions between the Fts proteins, where specific deletion mapping analysis of FtsQ and FtsI allowed the identification of essential regions for these interactions and demonstrated the suitability of the two-hybrid technique for mapping interactions of membrane spanning proteins (Karimova et al., 2005). The bacterial two hybrid assay is a powerful tool which have previously been used to identify and verify interactions between many *S. aureus* components, YychH and Yycl, the GTPase ERA and YbeY and YbeZ (Rohrer and Berger-Bächi, 2003).

### **3.1.1 Aims of this chapter**

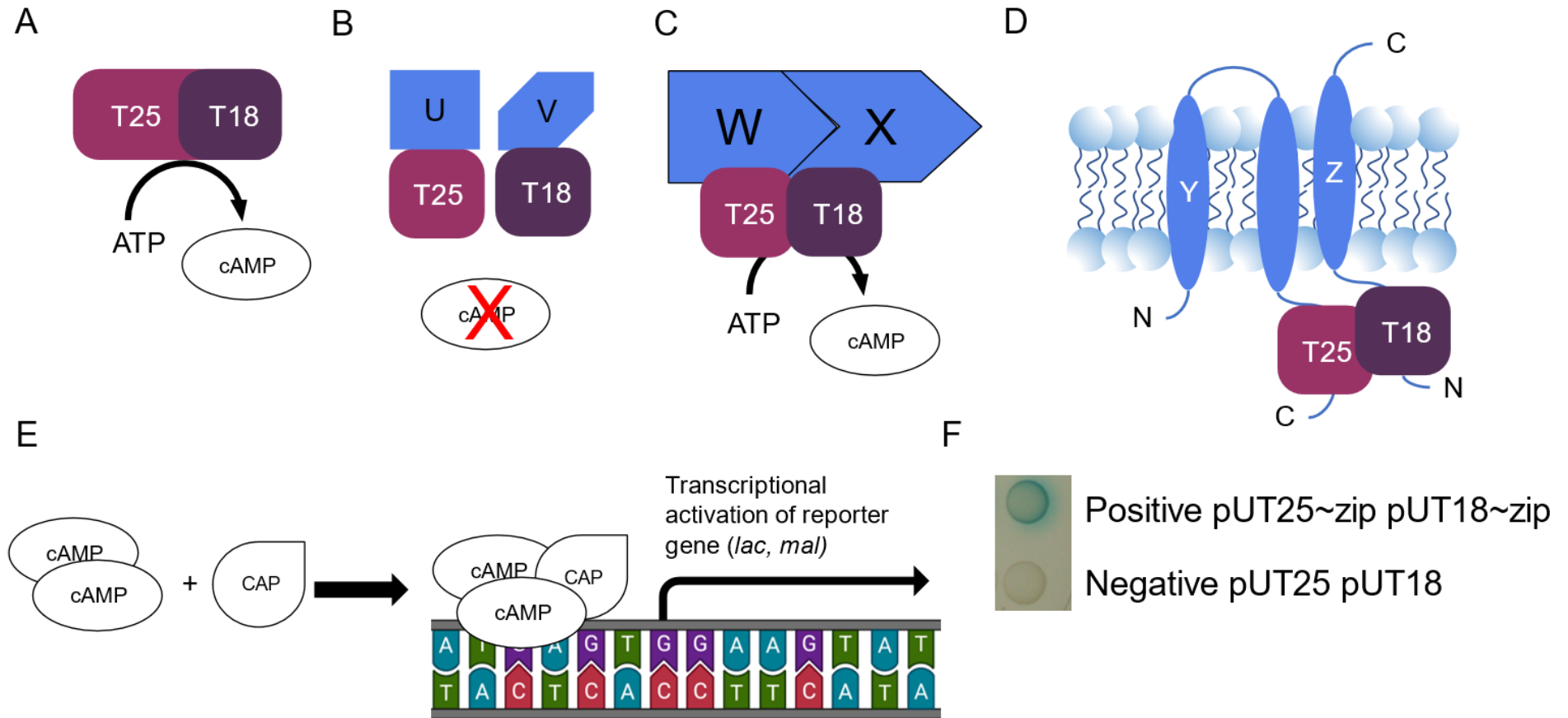
The overall aim of this chapter was to conduct bacterial two hybrid library screening to investigate the interactions between the penicillin binding proteins of *S. aureus* essential in cell growth, division, and maintenance of high-level antimicrobial resistance. We hypothesised that screening a bacterial two hybrid library of random genetic constructs could identify previously unknown interactions. The specific aims of this chapter were to:

- I. Develop and optimise a screening protocol for bacterial two hybrid libraries.
- II. Screen bacterial two hybrid libraries to identify novel interacting partners of PBP1, PBP2 and PBP2A.
- III. Test the novel putative interactions using full length gene constructs.

**Table 3.1. Methods used to characterise Protein-Protein interactions.**

Comparison of Scientific methods used to characterise and investigate protein-protein interactions.

Method	Scientific Principle	Key Considerations	Reference
Split-Luciferase	Nanometric measurement of fluorescence in relation to gene expression and interactions using the firefly luciferase enzyme that oxidizes D-luciferin in the presence of oxygen, yielding a quantifiable fluorescent product.	Live cells, can be used in any organism able to maintain required plasmids, requires multiple constructs for each protein and orientation requires testing.	(Kadonaga and Tjian, 1986; Puig et al., 2001; Schmitt et al., 1993; Smale, 2010)
Antibody based	Antibody based assays such as pulldowns and co-immunoprecipitation use a tag such as glutathione-S-transferase, or a fluorescent fusion. cells are lysed and can be fractionated, bait proteins tagged with protein fusion with suitable antibodies. Protein complexes are bound to antibodies conjugated to silica or magnetic beads and eluted for mass spectroscopy.	Expression in the organism of interest, requires antibodies to reporter proteins, successful (over)/expression of bait protein, but tagging of bait protein may disrupt localisation, posttranscriptional modifications, or conformation. Global assay, useful in characterising proteome as part of large-scale functionality studies, identification of hub proteins that are integral to cellular growth.	(Cherkasov et al., 2011; Iqbal et al., 2018)
Bacterial Two Hybrid	Protein proximity reconstitutes a protein split into two subunits resulting in cyclic AMP pathway activation resulting in reporter gene expression. Transcriptional repression and three hybrid systems have also been developed.	Can screen complex protein libraries, Allows interrogation in bacteria of bacterial interactions. Performed in <i>E. coli</i> .	(Karimova et al., 2017, 2000, 1998; Licitra and Liu, 1996)
Yeast Two Hybrid	Interaction between two proteins result in activation of reporter genes enabling growth on specific media or production of a colour.	Can be automated for high throughput screening, inexpensive and easily implemented but original methodology was restricted to interactions occurring in the yeast nucleus.	(Brückner et al., 2009)
Crosslinking Mass Spectroscopy	Cells are chemically cross linked and enzymatically digested and analysed by mass spectroscopy and data analysed using knowledge of secondary structure cross linking, previous network analysis and distance constraints.	The choice of cross-linking agent must consider how well they penetrate the cell or tissue sample, whether a cleavable cross linker is required and the impacts of the modifications that might occur to amino acids as a result of cross linking.	(Götze et al., 2019; Leitner et al., 2016; Petrotchenko and Borchers, 2010; Yu and Huang, 2018)



**Figure 3.1 Principle of the bacterial two hybrid (BACTH) assay for determining protein-protein interactions *in vivo*.**

The adenyl cyclase toxin produced by *Bordetella pertussis* which catalyses the production of cyclic AMP (A) was previously split into two portions (B) one 18 kDa and one 25 kDa which can be fused to potential interacting proteins (U and V), (C) when paired with interacting proteins W and X they reconstitute the cAMP signalling pathway. Reporter proteins can also be fused to membrane spanning proteins to identify interactions (D). Production of cAMP results in the transcriptional activation of reporter genes (E) resulting in a colour change on chromogenic agar (F). Adapted from Battesti and Bouveret (2012).

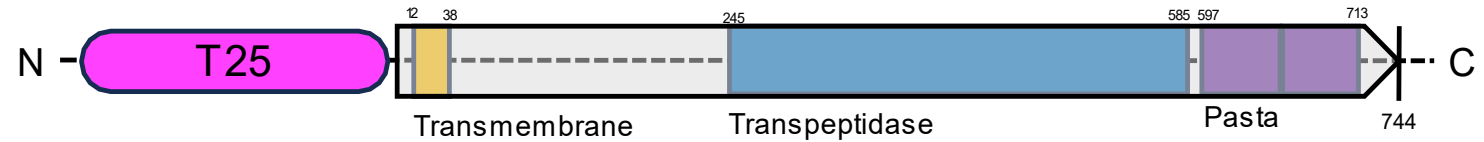
## **3.2 Results**

### **3.2.1 Screen of bacterial two-hybrid libraries**

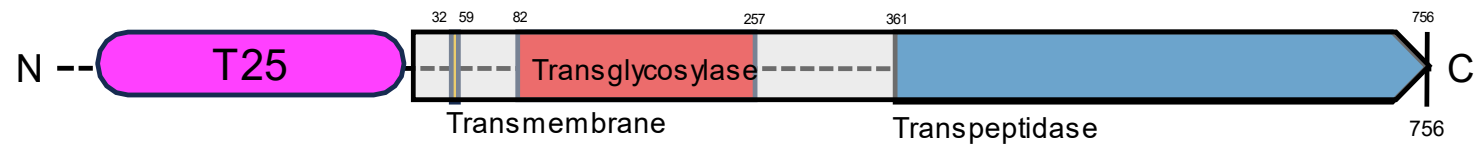
The screen aimed to investigate interactions between native staphylococcal PBP1, PBP2 and the high-level resistance determinant PBP2A. Fusions detailed in Figure 3.2 were used to perform the screening of the two-hybrid library.

N terminal T25 fusions of PBP1 were used to avoid disruption of the transpeptidase and two pasta domains (Sandro F. F. Pereira et al., 2009), N terminal fusions of PBP2 and both N and C T25 terminal fusions of PBP2A were used to maximise detection of interacting partners in this screen. Diagrammatical representations of the PBP fusions chosen for this screen are shown in Figure 3.2.

T25~PBP1 (SJF 2406)



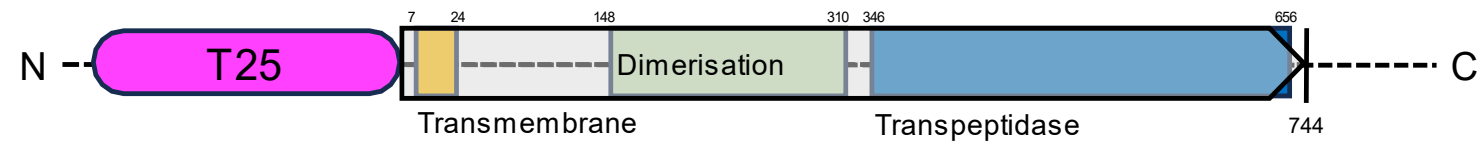
T25~ PBP2 (SJF 2329)



PBP2A~T25 (SJF 5258)



T25~ PBP2A (SJF 5259)



**Figure 3.2. Diagrammatical scale representation of the penicillin binding proteins fused to bacterial two hybrid T25 reporter proteins used in this study.**

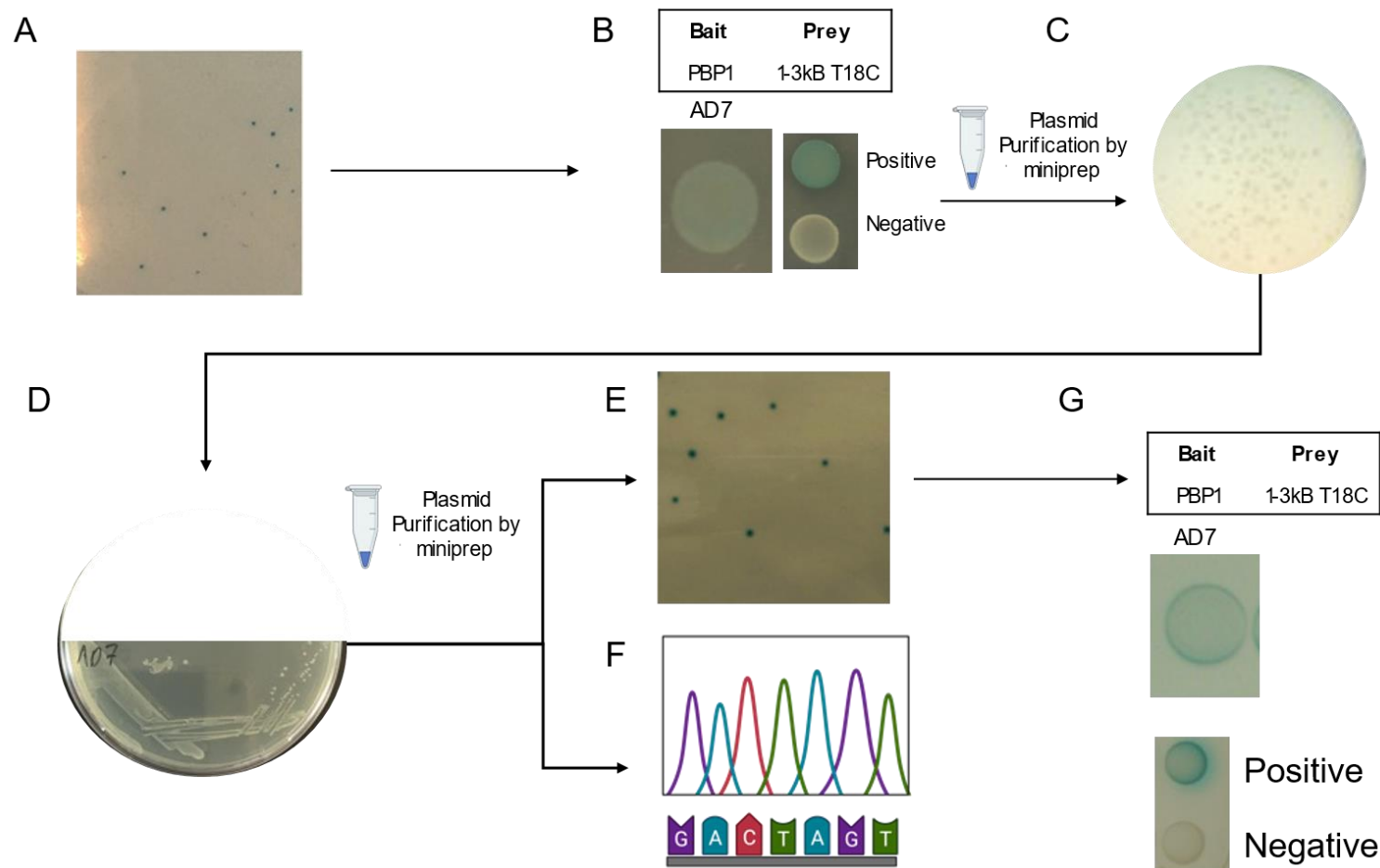
Each of penicillin binding proteins (grey block arrows) 1, 2 and 2A with N or C terminal T25 bacterial two hybrid fusions. Domain position and protein length (aa) shown for each PBP and relevant domains. Shown to scale.

### 3.2.2 Establishing the two hybrid library screening protocol

A protocol for screening bacterial two hybrid libraries was developed which allowed clones to be analysed for interactions with bait proteins of interest while minimising the number of false positive samples identified (Figure 3.3).

To ensure the most library fragments (prey) could be screened against bait proteins as possible, the library was transformed into chemically competent cells containing the bait protein expressing constructs of interest (Figure 3.3.A), instead of co-transformation. Positive interactions were verified by sub-culture on X-GAL containing media that ensured the interaction could still be discerned visually from a negative control (Figure 3.3.B). To verify the strain hadn't generated spontaneous mutations such as in the *cya*<sup>-</sup> gene such resulting in X-GAL precipitation plasmids were isolated by miniprep and retransformed into the parental bacterial two hybrid strain BTH101 (See section 2.3.2) the vector containing the library fusion was selected for using the appropriate antibiotic for the pUT18 vector (Figure 3.3.C). Resulting clones containing the T18 prey plasmids were purified on X-GAL media to confirm no blue coloration could be observed (Figure 3.3.D). To confirm interactions T18 prey plasmids were again purified by miniprep and transformed into bait (PBP) containing competent cells. Clones were grown in selective broth and plated on X-GAL medium as verification of positive interactions (Figure 3.3.E). The second miniprep of the T18 clone was used for Sanger sequencing using T18 specific primers (See primers table Table 2.4). To identify fusion proteins of interest (Figure 3.3.F).

Figure 3.3 details how an individual sample, AD07, progresses through the bacterial two hybrid screening progress.



**Figure 3.3 Progression of a sample through the bacterial two hybrid screening workflow**

(A) Library transformation of genetic library into chemically competent cells containing bait protein constructs fused to reporter genes onto LB X-Gal containing antibiotics selecting clones containing T25 and T18 fusions, blue colonies indicate positive interactions. (B) isolated, purified positive, positive clone showing blue colouration on LB X-Gal agar. (C) Two hybrid reference strain transformed with purified plasmid DNA, selecting for prey protein constructs only using appropriate antibiotic for T18 reporter constructs. (D) Purification of prey protein expressing construct on X-Gal agar to ensure no autoactivation of reporter genes (E) Isolated prey retransformed into competent cells containing original bait protein constructs onto LB X-Gal (F) samples were sanger sequenced using primers specific to the prey proteins two hybrid reporter fusion (G) individual colonies of positive clones were grown in LB X-Gal for at 37 °C 3 hours with shaking and spotted onto X-Gal agar to verify interactions.

### 3.2.3 Screening bacterial two hybrid libraries for PBP interactions

The bacterial two hybrid libraries were kindly provided by Dr. Rebecca Corrigan (University of Sheffield), prepared as described in Wood et al, (2019). Briefly, the libraries were prepared by partial digestion of five independent genomic DNA samples of *S. aureus* with Sau3AI. Digested DNA was run on an agarose gel and fragments of 0.5 – 1 kbp and 1 -3 kbp were extracted and purified. Fragments were ligated into BamHI restriction site of pUT18C or pUT18 (N) and *E. coli* DH5 $\alpha$  transformed with the resulting constructs and plated onto LB agar containing carbenicillin. Plates were scraped and plasmids isolated using a GeneJET plasmid purification kit. Therefore, the combinations of PBP and each library enabled comprehensive screening is shown in Table 3.2. Based on 0.5 kbp fragments in each library created from the 2.8 mbp staphylococcal genome, and assuming a normal distribution of library coverage to achieve 95% genomic coverage > 12,000 colonies needed to be screened for each combination, this has been exceeded with no fewer than 23,000 colonies screened for each combination with the maximum colonies screened for any individual combination being 1.1 million with the bait T25~PBP2A and library 0.5 -1 kbp due to multiple repeats of the transformations of this library being performed on large plates.



**Table 3.2 Total colonies screened for each combination of Bacterial two hybrid libraries and PBP expressing constructs.**

Total number of colonies screened for each bait (PBP) and prey (library) combination.

<b>Bait proteins T25 fusions (SJF Strain number)</b>	<b>T18 C terminal Libraries</b>		<b>T18 N terminal Libraries</b>	
	0.5 -1 kbp	1-3 kbp	0.5 -1 kbp	1-3 kbp
T25~PBP1 (SJF 2406)	75026	23978	23139	25764
T25~ PBP2 (SJF 2329)	57786	172861	55188	63643
PBP2A~T25 (SJF 5258)	26780	28095	34246	39009
T25~ PBP2A (SJF 5259)	1189318	860698	56695	36891

### **3.2.3.1 C terminal T18 fusion library screening**

For each interaction screen using 4 bait constructs (PBP1, PBP2, PBP2A C and PBP2A N and the two T18 C libraries (0.5 - 1 and 1 - 3 kbp), at least 23,000 clones were screened. All screens yielded at least one initial positive clone. During the rigorous verification process there was a steady attrition of positive hits. In fact, after full screening only four interaction trials yielded clones to take forward for sequencing (Table 3.3). In particular PBP1, T25 screened against the 0.5 – 1 KBP C-terminal T18 library was the most successful with 68 clones sequenced. Only a total of 6 verified clones progressed through to sequencing from all the other Prey/Bait combinations. Bioinformatics was then carried out on all sequences to identify potential interacting fusions.

The PBP1 screen identified 184 positive clones from 75026 negative clones. Only 82 clones showed positive interactions in the interaction assay. Bioinformatics analysis of 49 sequences resulted in one positive in frame fusion (Appendix 6). The PBP2 screen identified 251 positive clones from 57786 negative clones. Only three of the isolated 33 positive clones from the screening plates showed a positive interaction in the interaction assay. The 1-3 kbp T18 C library yielded no positive interactions at the end of the two-hybrid pipeline for any bait proteins despite identifying 372 positive clones from initial screening and screening more than 20,000 clones for each bait protein,

**Table 3.3 Summary of bacterial two hybrid screening of C terminal T18 fusion libraries of 0.5- 1 kbp and 1-3 kbp sized fragments**

Strains of chemically competent cells containing PBP1 T25, PBP2 T25, PBP2A N T25, PBP2A C T25 were transformed with genomic libraries of 0.5- 1 kbp and 1-3 kbp sized fragments from genomic digest ligated into the pUT18C vector. At each stage, the number of colonies that passed the verification step are shown in black and the number of colonies that failed to give the expected result are shown in red.

Prey	0.5-1kbp T18C								1-3kbp T18C							
	PBP1 T25		PBP2 T25		PBP2A N T25		PBP2A C T25		PBP1 T25		PBP2 T25		PBP2A N T25		PBP2A C T25	
Bait	+	-	+	-	+	-	+	-	+	-	+	-	+	-	+	-
Library Transformation Plate	184	75026	251	57786	2	26780	224	1189318	44	23978	194	172861	1	28095	133	860698
Isolated from screening plate	179	0	33	0	2	0	21	0	30	0	20	0	1	0	35	0
Isolated pure culture	169	10	30	3	2	0	21	0	20	10	16	4	1	0	30	5
Verified Positive (Patch Plate)	119	50	24	6	2	0	12	9	15	5	8	8	1	0	10	20
Verified White (Sub-culture)	115	4	24	0	2	0	11	1	13	2	8	0	1	0	8	2
Positive when retransformed against PBP	115	32	16	8	2	0	11	0	13	0	8	0	1	0	8	0
Positive in Interaction Assay	83	21	3	13	0	2	2	9	4	9	0	8	0	1	0	8
Sequencing	62	13	3	0	0	0	2	1	3	1	0	0	0	0	0	0
Bioinformatics	49	0	3	0	0	0	1	0	3	0	0	0	0	0	0	0

### **3.2.3.2 N terminal T18 fusion library screening**

For each interaction screen using four bait constructs (PBP1, PBP2, PBP2A C and PBP2A N T25) and the two T18 N libraries (0.5 - 1 and 1 - 3 KBP), at least 23,000 clones were screened. All screens apart from PBP2 T25 vs the 1-3 kbp T18N library yielded at least one initial positive clone. During the rigorous verification process there was a steady attrition of positive hits.

Use of PBP1 as a bait against the 0.5 -1 kbp library resulted in four positive clones during sequence analysis for in frame fusions, from the 15 colonies isolated during initial screening. PBP2 Screening of both the N terminal 0.5 – 1 kbp and 1- 3 kbp libraries with the bait protein PBP2 yielded no positive interactions at the end of the two-hybrid pipeline despite screening more than 55,000 clones for each library. PBP2A N screening resulted in eight samples through to bioinformatics. In particular PBP2A C T25, screened against the 1-3 kbp T18 N library was the most successful with 18 clones sequenced. After full screening six of the eight interaction trials yielded clones to take forward for sequencing Table 3.4. In total 39 verified clones progressed through to sequencing from all the other Prey/Bait combinations. Bioinformatics was then carried out on all sequences to identify potential interacting fusions.

**Table 3.4. Summary of bacterial two hybrid screening of N terminal T18 fusion libraries of 0.5- 1 kbp and 1-3 kbp sized fragments**

Strains of chemically competent cells containing PBP1 T25, PBP2 T25, PBP2A N T25, PBP2A C T25 were transformed with genomic libraries of 0.5- 1 kbp and 1-3 kbp sized fragments from genomic digest ligated into the pUT18 (N) vector). At each stage, the number of colonies that passed the verification step are shown in black and the number of colonies that failed to give the expected result are shown in red.

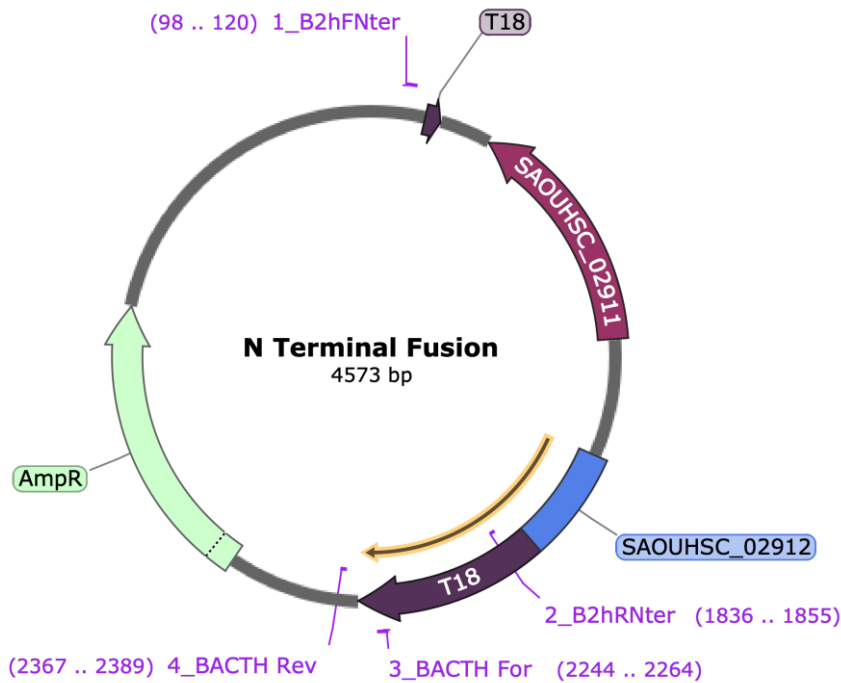
Prey	0.5-1kbp T18N								1-3kbp T18N							
	PBP1 T25		PBP2 T25		PBP2A N T25		PBP2A C T25		PBP1 T25		PBP2 T25		PBP2A N T25		PBP2A C T25	
Bait	+	-	+	-	+	-	+	-	+	-	+	-	+	-	+	-
Library Transformation Plate	15	23139	0	55188	7	34246	54	56695	29	25764	0	63643	25	39009	45	36891
Isolated from screening plate	15	0	0	0	7	0	47	0	24	0	0	0	25	0	45	0
Isolated pure culture	13	2	0	0	7	0	47	0	20	4	0	0	25	0	45	0
Verified Positive (Patch Plate)	8	5	0	0	3	4	37	10	10	10	0	0	21	4	29	16
Verified White (Sub-culture)	8	0	0	0	3	0	34	3	10	0	0	0	20	1	29	0
Positive when retransformed against PBP	8	0	0	0	3	0	34	0	10	0	0	0	20	0	29	0
Positive in Interaction Assay	7	1	0	0	1	2	12	22	8	2	0	0	11	9	22	7
Sequencing	7	0	0	0	1	0	11	1	8	0	0	0	10	1	20	0
Bioinformatics	4	3	0	0	1	0	9	1	6	2	0	0	8	2	18	2

The comprehensive library screening performed resulted in over 2.5 million individual colonies being screened for possible interactions between the proteins encoded by the vectors and the bait proteins. Colonies were most likely to be identified as being a false positive during their verification for X-Gal hydrolysis on a patch plate. Screening of the N terminal libraries was the most successful identifying over 39 positive hits. In total 1208 positive clones were isolated as positive transformants during the library transformation stage however only 41 of these were positive hits after sequencing and bioinformatics analysis had been completed.

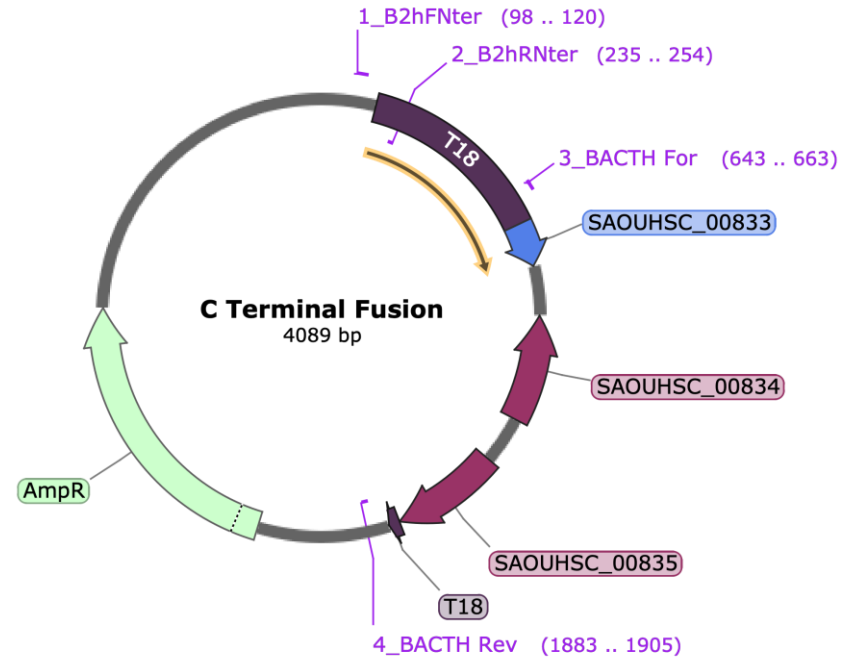
### **3.2.3.3 Identifying interacting protein partners**

To identify the proteins of interest fused to the bacterial two hybrid reporter genes samples were submitted for Sanger sequencing at Source Biosciences (Cambridge, UK). Primers specific to the N and C termini of the bacterial two hybrid vectors (N terminal primers 1 and 2, C terminal primers 3 and 4) were used to identify in frame fusions (Figure 3.4). Figure 3.4 shows the bacterial two hybrid vectors pUT18 (N) and pUT18(C) and BamHI restrictions site ligations of regions of gDNA from the *S. aureus* genome to illustrate how in frame fusions of proteins to reported genes occur during library construction.

A. pUT18 (N)



B. pUT18C



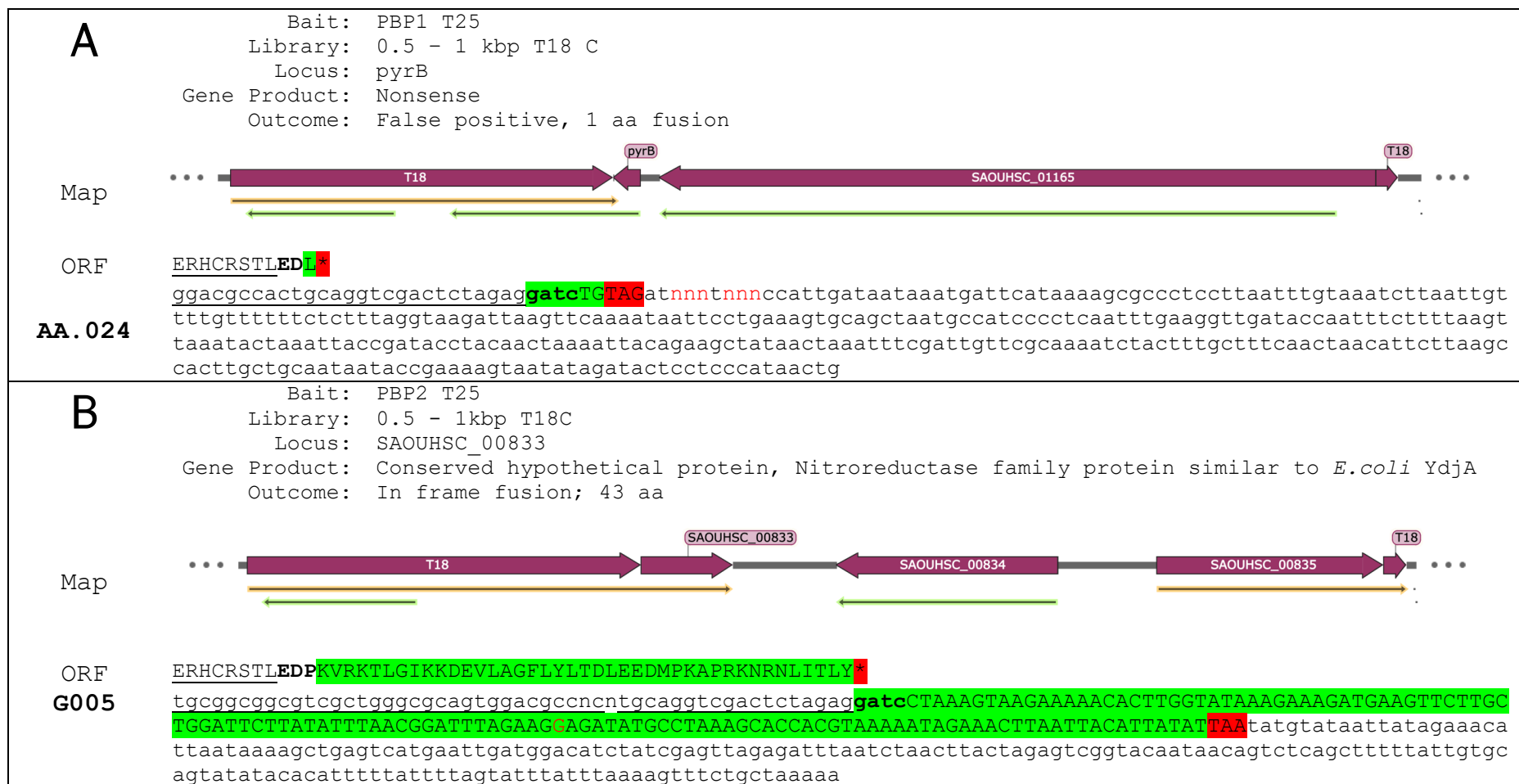
**Figure 3.4 Plasmid maps of bacterial two hybrid vectors pUT18(N) and pUT18(C) with a gDNA fragment ligated into the BamHI restriction site**

Bacterial Two hybrid vectors showing two hybrid primers (purple) used for sequencing inserted genes shown in purple flanking N and C terminal BamHI restriction site. Open reading frame in frame with T18 two hybrid reporter shown as black arrow and the gene of interest (Blue) fused to the two hybrid reporter (T18) in frame fusion shown in blue. Insert size in ligated pUT18(N) 1550 bp (A), in ligated pUT18(C) 1072 bp (B).

Resulting sequences were aligned to the *S. aureus* genome (NCTC8325, accession number [NC\\_007795.1](#)) using SnapGene Software.

Appendix 1 details, for each library and bait protein screened the loci nearest to the T18 reporter gene, and details of the length of fusion. *In silico* analysis of DNA fragments was used to assemble plasmid maps to identify in frame fusions of proteins of interest to the bacterial two hybrid T18 reporter gene product. Diagrams of inserts, DNA sequence and amino acid translations can be found in Appendix 2. Fusions were identified as being over 10 amino acids in frame of a known protein coding sequence in frame with the T18 reporter protein encoding gene Figure 3.5.





**Figure 3.5 Example analysis of in frame negative (A) and positive (B) fusions from bacterial two hybrid screen.**

Analysis of sequencing data to identify in frame fusions of genes of interest with the bacterial two hybrid reporter T18. (A) False Positive result and (B) positive in frame fusion with reporter gene products. Gene product identified by protein BLAST of in frame amino acid sequence. Vector DNA sequence underlined, with restriction site in bold Stop highlighted in **red**, amino acid stop codons denoted by \* and translated fusion region highlighted in **green**.

Fusions were classified as in frame fusions, denoting positive interactions, false positives, denoting nonsensical amino acid sequences that don't align to translated proteins. Summaries of the protein fusions can be found in (Appendix 2). Fusions, and their aligned genes are summarised by library in Table 3.5.

#### **3.2.3.4 Bioinformatics analysis of putative hits**

Table 3.5 shows the outcome of bioinformatics analysis of the sequencing data obtained. All the screened libraries aside from 1 – 3 KBP T18 C resulted in successful in frame fusions with a total of 12 genes identified. In total fusions of between 10 and 132 aa in length were identified.

Screening of the 1-3 kbp T18N library identified a 10 aa segment of SAOUHSC\_01868, the dipeptidase, *pepV*, which has homology to the  $Mn^{2+}$  dipeptidase *Sapep*, as interacting with the bait protein PBP2A C T25. The same library also identified interactions with the alternative T25~PBP2A N construct which was demonstrated as interacting with a 21 aa segment of SAOUHSC\_03015, HisZ, a regulatory subunit of ATP phosphoribosyltransferase. The bait protein PBP2 T25 was demonstrated as interacting with a 128 aa segment of SAOUHSC\_00531, a hypothetical protein with homology to multispecies amidohydrolases during screening of this library.

In the screen of the 0.5 – 1 kbp T18 C library the bait protein PBP2 T25 was demonstrated as interacting with a 43 aa segment of SAOUHSC\_00833, a hypothetical protein from the nitroreductase family of proteins, and the bait protein PBP1 T25 was demonstrated as interacting with a 109 aa segment of SAOUHSC\_00835, arsenate reductase.

In screening the 0.5 – 1 kbp T18 C and the T18 N libraries the bait proteins PBP1 and PBP2 T25 were shown to have interactions with portions of SAOUHSC\_00833 and SAOUHSC\_00835, two genes from the same operon. These repeated interactions arising from different screens could indicate genes involved in the same processes and therefore interacting in the cell. SAOUHSC\_00834 was therefore treated as a putative interacting partner,

Fusions of the same three genes SAOUHSC\_00435, 02134 and 02773 were independently isolated multiple times within the library screening. SAOUHSC\_02773 was identified as a positive interacting in frame fusion in screens of the 1 – 3 kbp T18 N library with both the bait proteins PBP2A C T25 and N T25.

### **3.2.4 Confirmation of novel interactions using full length gene constructs of identified proteins**

Due to the library preparation process (See 3.2.1), genes identified in this study are partial fusions in frame with bacterial two hybrid reporter genes. To confirm and characterise interactions between the genes of interest (GOIs), full length fusions were screened against the bait proteins they were identified as interacting with.

#### **3.2.4.1 Gibson Assemblies**

The Gibson assembly technique (Figure 3.6) was chosen to construct in frame fusions of genes of interest to the N or C termini of T18. Genes of interest were amplified by PCR of SH1000 gDNA using Gibson assembly primers. Detailed for each construct in Figure 3.8 and Figure 3.8. Positive clones were identified using colony PCR using the same primers. Positive clones were verified by plasmid extraction, and restriction digest using enzymes specific to the insert and vector (Figure 3.8 and Figure 3.8). Plasmids were sequenced using Gibson assembly primers by Source Biosciences to verify fusions.

#### **3.2.4.2 Commercial Gene synthesis**

The samples detailed in Table 3.6 were subcontracted to Genewiz and the details of their construction and results of internal QC can be found in Appendix 3 (Genewiz order reference 40-541290844-07-27-2021\_074346).

**Table 3.5 Summary of in frame fusions by library from bacterial two hybrid screening.**

The library origin and the bait proteins which generated positive interacting clones are shown as is the number of times the same fusion was identified from the library. The length of the fusion in frame with the T18 bacterial two hybrid reporter and the putative gene products identified from protein-protein BLAST search (genome used [NC\\_007795.1](#)) and their subcellular localisation, is also shown.

Library	Bait	Gene Locus	Number of Gene Hits	Fusion length	Gene Product
0.5-1kbp T18C	PBP1 T25	No locus tag	1	21	hypothetical protein BIT38_13765
	PBP2 T25	00833	1	43	Conserved hypothetical protein, Nitroreductase family
0.5-1kbp T18N	PBP1 T25	00835	1	109	Arsenate reductase
	PBP2A C T25	00435	9	47	Glutamate Synthase, Large Subunit
1-3kbp T18N	PBP1 T25	00531	1	128	Hypothetical protein; homology to MULTISPECIES: amidohydrolase
		02134	2	132	Nitric oxide synthase oxygenase
	PBP2A C T25	01868	1	10	Dipeptidase pepV; Homology to Mn(2+)-dependent dipeptidase <i>Sapep</i>
		02773	15	27	Putative Transporter, Homology to AbgT putative transporter family
		02912	1	106	Unknown Protein, Homology to glyoxalase/bleomycin resistance/extradiol dioxygenase family protein
	PBP2A N T25	03015	1	21	HisZ, ATP phosphoribosyltransferase regulatory subunit
		02773	7	27	Putative Transporter, Homology to AbgT putative transporter family
		02333	1	16	MULTISPECIES: NADH-dependent flavin oxidoreductase

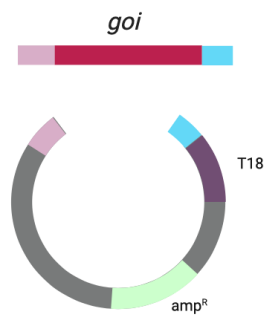
① Inserts amplified from SH1000 gDNA with gibson overhang primers



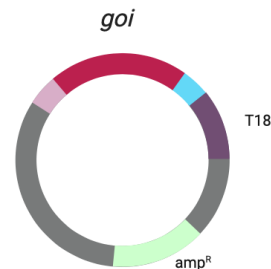
② Vector linearised by restriction digest



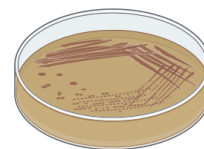
③ Gibson assembly



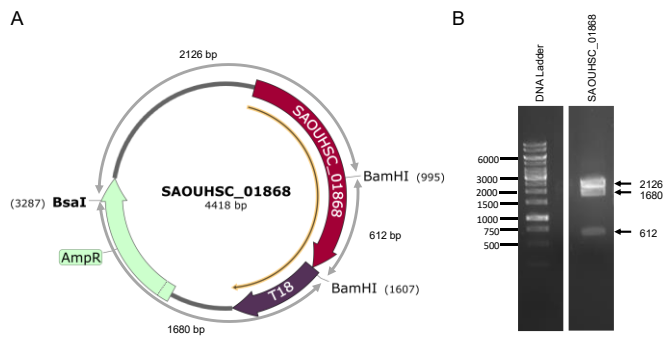
④ Assembled vector



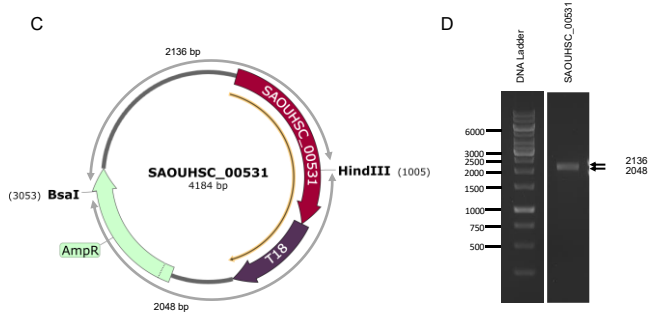
⑤ Bacterial transformation and confirmation by colony PCR



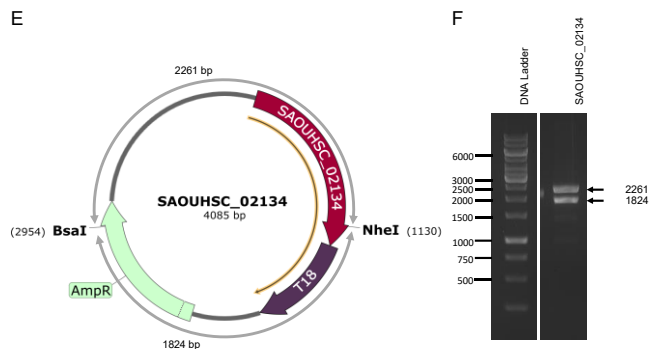
**Figure 3.6 Schematic of Gibson assembly to create in frame fusion of gene of interest (*goi*) fusions to BACTH reporter (T18) in pUT18 vectors.**  
*amp<sup>R</sup>* Ampicillin resistance cassette



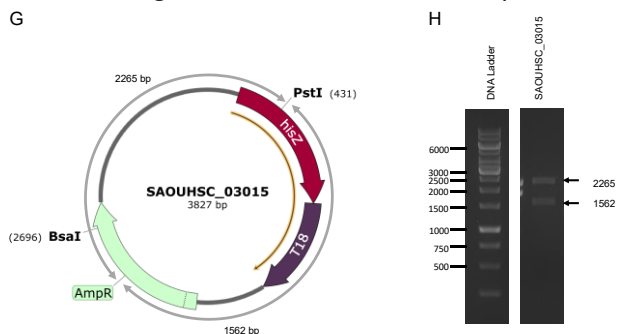
A. SAOUHSC\_01868 (primers 7 and 8) fusion pUT18 with in frame T18, vector digested with HindIII and PstI.  
 B. Verification digest BamHI and BsaI (Bands of expected sizes at 2126, 1680 and 612 bp).



C. SAOUHSC\_00531 (primers 23 and 24) fusion pUT18 with in frame T18, vector digested with HindIII and PstI.  
 D. Verification digest HindIII and BsaI (Bands of expected sizes at 2136 and 2048 bp).



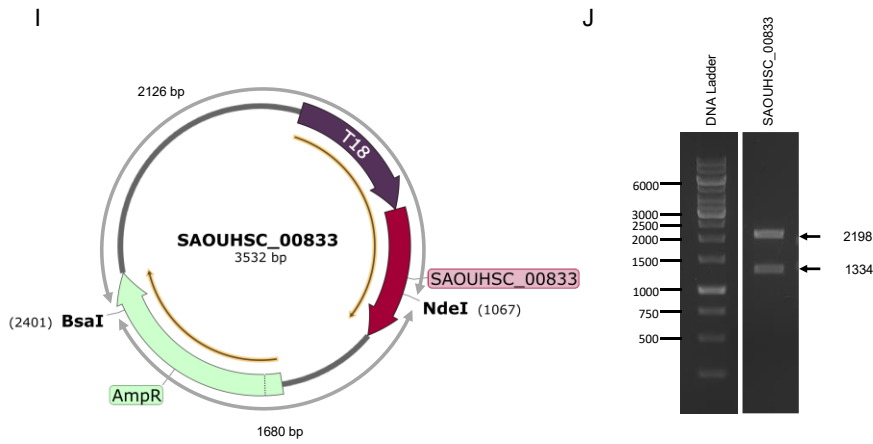
E. SAOUHSC\_02134 (primers 13 and 14) fusion pUT18 with in frame T18, vector digested with HindIII and PstI.  
 F. Verification digest BamHI and BsaI (Bands of expected sizes at 2261 and 1824 bp).



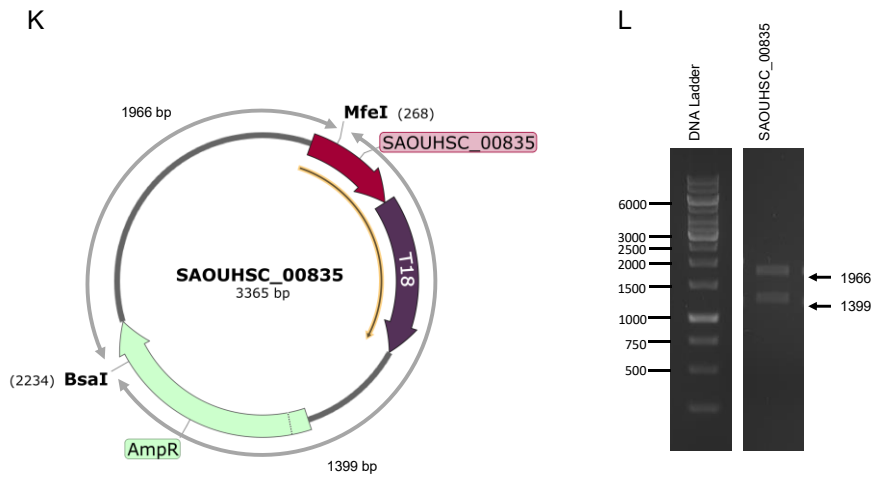
G. SAOUHSC\_03015 (primers 21 and 22) fusion pUT18 with in frame T18, vector digested with HindIII and PstI.  
 H. Verification digest PstI and BsaI (Bands of expected sizes at 2265 and 1562 bp).

**Figure 3.7 Plasmid maps and restriction digests of B2H constructs.**

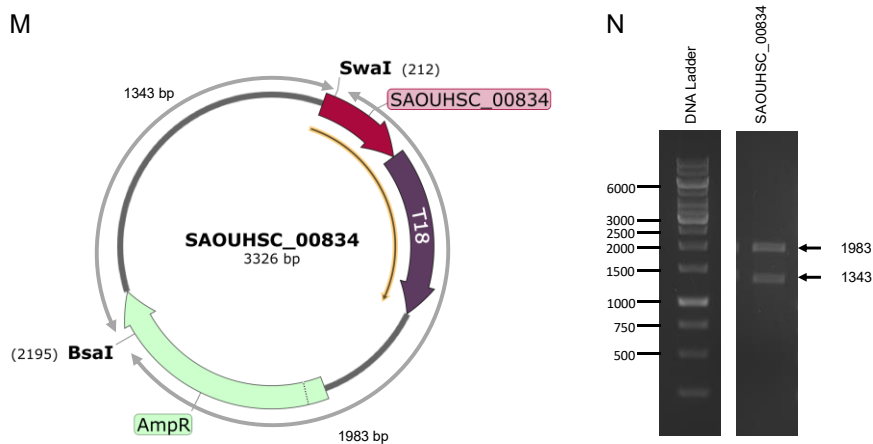
Fragments of correct size indicated by arrows; Inserts were also sequenced using T18 vector specific primers.



I. SAOUHSC\_00833 (primers 11 and 12) fusion pUT18 with in frame T18, vector digested with BamHI and EcoRI.  
 J. Verification digest NdeI and BsaI (Bands of expected sizes at 2198 and 1334 bp).



K. SAOUHSC\_00835 (primers 19 and 20) fusion pUT18 with in frame T18, vector digested with HindIII and PstI.  
 L. Verification digest MfeI and BsaI (Bands of expected sizes at 1966 and 1399 bp).



M. SAOUHSC\_00834 (primers 59 and 60) fusion pUT18 with in frame T18, vector digested with HindIII and PstI.  
 N. Verification digest SwaI and BsaI (Bands of expected sizes at 1983 and 1343 bp).

**Figure 3.8 Plasmid maps and restriction digests of B2H constructs.**

Fragments of correct size indicated by arrows; Inserts were also sequenced using T18 vector specific primers.

**Table 3.6. Sub-contracted BACTH constructs**

<b>Gene Locus</b>	<b>Genewiz Reference</b>	<b>Vector</b>
SAOUHSC_02912	p2941-Glyoxalase6	pUT18 (N)
SAOUHSC_00435	p2941-GluSynth9	pUT18 (N)
hypothetical protein B1T38_13765	p1956-hypprot b1t38_13765 10	pUT18C
SAOUHSC_02773	p1956-AbgT Transp 8	pUT18C



### 3.2.4.3 Solid media assay

Verification of interactions between the bait proteins chosen for this screen and the novel interacting partners, were confirmed by using the validated constructs of full-length genes in frame with bacterial two hybrid reporter genes. The constructs containing novel interacting protein partners were screened against the bait proteins that they were shown to interact with in the bacterial two hybrid library screen (Table 3.5), but also against the other bait proteins used in the screening to identify any shared interactions.

Chemically competent cells containing original bait proteins were transformed as described in section 2.13.1.2 with the validated constructs (see section 3.2.4.1). Control strains used to qualitatively discern positive interactions were two hybrid reporter genes fused to leucine zippers (pKT25~zip pUT18~zip) and negative interactions, empty bacterial two hybrid vectors (pKT25 pUT18).

9 of the putative interacting genes fused to the T18 bacterial two hybrid reporters gave rise to positive interactions (colouration discernible from BTH101 transformed with empty vectors) when transformed into *E. coli* BTH101 containing the bait proteins used in the library screen (Figure 3.9).

T25~PBP1 interacted with full length gene fusions of SAOUHSC\_00835 (Arsenate reductase), SAOUHSC\_02134 (Nitric oxidase synthase oxygenase), SAOUHSC\_00531 (a hypothetical protein with homology to aminohydrolase) and SAOUHSC\_00435 (large subunit of glutamate synthase). T25~PBP2 didn't show any interactions with any of the proteins identified from the screen.

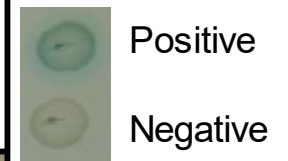
T25~PBP2A showed positive interactions with SAOUHSC\_00833 (conserved hypothetical protein in the nitroreductase family), SAOUHSC\_02773 (putative transporter protein, homology to AbgT transporter family), SAOUHSC\_02912 (a protein with homology to glyoxalase/bleomycin resistance/ extradiol dioxygenase family protein). The C terminal fusion of PBP2A (PBP2A~T25) showed positive interaction with SAOUHSC\_01868 (dipeptidase PepV).

### 3.2.5 Preliminary liquid assay investigation of interacting protein partners

While the bacterial two hybrid technique is widely used to investigate interacting protein partners it is important to confirm and quantify interactions by liquid assay prior to further investigation. For the genes identified in this screen two liquid assays were performed one each for PBP1~T25 vs T18~SAOUHSC\_00835 and one for PBP2A~T25 vs T18~PepV as they were

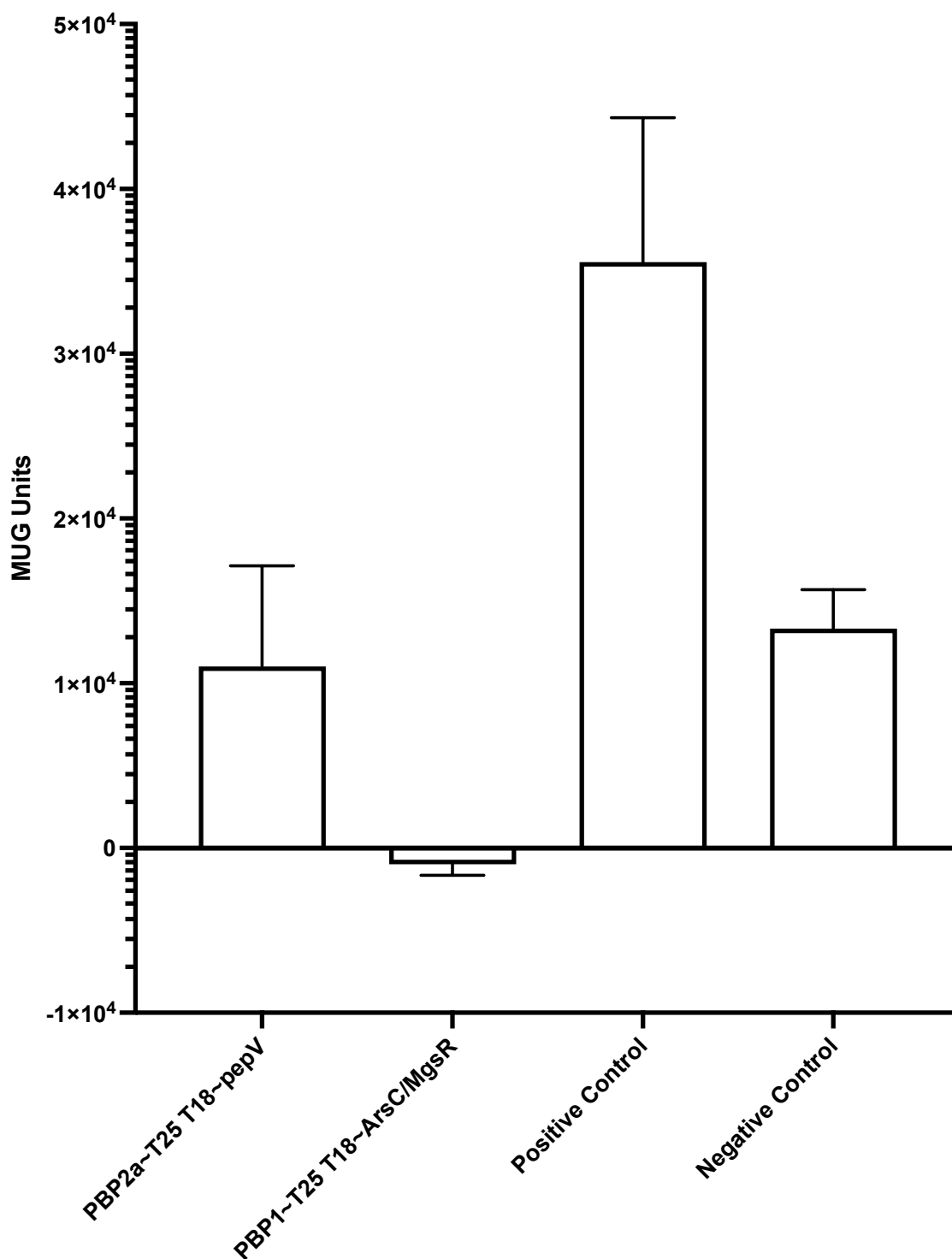
some of the weakest and strongest observable interactions on the plate assay. Figure 3.10 shows these interactions are not discernible from the negative control performed in liquid media. Due to these constructs not reliably demonstrating observable interactions in liquid culture we are unable to confirm these interactions.

	Hypothetical protein B1T38_13765	Homology to ArsC MgsR	Nitric oxide synthase oxygenase	Hypothetical protein; homology to multispecies: amidohydrolase	Conserved hypothetical protein, nitroreductase family	Glutamate synthase, large subunit	Dipeptidase pepv; homology to mn (2+)-dependent dipeptidase sapep	Putative transporter, homology to abgt putative transporter family	Unknown protein, homology to glyoxalase/bleomycin resistance/extradial dioxygenase family protein	Hisz	Putative transporter, homology to abgt putative transporter family	MULTISPECIES: NADH-dependent flavin oxidoreductase
Gene designation	No tag	835	2134	531	833	435	1868	2773	2912	3015	2773	02333
<i>pbpA</i> ~T25										NT		NT
<i>pbp2</i> ~T25								NT		NT		
PBP2A ~T25										NT		
T25~PBP2A										NT		



**Figure 3.9 Summary of solid media assay of full-length gene constructs of proteins identified in bacterial two hybrid library screen.**

Chemically competent *E. coli* BTH101 cells containing bait proteins were transformed with plasmids encoding full length constructs of prey proteins in frame with the T18 bacterial two hybrid reporters. Blue or green colouration, bold outline, indicate positive interactions, white cells indicate negative interactions and N/T, not transformed due to inability to generate clones.



**Figure 3.10 Preliminary  $\beta$ -Galactosidase activity of bacterial two hybrid interacting partners identified in library screening.**

Quantification of interactions between proteins of interest with complimentary T18 and T25 fusions identified in library screening. Activity is shown as standardised MUG units of activity, adjusted of optical density of each sample. Results shown are the mean from biologically independent samples performed in triplicate. Error bars represent the standard deviation of each sample.

### 3.3 Discussion

In *S. aureus* the bacterial two hybrid system has been used to characterise the constituents of the divisome (Steele et al., 2011) and recently the role of the PASTA domain of the essential transpeptidase PBP1, in interactions with DivIB and FtsW (Wacnik et al., 2022). My study was based on the use of a bacterial two hybrid library previously used in a screen to identify novel interactions between Era (pKNT25-*era*) and other proteins in the cell, resulting in elucidating its interaction with *cshA*, encoding a dead box RNA helicase (Wood et al., 2019). My screen aimed to identify previously unknown protein-protein interactions of PBP1 and PBP2 and the antibiotic resistance determinant PBP2A to developing understanding of their role in *S. aureus* growth and division.

The screen designed a comprehensive methodology to reduce the number of false positive fusions screened while maximising throughput. The screen initially identified 1208 positive clones and the screening process removed 353 constructs from the screen by verifying their negativity. This screen is comprehensive as it covered the 2.8 mbp *S. aureus* genome (accession number [NC\\_007795.1](#)) by screening greater than 23,000 clones from the library for each bait protein. This method gave a robust screening of the bacterial two hybrid libraries against the bait proteins of interest. In the future this could be repeated using this library and other *S. aureus* proteins.

Having independently isolated multiple fusions of the same genes is perhaps indicative of library bias or of real hits, these fragments might have more readily ligated into the B2H vector, resulting in a library bias when harvesting. Conversely, this could indicate interactions that occur more frequently or involve closer association or binding. The in-frame fusions identified in this screen had never previously been characterised or used in bacterial two hybrid screening in the context of the PBPs, or staphylococcal metabolism.

The genes identified are involved in multiple processes within the cell and consist mainly of proteins involved in biosynthetic and metabolic pathways. This study created 12 constructs that are useful for future investigations into the interactions of proteins in *S. aureus* using the bacterial two hybrid system. Of these constructs nine showed putative positive interaction when full length constructs were screened against bait proteins of interest.

The potential positive protein interactions observed are T25-PBP1 and the hypothetical protein BIT38\_13765. T25-PBP1 interacted with full length gene fusions of SAOUHSC\_00835 (Arsenate reductase) and SAOUHSC\_02134 (a putative Nitric oxidase synthase oxygenase). Mutant strains deficient in activity of nitric oxidase genes have been shown to reduce

development of skin abscesses in mice and increase antibiotic susceptibility (Van Sorge et al., 2013). SAOUHSC\_00531 (a hypothetical protein with homology to aminohydrolase) and SAOUHSC\_00435 (large subunit of glutamate synthase) have potential roles in cell wall synthesis as glutamate is part of the pentapeptide peptidoglycan constituent (X. Liu et al., 2016).

T25~PBP2 didn't show any interactions with any of the genetic constructs of the putative interacting partners, despite having identified a conserved hypothetical protein in the nitroreductase family during the screen.

In this context bacterial to hybrid is an exploratory technique that enables more thorough alternative investigations and requires liquid assays and/or another independent method to validate interactions. As mentioned previously, the two-hybrid system can be used to characterise the impact of deletions of domains to further investigate the function of given proteins (Wacnik et al., 2022). This means that the initial shorter fusions created during assembly of the library could be demonstrating independent affinity to the bait proteins irrespective of protein function, bringing the reporter genes into proximity with the T25 reporter.

As a technique in a surrogate organism the bacterial two hybrid system is limited. Interactions must subsequently be confirmed by an independent method, ideally in the organism of interest (Table 3.1).

The random genetic fusion library used in this study comprises of fragments prepared using a partial genomic digest using Sau3AI (Wood et al., 2019). The library suitability is dependent on three things: the digested fragment being successfully ligated into the vector containing genes of interest, an open reading frame between the restriction sites, and an in-frame fusion with the reporter gene when ligated in the correct orientation. The two size ranges of inserts of 0.5 – 1 kbp and 1 – 3 kbp automatically exclude genes smaller than 0.5 kbp and larger than 3 kbp. The restriction enzyme used also automatically excludes genes not in frame with the restriction sites. Different enzymes could be used for the genomic DNA digest that might include in frame fusions of known and novel interacting partners.

The screen used both the pUT18 (N) and pUT18(C) vectors allowing for N and C terminal fusions of the reporter genes. This facilitates the detection of interactions irrespective of if one protein region features an interaction site that is disrupted by the presence of the reporter gene, or where a protein is transmembrane and reporter proteins are present in different cellular compartments. For example, T25~PBP2 shouldn't show a positive interaction with PBP2~T18 despite its previously reported homodimerization due to the C and N termini

of the protein being in the exoplasm and cytoplasm respectively (Contreras-Martel et al., 2017; Łęski and Tomasz, 2005; Pinho et al., 2001).

T25~PBP2A showed positive interactions with SAOUHSC\_00833 (conserved hypothetical protein in the nitroreductase family), SAOUHSC\_02773 (putative transporter protein, homology to AbgT transporter family), SAOUHSC\_02912 (a protein with homology to glyoxalase/bleomycin resistance/ extradiol dioxygenase family protein). PBP2A~T25 showed positive interaction with SAOUHSC\_01868 (dipeptidase PepV). Whilst one might expect a narrow range of interactions due to its specific role in antibiotic resistance and it's being acquired from another species (Pinho et al., 2001), the screen didn't identify the expected interactions including folding partners *prsA* and *htrAI* and PBP2 (Roch et al., 2019). FloA and PBP2A have previously been shown to interact using B2H and pull-down experiments (García-Fernández et al., 2017). This could indicate its proximity and potential interactions with other constituent parts of membrane microdomains and associated proteins essential to its' function.

PBP2A interacting with a putative transporter highlights its membrane associated localisation and could potentially suggesting involvement with efflux given the homology of this protein to members of the AbgT transporter family proteins well characterised in other organisms (Delmar and Yu, 2016). PBP2A has different interactions with PBP2 when the latter is acylated (Fuda et al., 2004) in the presence of oxacillin might give different interactions, especially due to shared function during peptidoglycan biosynthesis (Pinho et al., 2001). This again highlights, how any interactions of PBP2A in the model two hybrid system must be confirmed in MRSA strains in the presence of antibiotics as there could be different interactions, or changes in partners (Lim and Strynadka, 2002).

Due to the nature of the two hybrid reporters, screening is reliant on the qualitative interpretations of growth on reporter plates, especially when screening many colonies per plate. This could be improved in future by plating a higher dilution factor of transformants or using less library DNA in transformations. In repeating the screening, the use of alternative media including MacConkey with maltose, or M63 in tandem, or more selective media such as minimal media might allow better discrimination between interactions in both the screening and assaying for interaction stages (Battesti and Bouveret, 2012).

A comprehensive screen of a random library of genetic constructs was performed using penicillin binding proteins 1, 2 and 2A. this identified 12 potential novel putative interacting partners, none of which have been associated with interacting with the PBPs previously. However, these require further screening using alternative protein-protein interaction

methodologies and global protein-protein interaction techniques to characterise the interactions of PBP2A during cell growth division and the maintenance of high-level antimicrobial resistance (Cherkasov et al., 2011) to confirm and validate these interactions.

This study indicates a need for caution using libraries for screening and relying on *in vitro* techniques in model organisms such as the BTH101 *E. coli* *cyo*<sup>-</sup> strain as this can result in many assays being required solely to confirm multiple false positive results. More directed screening using previously validated constructs to screen for interactions against specified bait proteins of interest, would enable the design of more targeted experimental investigations of protein-protein interactions. This could be used to examine interactions between proteins involved in specific processes from cell division, protein trafficking and display, specific cellular phenotypes, and antibiotic resistance.



# Chapter 4 Directed analysis of protein-protein interactions

## 4.1 Introduction

Cell division in *S. aureus* requires a complex remodelling of the cell wall structure to permit morphogenesis. The final stage is cell scission which occurs within a millisecond and is dependent on the mechanical stress exerted by turgor pressure on the peripheral mother cell wall that connects the two daughter cells (Zhou et al., 2015). Such dynamics pose a considerable challenge for the cell, requiring both spatial and temporal control. A protein complex called the divisome has been found to be crucial to allow optimal division (Daniel et al., 2006).

The divisome is highly conserved across species with several essential protein members (Steele et al., 2011). The B2H technique has been used to screen for interactions of potential divisome components and direct further physiological investigations, Bottomley et al (2011) used B2H to identify interactions between cell division proteins in *S. aureus*, resulting in a complex map of proteins with linked functions. These include the core complex of EzrA, PBP1, PBP2, DivIB, DivIC, FtsL, and FtsZ which are all required for cell division.

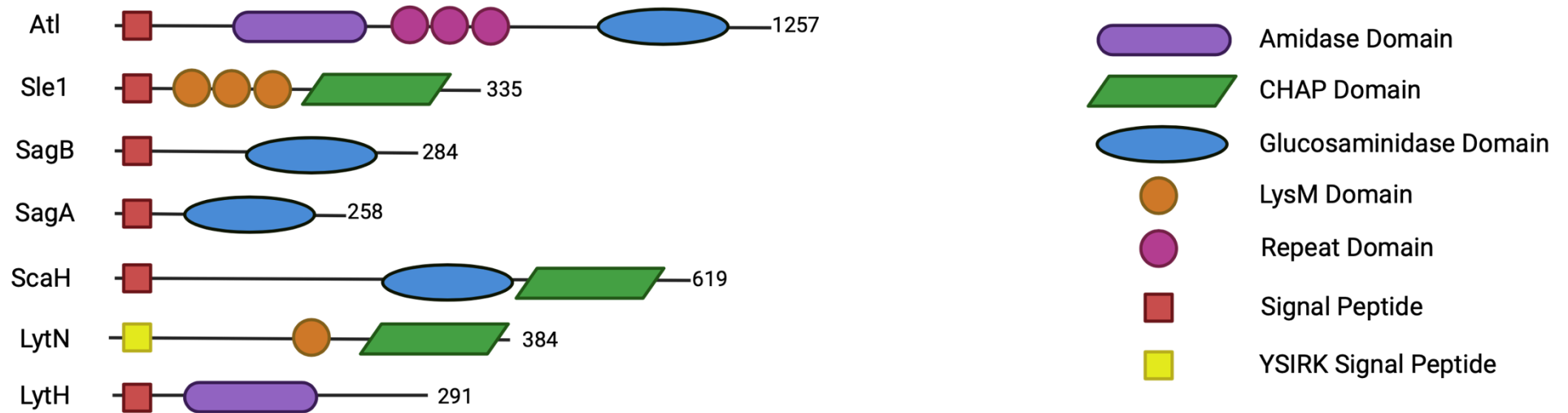
One division associated protein factor which hasn't been comprehensively investigated for its protein-protein interactions through directed B2H screening is GpsB. The depletion of GpsB has been reported to result in cell lysis due to arrested cell division highlighting its role in co-constricting with the division machinery (Cleverley et al., 2019; Sutton et al., 2023). Importantly GpsB is responsible for the direct regulation and bundling of FtsZ filaments (Eswara et al., 2018). FtsZ is one of the first proteins recruited to the site of cell division (Monteiro et al., 2018)

It has also been reported that GpsB shares common N terminal sequence motifs with DivIVA (Sacco et al., 2022). Both the late-stage cell division proteins DivIVA and GpsB bind lipids and have an important functional relationship through the structural basis of interactions with their ligands (Halbedel and Lewis, 2019). Despite this shared domain organisation and common motifs these proteins play separate roles during cell division. Their separate roles include DivIVA determining the site of division and controlling peptidoglycan homeostasis whereas GpsB controls penicillin binding protein activity (Halbedel and Lewis, 2019). Examined briefly during screens of cell wall constituents, GpsB was shown to be an interacting partner of EzrA and FtsA (Steele et al., 2011) as well as LcpC, LcpA and TarO (Kent, 2013). Other studies have

demonstrated direct interactions of GpsB with FtsZ and TarG by both B2H and colocalization microscopy (Hammond et al., 2022).

Mutations in *gpsB* lead to an increasingly spherical phenotype in comparison to wild type *S. aureus* (Sutton et al., 2023). The authors noted a decrease in peripheral cell wall synthesis correlated with increased PBP2 and 3 localisation at the septum (Sutton et al., 2023). In *S. pneumoniae* and *B. subtilis* GpsB also interacts with peptidoglycan synthases (Cleverley et al., 2019). In *S. aureus* GpsB protomers associate with the N terminal, membrane spanning domains of PBPs (Sacco et al., 2022).

Cell wall dynamics during division requires the coordinated activity of multiple peptidoglycan hydrolases to allow remodelling and morphogenesis, one example is during cell scission where the mother cell wall is cleaved to allow daughter cell separation (Salamaga et al., 2021). Staphylococcal cell wall hydrolases therefore have an important role in growth and division (Wheeler et al., 2015). Representative *S. aureus* hydrolases and their modular structure is shown diagrammatically in Figure 4.1



**Figure 4.1 Peptidoglycan hydrolases.**

The modular structure of peptidoglycan hydrolases and their relevant catalytic and regulatory domains. Created with BioRender.com.

Cell separation or scission involves several hydrolases including Atl, Sle1 and LytN (Frankel et al., 2011; Komatsuzawa et al., 1997; Veiga et al., 2023). PG hydrolysis is also important in antibiotic resistance, LytH has been identified as a potentiator of resistance whereby its deletion/mutation increase methicillin resistance from 6.3 to 1600  $\mu\text{g}/\text{mL}$ , (Fujimura and Murakami, 1997). LytH conducts the exclusive cleavage of newly synthesised peptidoglycan that has not yet been cross linked by pentaglycine bridges acting differently from other hydrolases (Do et al., 2020). The localisation of LytH coordinates cell division and FtsZ is mislocalised in  $\Delta\text{lytH}$  strains resulting in division defects such as multiple septa and larger cells in comparison to wild type (Do et al., 2020).

LytN is a hydrolase secreted into the cross wall of *S. aureus* that facilitates cell envelope assembly and daughter cell separation by promoting peptidoglycan lysis required to complete the cell cycle (Frankel et al., 2011). Deletion of LytN results in a growth defect phenotype of lower stationary phase optical density and reduced doubling times (Frankel et al., 2011). The same study demonstrated how *lytN* mutagenesis resulted in altered cellular morphology due to reduced hydrolysis of peptidoglycan and growth defects (Frankel et al., 2011).

PGH also have a role in virulence, both due to their role in the cell cycle but also affecting the display of virulence factors. LytN contributes to the release of SpA from the cell wall with a significant role during the pathogenesis of *S. aureus* in the host (Becker et al., 2014). The cell wall localisation of peptidoglycan hydrolases means they not only mediate the organism's bacterial growth and fitness but also virulence (Wang et al., 2022) through host cell adhesion and internalisation alongside immune evasion through SpA release, inflammatory responses, and biofilm formation (McCarthy et al., 2016; Schlesier et al., 2020; Sutton et al., 2021).

Methicillin resistance is determined by the presence of *mecA*, which encodes PBP2A that has a low affinity for  $\beta$ -lactams and can take over transpeptidase activity in their presence. In Chapter 3, PBP2A was subjected to a library screen to identify novel interacting partners of this resistance determinant. Another approach would be to use existing B2H constructs to take a candidate approach to the identification of PBP2A protein partners. This Chapter uses a targeted approach to build on current knowledge of the divisome and cell morphogenesis/lysis machinery by performing directed screening to characterise the protein interactions of GpsB, LytH, LytN and PBP2A.

Our existing library of B2H constructs include many cell division components such as FtsL, DivB and DivC which associate with PBPs (PBP 1 and 3), membrane spanning components such as FtsW and RodA or intracellular proteins such as FtsA or FtsZ (Bottomley et al., 2017; Kent, 2013). The library also contains the major biosynthesis proteins, LtaS, LtaA and YpfP, as

LTA is an important cell wall component with a role in growth and division (Kiriukhin et al., 2001). A variety of other proteins are in the library such as the FtsZ anchors YlmF/SepF (White and Eswara, 2021) and cell division regulator SosaA, which prevents cells from dividing in response to DNA damage (Bojer et al., 2019) and also proteins with other important roles in the cell cycle including MreD, which provides molecular scaffolding for distributing proteins involved in lipid metabolism (García-Lara et al., 2015; Tavares et al., 2015). Finally, a range of components important in general cellular physiology including, the phospholipid biosynthetic enzyme CdsA (Weihs et al., 2018), the heat shock associated protein DnaK, which facilitates protein folding under cellular stress conditions (Singh et al., 2012) and ParC, a subunit of the DNA topoisomerase IV (Li et al., 1998) are in the collection.

The T18 array of protein constructs also includes constructs designed in section 3.2.4 as they are previously uncharacterised in terms of interactions and could generate data useful to support development of their understanding in staphylococcal processes.

#### **4.1.1 Aims of this Chapter**

This Chapter aims to use directed B2H screening to investigate and verify interactions between proteins involved in cell wall hydrolysis and morphogenesis, while furthering knowledge of interactions with the resistance determinant PBP2A. We hypothesised that directed screening of previously used B2H constructs could identify unknown interactions. It was also hypothesised that the localisation of PBP2A might follow a comparable pattern to that of PBP2 when using a fluorescent fusion. The specific aims of this chapter were:

- i. Perform directed screening using the B2H system with:
  - a. The resistance determinant PBP2A
  - b. The cell wall morphogenesis factor GpsB
  - c. The cell wall hydrolases LytH and LytN
- ii. Verification of interactions using liquid media assays
- iii. Construction and verification of methodology for localisation and co-immunoprecipitation of PBP2A using GFP nanotraps.

## **4.2 Results**

### **4.2.1 Directed B2H screening.**

An array of 70 T25 and 71 T18 B2H constructs was prepared by miniprep (Section 2.10.2). Interactions between bait proteins in this screen were evaluated by transforming an array of

T18 and T25 constructs into chemically competent cells containing T25 or T18 reporter fusions to proteins of interest (as section 2.13.5). Data is presented by each protein screened against the T25 and T18 libraries, where constructs were available. Constructs used included those previously designed and verified to characterise the divisome (Kent, 2013; Steele et al., 2011), constructs of PBP1 including PBP1<sup>PASTA</sup> and PBP1<sup>STOP</sup> designed by Dr Kasia Wacnik (Wacnik et al., 2022) and those designed in Chapter 3. The details of these constructs are shown in Appendix 1.

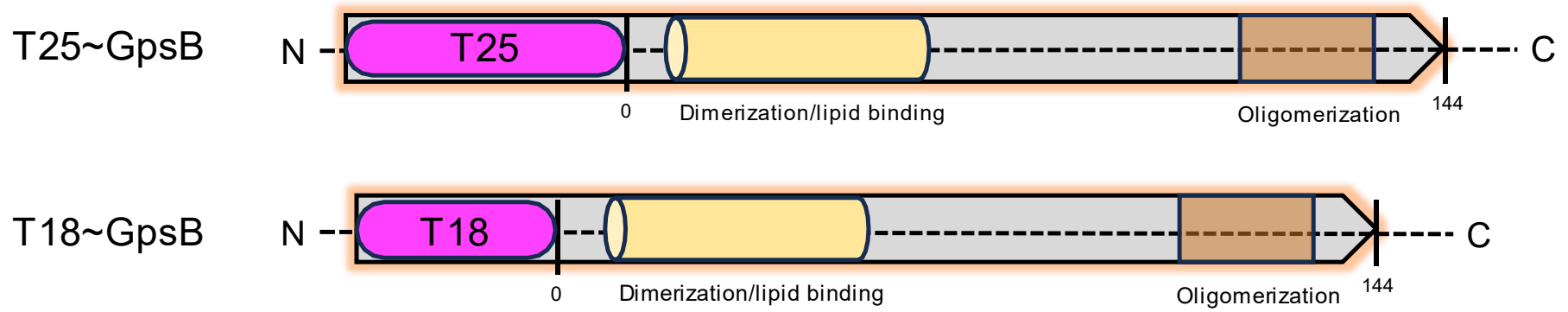
For each T18 or T25 bait protein (GpsB, LytH, LytN and PBP2A) chosen, an array of two hybrid constructs were transformed in a 96 well plate format as described in section 2.13.5. Single colonies were inoculated into 100 µL minimal media broth containing IPTG, kanamycin and ampicillin and incubated with shaking for 3 hours. 5 µL was spotted onto Minimal media agar with 100 µg / mL Ampicillin, 50 µg / mL Kanamycin, 0.5 mM IPTG and 160 µg / mL X-Gal. (as described in section 2.13.6) and incubated for 48 hrs at 30 ° C. The control strains used to enable qualitative differentiation between positive and negative interactions were two hybrid reporter genes fused to leucine zippers (pKT25~zip pUT18~zip) and negative interactions, empty B2H vectors (pKT25 pUT18). To increase ease of differentiating between positive and negative interactions the product of X-Gal hydrolysis was left to precipitate at 4° C for 12 hrs.

#### **4.2.1.1 Cell wall morphogenesis factor: GpsB**

To screen for interactions with GpsB, both T25 and T18 fusions from Steele et al. (2011) were used. These constructs are represented diagrammatically in Figure 4.2.

In the screening of the T25 constructs (Figure 4.3) interactions with T18 GpsB discernible from the negative controls during screening of the T25 array of B2H constructs were PBP3, GpsB, YpsA, DivIB, FtsA, PBP2, EzrA, FtsZ, ZapA, FtsA, ParC, ParE, PBP1, MreC, DivIB, FtsL, FtsA, PBP2A (N terminal), PBP1<sup>Stop</sup> and LytN. In screening T25 constructs interactions between DnaK, LtaA and YpfP with GpsB were demonstrated when reporters were fused to both the N and C termini of the bait proteins.

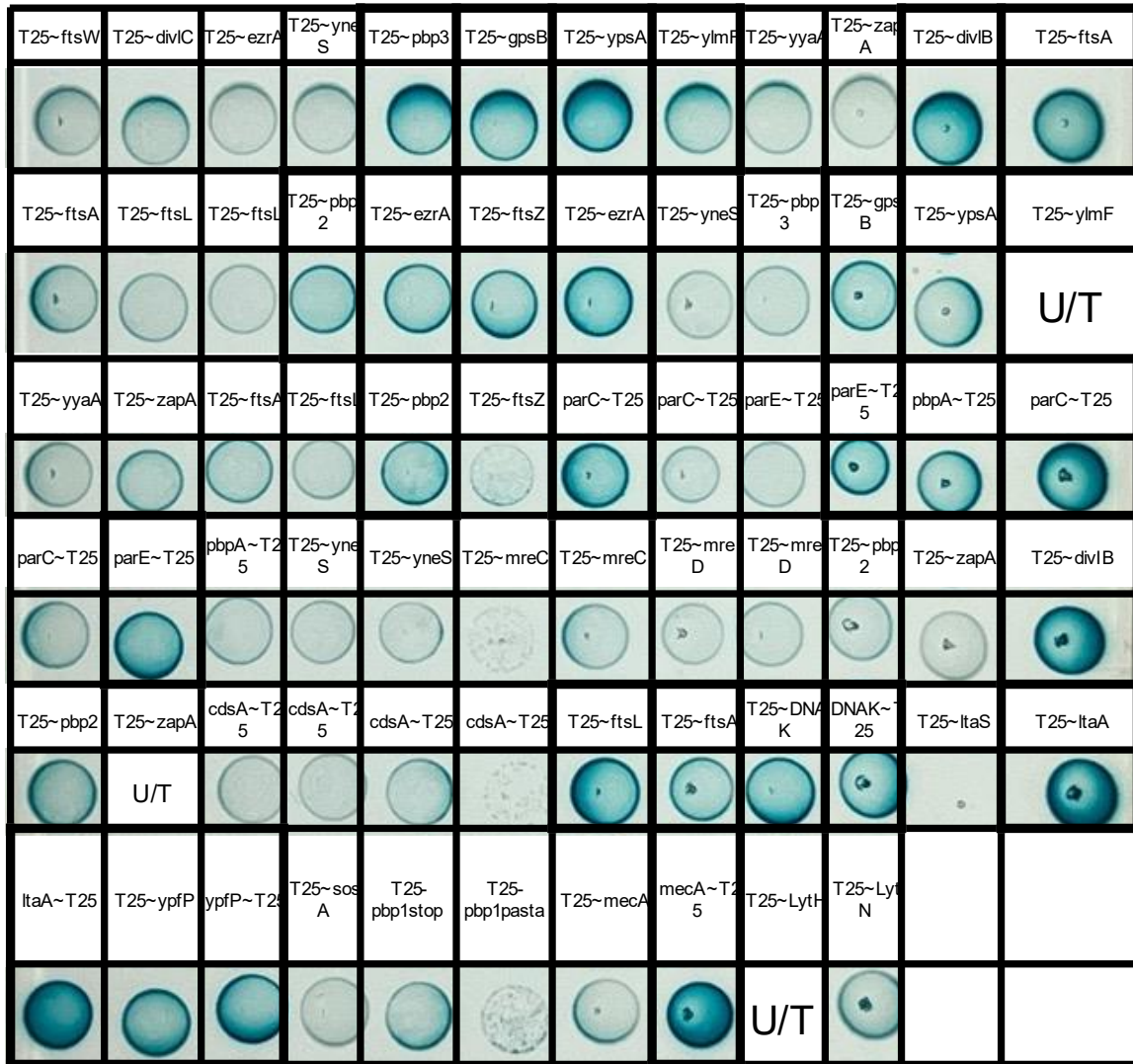
The array of T18 constructs (Figure 4.4) gave positive interactions with YsxC, FtsZ, GpsB, LtaS YpfP, and MecA. The constructs from Chapter 3, SAOUHSC\_01868, SAOUHSC\_00531, SAOUHSC\_02134 and SAOUHSC\_03015 also gave rise to positive interactions.



**Figure 4.2 Diagram of GpsB in frame fusions with B2H T25 and T18**

GpsB constructs for B2H screening showing coiled coil domain, yellow. Open reading frame inclusive of the B2H reporter in orange. Not to scale.

A



B

Positive interactions T18 GpsB		
N Terminal	C Terminal	N and C Terminal
T25~pbp3	T25~ftsZ	
T25~gpsB	T25~ezrA	parC~T25
T25~ypsA	T25~gpsB	parC~T25
T25~ylmF	T25~ypsA	pbpA~T25
T25~divIB	T25~pbp2	parE~T25
T25~ftsA	T25~divIB	parE~T25
T25~pbp2	T25~ftsL	mecA~T25
T25~ezrA	T25~ftsA	
		T25~DNAK, DNAK~T25
		T25~ItaA, ItaA~T25
		T25~ypfP, ypfP~T25

T25~zip	T25
T18~zip	T18

**Figure 4.3. Solid media assay of T25 array of B2H constructs screened against GpsB T18**

(A) Interaction assay of T25 array of prey proteins against bait protein GpsB T18 on minimal media agar. Positive controls were two hybrid reporter genes fused to leucine zippers (pKT25~zip pUT18~zip) and negative interactions, empty B2H vectors (pKT25 pUT18). (B) Summary of positive interactions. U/T, Untested.



A

T18~ysxC	T18~rpsE	T18~rpsJ	T18~rplQ	T18~glpD	T18~tuf	T18~secA	T18~rpsB	T18~ftsW	T18~ftsZ	T18~divC	T18~ezrA
T18~yneS	T18~gpsB	T18~ypsA	T18~ylmF	T18~yyaA	T18~zapA	T18~divB	T18~divC	T18~ftsA	T18~ftsl	T18~pbp2	T18~yneS
T18~ftsW	T18~ftsZ	T18~divC	T18~ezrA	T18~parC	T18~yneS	T18~gpsB	T18~ypsA	T18~ylmF	T18~yyaA	T18~zapA	T18~ezrA
		U/T									
T18~ftsZ	T18C~zapA	T18~spaSS2	spaSS1~T18	T18~ltaS	T18~pbp4	cdsA~T18	cdsA~T18	T18~gpsB	T18~ylmF	T18~DNAK	DNAK~T18
T18~LtaS	T18~LtaA	LtaA~T18	T18~ypfP	ypfP~T18	T18~sosA	T18~pbp1stop	T18~pbp1pasta	mecA~T18	T18~mecA	SAOUHSC_01868~T18	SAOUHSC_00531~T18
SAOUHSC_02134~T18	SAOUHSC_03015~T18	T18~SAOUHSC_00833	SAOUHSC_02912~T18	SAOUHSC_00835~T18	SAOUHSC_02773~T18	T18~SAOUHSC_00435	B1T38_13765~T18	SAOUHSC_00834~T18	T18~LytH	T18~LytN	

B

Positive interactions T25 GpsB		
N Terminal	C Terminal	N and C Terminal
T18~gpsB T18~gpsB T18~ezrA T18~zapA T18~mecA	ypfP~T18 SAOUHSC_01868~T18 SAOUHSC_03015~T18	None

T25~zip T18~zip	T25 T18

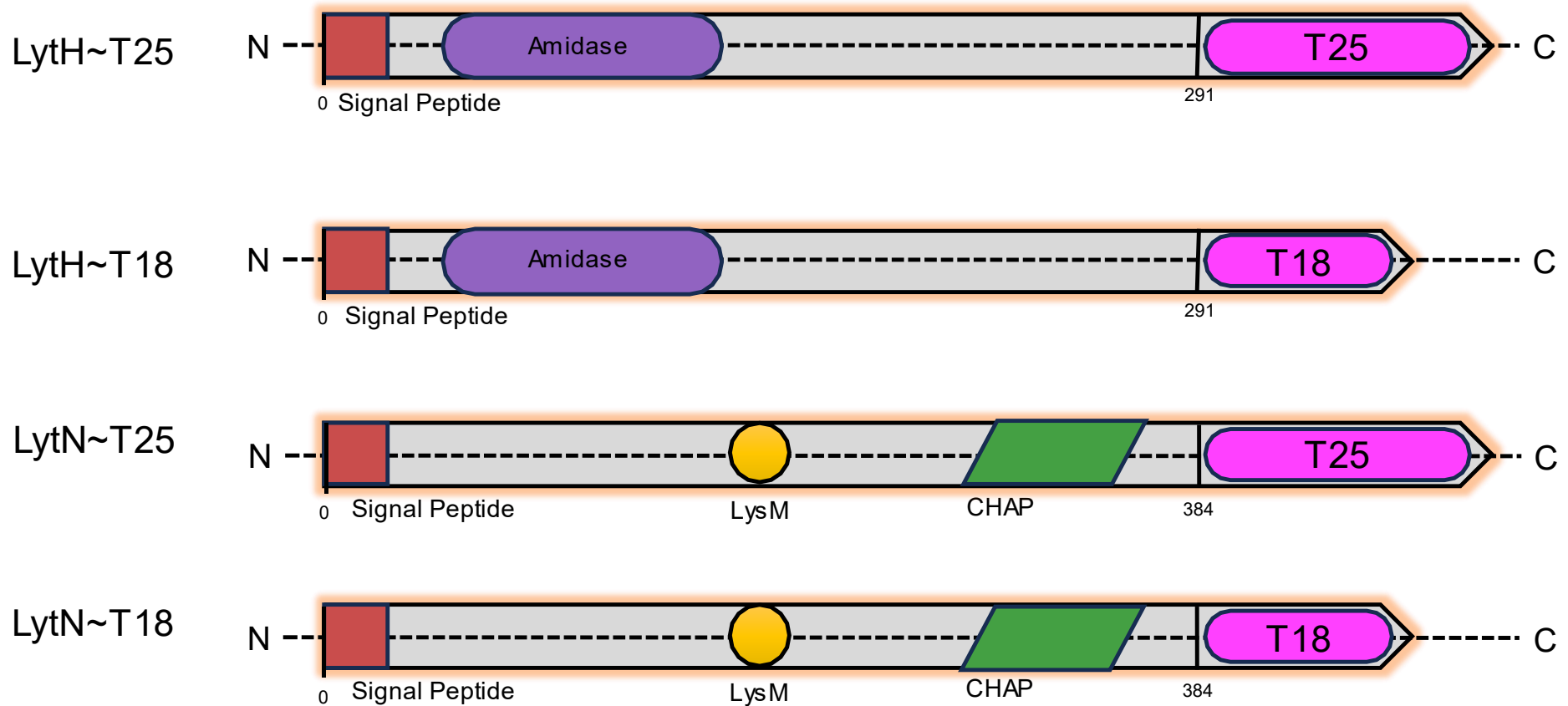
**Figure 4.4. Solid media assay of T18 array of B2H constructs screened against GpsB T25**  
 (A) Interaction assay of T18 array of prey proteins with bait protein GpsB T25 on minimal media agar with X-Gal. Positive controls were two hybrid reporter genes fused to leucine zippers (pKT25~zip pUT18~zip) and negative interactions, empty B2H vectors (pKT25 pUT18).  
 (B) Summary of positive interactions. U/T, Untested.

### 4.2.1.2 Cell wall hydrolases

Two hybrid constructs of the cell wall hydrolases LytH (gene: SAOUHSC\_01739, Genewiz reference: P1956-LytH13, vector: pUT18C) and LytN (gene: SAOUHSC\_01219, Genewiz reference: p2941-LytN12, vector: pUT18 (N)) were designed and were subcontracted to Genewiz and the details of their construction and results of internal QC can be found in Appendix 4. The resulting constructs are shown diagrammatically in Figure 4.5. Both LytH and LytN have an N terminal signal peptide (Wheeler et al., 2015) and therefore only C terminal B2H constructs can be expressed without disrupting their localisation. These were used to screen the B2H T25 and T18 Libraries for interacting protein partners. Some proteins such as PBP4 were omitted from the interaction assays as they reliably failed to successfully transform into the chemically competent cells containing the bait proteins.

#### 4.2.1.2.1 LytH

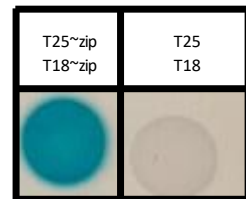
LytH-T25 and LytH-T18 were used to screen for interactions against the two hybrid arrays. There were no interactions discernible from the negative controls when screening T25 against the bait protein LytH-T18 (Figure 4.6). Screening using the T25 LytH construct (Figure 4.7) gave several interactions discernible from the negative controls: T18 fusions of ~DivIC, ~FtsA, ~PBP2, ~LtaS, YpfP~, ~PBP1<sup>STOP</sup> and ~PBP1<sup>PASTA</sup>.



**Figure 4.5 Diagrammatical representation of cell wall hydrolases LytH and LytN with T25 and T18 B2H reporters.**

LytH and LytN constructs for B2H screening showing Signal peptides, and relevant domains, CHAP: cysteine, histidine-dependent amidohydrolase/peptidase. Open reading frame inclusive of the B2H reporter in orange. Not to scale.

T25~ftsW	T25~divIC	T25~ezrA	T25~yneS	T25~pbp3	T25~gpsB	T25~ypsA	T25~ylmF	T25~yyaA	T25~zapA	T25~divIB	T25~ftsA
T25~ftsA	T25~ftsL	T25~ftsL	T25~pbp2	T25~ezrA	T25~ftsZ	T25~ezrA	T25~yneS	T25~pbp3	T25~gpsB	T25~ypsA	T25~ylmF
T25~yyaA	T25~zapA	T25~ftsA	T25~ftsL	T25~pbp2	T25~ftsZ	parC~T25	parC~T25	parE~T25	parE~T25	pbpA~T25	parC~T25
parC~T25	parE~T25	pbpA~T25	T25~yneS	T25~yneS	T25~mreC	T25~mreC	T25~mreD	T25~mreD	T25~pbp2	T25~zapA	T25~divIB
T25~pbp2	T25~zapA	cdsA~T25	cdsA~T25	cdsA~T25	cdsA~T25	T25~ftsL	T25~ftsA	T25~DNAK	DNAK~T25	T25~ltaS	T25~ltaA
ltaA~T25	T25~yfpP	yfpP~T25	T25~sosA	T25- pbp1stop	T25- pbp1pasta	T25~mecA	mecA~T25	T25~LytH	T25~LytN		



**Figure 4.6 Solid media assay of T25 array of B2H constructs screened against LytH T18**  
Interaction assay of T25 Array of prey proteins bait protein LytH T18 on minimal media agar with X-Gal. Positive controls were two hybrid reporter genes fused to leucine zippers (pKT25~zip pUT18~zip) and negative interactions, empty B2H vectors (pKT25 pUT18).

A

T18~ysxC	T18~rpsE	T18~rpsJ	T18~rplQ	T18~glpD	T18~tuf	T18~secA	T18~rpsB	T18~ftsW	T18~ftsZ	T18~divC	T18~ezrA
		U/T					U/T		U/T		U/T
T18~yneS	T18~gpsB	T18~ypsA	T18~ylmF	T18~yyaA	T18~zapA	T18~divB	T18~divC	T18~ftsA	T18~ftsL	T18~pbp2	T18~yneS
									U/T		U/T
T18~ftsW	T18~ftsZ	T18~divC	T18~ezrA	T18~parC	T18~yneS	T18~gpsB	T18~ypsA	T18~ylmF	T18~yyaA	T18~zapA	T18~ezrA
									U/T		U/T
T18~ftsZ	T18C~zapA	T18~spa5S2	spa5S1~T18	T18~ltaS	T18~pbp4	cdsA~T18	cdsA~T18	T18~gpsB	T18~ylmF	T18~DNAK	DNAK~T18
					U/T			U/T			U/T
T18~LtaS	T18~LtaA	LtaA~T18	T18~ypfP	ypfP~T18	T18~sosA	T18~pbp1stop	T18~pbp1pasta	mecA~T18	T18~mecA	SAOUHSC_01868~T18	SAOUHSC_00531~T18
					U/T				U/T		
SAOUHSC_02134~T18	SAOUHSC_03015~T18	T18~SAOUHSC_00833	SAOUHSC_02912~T18	SAOUHSC_00835~T18	SAOUHSC_02773~T18	T18~SAOUHSC_00435	B1T38_13765~T18	SAOUHSC_00834~T18	T18~LytH	T18~LytN	
				U/T	U/T						

B

Positive interactions T25 LytH		
N Terminal	C Terminal	N and C Terminal
T18~divC		
T18~divC		
T18~ftsA		
T18~pbp2		
T18~divC	ypfP~T18	
T18~ltaS		None
T18~pbp1stop		
T18~pbp1pasta		



**Figure 4.7 Solid media assay of T18 array of B2H constructs screened against LytH T25**

(A) Interaction assay of T18 Array of prey proteins bait protein LytH T25 on minimal media agar with X-Gal. Positive controls were two hybrid reporter genes fused to leucine zippers (pKT25~zip pUT18~zip) and negative interactions, empty B2H vectors (pKT25 pUT18). (B) Summary of positive interactions. U/T, Untested.

#### **4.2.1.2.2 LytN**

The cell wall hydrolase LytN was screened against the library of B2H proteins to identify interacting protein partners. The screening of B2H T25 constructs against the LytN-T18 bait proteins are shown in Figure 4.8, where no positive interactions are discernible from the negative control. The screening of B2H T18 constructs against the LytN-T25 bait protein are shown in Figure 4.9. Interactions with T25- LytN are observed for the T18 constructs T18-DivIC and T18-PBP2A.

T25~ftsW	T25~divIC	T25~ezrA	T25~yneS	T25~pbp3	T25~gpsB	T25~ypsA	T25~ylmF	T25~yyaA	T25~zapA	T25~divIB	T25~ftsA
	U/T		U/T								
T25~ftsA	T25~ftsL	T25~ftsL	T25~pbp2	T25~ezrA	T25~ftsZ	T25~ezrA	T25~yneS	T25~pbp3	T25~gpsB	T25~ypsA	T25~ylmF
		U/T									
T25~yyaA	T25~zapA	T25~ftsA	T25~ftsL	T25~pbp2	T25~ftsZ	parC~T25	parC~T25	parE~T25	parE~T25	pbpA~T25	parC~T25
								U/T			
parC~T25	parE~T25	pbpA~T25	T25~yneS	T25~yneS	T25~mreC	T25~mreC	T25~mreD	T25~mreD	T25~pbp2	T25~zapA	T25~divIB
T25~pbp2	T25~zapA	cdsA~T25	cdsA~T25	cdsA~T25	cdsA~T25	T25~ftsL	T25~ftsA	T25~DNAK	DNAK~T25	T25~ltaS	T25~ltaA
					U/T						
ltaA~T25	T25~yfpP	yfpP~T25	T25~sosA	T25~pbp1stop	T25~pbp1nasta	T25~mecA	mecA~T25	T25~LytH	T25~LytN		
					U/T						

T25~zip T18~zip	T25 T18

**Figure 4.8 Solid media assay of T25 array of B2H constructs screened against LytN T18**

Interaction assay of T25 array of prey proteins against bait protein LytN T18 on minimal media agar with X-Gal. Positive controls were two hybrid reporter genes fused to leucine zippers (pKT25~zip pUT18~zip) and negative interactions, empty B2H vectors (pKT25 pUT18). U/T, Untested.

A

T18~ysxC	T18~rpsE	T18~rpsJ	T18~rplQ	T18~glpD	T18~tuf	T18~secA	T18~rpsB	T18~ftsW	T18~ftsZ	T18~divIC	T18~ezrA
T18~yneS	T18~gpsB	T18~ypsA	T18~ylmF	T18~yyaA	T18~zapA	T18~divIB	T18~divIC	T18~ftsA	T18~ftsL	T18~pbp2	T18~yneS
T18~ftsW	T18~ftsZ	T18~divIC	T18~ezrA	T18~parC	T18~yneS	T18~gpsB	T18~ypsA	T18~ylmF	T18~yyaA	T18~zapA	T18~ezrA
T18ftsZ	T18C~zapA	T18~spaSS2	spaSS1~T18	T18~ltaS	T18~pbp4	cdsA~T18	cdsA~T18	T18~gpsB	T18~ylmF	T18~DNAI	DNAK~T18
					U/T						
T18LtaS	T18~LtaA	LtaA~T18	T18~ypfP	ypfP~T18	T18~sosA	T18pbp1stop	T18 pbp1pasta	mecA~t18	T18~mecA	SAOUHSC_01868~T18	SAOUHSC_00531~T18
SAOUHSC_02134~T18	SAOUHSC_03015~T18	T18~SAOUHSC_00833	SAOUHSC_02912~T18	SAOUHSC_00835~T18	SAOUHSC_02773~T18	T18~SAOUHSC_00435	SB1T38_13765~T18	SAOUHSC_00834~T18	T18~LytH	T18~LytN	

B

**Positive interactions T25 LytN**

N Terminal                      C Terminal                      N and C Terminal

T18~divIB                      None                      None  
T18~mecA

T25~zip T18~zip	T25 T18

**Figure 4.9 Solid media assay of T18 array of B2H constructs screened against LytN T25**

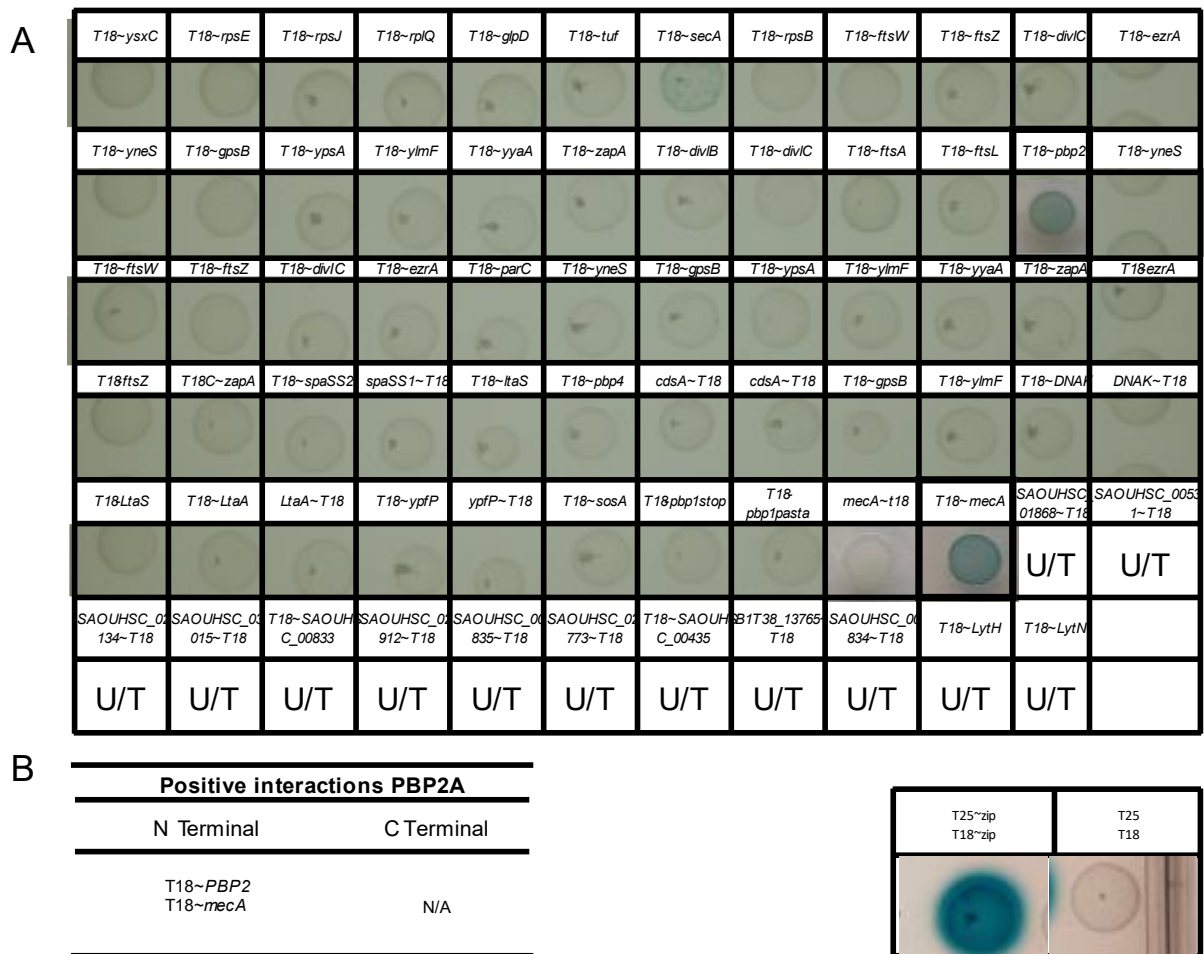
(A) Interaction assay of T18 array of prey proteins against bait protein LytN T25 on minimal media agar with X-Gal. Positive controls were two hybrid reporter genes fused to leucine zippers (pKT25~zip pUT18~zip) and negative interactions, empty B2H vectors (pKT25 pUT18).

(B) Summary of positive interactions. U/T, Untested.



#### **4.2.1.3 Investigating Antibiotic resistance determinant: PBP2A**

Having conducted a library screen in Chapter 3 of PBP2A to little avail, screening of PBP2A against a selection of relevant cell division proteins could be insightful and allow insights into key mechanisms of this extra species facilitator of resistance. The antibiotic resistance determinant PBP2A, expressed in the B2H system, was screened against the library of B2H proteins to identify interacting protein partners. The screening is shown in Figure 4.10. Interactions were observed with itself and PBP2 and only when its respective T25 or T18 fusions were fused to the same terminal of the gene.



**Figure 4.10 Solid media assay of T18 constructs of Staphylococcal proteins screened against PBP2A**

(A) Interaction assay of T18 array of prey proteins against bait protein PBP2A T25. Performed on minimal media agar with X-Gal. Positive controls were two hybrid reporter genes fused to leucine zippers (pKT25~zip pUT18~zip) and negative interactions, empty B2H vectors (pKT25 pUT18). (B) Summary of positive interactions. This figure uses composite images and not all assays were performed on the same plate. U/T, Untested.

**A**

<i>T25-ftsW</i>	<i>T25-divIC</i>	<i>T25-ezrA</i>	<i>T25-yneS</i>	<i>T25-pbp3</i>	<i>T25-gpsB</i>	<i>T25-ypsA</i>	<i>T25-ylmF</i>	<i>T25-yyaA</i>	<i>T25-zapA</i>	<i>T25-divIB</i>	<i>T25-ftsA</i>
<i>T25-ftsA</i>	<i>T25-ftsL</i>	<i>T25-ftsL</i>	<i>T25-pbp2</i>	<i>T25-ezrA</i>	<i>T25-ftsZ</i>	<i>T25-ezrA</i>	<i>T25-yneS</i>	<i>T25-pbp3</i>	<i>T25-gpsB</i>	<i>T25-ypsA</i>	<i>T25-ylmF</i>
				U/T					U/T	U/T	
<i>T25-yyaA</i>	<i>T25-zapA</i>	<i>T25-ftsA</i>	<i>T25-ftsL</i>	<i>T25-pbp2</i>	<i>T25-ftsZ</i>	<i>parC-T25</i>	<i>parC-T25</i>	<i>parE-T25</i>	<i>parE-T25</i>	<i>pbpA-T25</i>	<i>parC-T25</i>
<i>parC-T25</i>	<i>parE-T25</i>	<i>pbpA-T25</i>	<i>T25-yneS</i>	<i>T25-yneS</i>	<i>T25-mreC</i>	<i>T25-mreC</i>	<i>T25-mreD</i>	<i>T25-mreD</i>	<i>T25-pbp2</i>	<i>T25-zapA</i>	<i>T25-divIB</i>
<i>T25-pbp2</i>	<i>T25-zapA</i>	<i>cdsA-T25</i>	<i>cdsA-T25</i>	<i>cdsA-T25</i>	<i>cdsA-T25</i>	<i>T25-ftsL</i>	<i>T25-ftsA</i>	<i>T25-DNAK</i>	<i>DNAK-T25</i>	<i>T25-ltaS</i>	<i>T25-ltaA</i>
			U/T								
<i>ltaA-T25</i>	<i>T25-ypfP</i>	<i>ypfP-T25</i>	<i>T25-sosA</i>	<i>T25-pbp1stop</i>	<i>T25-pbp1stop</i>	<i>T25-mecA</i>	<i>mecA-T25</i>	<i>T25-LytH</i>	<i>T25-LytN</i>		
U/T			U/T						U/T		

**B**

Positive interactions PBP2A	
N Terminal	C Terminal
<i>T25-PBP2</i> <i>T25-mecA</i>	N/A

<i>T25~zip</i> <i>T18~zip</i>	<i>T25</i> <i>T18</i>

**Figure 4.11 Solid media assay of T25 constructs of Staphylococcal proteins screened against PBP2A**

(A) Interaction assay of T25 array of prey proteins against bait protein PBP2A T18. Performed on minimal media agar with X-Gal. Positive controls were two hybrid reporter genes fused to leucine zippers (pKT25~zip pUT18~zip) and negative interactions, empty B2H vectors (pKT25 pUT18). (B) Summary of positive interactions. This figure uses composite images and not all assays were performed on the same plate. U/T, Untested.

## 4.2.2 Liquid Media Assays

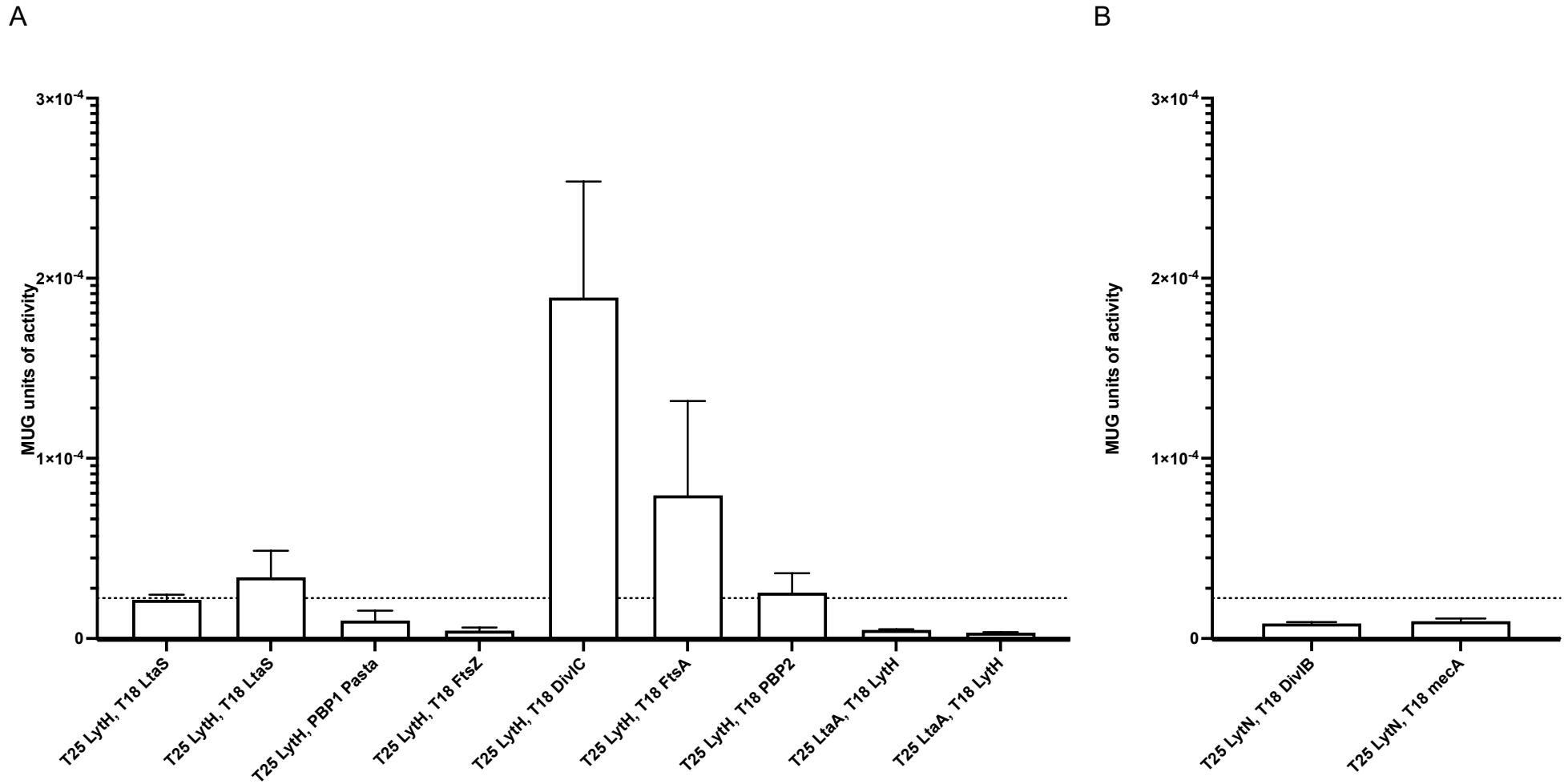
For each interacting partner identified on solid media assays, quantitative liquid media assays using the previously described liquid assays for  $\beta$ -galactosidase activity (section 2.13.7) were used. Strains that gave rise to positive interactions on minimal media were sub-cultured and single colonies used to inoculate triplicate broths for liquid media assays. Liquid media interactions for PBP2A were not performed due to time limitations.

The results of liquid assays for the combinations of LytH and LytN and their potential interacting partners are shown in Figure 4.12. These are displayed separately, in A and B as they were performed using a separate calibration curve, on different days.

Positive interactions above the negative cut-off are observed between LytH and LtaS, DivIC, FtsA and PBP2. However, for LytN no positive interactions were found using the 4x negative control cut off as previously used in Steele et al. (2011).

In Figure 4.13 quantification of  $\beta$ -galactosidase activity for interacting partners of T25-GpsB was performed. T25-GpsB has apparently interacted with T18-GpsB, YsxC, FtsZ, LtaS and EzrA, in at least one replicate, greater than the 4x negative control cut off, but due to high standard deviations, all are reported as preliminary positive interacting proteins.

Figure 4.14 shows the quantification of  $\beta$ -galactosidase activity for interacting partners of T18-GpsB. 17 protein interacting partners were screened with nine confirmed positive interactions, T25-GpsB, YpsA, ParC, FtsA, LtaA, YpfP (N and C terminal fusions) and PBP2, above the negative control cut-off. For the T25 prey protein, the remaining eight samples had high standard deviations meaning results are only preliminary but can be interpreted alongside the solid media, as interactions which require further investigation.

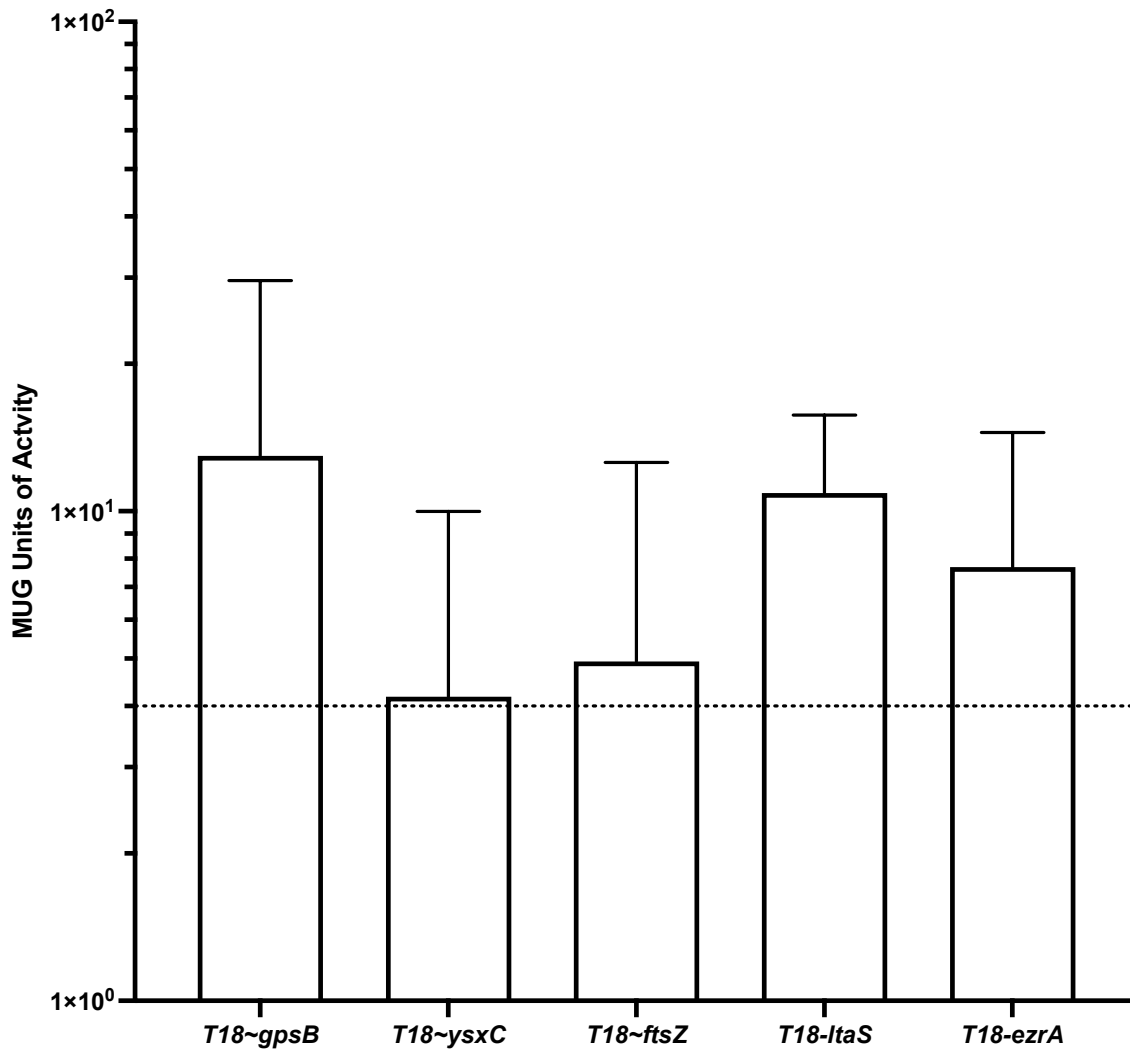


**Figure 4.12 Identification of B2H interacting partners of LytH and LytN determined by liquid  $\beta$ -galactosidase assay.**

Quantification of interactions between proteins of interest with complimentary T18 and T25 fusions for LytH and LytN. Activity is shown as standardised MUG units of activity, adjusted to the optical density of each sample. Results shown are the mean from biologically independent samples performed in triplicate. Error bars represent the standard deviation of each sample. A dotted line on each graph represents cut off level of four times the activity of each plate's negative control. A and B used different calibration curves and were performed independently.

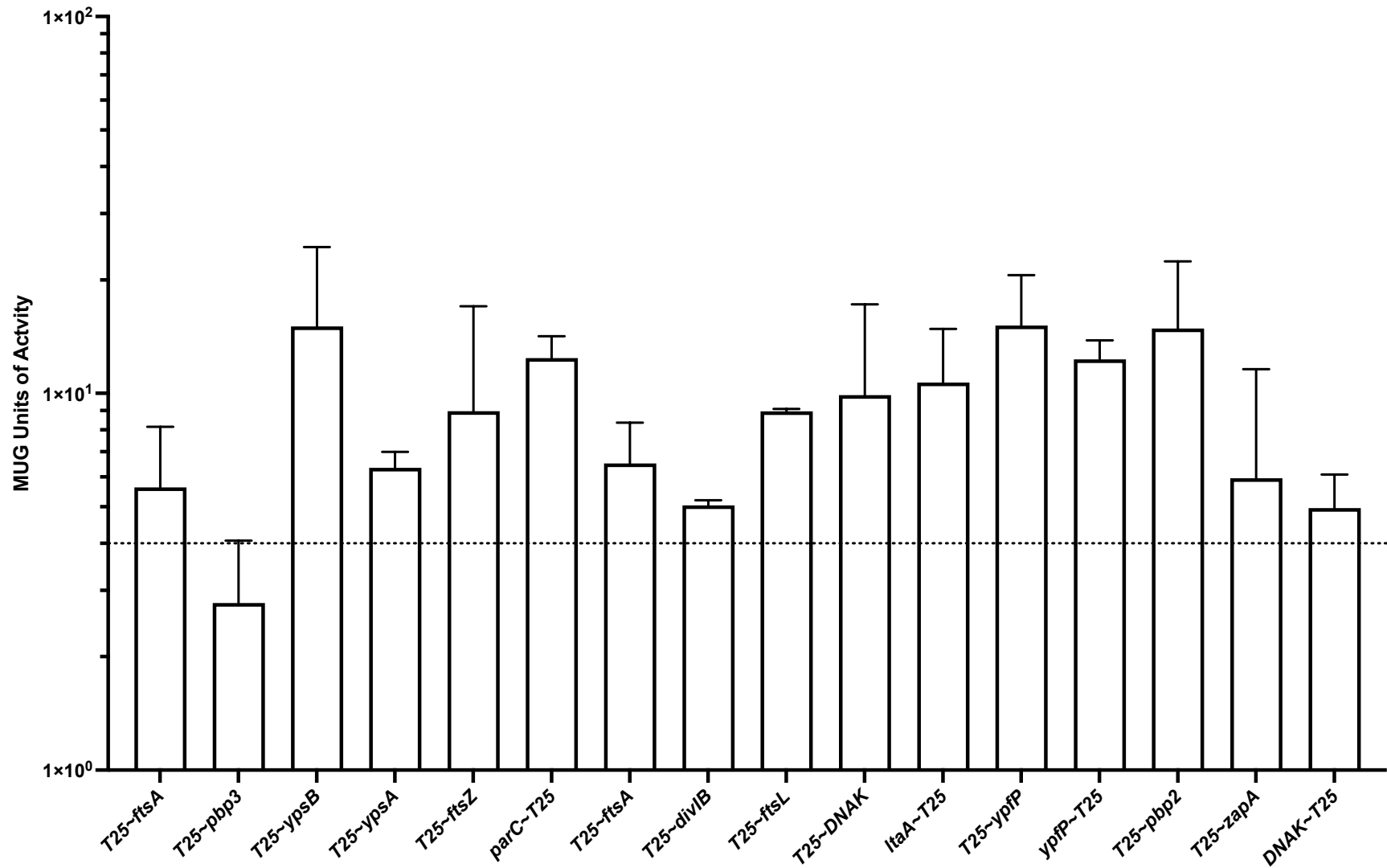
### **4.2.3 Protein interaction mapping**

B2H library screening identified potential protein-protein interactions. Cytoscape (version 3.10.1) (Shannon et al., 2003) was used to visualise protein interactions in Figure 4.15. This was prepared using literature sources and data from this study. To differentiate interactions confirmed by  $\beta$ -galactosidase liquid assays, Figure 4.15 uses dotted lines. The diagram shows novel interactions identified in this study between different proteins.



**Figure 4.13 Identification of B2H interacting partners of T25-GpsB determined by  $\beta$ -galactosidase liquid assay.**

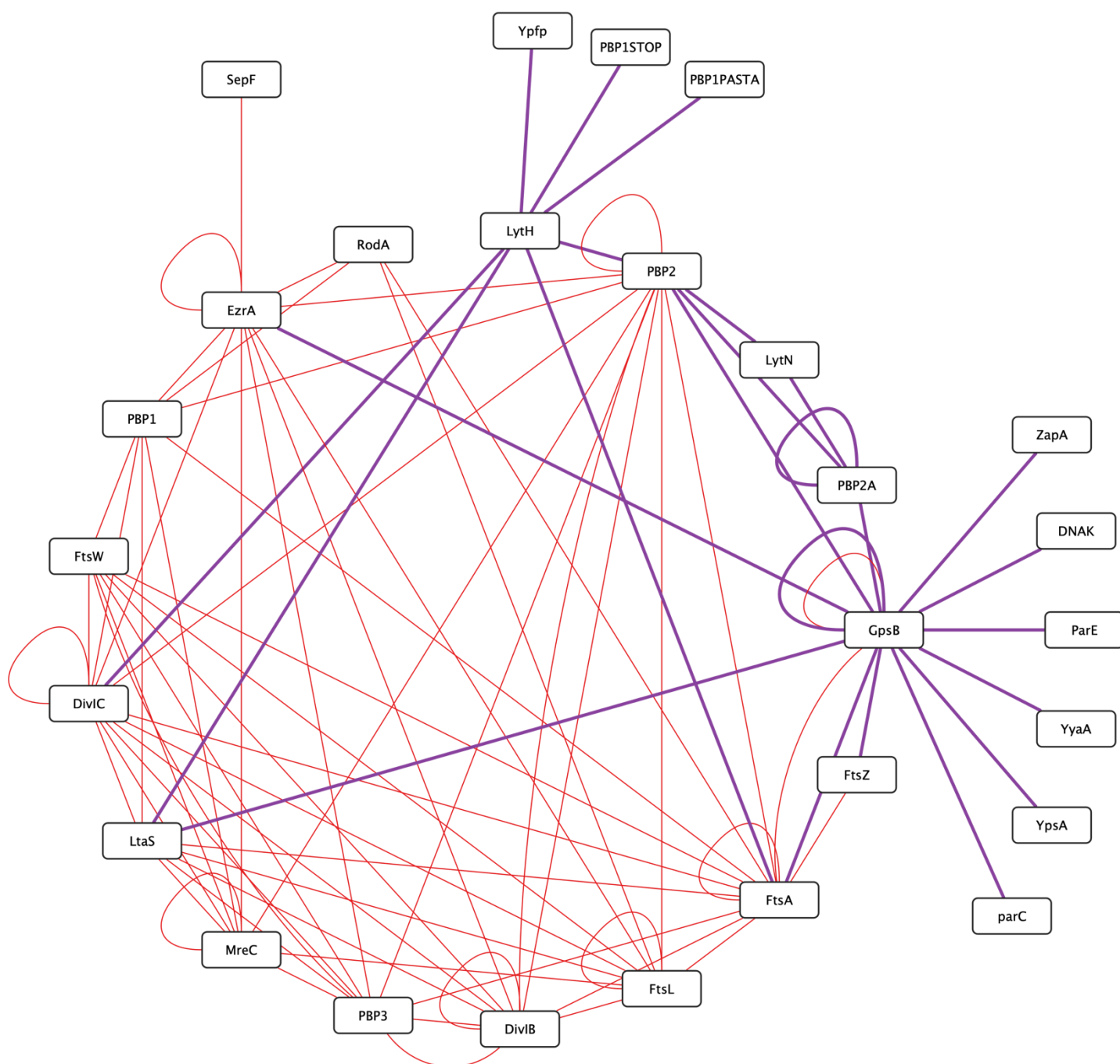
Quantification of interactions between proteins of interest with complimentary T18 and T25 fusions. Activity is shown as standardised MUG units of activity, adjusted to the optical density of each sample. Results shown are the mean from biologically independent samples performed in triplicate. Error bars represent the standard deviation of each sample. A dotted line on each graph represents cut off level of four times the activity of the negative control.



**Figure 4.14 Identification of B2H interacting partners of T18 GpsB determined by  $\beta$ -galactosidase liquid assay.**

Quantification of interactions between proteins of interest with complimentary T18 and T25 fusions. Activity is shown as standardised MUG units of activity, adjusted to the optical density of each sample. Results shown are the mean from biologically independent samples performed in triplicate. Error bars represent the standard deviation of each sample. A dotted line on each graph represents cut off level of four times the activity of the negative control.





**Figure 4.15 Protein interaction mapping of *S. aureus* as determined by two hybrid analysis in the context of the literature.**

Interacting web of protein partners determined by B2H assays. Interactions from this study are shown in purple, interactions from literature are shown in red (Bottomley et al., 2017; Steele et al., 2011; Wacnik et al., 2022). Self-interactions are depicted by a curved arrow. Detail is not shown on orientation/specific B2H fusions of interactions for ease of interpretation of this diagram.

#### 4.2.4 Investigating protein interactions using co-immunoprecipitation

In both Chapter 3, and this Chapter, the interacting partners of the methicillin resistance determinant, PBP2A were determined. The B2H technique lacks the ability to probe interactions between this resistance determinant and proteins of interest directly in *S. aureus* as it requires the use of the model *E. coli* BTH101 strains also investigations into interactions in the presence of methicillin are not possible. A previous study Panchal (2018) and Pinho et al (2001) investigated the localisation of PBP2A and its role in resistance to antibiotics. This highlights the ease of using fluorescently labelled functional PBP2A fusions for the imaging and localisation of the protein during distinct stages of the cell growth and division cycle.

Here I aimed to create and validate GFP fusions for use in co-immunoprecipitation experiments. To verify the developed co-immunoprecipitation methodology a protocol for cell breakage and fractionation was established (Section 2.12.5).

##### 4.2.4.1 CO-IP experimental design

Co-IP is dependent on the identification of specific interactions. Thus, it is essential to reduce non-specific pull down of proteins by the antibodies and so it was important to use  $\Delta spa$  strains were important as SpA binds immunoglobulins (R. Zhang et al., 2021).

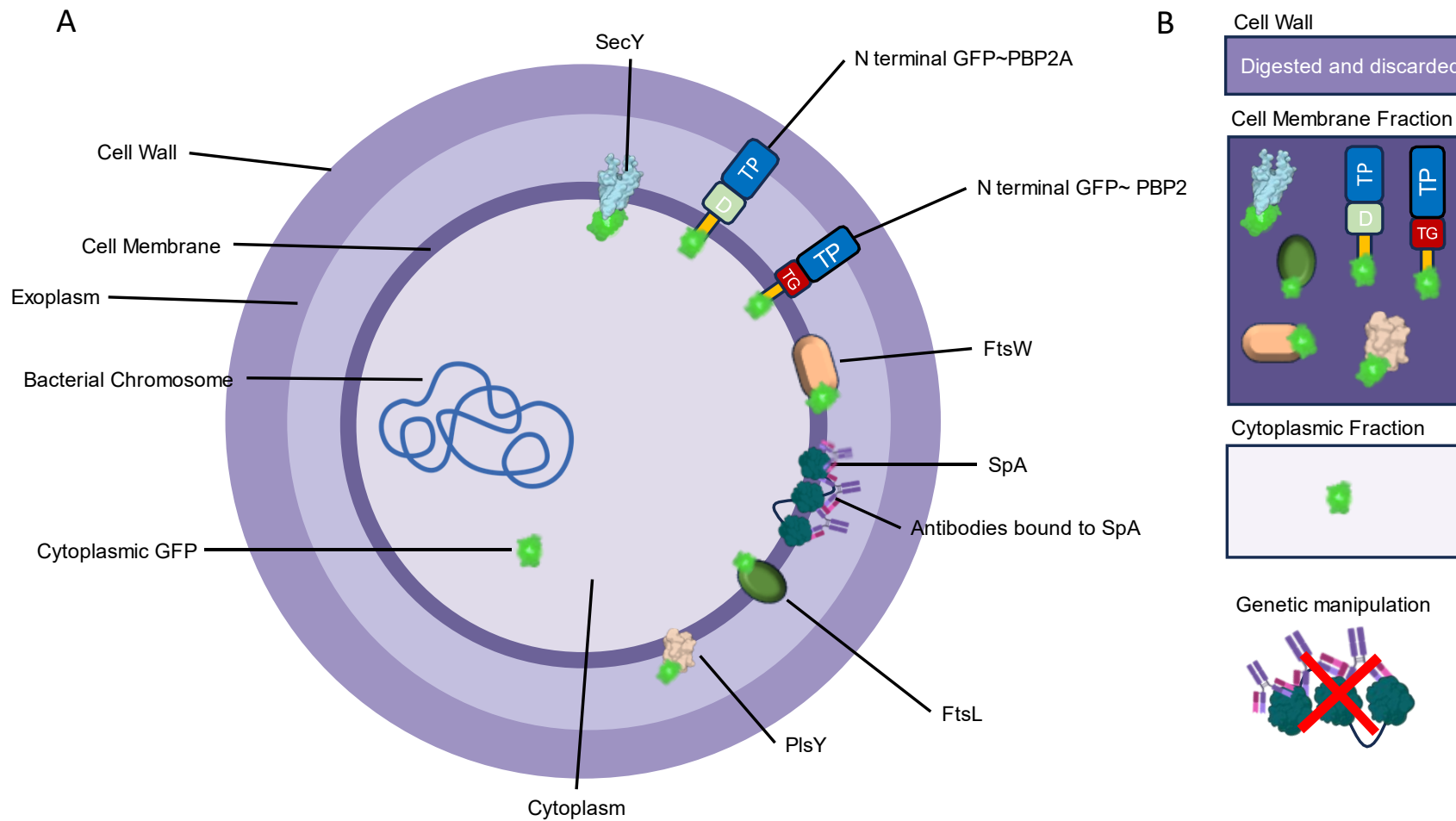
Experimental controls for the PBP2A experiments include chromosomally expressed tagged membrane bound proteins SecY-GFP (SJF 2103) and PlsY-GFP (SJF 4772) alongside cytoplasm expressed free GFP (pMa1M-GFP SJF 4618), and membrane associated FtsW from the divisome, to be used to validate the cell fractionation steps. Figure 4.16 shows compartmental localisation of these fragments and the expected fractions, they are present in after purification of samples.

Experimental controls with well characterised interactions were also chosen to aid the interpretation of data and to provide insights into their own interaction characteristics. The chosen control strains were *spa::kan* pLOW Ppcn GFP-PBP2 (SJF 5816), *spa::kan* pLOW PPCN FtsW-GFP (SJF 5817) and  $\Delta spa$  pKASBAR Pspac FtsL GFP (SJF 5818).

The system used to study PBP2A interactions allows its production to be controlled and functionality assessed by virtue of its ability to lead to  $\beta$ -lactam resistance. The use of a strain background with the *rpoB*<sup>H924Q</sup> mutation allows the role of the potentiated PBP2A (Panchal, 2018) to be examined.

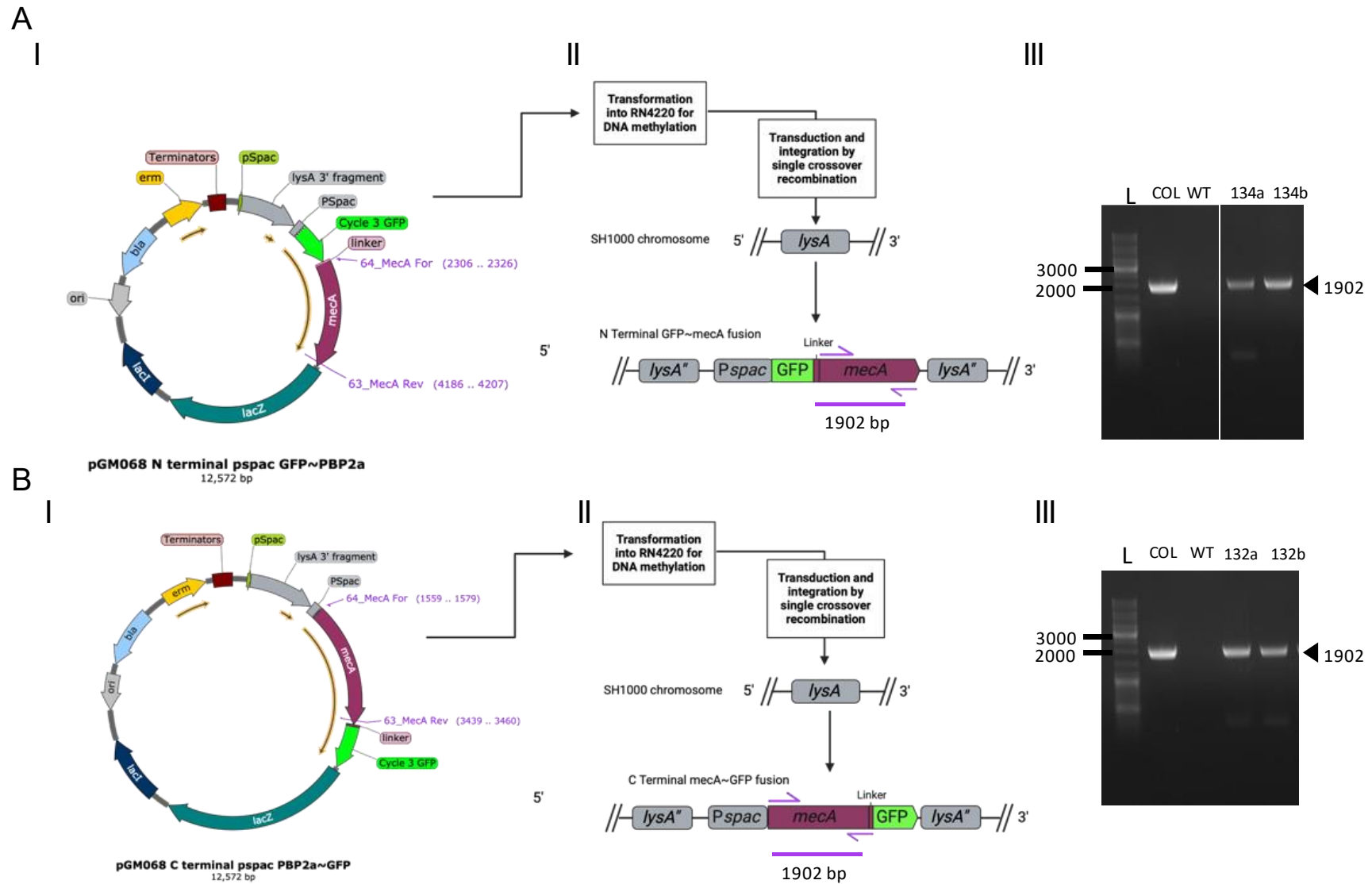
#### 4.2.4.2 Design of PBP2A fluorescent fusions

To investigate the role of PBP2A, constructs were designed using the same flexible 2x((4xGLY)Ser) linker to allow independent folding of both PBP2A and GFP as previously used for the localisation of PBPs (Wacnik et al., 2022) and DivIC (Tinajero-Trejo et al., 2022) under the control of *Pspac*, the widely used IPTG inducible promoter (Yansura and Henner, 1984). Both single gene copy, using pGM068 (SJF 3538) for single crossover recombination at *lysA* and multicopy pLOW (SJF 3543) constructs were designed. Plasmids were subcontracted to Genewiz (Appendix 5). Diagrammatical representation of the assembly of the strains is shown in Figure 4.17.



**Figure 4.16 Location of key GFP tagged proteins in a representative cell**

Representative staphylococcal cell (A), showing key structures and location of GFP tagged proteins used in this study. (B) theoretical contents of the cell membrane and cytoplasmic fractions, also showing genetic manipulation to knock out the immunoglobulin SpA gene (García-Lara et al., 2015).



**Figure 4.17 Construction of chromosomal *mecA* GFP fusions in *S. aureus***

Diagrammatic representation of the construction of *S. aureus* single copy chromosomal *mecA* (from high-level resistant strain COL) with N and C terminal GFP transcriptional fusions, (A.I. and B.I. respectively). Schematic representation of the *lysA* region post integration of N terminal *Pspac* GFP~*mecA* (A.II.) and C terminal *Pspac* *mecA* ~GFP (B.II.) by transformation and then phage transduction. Chromosomal integration verified by PCR using *mecA* specific primers, Purple (primers 63 and 64) COL, high-level MRSA (*mecA* and *rpo*<sup>\*</sup>), WT represents the SH1000 negative control. N terminal *Pspac* GFP~ *mecA* (134 a and b) and C terminal *Pspac* *mecA* ~GFP (132 a and b,) performed in duplicate (A.III. and B.III.).

#### 4.2.4.3 Strain construction and method development for CO-IP

Our previous studies have shown apparent toxicity of *S. aureus* PBPs when expressed in *E. coli*, and so plasmids from Genewiz were immediately transformed into electrocompetent *S. aureus* (RN4220 SJF 0684) as described in section 2.13.2.

#### 4.2.4.4 Strain validation

The expression of *mecA* under the control of *Pspac* allows the functionality of the fusions to be validated by measuring subsequent antibiotic resistance levels. To examine a range of possibilities both the N and C terminal fusions and multicopy (plasmid based, pLOW) and single copy (single crossover, pMG068 based) PBP2A GFP fusions, were used.

Table 4.1 shows the levels of oxacillin resistance of different SH1000 strains containing GFP tagged PBP2A. Oxacillin MICs ranged from 0.5 – 8 µg/mL for SH1000 strains containing PBP2A constructs in comparison to an MIC of 0.38 µg/mL for the wild type strain, or wild type strains with a  $\Delta spa$  mutation. The presence of IPTG did not affect the level of oxacillin resistance exhibited by control strains, shown as bold Table 4.1.

Plasmids expressing N or C terminal fusions of PBP2A to GFP did not reliably transduce into strains with the *rpoB*<sup>H929Q</sup> mutation or result in high-levels of oxacillin resistance of  $\geq 256$  µg/mL. Single copy, chromosomally expressed PBP2A tagged with GFP (constructed with pGM068, Strains 132, 134, 154, 155, 164 and 166) exhibit increased levels of oxacillin resistance compared to SH1000. No single copy strains (genotype: *lysA::kan rpoB*<sup>H929Q</sup> *Pspac* GFP-PBP2A or PBP2A-GFP) were constructed with *rpoB*\* mutations due to time limitations as transductions proved unreliable .

#### 4.2.4.5 Verification of strains using $\alpha$ -GFP antibodies

Prior to pulldown experiments using GFP traps (ProteinTech, UK) the strains were validated using  $\alpha$ -GFP and  $\alpha$ -PBP2 to verify the relevant staphylococcal strains containing functional GFP fusions. The presence of the *spa/sbi* band at ~50 kDa necessitates the use of SpA as it highlights the cross reactivity to the antibodies used.

#### 4.2.4.6 Verification of SpA strains for CO-IP

In order to remove SpA, a range of  $\Delta spa$  mutations were used. Primers 164 and 165 were used to amplify the *spa* region. To allow strain construction a *spa* knockout strain was used, *spa::kan* (SJF 2978)) and the *spa::tet* (SJF 1942). Figure 4.19 shows strains where the *spa* has been used in this study where the mutation has been introduced into another background.

#### 4.2.4.7 Microscopy of strains for Co-immunoprecipitation

Genetically verified strains were prepared for structured illumination microscopy (SIM) as described in section 2.15 and SIM performed with Dr. Mariana Tinajero-Trejo and Dr. Lucia Lafage.

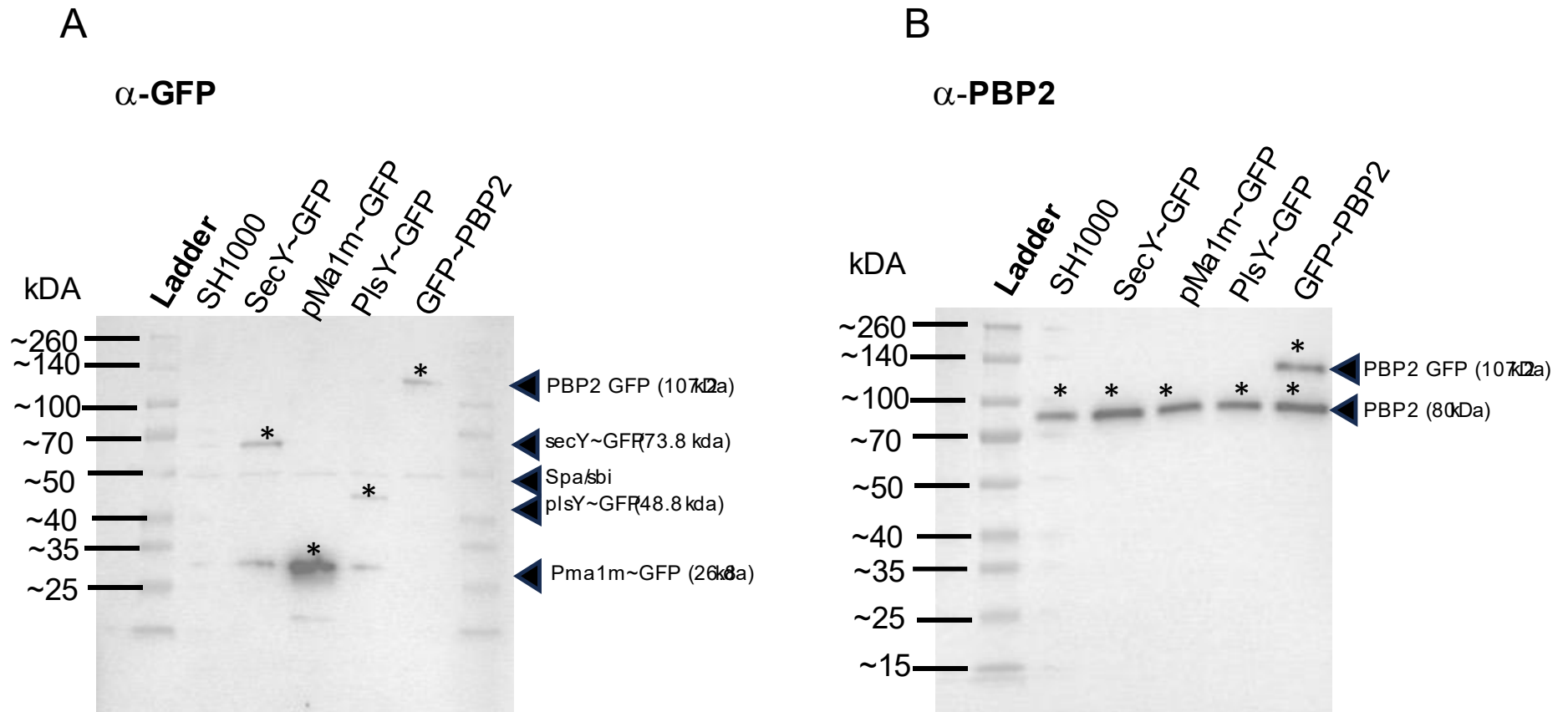
To avoid bleaching of GFP, samples were stained with NHS-ester to allow localisation and visualisation of the cell and the cell wall.

Figure 4.20 shows NHS-ester<sub>355nm</sub> and GFP<sub>488nm</sub> imaging of representative fluorescent strains SH1000  $\Delta spa$  (SJF) SH1000 exhibiting no fluorescence at 488nm (GFP), Cytoplasmic fluorescence control Pma1M-GFP (2103) with cytoplasmic GFP localisation, and  $\Delta spa ppcn$  FtsW-GFP, showing this strains characteristic septal localisation (unpublished data from Dr. Mariana Tinajero-Trejo, University of Sheffield) as well as the SH1000  $\Delta spa$  pLOW *Pspac* GFP-PBP2A showing cells with aberrant cell wall associated GFP-PBP2A

**Table 4.1 Minimum inhibitory concentrations of strains designed for co-immunoprecipitation using GFP tagged PBP2A by Etest.**  
 Etests of strains of SH1000, relevant genotypes, plasmids and oxacillin MIC in the presence and absence of IPTG. Control strains shown in bold.

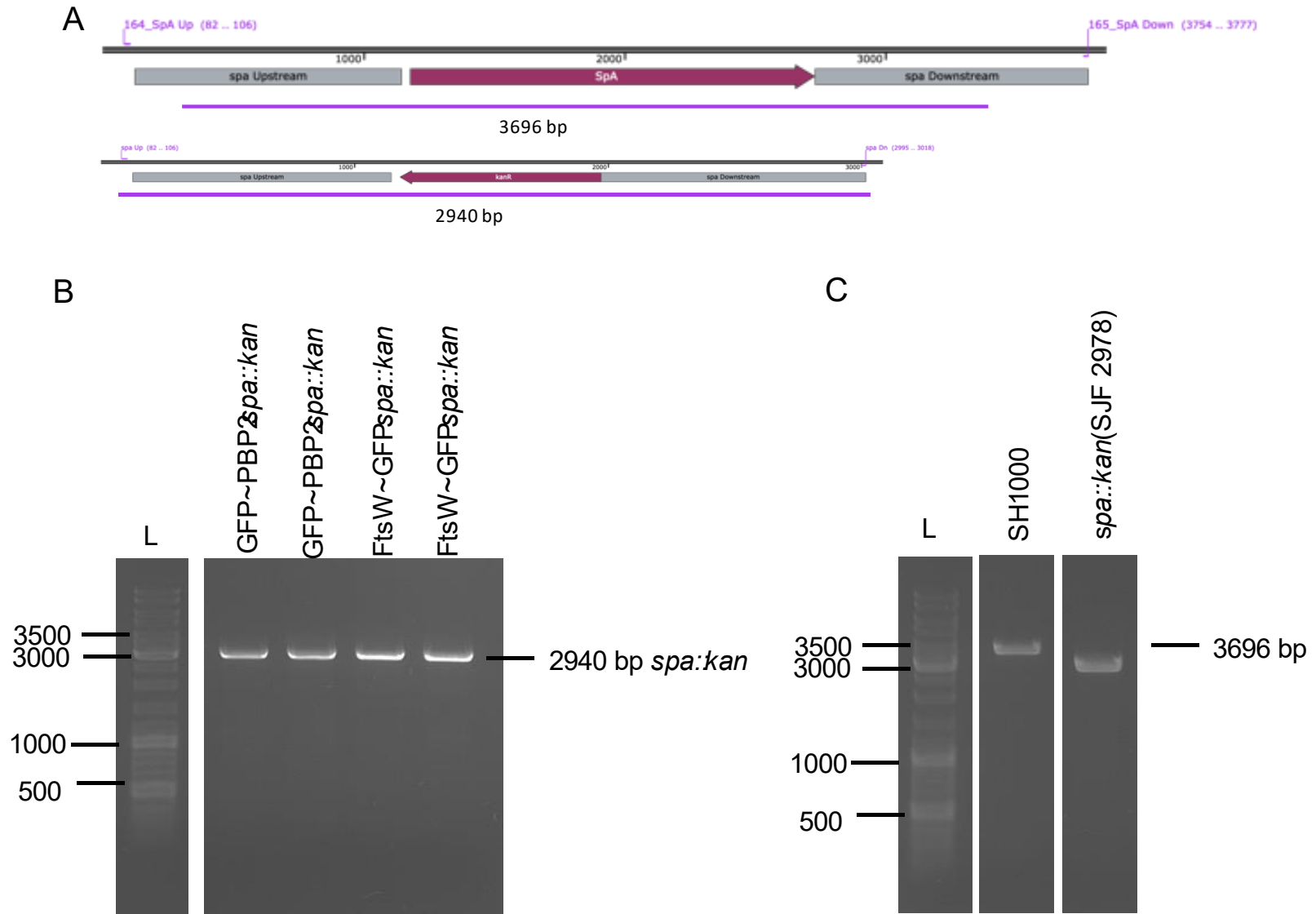
Strain	Relevant Genotype	Plasmid	Oxacillin MIC
			TSA IPTG 0.1 M
<b>SJF 0682</b>	<b>Wild Type SH1000</b>		<b>0.38</b>
6132	<i>Pspac</i> PBP2A ~GFP		8
6133		pLOW <i>Pspac</i> PBP2A ~GFP	1.5
6134	<i>Pspac</i> GFP~PBP2A		6
6135		pLOW <i>Pspac</i> GFP~PBP2A	0.38
<b>136 SJF 5915</b>	<b><math>\Delta</math><i>spa</i></b>		<b>0.38</b>
6140	$\Delta$ <i>spa</i> <i>Pspac</i> PBP2A ~GFP		6
6138	$\Delta$ <i>spa</i>	pLOW <i>Pspac</i> PBP2A ~GFP	1.5
6141	$\Delta$ <i>spa</i> <i>Pspac</i> GFP~PBP2A		8
6139	$\Delta$ <i>spa</i>	pLOW <i>Pspac</i> GFP~PBP2A	0.5
<b>5010</b>	<b><i>lysA::kan rpoB<sup>H929Q</sup></i></b>		<b>0.19</b>
	N/A	<i>lysA::kan rpoB<sup>H929Q</sup> Pspac</i> PBP2A ~GFP	No suitable transductants
6136		<i>lysA::kan rpoB<sup>H929Q</sup></i>	No suitable transductants
	N/A	<i>lysA::kan rpoB<sup>H929Q</sup> Pspac</i> GFP~PBP2A	No suitable transductants
6137		<i>lysA::kan rpoB<sup>H929Q</sup></i>	0.5





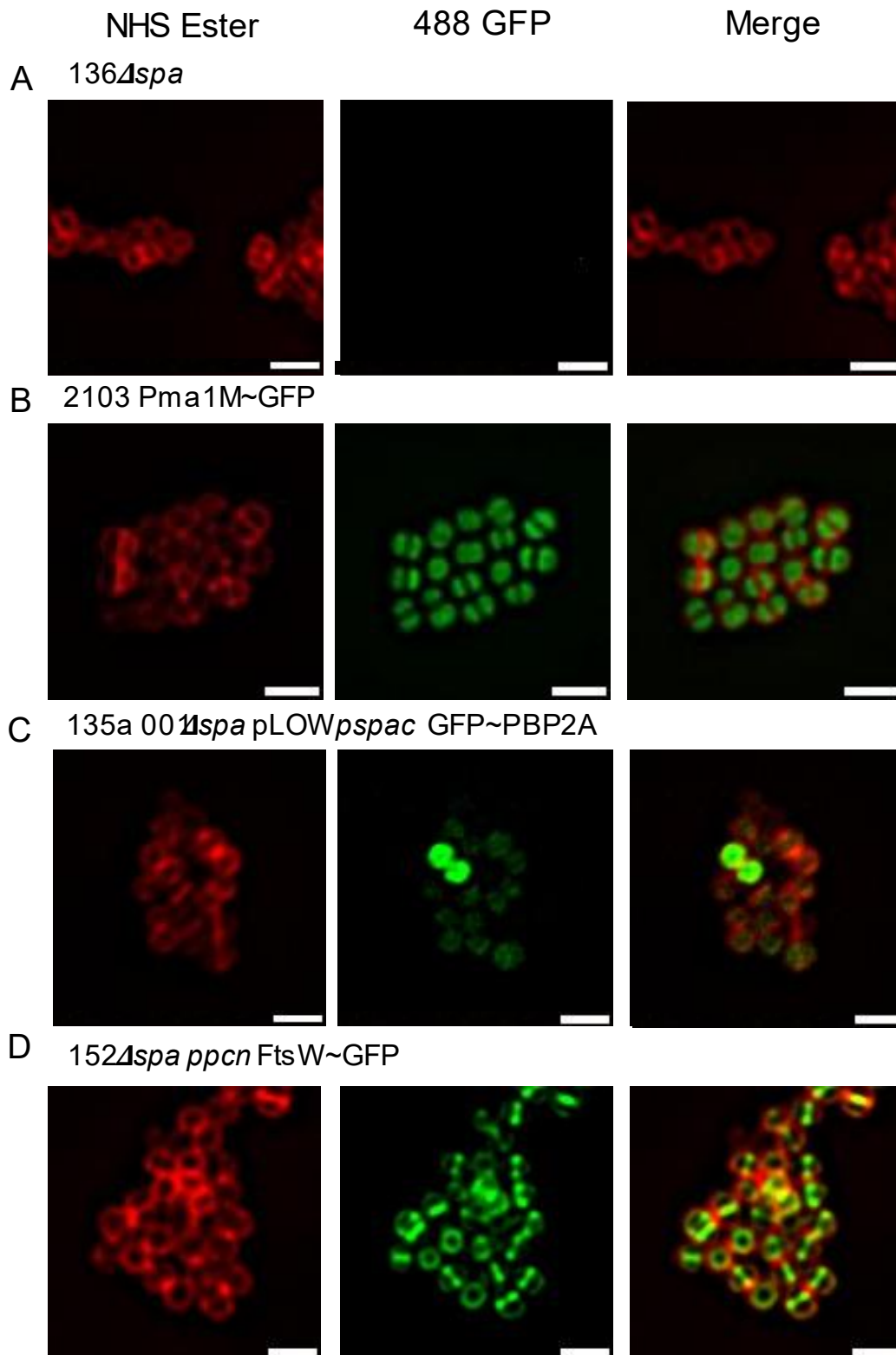
**Figure 4.18 Western blots to verify control strains for co-immunoprecipitation using  $\alpha$ -GFP (A) and  $\alpha$ -PBP2 (B)**

Whole cell lysates of WT SH1000 and derivatives: SecY~GFP, pma1m~GFP, pCQ11 PlsY~GFP and pLOW GFP~PBP2 were probed with  $\alpha$ -GFP (A) and  $\alpha$ -PBP2 (B) at a 1:1000 dilution. Arrows indicate bands of interest on each gel with approximate molecular weights. The Western blot using  $\alpha$ -GFP (A) shows the following bands SecY~GFP (73.8 kDa), pMa1m~GFP (26.8 kDa), PlsY~GFP (48.8 kDa) and GFP~PBP2 (107.2 kDa). Consistent binding of  $\alpha$ -GFP by SpA is observed at approximately 50 kDa. The western blot using  $\alpha$ -PBP2 (B) shows all strains with PBP2 (80 kDa) and the pLOW GFP~PBP2 construct with a GFP~PBP2 band at 107.2 kDa.



**Figure 4.19 DNA electrophoresis of PCR products confirming *spa* inactivation in strains for Co-immunoprecipitation.**

Physical map showing expected PCR product size of wild type *spa* gene (3696 bp) (A), PCR products from amplification using *spa* specific primers independent biological replicates of *spa::kan* knockouts expressing GFP~PBP2 and FtsW~GFP (B) and controls SH1000 and *spa::kan* (C).



**Figure 4.20 Structured illumination microscopy (SIM) of strains expressing fluorescently tagged proteins of interest for co-immunoprecipitation and investigation of cellular localisation.**

NHS-ester355nm and GFP488nm were used to image (A) SH1000 *spa::kan* (SJFCHK), (B) Cytoplasmic fluorescence control Pma1M~GFP (2103), (C) SH1000 *spa* pLOW Pspac GFP~PBP2A and (D) *spa* Ppcn FtsW~GFP. Cells were grown for in the presence of 2  $\mu$ g/mL methicillin and IPTG 0.1 mM to induce expression of fusion proteins. Treated with NHS-ester to stain cell walls. Images are average intensity projections of z-stacks. Scale bars shown are 2  $\mu$ m.

### 4.3 Discussion

Here, I aimed to identify novel interactions of cell growth and division proteins in *S.aureus*, I developed and used a 96-well transformation to streamline and carry out directed B2H interaction screening of proteins of interest. Also, the methodology for a CO-IP system, to permit interactions to be identified was developed. Having two independent methods allows interactions to be verified. My B2H extended previous analysis on cell division and growth associated proteins (Bottomley, 2011; Kent, 2013; Steele et al., 2011).

My screen identified many novel interactions however, many of the detected interactions on solid media were not confirmed by liquid assay. Thus, further investigations are required to troubleshoot the liquid assay. Whilst aspects of my study are incomplete, it sheds further light on the complex and multi-fold interactions of proteins involved in growth and division. It also alludes to a complex interplay of both enzymatic and regulatory components.

Previous studies have suggested that the combined action of GpsB and DivIVA link teichoic and cell division in a regulatory manner (Sutton et al., 2023). My study demonstrated an interaction between LtaS and GpsB. LtaS is a crucial enzyme in LTA biosynthesis (Reichmann et al., 2014) and coordinating its localisation with cell division proteins may be important. Additionally, GpsB was found to interact with YpfP. YpfP is a diacylglycerolglucosyltransferase which facilitates LTA anchorage to the cell membrane (Fedtke et al., 2007).

My study supports a key interaction between *S. aureus* GpsB and PBP2 and while this would need further confirmation using an alternative protein-protein interaction methodology, the detection of a strong positive interaction on solid media and in the liquid assays highlights an important biological relevance.

Interestingly, as a spheroid bacterium *S. aureus* does not require overarching relocation of PBPs between elongation and division sites, whereas in *B. subtilis* GpsB has been identified as interacting with EzrA as part of its facilitation of PBP transfer between elongation and division (Claessen et al., 2008). The discovery of a GpsB and PBP2 interaction in my study points to a cooperative mechanism of GpsB and peptidoglycan synthase interaction and localisation as found in other organisms (Cleverley et al., 2019; Sacco et al., 2022). This is further evidenced by *gpsB* mutants which have been observed to demonstrate increased PBP2 and 3 localisation at the septum and a decrease in peripheral cell wall synthesis (Sutton et al., 2023).

LytH has potential interactions with T18 fusions of DivIC, FtsA, PBP2, LtaS, YpfP<sup>-</sup>, PBP1<sup>STOP</sup> and PBP1<sup>PASTA</sup>. Notably, interactions between truncated PBP1 strains and not wild type PBP1 is interesting as this may occur via the PBP1 membrane spanning domain. LytH also interacts with

PBP2 and so is linked to major essential PG biosynthesis enzymes. LytH has an important function in PG homeostasis (Do et al., 2020) and so complex formation would optimise this role. Interactions between PBP2 and LytH is interesting when LytH is considered to be a potentiator of oxacillin/ $\beta$ -lactam resistance (Fujimura and Murakami, 1997). This suggests that LytH has a combined role with PBP2 in promoting antibiotic resistance.

A newly identified potential LytN-PBP2A interaction is very interesting as PBP2A does not have many partners in *S. aureus*. LytN has a role in division and so this may enhance the ability of PBP2A to take over the activity of the native enzymes in the presence of antibiotics. Despite these results this data set is incomplete primarily because of time limitations which, therefore necessitate further investigation, using other methods for the determination of protein-protein interactions. Further inclusion of cell wall hydrolases in the screening array would enable insight into how interactions between hydrolases facilitate the control and regulation of morphogenesis.

My study supports a cooperative interaction between PBP2 and PBP2A. PBP2A acts as a dimer (Lim and Strynadka, 2002). PBP2 and PBP2A may form a heterodimer in the presence of antibiotics, suggesting that the function of PBP2A requires the dimerization with PBP2 to accommodate and facilitate the transpeptidation of the peptidoglycan strands in the synthesis of the new cell wall. This would allow PBP2A to be an active transpeptidase but driven by the interaction of PBP2 with other proteins.

In this Chapter a methodology was designed to screen and characterise interactions by co-immunoprecipitation This was based on GFP fusions and their pull down with  $\alpha$ -GFP antibodies. Initial studies showed constructs expressing PBP2A GFP did result in increased antibiotic resistance indicating functionality. However, PBP2A GFP localisation was not fully verified to allow further use in pulldowns. A previous SNAP tagged PBP2A (Panchal, 2018) also showed a localisation not entirely expected. Thus, increased resistance may occur even with an unstable protein fusion.

Future studies should aim to further verify interactions that have been briefly examined here, using different methodologies ideally performed in *S. aureus*. This would support the development of databases, such as STRING (Szklarczyk et al., 2023) to build protein-protein interaction networks. These can be interrogated to reveal potential functional connections, unravelling the complex processes that underpin cellular physiology.

# Chapter 5 Analysis of the mechanism of action of resensitising agents that modulate $\beta$ -lactam resistance in MRSA.

## 5.1 Introduction

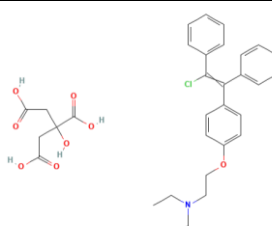
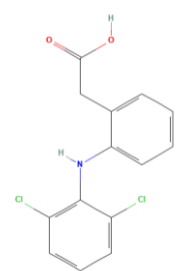
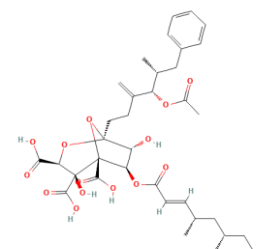
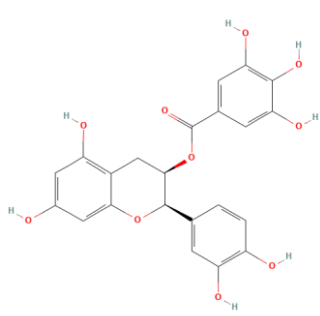
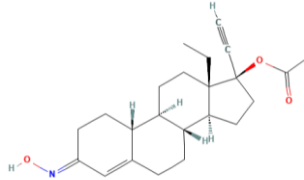
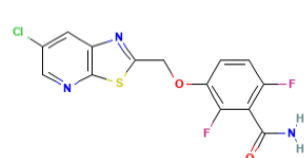
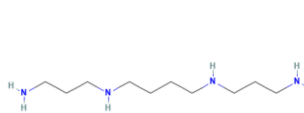
*S. aureus* requires the acquisition of the PBP2A to develop low level resistance to  $\beta$ -lactam antibiotics. High-level resistance to  $\beta$ -lactams, develops due to mutations in potentiator genes (Bilyk et al., 2022; Panchal et al., 2020). These mutations in genes encoding components such as RNA polymerase subunits B and C (*rpoB*, *rpoC*) and *rel* (*relA* and *relQ*) occur clinically (Aiba et al., 2013; Mwangi et al., 2013; Panchal et al., 2020). How potentiator gene mutations lead to increased resistance is unknown.

Chemical adjuvants can synergize with existing antibiotics to overcome resistance. The  $\beta$ -lactamase inhibitor clavulanic acid (discovered in 1977) exemplifies this strategy, resensitising resistant bacteria like penicillin resistant *S. aureus* to the effects of  $\beta$ -lactams (Ba et al., 2015; Neu and Fu, 1978; Reading and Cole, 1977). A plethora of diverse natural and synthetic chemicals have been found to modulate methicillin resistance in *S. aureus* (Stapleton and Taylor, 2002). These resensitising agents, with origins ranging from plants to bacteria, hold potential as adjuvants to existing antibiotics. They also provide tools to give mechanistic insight into resistance evolution. To highlight the variety and diversity of these compounds, examples of these chemicals and their origins are shown in Table 5.1.

Some resensitising agents are FDA approved drugs or extracts from tea suggesting their clinical use could be expedited (Foster, 2019). One such FDA approved drug is clomiphene citrate, an affordable first line therapy for infertility and has been used for 40 years to yield a high birth rate with few side effects (Homburg, 2005). During antagonistic screens of inhibitors of cell wall synthesis, Clomiphene citrate was identified as an inhibitor of undecaprenyl diphosphate synthase resulting in sensitisation to methicillin (Farha et al., 2015).

**Table 5.1 Table of Resensitising agents**

Compounds shown are all known sensitising agents, highlighting the diversity of compounds able to re-sensitise MRSA to the effects of  $\beta$ -lactams.

Compound	Origin and Details	Structure	References
Clomiphene Citrate	Infertility treatment, inhibitor of undecaprenyl diphosphate synthase, FDA approved. A mixture which consists of citric acid and Zuclomiphene.		(Farha et al., 2015; Homburg, 2005)
Diclofenac	Widely used non-steroidal anti-inflammatory drug used in Voltarol <sup>®</sup> .		(Sharma and Gutheil, 2023; S. Zhang et al., 2021)
Zaragozic Acid	A statin that inhibits membrane microdomain assembly		(García-Fernández et al., 2017)
Epicatechin Gallate	A galloyl catechin extracted from green tea. Studies show its ability to resensitise increased angiogenesis and modulates human inflammatory responses in the presence of elevated vascular endothelial growth factor (VEGF).		(Bernal et al., 2010; Rosado et al., 2015; Stapleton et al., 2007)
Norgestimate	An acetylated progestin used as a fertility treatment. FDA approved.		(Yoshii et al., 2017)
PC190723	An inhibitor of FtsZ resulting in the delocalisation of PBP2.		(Tan et al., 2012)
Spermine	A linear polyamine with important physiological roles in cell growth and differentiation.		(Oille, 1986; Pawar et al., 2019; Yao and Lu, 2012)

The active ingredient in the widely used topical pain reliver Voltarol® is diclofenac which also reduces resistance levels MRSA and can be used synergistically with the antibiotic to prevent the development of medical device implant infections (S. Zhang et al., 2021). One compound that sensitises MRSA, the statin Zaragozic acid inhibits PBP2A activity by disrupting the formation of lipid rafts, PBP2A maturation and oligomerization to stop its activity and therefore the maintenance of high-level resistance (García-Fernández et al., 2017). The design of compounds to resensitise MRSA to the effects of  $\beta$ -lactams using computational studies has resulted in novel compounds such as PC190723 (Tan et al., 2012).

MRSA resensitising agents can also act at the level of membrane homeostasis. Polyamines interact with the cell membrane and affect its fluidity (Yao and Lu, 2012). Linear polyamines from putrescine to spermidine and spermine, have been shown to re-sensitise MRSA to the effects of  $\beta$ -lactams (Yao and Lu, 2012). In synergy with oxacillin, Spermine impacts cell wall synthesis and global gene regulation (Pawar et al., 2019). In studies using directed evolution, a PBP2 mutation in the TP domain removed spermine's ability to re-sensitise MRSA to the effects of  $\beta$ -lactams through complex modulation of protein expression (Yao and Lu, 2012).

Compounds extracted from green tea include the polyphenols (-)-epicatechin gallate (ECg) and (-)-epigallocatechin gallate (EGCG), known to exhibit bacteriostatic effects against MRSA through destruction of cell membranes and resultant ROS-mediated stress (Zhong et al., 2023). The mechanism of ECg in animal cells is to bind to the membrane and integrate deep into the lipid palisade regulating the fluidity of the bilayer (Rosado et al., 2015). (-)-epicatechin homologs lacking the galloylated moiety can also facilitate ECg entry into the membrane (Palacios et al., 2014). When intercalated into the lipid membrane the galloyl moiety bound to the C ring is critical in the inhibition of fatty acid synthesis demonstrating cytotoxicity to human cancer cells (Wang et al., 2003). Galloyl catechins have been evaluated as clinical inhibitors of MRSA (Palacios et al., 2014). Other gallates such as Octyl Gallate have been shown to resensitise MRSA to the effects of penicillin and other antimicrobials thought to be through increasing cell wall permeability (Tamang et al., 2022).

Studies have also demonstrated that the combination of ECg and oxacillin can delocalize a plasmid-encoded GFP-PBP2 fusion protein from the septum in *S. aureus* MRSA strain COL (Bernal et al., 2010) ECg also disrupts the resistance mediated by PBP2A in strains EMRSA and Mu50 (Bernal et al., 2010). Interestingly, while ECg alters the cell wall, it neither directly affects penicillin binding to PBP2A, 3, or 4 nor influences the cellular level of PBP2A (Bernal et al., 2010; Stapleton et al., 2007). However, its addition to isolated membrane preparations significantly



reduces penicillin binding to PBP1 (Stapleton et al., 2007). This suggests that the primary target of ECg might be PBP1.

Inhibiting PBP1 could explain the observed delocalization of PBP2 from the divisome. PBP1 plays a crucial role in cell wall synthesis and septum formation (Wacnik et al., 2022). Without proper septal localization of PBP2, on which PBP2A relies, the key enzyme for methicillin resistance, would be unable to effectively maintain its high activity, leading to reduced resistance in the COL background. The resensitising compound Norgestimate, an oral contraceptive and hormone replacement therapy (Yoshii et al., 2017), has been demonstrated to result in increased expression levels of PBP2 and re-sensitisation of MRSA to the effects of  $\beta$ -lactam antibiotics through changes in cell wall morphology, including increased cell wall thickness (Yoshii et al., 2017).

Thus, a promising range of MRSA re-sensitising agents have been described. They give the hope of adjuvants to reinvigorate the use of clinically important  $\beta$ -lactams in human treatment. They can also be used to probe the molecular mechanism of resistance as mostly their modes of action are obscure.

### 5.1.1 Aims

We have established an experimental framework to study MRSA mechanisms in the well characterised SH1000 strain background (Panchal et al., 2020). High-level  $\beta$ -lactam resistance requires both the *mecA* gene (encoding PBP2A) and a potentiator mutation (such as *rpoB*<sup>H929Q</sup>) (Bilyk et al., 2022; Panchal et al., 2020). This provides a platform for which to investigate the activity of resensitising agents. We hypothesised that exposure to resensitising compounds would result in the generation of spontaneous mutations in genes related to antimicrobial resistance. The specific aims of this chapter were to:

- i. To use directed evolution to generate strains of MRSA resistant to the effects of the re-sensitising compound ECg.
- ii. Identify and characterise genes involved in resistance to the effects of ECg and other re-sensitising compounds.
- iii. Investigate the molecular mechanisms of resistance to the effects of re-sensitising compounds.

## 5.2 Results

### 5.2.1 (-)-epicatechin gallate sensitises MRSA.

To evaluate the effect of ECg, a range of strains were used: Methicillin sensitive SH1000 (SJF0682), low level resistant SH1000 *lysA::pmecA* (SJF 4996), high-level resistant SH1000 *lysA::pmecA rpoB<sup>H929Q</sup>* (SJF 5003), *mecA* cured sensitive SH1000 *lysA::kan rpoB<sup>H929Q</sup>* (SJF 5010) and high-level resistant SH1000 *lysA::pmecA rpoC<sup>G740R</sup>* (SJF 5034).

The MIC of ECg was evaluated in liquid MIC as described in section 2.8.1. The maximum tested concentration of 200 µg/mL had no effect on the growth of all the representative strains. We chose to use 50 µg / mL ECg in the context of previous literature (Stapleton et al., 2007), and this being an amount that resulted in a definitive change in resistance for our strains, without affecting the growth of the organism in pilot studies (data not shown).

To evaluate the effect of ECg on the resistance of the strains, the MIC of oxacillin in the presence of 50 µg / mL ECg was tested by Etest as described in section 2.9.1 and is shown in Table 5.2. The sensitising effect of ECg reduced the resistance of all strains that exhibit low- or high-level resistance to oxacillin. This was most dramatic for high-level resistant strains *lysA::pmecA rpoB<sup>H929Q</sup>* and *lysA::pmecA rpoC<sup>G740R</sup>*, which reduced from  $\geq 256$  µg/mL to 4 and 6 µg/mL, respectively.

**Table 5.2. Minimum inhibitory concentration (MIC) by Etest Oxacillin ( $\mu\text{g/mL}$ ) on TSA and in the presence of (-)-epicatechin gallate (50  $\mu\text{g/mL}$ )**

Strain (SJF Reference)	TSA	(-)-epicatechin gallate (50 $\mu\text{g/mL}$ )
SH1000 (SJF0682)	0.25	0.5
SH1000 <i>pmecA</i> (SJF4996)	2	1
SH1000 <i>pmecA</i> <i>rpoB</i> <sup>H929Q</sup> (SJF5003)	$\geq 256$	4
SH1000 <i>rpoB</i> <sup>H929Q</sup> (SJF5010)	0.19	0.5
SH1000 <i>pmecA</i> <i>rpoC</i> <sup>G740R</sup> (SJF5034)	$\geq 256$	6

**Reference Oxacillin MIC shading key**

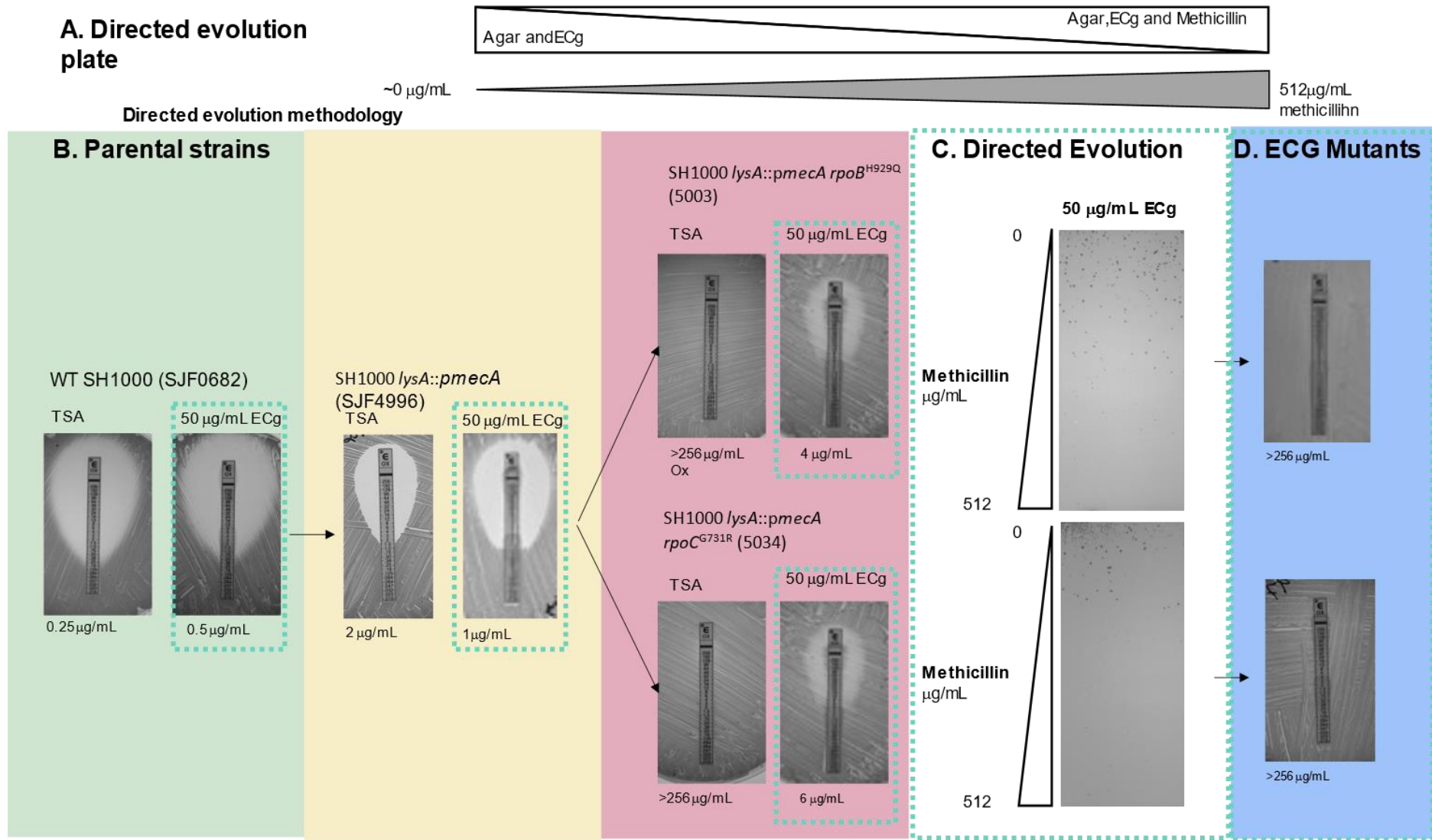
$\leq 1 \mu\text{g/mL}$	1-20 $\mu\text{g/mL}$	$\geq 20 \mu\text{g/mL}$	Not Done
-------------------------	-----------------------	--------------------------	----------

### 5.2.2 Isolation of ECg insensitive derivatives of MRSA

Mutations in *rpoB*<sup>H929Q</sup>(SJF5003) and *rpoC*<sup>G740R</sup>(SJF5034) result in high-level methicillin/oxacillin resistance in *pmeCA* strains (Panchal et al., 2020; Panchal, 2018). To investigate the development of resistance to the effects of the sensitising compound (-)-epicatechin gallate (ECg), a directed evolution experiment was proposed using a modified gradient plate technique (section 2.9.2), Figure 5.1.A (Bryson and Szybalski, 1952).

The premise of the experiment was that spontaneous mutations in genes associated with the resensitising effects of ECg would lead to derivatives more resistant to methicillin in the presence of ECg. To determine changes in antibiotic resistance E- test strips were used. As Methicillin Etest strips are not commercially available, we used oxacillin test strips for solid media. Methicillin was used in liquid media to corroborate results. Figure 5.1.B shows oxacillin Etest strips for all parental strains and their MICs, with ECg where appropriate, as summarised in Table 5.2. Figure 5.1.C shows the growth of single isolated colonies on gradient plates demonstrating the directed evolution of clones able to grow at high methicillin concentrations in the presence of ECg and in Figure 5.1.D two of the resulting ECg insensitive strains. Despite no identifiable MICs of ECg having been identified in 5.2.1, the gradient plate using the higher concentration of 50 µg/mL ECg shows reduced levels of growth across the plate due to likely diffusion of methicillin.

A total of 28 isolates were selected from gradient plates (Figure 5.1.C), for further characterisation. Sensitiser resistant MRSA strains were first verified by multiplex PCR to verify the maintenance of PBP2A and then Etest in the presence of 50 µg/mL ECg as described in section 2.9.1. This gave 5 highly resistant, stable clones from *rpoB*<sup>H929Q</sup>(SJF5003) evolution and 10 clones from *rpoC*<sup>G740R</sup>(SJF5034) evolution. Examples are shown in Figure 5.1.D The oxacillin MICs for these strains can be found in Table 5.3.



**Figure 5.1. Generation of (-)-epicatechin gallate (ECg) insensitive strains of MRSA**

An adapted gradient plate with a top layer containing 512 µg/mL methicillin and both layers containing ECg (A) was used for directed evolution of parental high-level oxacillin resistant strains (B), their respective resistance determined by Etest on TSA and in the presence of epicatechin gallate. Gradient plates were used to select for high-level (methicillin) β-lactam resistance in the presence of the sensitising compound ECg (C) and the resulting mutants' oxacillin resistance in the presence of ECg determined by Etest (D).

**Table 5.3. List of ECg insensitive methicillin resistant strains generated by directed evolution in the presence of (-)-epicatechin gallate on a gradient of methicillin.**

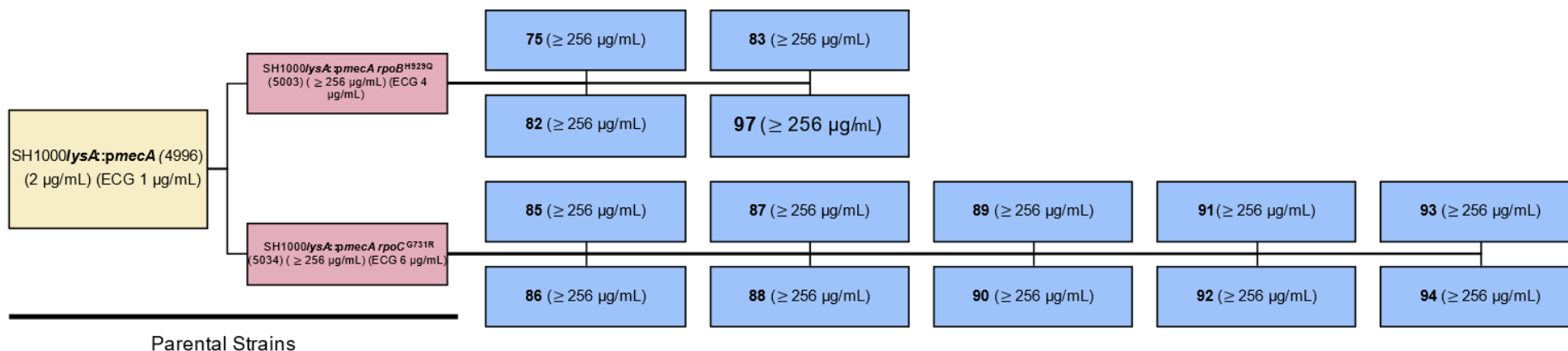
Strain reference	Oxacillin MIC Etest( $\mu\text{g}/\text{mL}$ ) 50 $\mu\text{g}/\text{mL}$ Epicatechin gallate,
<b>Parental Strain <i>pmeCA rpoB</i><sup>H929Q</sup> (SJF5003)</b>	<b>4</b>
ECg_75	$\geq 256$
ECg_82	$\geq 256$
ECg_83	$\geq 256$
ECg_96	$\geq 256$
ECg_97	$\geq 256$
<b>Parental Strain <i>pmeCA rpoC</i><sup>G740R</sup> (SJF5034)</b>	<b>6</b>
ECg_85	$\geq 256$
ECg_86	$\geq 256$
ECg_87	$\geq 256$
ECg_88	$\geq 256$
ECg_89	$\geq 256$
ECg_90	$\geq 256$
ECg_91	$\geq 256$
ECg_92	$\geq 256$
ECg_93	$\geq 256$
ECg_94	$\geq 256$

Reference Oxacillin MIC shading key			
$\leq 1 \mu\text{g}/\text{mL}$	1-20 $\mu\text{g}/\text{mL}$	$\geq 20 \mu\text{g}/\text{mL}$	Not Done

### 5.2.2.1 Identification of chromosomal mutations in sensitiser resistant strains

To characterise the genetic alterations that led to increased  $\beta$ -lactam resistance in the derived clones, whole genome analysis was carried out. SH1000 and the parental *pmecA*, *rpoB*<sup>H929Q</sup> and *rpoC*<sup>G740R</sup> strains were submitted along with the evolved sensitiser resistant MRSA clones for whole genome sequencing (MicrobesNG, Birmingham, UK) using Illumina sequencing. Reads from strains were mapped to the reference genome NCTC8325 (NC\_007795). Variant calling was performed using VarScan (MicrobesNG, Birmingham, UK). Complete variant calling is shown in Appendix 6. In total 15 evolved strains were sequenced, one strain, due to insufficient read depth E96 did not yield data of appropriate quality to perform variant calling. The remaining 14 strains with their lineage shown in Figure 5.2.

Mutations occurring with at least 90x coverage in the variant calling from WGS data are shown in an evolutionary lineage in Table 5.4. No other mutations leading to non-synonymous changes to protein sequence or truncations were found. Mutations were found in a total of 13 independent genes. Mutations in SAOUHSC\_01742 and SAOUHSC\_00942 occurred in clones derived from both *rpoB*<sup>H929Q</sup> and *rpoC*<sup>G740R</sup> MRSA backgrounds. Of the 10 mutant strains generated in the *mecA rpoC*<sup>G731R</sup> background, independent mutations in the genes SAOUHSC\_01742 and SAOUHSC\_00942 occurred repeatedly in 4 and 3 strains, respectively.



**Figure 5.2 Lineage of parental strains and ECg insensitive strains generated by the directed evolution of high-level resistant strains.**

The MIC for oxacillin for all strains is shown in the presence of 50 µg/mL ECg. Parental strain SH1000 *lysA::pmecA* (4996, yellow) was previously evolved in the presence of methicillin into the characteristic high-level β-lactam resistant (Oxacillin MIC of ≥256 µg/mL) strains SH1000 *lysA::pmecA rpoB<sup>H929Q</sup>* (5003) and SH1000 *lysA::pmecA rpoC<sup>G731R</sup>* (5034, pink) (Panchal et al., 2020). These strains can be sensitised by (-)-epicatechin gallate (50 µg/mL) to oxacillin resistance of 4 µg/mL and 6 µg/mL respectively. All evolved strains have an oxacillin MIC of ≥256 µg/mL in the presence of (-)-epicatechin gallate (50 µg/mL). Evolved strains (Blue) are shown with strain reference from directed evolution experiments.



In Table 5.4 the variant calling and the impact of the mutations on the genes of interest is summarised. Genes were identified by sequence alignment using BLAST (<https://blast.ncbi.nlm.nih.gov/Blast.cgi>) with the NCTC 8325 genome and UNIPROT. Figure 5.3 graphically depicts where the mutations effect each of the encoded proteins. One of the most striking observations from the data interpretation and analysis was the repeated mutagenesis of genes *relA* (SAOUHSC\_01742) and *relQ* (SAOUHSC\_00942) in independent strains. *relA* and *relQ* respectively have significant roles in the regulation of the stringent response (Atkinson et al., 2011; Gentry et al., 2000; Gratani et al., 2018). One strain contains a dual SNP in *relA*<sup>V654D, L656\*</sup> (E82) resulting in a 73 bp 3' truncation of the gene.

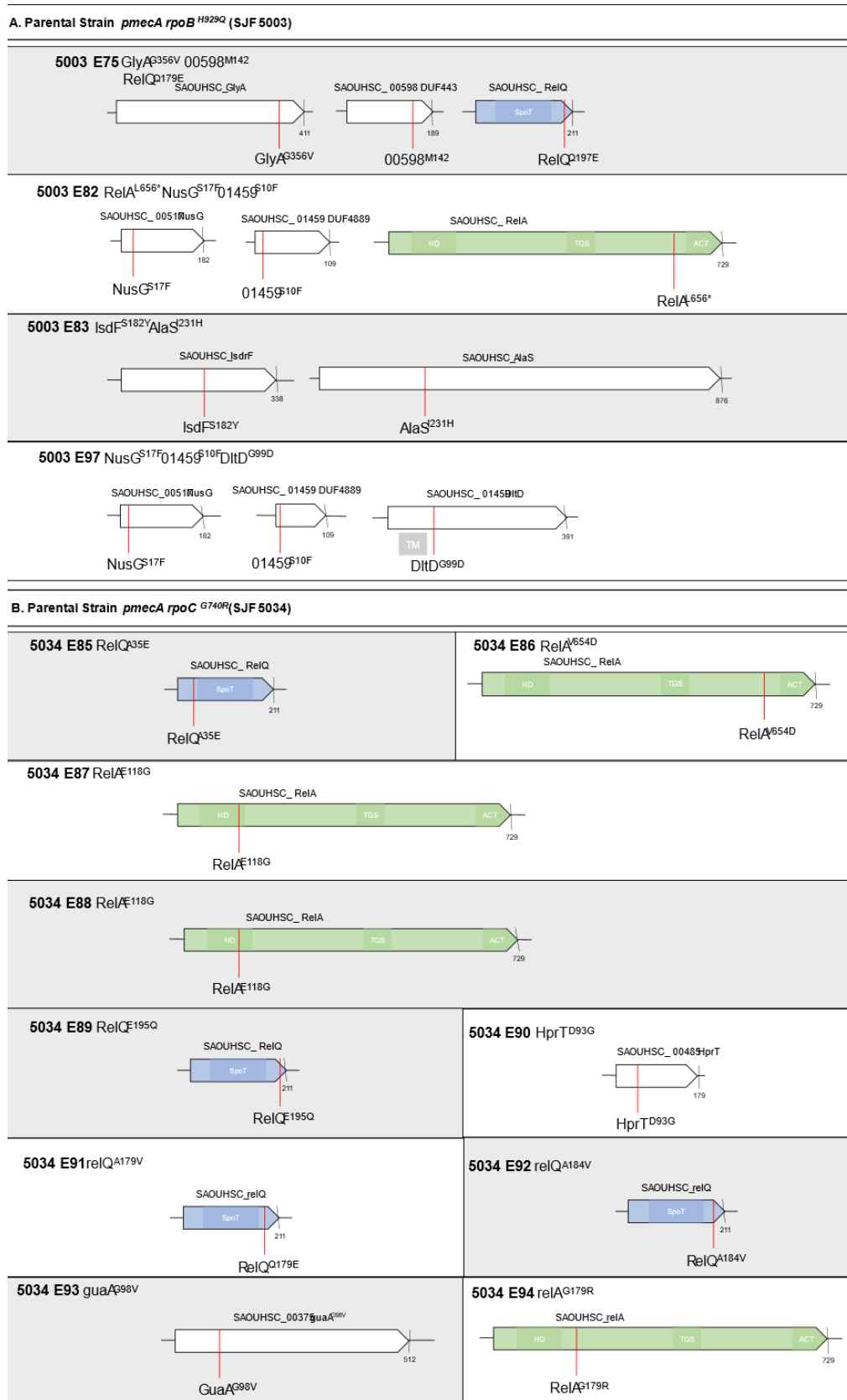
SNPs were also observed in genes encoding the previously characterised GlyA, GuaA, HprT, DltD and AlaS. Mutations in other genes encoding proteins such as a DUF 4889 containing protein (SAOUHSC\_01459), NusG (SAOUHSC\_00517) and a ferrichrome ABC transporter permease (SAOUHSC\_00654) were also found.

**Table 5.4 Summary of Variant Calling for (-)-epicatechin gallate (ECg) resistant strains.**

Summary of variant calling from whole genome sequencing of strains resistant to the effects of ECg evolved from SJF5003 and SJF5034, the locus, nucleotide and amino acid changes protein affected and putative function or localisation.

Sample(s)	Locus tag (Gene)	Mutation location	Nucleotide Change	Amino Acid Change	Protein	Putative Function
<b>Parental Strain <i>pmecA rpoB<sup>H929Q</sup></i> (SJF 5003)</b>						
	<i>glyA</i>	2176486	gGt/gTt	G356V	GlyA	Serine hydroxymethyltransferase
E75	<i>SAOUHSC_00598</i>	593607	aTg/aAg	M142K	Putative membrane spanning DUF443	Unknown
	<i>SAOUHSC_00942</i>	914769	Caa/Gaa	Q197E	RelQ	GTP pyrophosphokinase family protein
	<i>SAOUHSC_00517</i>	517977	tCt/tTt	S17F	Transcription antitermination protein	NusG-like Transcription termination factor
E82	<i>SAOUHSC_01459</i>	1417217	tCt/tTt	S10F	DUF4889 domain containing protein	Cytoplasmic membrane associated DUF4889 containing protein with a transmembrane helix
	<i>SAOUHSC_01742</i>	1644371	tta/	L656*	RelA	GTP pyrophosphokinase, bifunctional ppGpp synthetase.
E83	<i>alaS</i>	1627198	cTt/cAt	L231H	AlaS	Alanyl-tRNA synthetase
	<i>SAOUHSC_00654</i>	643579	tCt/tAt	S182Y	Iron-regulated surface determinant protein F	Ferrichrome ABC transporter permease
	<i>SAOUHSC_00872</i>	837489	gGt/gAt	G99D	D-alanyl lipoteichoic acid biosynthesis protein DIdD	Lipoteichoic biosynthesis protein with a 33 aa signal peptide and a transmembrane helix
E97	<i>SAOUHSC_00517</i>	517977	tCt/tTt	S17F	Transcription antitermination protein	transmembrane N terminally anchored, Observed mutation in start of extra cellular topological domain. NusG-like transcription termination factor
	<i>SAOUHSC_01459</i>	1417217	tCt/tTt	S10F	DUF4889 domain containing protein	Cytoplasmic membrane associated DUF4889 containing protein with a transmembrane helix
<b>Parental Strain <i>pmecA rpoC<sup>G740R</sup></i> (SJF 5034)</b>						

E85	SAOUHSC_00942	914284	gCg/gAg	A35E	RelQ	GTP pyrophosphokinase family protein
E86	SAOUHSC_01742	1644378	gTt/gAt	V654D	RelA	GTP pyrophosphokinase, bifunctional ppGpp synthetase.
E87	SAOUHSC_01742	1645986	gAa/gGa	E118G	RelA	GTP pyrophosphokinase bifunctional pppGpp synthetase.
E88	SAOUHSC_01742	1645986	gAa/gGa	E118G	RelA	GTP pyrophosphokinase bifunctional ppGpp synthetase.
E89	SAOUHSC_00942	914763	Gaa/Caa	E195Q	RelQ	GTP pyrophosphokinase family protein
E90	SAOUHSC_00485	482873	gAc/gGc	D93G	HprT hypoxanthine phosphoribosyltransferase	Synthesizes IMP from hypoxanthine as part of the GMP metabolism and salvage pathway. Involved in purine metabolism.
E91	SAOUHSC_00942	914716	gCg/gTg	A179V	RelQ	GTP pyrophosphokinase family protein
E92	SAOUHSC_00942	914731	gAa/gTa	E184V	RelQ	GTP pyrophosphokinase family protein
E93	<i>guaA</i>	381996	gGt/gTt	G98V	glutamine hydrolysing GMP synthase	Purine metabolism/ribosomal protein interactions amidotransferase region
E94	SAOUHSC_01742	1645804	Ggt/Cgt	G179R	RelA	GTP pyrophosphokinase, bifunctional ppGpp synthetase.



**Figure 5.3 Strains generated by directed evolution and location of mutations in proteins represented diagrammatically.**

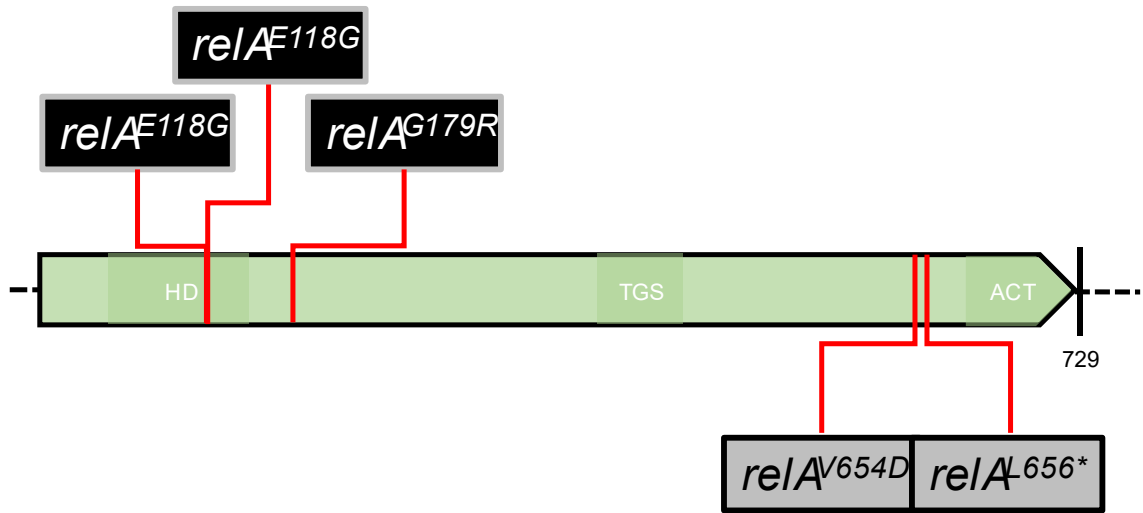
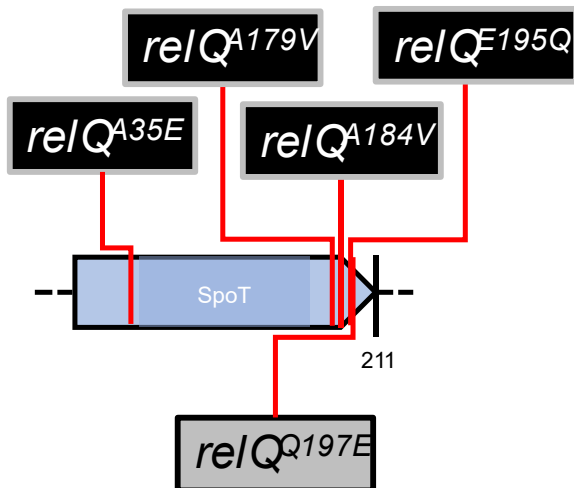
Strains generated by directed evolution of SH1000 *lysA::pmeCA rpoB*<sup>H929Q</sup> (5003) (A) and SH1000 *lysA::pmeCA rpoC*<sup>G731R</sup> (B). Key features annotated and transcribed using uniprot and AureoWiki. Proteins are shown to scale, with mutated amino acid denoted by a red line, and length by black line. RelA shown in green and RelQ shown in blue.

### 5.2.2.2 A common theme for mutated genes

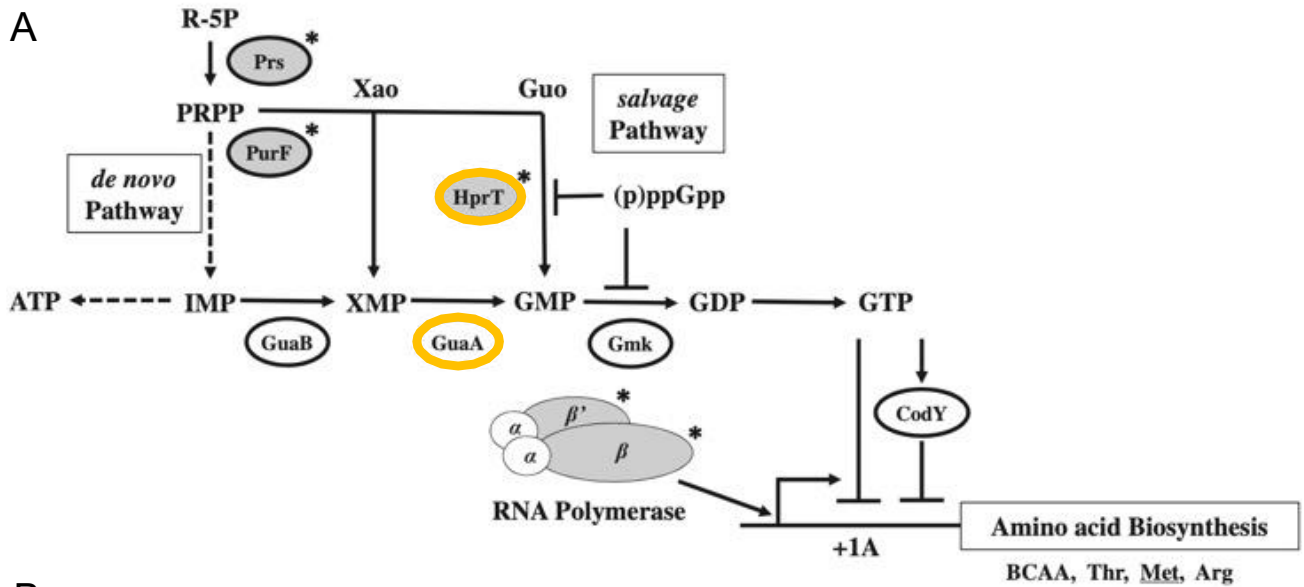
Our study identified multiple mutations occur independently in both backgrounds in the genes *relA* (SAOUHSC\_01742) and *relQ* (SAOUHSC\_00942) and mutations in genes such as *guaA*, *dltD* and *hprT* (Figure 5.3).

Mutations in genes related to RNA polymerase (Panchal et al., 2020), purine biosynthesis (Goncheva et al., 2019; Panchal et al., 2020), (p)ppGpp synthesis (Corrigan et al., 2016) and protein quality control (Boonsiri et al., 2020) have been found previously as supporters of  $\beta$ -lactam resistance. **Figure 5.5** details purine and ppGpp synthesis pathways. The *rel spoT* homologue (RSH) superfamily of proteins feature hydrolase and synthetase domains and a regulatory region to produce pppGpp and derivatives or the removal of the phosphate group (PPi) to recover GTP, GDP or GMP (Irving et al., 2020). *De novo* synthesis and salvage of (p)ppGpp and pppGpp requires conversion of IMP to XMP and by GuaA to GMP (Corrigan et al., 2016).

Figure 5.4 shows all the mutations identified in *relA* and *relQ*. Only one *relA* mutation is observed in the HD catalytic domain, but it occurred twice in independent strains. RelQ is a tetrameric protein, and the mutations are present in the final helix of each individual protomer, none of these mutations are present in the synthase domains, or the ppGpp binding domains. The mutation's effects on activity or protein conformation of both RelQ and RelA are unknown.

**A***SAOUHSC\_reIA***B***SAOUHSC\_reIQ***Figure 5.4 Mapping SNP changes on Rel proteins.**

Mutations found in (A) *relA* and (B) *relQ*, during directed evolution screen. Parental *rpoB<sup>H929Q</sup>* strains shown in grey and mutations found in *rpoC<sup>G740R</sup>* strains shown in black.



**Figure 5.5 Purine and ppGpp biosynthesis pathways.**

(A) Schematic of purine nucleotide biosynthesis pathway in *Bacillus subtilis* and underlying transcriptional mechanism controlling intracellular GTP concentration. Taken from Osaka et al. (2020) (B) The synthetase domain (SYNTH; grey) of RSH (RelA/SpoT homologue) enzymes catalyses the transfer of a pyrophosphate group from ATP to the ribose moiety of GTP, GDP or GMP to produce guanosine pentaphosphate (pppGpp), guanosine tetraphosphate (ppGpp) or guanosine 5'-monophosphate 3'-diphosphate (pGpp), respectively. This reaction also generates a molecule of AMP. Conversely, the hydrolase domain (HD; orange) is responsible for removing the pyrophosphate group (PPI) to recover GTP, GDP or GMP. SNPs identified in directed evolution in the presence denoted by yellow outline. Adapted from Irving et al., 2020).

### 5.2.3 Construction of sensitiser resistant, transposon insertion MRSA strains

To verify the role of genes identified in the directed evolution screen (Table 5.4), the Nebraska transposon mutant library (NTML) was used (Chaudhuri et al., 2009). NTML is an ordered library of mutations in non-essential genes, each marked by an erythromycin resistance cassette. Their use would evaluate if inactivation of the identified genes by transposon insertion matches the phenotype of the derived SNP's and therefore verify the role of the gene in ECg resistance.

Phage lysates of USA3000 strains from the NTML (Chaudhuri et al., 2009) were prepared and used to transduce mutations into the representative MRSA transposon recipient strains as described in section 2.14. The MRSA recipient strains feature a kanamycin resistance marked *pmeCA* as opposed to the erythromycin/lincomycin marked *pmeCA* used in the screen (Panchal et al., 2020). The resistance properties and effect of ECg on these parental strains were verified, (Table 5.5). This showed that they are similarly affected by the presence of ECg with *pmeCA rpoB*<sup>+</sup> and *rpoC*<sup>+</sup> showing a reduction in oxacillin resistance from  $\geq 256$   $\mu\text{g}/\text{mL}$  to 2.5 and 10  $\mu\text{g}/\text{mL}$  respectively despite their alternative antibiotic markers and location of the genes.

Mutations were verified by antibiotic selection during transduction, sub-culture onto Baird parker agar (data not shown) and using PCR using either primers flanking the gene of interest (goi) or primers binding within the Nebraska transposon insertion and outside the goi. Figure 5.6 shows the Nebraska transposon mutagenesis insertion into *relA*, other genes are shown in Appendix 7. Due to there being no appropriate NTML mutants *dltD* and *relQ* were not further analysed.



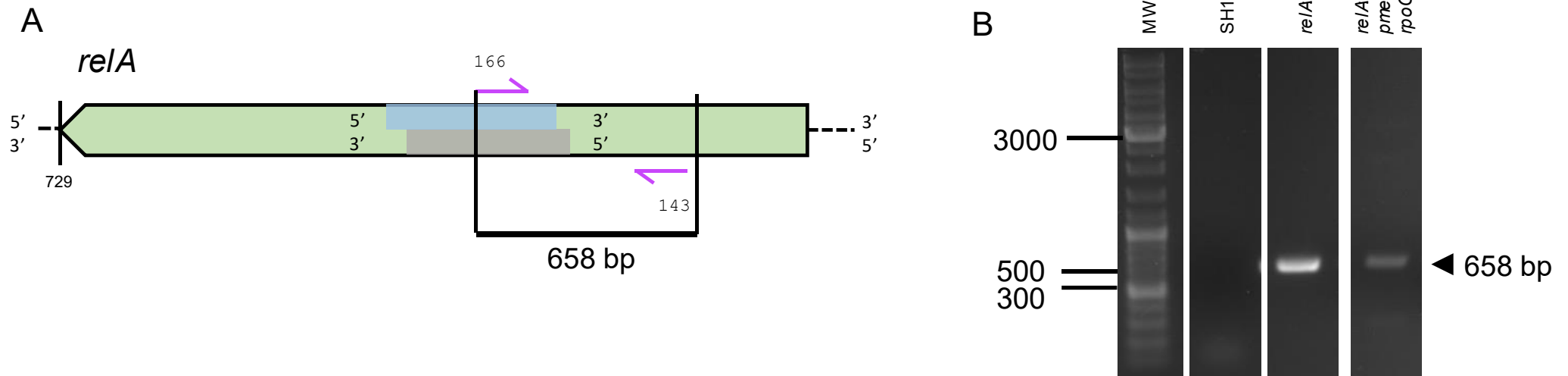
**Table 5.5 Antibiogram of parental strains in the presence of (-)-epicatechin gallate**

Oxacillin resistance by Etest of laboratory MRSA strains and kanamycin resistance marked transposon recipient strains in the presence of no treatment control (NTC) or (-)-epicatechin gallate (ECg) (50 µg/mL).  $\Sigma$  shows the number of repeats for that strain, where  $\Sigma=0$  this combination wasn't attempted, grey shading.

<b>SH1000 Strain Genotype (SJF Reference)</b>	<b>NTC</b>	<b><math>\Sigma</math></b>	<b>ECg</b>	<b><math>\Sigma</math></b>
SH1000 (SJF 0682)	0.28	4	0.25	1
<i>lysA::mecA</i> (SJF 4996)	1.75	4	1.50	1
<i>lysA::mecA rpoB<sup>H929Q</sup></i> (SJF 5003)	256	4	6	3
<i>lysA::kan rpoB<sup>H929Q</sup></i> (SJF 5010)	0.25	4	0.25	2
<i>lysA::mecA rpoC<sup>G731R</sup></i> (SJF 5034)	256	3	4	3

<b>SH1000 Strain Genotype (SJF Reference)</b>	<b>NTC</b>	<b><math>\Sigma</math></b>	<b>ECg</b>	<b><math>\Sigma</math></b>
<i>pmecA<sup>kan</sup></i> (SJF 5324)				
<i>rpoB<sup>H929Q</sup></i> (SJF 5320)	0.19	2	0.25	1
<i>rpoC<sup>G731R</sup></i> (SJF 5672)	0.13	2	0.13	1
<i>pmecA<sup>kan</sup> rpoB<sup>H929Q</sup></i> (SJF 5323)	256	3	2.50	2
<i>pmecA<sup>kan</sup> rpoC<sup>G731R</sup></i> (SJF 5673)	256	3	10	3



**Figure 5.6 Diagram of transposon mutagenesis of *relA* in *S. aureus*.**

(A) *relA* gene showing the location of the Nebraska transposon insertion and the internal (166) and external (143) primers, (B) DNA electrophoresis of PCR products amplified using primers 166 and 143.

### 5.2.3.1 Effects of sensitising compounds on transposon insertion strains

Strains were constructed with transposon insertions in genes that were identified with SNP's after directed evolution to selector MRSA clones no longer susceptible to ECg. The parental strains *pmeCA rpoB* and *pmeCA rpoC* both have an MIC of  $\geq 256$   $\mu\text{g}/\text{mL}$  oxacillin which is reduced to  $\leq 10$   $\mu\text{g}/\text{mL}$  oxacillin in the presence of ECg (Table 5.5). All the insertions led to MICs of  $\leq 40$   $\mu\text{g}/\text{mL}$  oxacillin (Table 5.6) indicating that inactivation of genes results in an intrinsic loss of resistance and so they are auxiliary factors. For some of the transposon insertions (*alaS*, *hprT*, *relA*, *DUF443*) the MIC only fell by  $\leq 4$  fold in the presence of ECg. This indicates their role in ECg sensitivity. However, in no case did gene inactivation recapitulate the dramatic results demonstrated by the SNP's.

**Table 5.6 Antibiogram of transposon insertion mutants in the presence of (-)-epicatechin gallate**

Oxacillin resistance by Etest of kanamycin resistance marked transposon recipient strains in the presence of no treatment control (NTC) or (-)-epicatechin gallate (ECg) (50 µg/mL).  $\Sigma$  shows the number of repeats for that strain, where  $\Sigma=0$  this combination wasn't attempted, grey shading.

SH1000 Strain Genotype (SJF Reference)	NTC	$\Sigma$	ECg	$\Sigma$
<i>alaS</i> ::TnNE1575 SH1000	0.19	3	0.25	2
<i>alaS</i> ::TnNE1575 <i>pmecA</i> <sup>kan</sup>	0.25	2	0.25	2
<i>alaS</i> ::TnNE1575 <i>pmecA</i> <sup>kan</sup> <i>rpoB</i> <sup>H929Q</sup>	40	2	20	2
<i>alaS</i> ::TnNE1575 <i>rpoB</i> <sup>H929Q</sup>	0.19	1	0.38	1
<i>alaS</i> ::TnNE1575 <i>pmecA</i> <sup>kan</sup> <i>rpoC</i> <sup>G731R</sup>	11	2	8	1
SH1000 Strain Genotype (SJF Reference)	NTC	$\Sigma$	ECg	$\Sigma$
<i>glyA</i> ::TnNE213 SH1000	0.13	1	8	1
<i>glyA</i> ::TnNE213 <i>pmecA</i> <sup>kan</sup> <i>rpoC</i> <sup>G731R</sup>	12	2	24	1
SH1000 Strain Genotype (SJF Reference)	NTC	$\Sigma$	ECg	$\Sigma$
<i>hprT</i> ::TnNE917 SH1000	0.19	1	0.19	1
<i>hprT</i> ::TnNE917 SH1000	0.25	3	0.38	3
<i>hprT</i> ::TnNE917 <i>pmecA</i> <sup>kan</sup> <i>rpoB</i> <sup>H929Q</sup>	32	1	16	1
<i>hprT</i> ::TnNE917 <i>rpoB</i> <sup>H929Q</sup>	0.19	1	0.25	1
<i>hprT</i> ::TnNE917 <i>pmecA</i> <sup>kan</sup> <i>rpoC</i> <sup>G731R</sup>	32	1	8	1
SH1000 Strain Genotype (SJF Reference)	NTC	$\Sigma$	ECg	$\Sigma$
<i>relA</i> :: TnNE1714	0.38	4	0.50	4
<i>relA</i> :: TnNE1714 <i>pmecA</i> <sup>kan</sup>	16	3	0.75	3
<i>relA</i> :: TnNE1714 <i>pmecA</i> <sup>kan</sup> <i>rpoB</i> <sup>H929Q</sup>	28	4	14	2
<i>relA</i> :: TnNE1714 <i>pmecA</i> <sup>kan</sup> <i>rpoC</i> <sup>G731R</sup>	12	2	8	1
<i>relA</i> :: TnNE1714 <i>rpoC</i> <sup>G731R</sup>	1.50	1	0.75	1
SH1000 Strain Genotype (SJF Reference)	NTC	$\Sigma$	ECg	$\Sigma$
DUF443 SAOUHSC_00598:: TnNE1093 SH1000	0.19	1	0.25	1
DUF443 SAOUHSC_00598:: TnNE1093 <i>pmecA</i> <sup>kan</sup> <i>rpoB</i> <sup>H929Q</sup>	32	3	8	2
DUF443 SAOUHSC_00598:: TnNE1093 <i>pmecA</i> <sup>kan</sup> <i>rpoC</i> <sup>G731R</sup>	12	1	8	1
SH1000 Strain Genotype (SJF Reference)	NTC	$\Sigma$	ECg	$\Sigma$
lsdF SAOUHSC_00654:: TnNE1468 SH1000	0.19	2	0.25	1
lsdF SAOUHSC_00654:: TnNE1468 <i>pmecA</i> <sup>kan</sup>	0.25	1		
lsdF SAOUHSC_00654:: TnNE1468 <i>pmecA</i> <sup>kan</sup> <i>rpoB</i> <sup>H929Q</sup>	0.50	1	0.38	1
Reference Oxacillin MIC shading key				
≤ 1 µg/mL	1-20 µg/mL	≥ 20 µg/mL	Not Done	

## 5.2.4 Investigating the effect of other compounds that sensitise MRSA to $\beta$ -lactams.

As discussed in chapter 5.1 a range of compounds such as diclofenac, clomiphene citrate and norgestimate can also be used to re-sensitise MRSA to the effects of  $\beta$ -lactam antibiotics. To build understanding of the mechanisms that permit re-sensitisation of MRSA by these compounds we hypothesised that strains generated by directed evolution in the presence of (-)-epicatechin gallate (ECg) (50  $\mu\text{g}/\text{mL}$ ) would also potentially exhibit resistance to other sensitising compounds. We first determined the MIC of the sensitising compounds for the MRSA strains (Table 5.7). The only observable MIC was for SH1000 *lysA::mecA rpoB<sup>H929Q</sup>* (SJF 5003) of which growth was inhibited at 40  $\mu\text{g}/\text{mL}$  Norgestimate and for all strains at 8  $\mu\text{g}/\text{mL}$  of clomiphene. The results were consistent for all strains used apart from SJF 5003 with Norgestimate which was four times lower than the other strains. The analysis allows sub-MIC levels of the compounds to be used in further re-sensitisation experiments.

### 5.2.4.1 Oxacillin resistance in the presence of sensitising compounds

Using the data derived from Table 5.7 working concentrations of Norgestimate (NRG) (10  $\mu\text{g}/\text{mL}$ ), diclofenac (DSS) (31.25  $\mu\text{g}/\text{mL}$ ) or clomiphene (CC) (4  $\mu\text{g}/\text{mL}$ ) were used.

For all compounds used, the MIC of high-level resistant MRSA strains (containing *mecA* and *rpo\** mutations show a decrease from  $\geq 256$  to  $\leq 12$   $\mu\text{g}/\text{mL}$  (Table 5.8). this substantiates the activity of all compounds as resensitising agents.

**Table 5.7 Minimum inhibitory concentrations (MIC) for sensitising compounds by broth microdilution in tryptone soya broth ( $\mu\text{g}/\text{mL}$ )**  
 The MICs of Norgestimate, Diclofenac sodium salt, and Clomiphene citrate were evaluated in broth microdilutions to the maximum concentration stated in the table. ND Not done.

Strain (SJFXXX)	Sensitising compound [Maximum tested concentration]		
	Norgestimate [160 $\mu\text{g}/\text{mL}$ ]	Diclofenac [500 $\mu\text{g}/\text{mL}$ ]	Clomiphene [64 $\mu\text{g}/\text{mL}$ ]
SH1000 (SJF 0682)	160	250	8
SH1000 <i>lysA::mecA</i> (SJF 4996)	160	250	8
SH1000 <i>lysA::mecA rpoB<sup>H929Q</sup></i> (SJF 5003)	40	250	8
SH1000 <i>lysA::kan rpoB<sup>H929Q</sup></i> (SJF 5010)	160	250	8
SH1000 <i>lysA::mecA rpoC<sup>G731R</sup></i> (SJF 5034)	160	ND	8

**Table 5.8 Oxacillin resistance of characteristic laboratory strains in the presence of sensitising compounds**

Effect of resensitising compounds on oxacillin resistance of MRSA and related strains No treatment control (NTC), (-)-epicatechin gallate (ECg) (50 µg/mL) for reference, Norgestimate (NRG) (10 µg/mL), diclofenac (DSS) (31.25 µg/mL) or clomiphene (CC) (4 µg/mL).  $\Sigma$  shows the number of repeats for that strain, where  $\Sigma=0$  this combination wasn't attempted, grey shading.

SH100 Strain Genotype (SJF Reference)	NTC	$\Sigma$	ECg	$\Sigma$	CC	$\Sigma$	NRG	$\Sigma$	DSS	$\Sigma$
SH1000 (SJF 0682)	0.28	4	0.25	1	0.21	4	0.25	2	0.25	2
<i>lysA::mecA</i> (SJF 4996)	1.75	4	1.50	1	0.94	4	1.67	3	1.25	4
<i>lysA::mecA rpoB<sup>H929Q</sup></i> (SJF 5003)	256	4	6	3					1.25	2
<i>lysA::kan rpoB<sup>H929Q</sup></i> (SJF 5010)	0.25	4	0.25	2	0.19	4	0.21	3	0.25	4
<i>lysA::mecA rpoC<sup>G731R</sup></i> (SJF 5034)	256	3	4	3	3	3	1	2	2	2

SH100 Strain Genotype (SJF Reference)	NTC	$\Sigma$	ECg	$\Sigma$	CC	$\Sigma$	NRG	$\Sigma$	DSS	$\Sigma$
<i>pmecA<sup>kan</sup></i> (SJF 5324)										
<i>rpoB<sup>H929Q</sup></i> (SJF 5320)	0.19	2	0.25	1						
<i>rpoC<sup>G731R</sup></i> (SJF 5672)	0.13	2	0.13	1						
<i>pmecA<sup>kan</sup> rpoB<sup>H929Q</sup></i> (SJF 5323)	256	3	2.50	2	1.50	1	1.50	2	3	2
<i>pmecA<sup>kan</sup> rpoC<sup>G731R</sup></i> (SJF 5673)	256	3	10	3	9	2	9	2	12	1

**Reference Oxacillin MIC shading key**

≤ 1 µg/mL	1-20 µg/mL	≥ 20 µg/mL	Not Done
-----------	------------	------------	----------

All the mutations evaluated, that were identified in the directed evolution screen, were assessed using the corresponding transposon insertions. In the parental high-level resistant strain (*mecA*<sup>+</sup> and *rpoB*<sup>\*</sup>), all three compounds led to a large decrease in MIC to oxacillin (Table 5.8). The transposon insertion functionally abrogated any resensitising effects (Table 5.9). As previously Table 5.5 the insertion led to a drop in MIC in the untreated samples. Thus, all compounds behave as ECg whereby their resensitising effects are reverted by mutation of genes identified in the directed evolution screen.

### **5.2.5 The stringent response as a modulator of high-level resistance in MRSA**

As previously noted (Section 5.2.2), a common feature of many genes identified in the directed evolution experiments was that they have a physiological relevance to nucleotide signalling and the stringent response. Several (*dltD* and *relA*) are known potentiators of  $\beta$ -lactam resistance (Bilyk et al., 2022), which highlights their involvement in regulatory responses spanning aspects of cellular physiology important for high-level resistance. The direct induction of the stringent response is also known to alter the levels of resistance to  $\beta$ -lactam antibiotics (Irving et al., 2020).



**Table 5.9 Antibiogram of transposon insertion mutants in the presence of sensitising compounds**

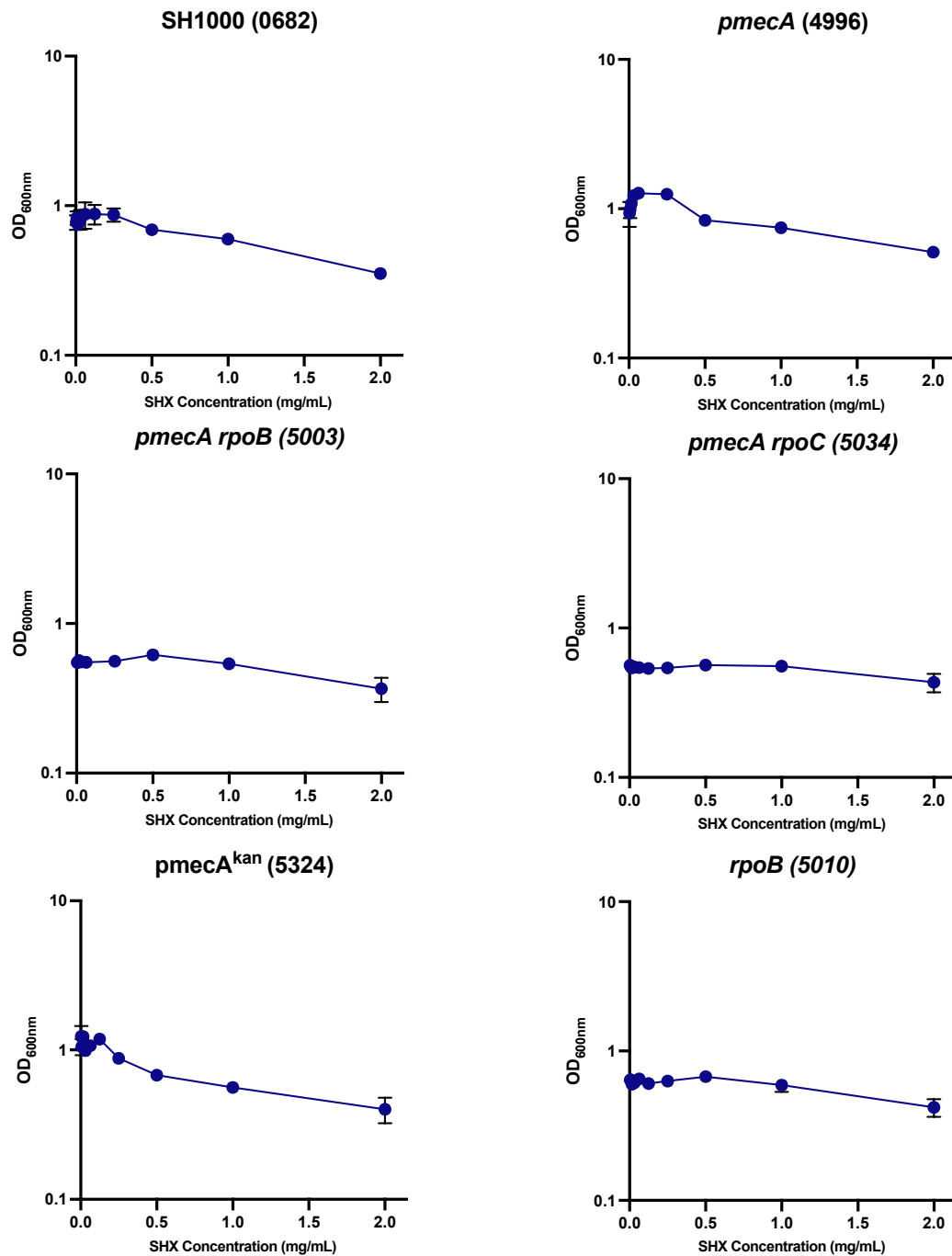
Oxacillin resistance by Etest of laboratory MRSA strains. transposon recipient strains and strains containing transposons from the NARSA mutant library in the presence of No treatment control (NTC), Norgestimate (NRG) (10 µg/mL), diclofenac (DSS) (31.25 µg/mL), clomiphene (CC) (4 µg/mL). Σ shows the number of repeats for each strain, combination wasn't attempted, grey shading. Results are shown as mean where appropriate.

<b>SH1000 Strain Genotype (SJF Reference)</b>	<b>NTC</b>	<b>Σ</b>	<b>ECg</b>	<b>Σ</b>	<b>CC</b>	<b>Σ</b>	<b>NRG</b>	<b>Σ</b>
<i>alaS</i> ::TnNE1575 SH1000 (SJF 6115)	0.19	3	0.19	2	0.19	2	0.19	1
<i>alaS</i> ::TnNE1575 <i>pmeCA<sup>kan</sup></i> (SJF 6111)	0.25	2	0.29	2	0.38	1	0.19	1
<i>alaS</i> ::TnNE1575 <i>pmeCA<sup>kan</sup></i> <i>rpoB<sup>H929Q</sup></i> (SJF 6114)	40	2	103.	3			96	1
<i>alaS</i> ::TnNE1575 <i>rpoB<sup>H929Q</sup></i> (SJF 6113)	0.19	1			0.50	1	0.25	1
<i>alaS</i> ::TnNE1575 <i>pmeCA<sup>kan</sup></i> <i>rpoC<sup>G731R</sup></i> (SJF 6112)	11	2	18	2	18	2	32	1
<b>SH1000 Strain Genotype</b>								
<i>glyA</i> ::TnNE213 SH1000 (SJF 6117)	0.13	1	22	2	4	1	48	1
<i>glyA</i> ::TnNE213 <i>pmeCA<sup>kan</sup></i> <i>rpoC<sup>G731R</sup></i> (SJF 6116)	12	2	32	2	18	2	48	2
<b>SH1000 Strain Genotype</b>								
<i>hprT</i> ::TnNE917 SH1000 (SJF 6118)	0.19	1						
<i>hprT</i> ::TnNE917 SH1000 (SJF 6119)	0.25	3						
<i>hprT</i> ::TnNE917 <i>pmeCA<sup>kan</sup></i> <i>rpoB<sup>H929Q</sup></i> (SJF 6120)	32	1	72	2	256	1	256	1
<i>hprT</i> ::TnNE917 <i>rpoB<sup>H929Q</sup></i> (SJF 6122)	0.19	1			0.38	1	0.25	1
<i>hprT</i> ::TnNE917 <i>pmeCA<sup>kan</sup></i> <i>rpoC<sup>G731R</sup></i> (SJF 6121)	32	1	48	1	6	1	48	1
<b>SH1000 Strain Genotype</b>								
<i>relA</i> :: TnNE1714 (SJF 5457)	0.38	4	0.41	4	0.56	4	0.57	4
<i>relA</i> :: TnNE1714 <i>pmeCA<sup>kan</sup></i> (SJF 5463)	16	3	1.63	4	16.5	2	13.3	3
<i>relA</i> :: TnNE1714 <i>pmeCA<sup>kan</sup></i> <i>rpoB<sup>H929Q</sup></i> (SJF 6124)	28	4	37.3	3	29	4	256	2
<i>relA</i> :: TnNE1714 <i>pmeCA<sup>kan</sup></i> <i>rpoC<sup>G731R</sup></i> (SJF 6123)	12	2	14	2	14	2	12	1
<b>SH1000 Strain Genotype</b>								
SAOUHSC_00598:: TnNE1093 SH1000 (SJF 6126)	0.19	1						
SAOUHSC_00598:: TnNE1093 <i>pmeCA<sup>kan</sup></i> <i>rpoC<sup>G731R</sup></i> (SJF 6125)	12	1	36	2	48	1		
<b>SH1000 Strain Genotype</b>								
SAOUHSC_00654:: TnNE1468 SH1000 (SJF 6128)	0.19	2	0.25	1				
SAOUHSC_00654:: TnNE1468 <i>pmeCA<sup>kan</sup></i> (SJF 6127)	0.25	1	0.19	1				
Reference Oxacillin MIC shading key								
≤ 1 µg/mL	1-20 µg/mL	≥ 20 µg/mL	Not Done					

### 5.2.5.1 Characterising resistance in the presence of a stringent response inducer

As the stringent response can directly modulate levels of resistance to  $\beta$ -lactam antibiotics, and our directed evolution results indicate a link between genes involved in nucleotide biosynthesis and regulation of the stringent response, we hypothesised we could use inducers of the stringent response to further interrogate the mode of  $\beta$ -lactam resistance in the presence of re-sensitising compounds.

Compounds that are able to modulate the stringent response include the use of sub-MIC levels of mupirocin, shown to greatly increase levels of oxacillin resistance in the presence of auxiliary mutations in the COL background (Kim et al., 2017) and serine hydroxamate (SHX), a serine analog that inhibits seryl-tRNA synthetase (resulting in the induction of the stringent response in *S. aureus*) (Geiger et al., 2012). Serine hydroxamate shows no bactericidal activity so we hypothesised that we could use SHX to modulate the levels of  $\beta$ -lactam resistance in the presence of re-sensitising compounds. Firstly, the effect of SHX alone on the parental and MRSA strains was determined by liquid MIC, as described in section 2.8.1. Figure 5.7 shows  $OD_{600nm}$  readings of strains grown in TSA broth microdilutions containing serine hydroxamate after 24 hrs growth at 37 ° C. These results are shown as line graphs to better illustrate levels of growth at different SHX concentrations, as this highlights its varied effects amongst the different strains. The presence of *rpoB\** or *rpoC\** in the SH1000 background results in a reduced growth yield. Even the maximum tested concentration of 2 mg/mL SHX did not prevent growth of these strains.



**Figure 5.7 Determination of the minimum inhibitory concentration of Serine hydroxamate for representative *Staphylococcus aureus* strains.**

Broth microdilution determination of the MIC of representative strains of *S. aureus* in the presence of serine hydroxamate. OD<sub>600nm</sub> readings taken after overnight incubation at 37 °C represented on a log scale. Performed in biological triplicate, error bars represent the standard deviation of the mean.

### 5.2.5.2 Induction of the stringent response decreases antimicrobial susceptibility.

As our range of SH1000 derived strains were all able to grow up to 2 mg/mL of serine hydroxamate increasing concentrations were used to demonstrate how it affects the level of oxacillin resistance of the non-potentiated SH1000 *lysA::mecA* (SJF 4996) strain. The MIC for oxacillin rose from 1.5 µg/mL to between 4-12 µg/mL in the absence or presence of 1 mg/mL serine hydroxamate demonstrating it has a modest effect on resistance. 1 mg/mL of serine hydroxamate results in increased levels of antibiotic resistance in wild type SH1000, low level MRSA (*lysA::pmecA*, SJF 4996) and SH1000 cured of *pmecA* (*lysA::kan rpoB<sup>H929Q</sup>* (SJF 5010)) (Figure 5.8). The resistance of the high-level resistant strains in the presence of SHX is unchanged  $\geq 256$  µg/mL to oxacillin in the presence of SHX. This demonstrates that induction of the stringent response using SHX has a generic effect on oxacillin resistance for those strains that do not already exhibit high-level resistance.



**Figure 5.8. Evaluation by Etest of the effects of serine hydroxamate on oxacillin resistance**

Oxacillin Etests of Wild type, and low and high-level resistant strains of SH1000 performed on TSA agar in the presence or absence of serine hydroxamate (SHX)

### 5.2.5.3 Rescuing MRSA from the effects of sensitising compounds via induction of the stringent response

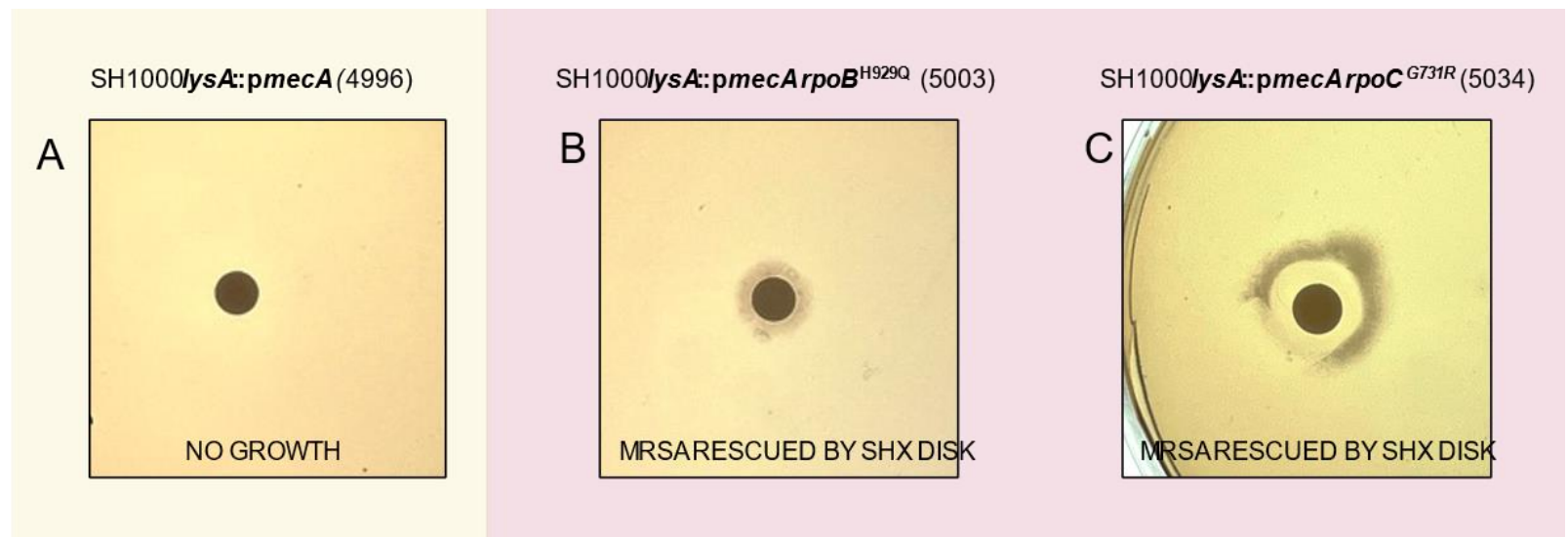
As SHX can increase the MIC to oxacillin we hypothesised that it could abrogate the effects of MRSA resensitising compounds. An experiment was designed that used a filter disk impregnated with SHX to rescue MRSA from the effects of methicillin in the presence of the sensitising compound ECg on an agar plate.

TSA was supplemented with 50 µg/mL ECg and 200 µg/mL methicillin. 100 µL of logarithmically grown ( $OD_{600nm} \sim 0.6$ ) MRSA (*mecA*<sup>+</sup> *rpoB*<sup>\*</sup>) was spread evenly over the surface of the agar. Filter disks were placed on each plate and 20 µL of SHX in solution (1 mg/mL) was pipetted onto the disks. Plates were incubated overnight at 37 °C. The combination of ECg and methicillin resulted in no growth. If, however, a filter disk containing SHX had been added to these plates a distinct zone of growth around the disc could be observed for high-level MRSA strains. This demonstrates that SHX has the capacity to rescue MRSA from the growth inhibitory synergistic effects of methicillin and ECg.

To further quantify the effect of SHX on the levels of oxacillin resistance in the presence of re-sensitising compounds, oxacillin Etest strips and agar containing SHX and re-sensitising compounds was used, Figure 5.10.

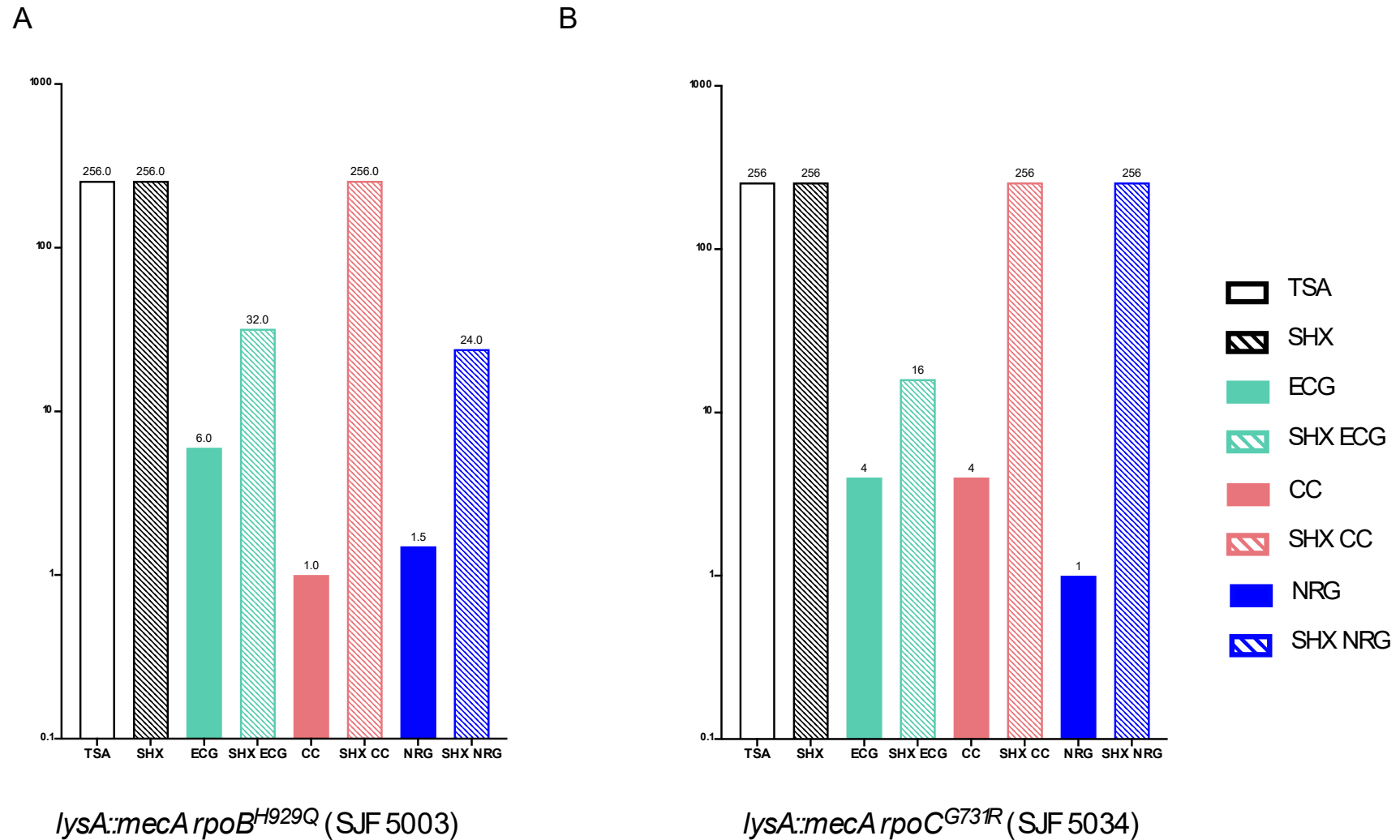
For both high-level resistant MRSA strains harbouring *rpoB*<sup>\*</sup> or *rpoC*<sup>\*</sup> mutations the MIC for oxacillin was  $\geq 256$  µg/mL with or without SHX. As expected, the resensitising agents ECg, clomiphene and Norgestimate led to a drop in MIC for oxacillin between 20-100 fold in all cases. The addition of SHX to the plates led to an increase in oxacillin MIC of between 2-100 fold for all samples. This clearly demonstrates that SHX has the capability to restore oxacillin resistance in the presence of resensitising agents of a range of different chemistries.

**DISK: SHX 1 mg/mL**  
Methicillin 200 µg/mL  
(-)-epicatechin gallate 50µg/mL



**Figure 5.9 Filter disk assay using SHX rescues growth of MRSA from a combination of methicillin and ECg.**

Use of serine hydroxamate disks to rescue MRSA from the synergistic effects of methicillin and (-)-epicatechin gallate. Strains wild type, low and high-level methicillin resistant strains of *S.* were spread evenly over the surface of TSA. TSA with 200 µg/mL methicillin (A,B,C) and TSA with 200 µg/mL methicillin 50 µg/mL (-)-epicatechin gallate (D,E,F). Filter paper impregnated with 20 µL of 1 mg/mL concentrations of serine hydroxamate solution were placed on the agar. Images were artificially re-coloured to highlight growth.



**Figure 5.10. Use of DL-serine hydroxamate to rescue MRSA from the effects of sensitising compounds.**

MRSA strains with *rpoB<sup>H929Q</sup>* (A) and *rpoC<sup>G731R</sup>* (B) mutations grown on TSA, and agar containing 1mg/mL serine hydroxamate (SHX), with or without either 50 µg/mL (-)-epicatechin gallate (ECg), 4 µg/mL Clomiphene Citrate (CC), 10 µg/mL Norgestimate (NRG), each had an oxacillin Etest strip applied to determine MIC value and plotted on a log scale with actual values shown above, N=3, Data as mean value.



### 5.3 Discussion

MRSA poses a threat to health worldwide (Murray et al., 2022). To begin to combat MRSA, a range of compounds have been identified that resensitise MRSA to the effects of  $\beta$ -lactams (Stapleton and Taylor, 2002). The re-sensitising green tea extract ECg independently shows no toxicity to MRSA but its synergy with oxacillin and ability to re-sensitise MRSA to its effects make it a promising candidate in the fight against antibiotic resistance (Bernal et al., 2010; Stapleton et al., 2007). My study shows ECg reduces the level of oxacillin resistance in our laboratory derived high-level resistant MRSA strains. While ECg has been proposed to bind to PBPs and intercalate into the phospholipid bilayer its specific mode of action and that of other sensitising compounds remain unknown (Stapleton et al., 2007).

Previous studies had obtained mutants insensitive to the effects of different sensitising compounds (Yao and Lu, 2012) and this chapter aimed to establish a directed evolution methodology using ECg to interrogate the mechanism of action of resensitising compounds. To develop understanding of how ECg acts to reduce the level of  $\beta$ -lactam resistance of MRSA we used an altered gradient plate to evolve MRSA derivatives resistant to the effects of sensitising compounds. Whole genome sequencing of strains generated by directed evolution revealed SNPs across the evolved strains. Mutations were found in 13 genes. Many of the genes identified encode proteins which are involved in nucleotide biosynthesis such as GuaA (Osaka et al., 2020), RelA and RelQ (Irving et al., 2020). Strains independently generated SNPs in the same genes such as SAOUHSC\_01742 (*relA*) and SAOUHSC\_00942 (*relQ*), genes involved in the stringent response (Irving et al., 2020).

To verify their role in resistance to the effects of sensitising compounds the Nebraska transposon library (Fey et al., 2013) was used as a resource for mutations to interrupt the genes of interest. To determine mode of action of other resensitising compounds we assessed the level of resistance of transposon mutants in their presence. We tried to genetically modify strains using transposon mutagenesis but none of the transposon strains recapitulated the phenotype of high-level resistance to oxacillin in the presence of ECg, but instead show an altered intermediate level of resistance. This could be attributed to the differences in the SNPs that occurred in directed evolution (section 5.2.2.1), which may not necessarily lead to a loss of function (like the transposons) and could lead to a gain in function especially in the case of *rel* (Gentry et al., 2000; Gratani et al., 2018). Therefore, we suggest that these factors might be auxiliary in nature, reducing the stress exerted by the exposure to oxacillin in the presence of the ECg enabling cellular growth and division.

MRSA requires the non-native penicillin binding protein 2A (PBP2A) and mutations in potentiator genes to maintain high-level resistance to antibiotics (Bilyk et al., 2022). Independently, mutation of *relA* has been shown to potentiate resistance in the *mecA* background (Bilyk et al., 2022). This commonality in genes related to the stringent response and nucleotide biosynthesis and even their independent reoccurrence in different mutant strains adds further support to the role of the stringent response in the maintenance of antibiotic resistance in MRSA (Aedo and Tomasz, 2016; Kim et al., 2013, 2017).

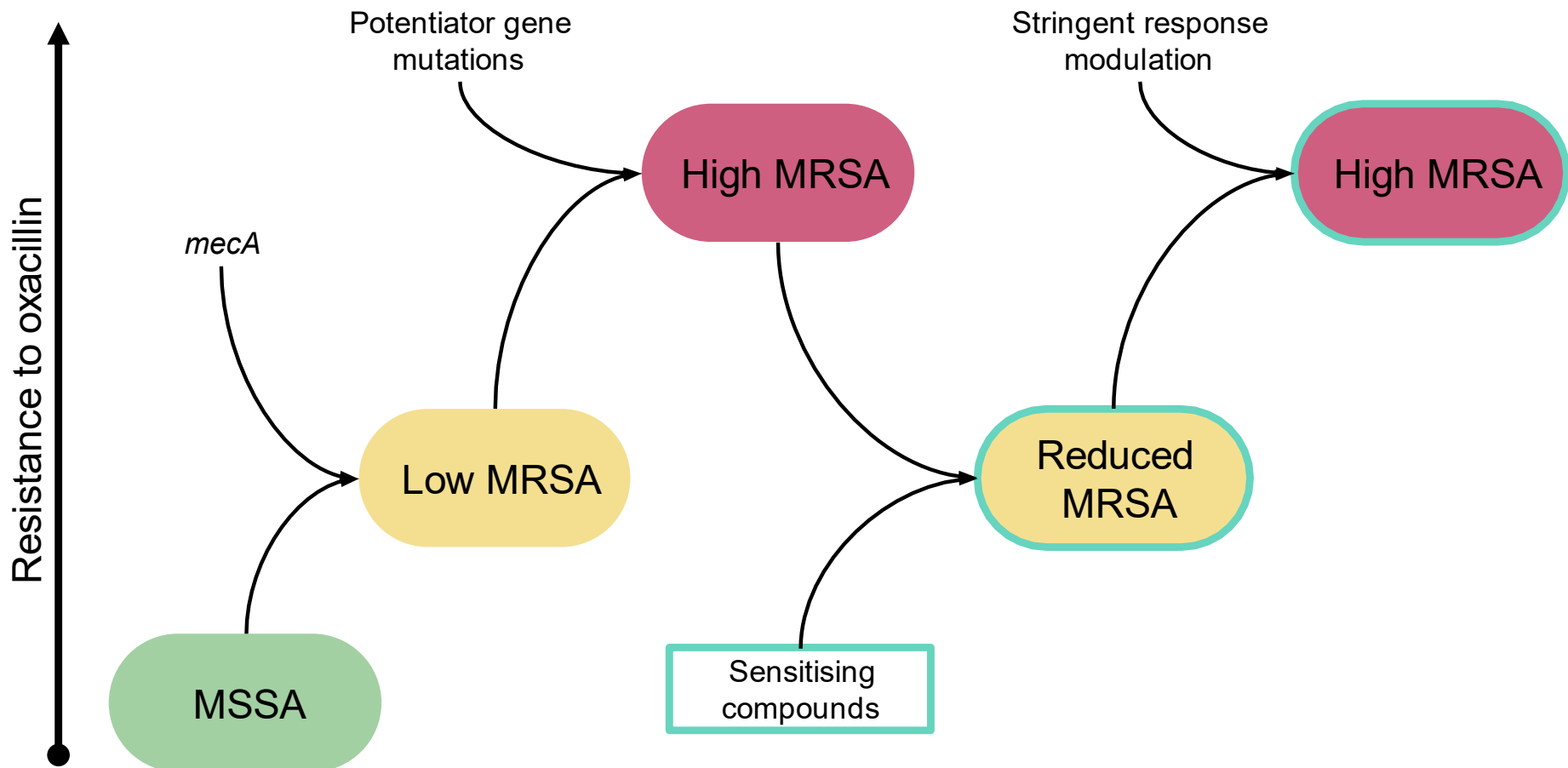
We can recapitulate the observed phenotype from the SNP's in *relA* and *relQ* using serine hydroxamate (SHX), a serine analog that inhibits seryl-tRNA synthetase, resulting in serine starvation and induction of the stringent response (Geiger et al., 2012; Tosa and Pizer, 1971). SHX had previously been shown to increase the level of resistance of strains containing plasmid borne PBP2A (Kim et al., 2013). While not directly toxic to characteristic lab strains SHX results in lower growth yields, different colony morphology and preliminary experiments showed it affects COL strains adversely (data not shown).

We hypothesised that, given the potential involvement of *relA* and *relQ* in resistance to the effects of sensitising compounds, we could use SHX mediated induction of the stringent response to rescue MRSA from the effects of sensitising compounds. SHX treatment potentiates resistance in wild type, increases resistance in *lysA::mecA* strains, and does not affect high-level MRSA strains. Also, in the presence of sensitising compounds SHX rescues MRSA from the effects of three tested sensitising compounds, clomiphene citrate, norgestimate and epicatechin gallate. The use of FDA approved drugs in my study which act in the same way as ECg to affect oxacillin resistance highlights their potential as adjuvants to treatment of  $\beta$ -lactam resistant staphylococcal infections.

In this study I have developed understanding of how the stringent response can be modulated, chemically, or genetically to overcome the effects of sensitising compounds. I am able to extend our previous model of high-level resistance to include using the stringent response to overcome the effects of sensitising compounds. Figure 5.11 shows an updated representation of our understanding of high-level resistance from (Bilyk et al., 2022) to incorporate our newfound knowledge of the interactions between the stringent response and re-sensitizing compounds.

Through directed evolution of well characterised MRSA strains in the presence of re-sensitising compounds my study has linked the action of sensitising compounds and the stringent response in MRSA. This work identifies previously unknown links between modulation of the stringent response and overcoming the effects of sensitising compounds

with implications for the understanding of cell growth and division in the presence of antibiotics. My study has identified how modulation of the stringent response in MRSA confers insensitivity to the effects of resensitising compounds. Future work could include examining how cells are able to divide in the presence of the antibiotics and sensitising compounds, also as the stringent response alters cellular metabolism (Aedo and Tomasz, 2016; Kim et al., 2013). There are a wide range of clinical MRSA strains with a variety of *SCCmec* types (Lakhundi and Zhang, 2018) extending my work to determine the role of the stringent response in other strains would establish the wider applicability of my findings. Also, determination of the role of stringent response in resistance to other antibiotics would be of great interest.



**Figure 5.11 The stringent response modulates MRSA resistance to oxacillin in the presence of sensitising compounds.**

Diagram of how *S. aureus* develops low level resistance to antibiotics via acquisition of *mecA* (encoding PBP2A) and high-level resistance through mutations in potentiator genes. MRSA strains can be “re-sensitised” to  $\beta$ -lactam antibiotics by sensitising compounds, the effects of which can be overcome by chemical or genetic modulation of the stringent response.

## Chapter 6 General Discussion

### 6.1 The danger of antimicrobial resistance

It is estimated that AMR may cost 10 million lives every year by 2050 (O'Neill, 2018). It is therefore a worldwide concern that not enough new antimicrobials are being developed to treat the rising tide of antibiotic resistant infections. Also resistance to recently developed antibiotics emerges rapidly (WHO, 2015). Methicillin resistant *S. aureus* (MRSA) is an antibiotic resistant pathogen and is the second leading cause of deaths associated with resistance (Murray et al., 2022), leading to 19,832 deaths in the USA alone in 2017.

MRSA infections are difficult to treat as resistance develops to virtually all  $\beta$ -lactam antibiotics. This is due to the acquisition of the *mecA* gene, expressing *mecA* a transpeptidase with a low affinity for  $\beta$ -lactams (Hartman and Tomasz, 1984). It has been shown in numerous studies that the expression of PBP2A, carried on *SCCmec*, is sufficient to allow low level antimicrobial resistance (Pinho et al., 2001) but the conversion to homogenous high-level resistance requires mutations in "potentiator" genes (Bilyk et al., 2022; Panchal et al., 2020). Understanding the complex mechanism by which PBP2A supports antimicrobial resistance has formed the basis for my project.

### 6.2 Insights into PBP2A protein-protein interactions

PG biosynthesis during growth and division is highly organised to allow morphogenesis. How PBP2A, as a gene product from an exogenous source, can take over the transpeptidase activity of the endogenous enzymes in the presence of antibiotics is intriguing. PG biosynthesis requires a complex interaction of multiple proteins into which PBP2A activity must be integrated. Previous studies using bacterial two hybrid analysis has defined protein complexes in *S. aureus* (Bottomley et al., 2017; Steele et al., 2011; Wacnik et al., 2022). My work has added important insights into this process.

The range of constructs screened gave rise to only one interaction between PBP2A and the multifunctional transpeptidase and transglycosylase PBP2 (Łęski and Tomasz, 2005; Pinho and Errington, 2005). This interaction is telling as it may allow PBP2A to "piggyback" onto the widely documented native interactions of PBP2 (Łęski and Tomasz, 2005; Pinho and Errington, 2005; Steele et al., 2011). As PBP2 is known to form dimers (Łęski and Tomasz, 2005), this is perhaps indicative of a heterodimer forming between PBP2 and 2A, allowing PBP2 to give the control and PBP2A the activity required in the presence of  $\beta$ -lactams. The presence of both proteins

is necessary, as PBP2 has transglycosylase activity and may function as a biochemical regulator, similarly to PBP1 (Adedeji-Olulana Unpublished and Wacnik, 2024; Wacnik et al., 2022).

Due to the limitations of bacterial two hybrid system, my study also developed constructs of PBP2A fused to GFP to be used for investigating of interactions through Co-IP and localisation using fluorescence microscopy allowing examination of these interactions in *S. aureus*. The *mecA*-GFP constructs resulted in an increase in antibiotic resistance demonstrating functionality, however fluorescence microscopy showed no specific location, comparable to that in previous studies, using a SNAP tagged version (Panchal, 2018). The PBP2A fusion protein may be unstable with sufficient functional protein to demonstrate an increase in  $\beta$ -lactam MIC, but the bulk of the protein is degraded.

The localisation of PBP2A, that is facilitated by interaction with PBP2, is integral to antibiotic resistance at high-levels (Pinho et al., 2001), where potentiator mutations tailor cell physiology to allow cells to grow in the presence of high concentrations of  $\beta$ -lactams (Bilyk et al., 2022). Naturally occurring clinical isolates demonstrate heterogeneous resistance, whereby the acquisition of *SCCmec* leads to only a modest methicillin resistance level to most of the population (De Lencastre et al., 1994b; Hartman and Tomasz, 1986) . However, a small proportion of the cells are high-level resistant. Once treated with antibiotics these are selected for and take over to become homogeneous high-level resistant MRSA. This process has also been recapitulated in various lab studies to highlight the identity of potentiator genes (Bilyk et al., 2022; Panchal, 2018) To combat the scourge of MRSA, many compounds have been identified that can resensitise MRSA to  $\beta$ -lactams, but their mode of action is largely unknown (Stapleton et al., 2007; Stapleton and Taylor, 2002).

I combined our well-defined, lab-based, high-level resistant MRSA (Panchal et al., 2020), with a directed evolution screen to identify mutations that led to loss of activity of the resensitising compound ECg. I found mutations in genes all related to the stringent response and nucleotide signalling (Corrigan et al., 2016, 2015; Irving et al., 2020). The role of the mutated genes was partially verified using transposon insertion mutants. I then showed that loss of sensitivity to ECg was also mirrored by the same effect on the activity of other resensitising compounds. Thus, either the compounds have a similar mode of action or that alterations to nucleotide signalling can give a generalised resistance to these diverse range of compounds. ECg has been the subject of a number of studies to determine its mode of action and has been proposed to intercalate into the cell membrane and to lead to delocalisation of PBP2A (Bernal et al., 2010). Another resensitising agent, Zaragozic acid (a statin), has also been found to inhibit PBP2A

oligomerization by adversely affecting lipid raft formation (García-Fernández et al., 2017). Both of these compounds may therefore adversely affect the PBP2 and PBP2A interaction.

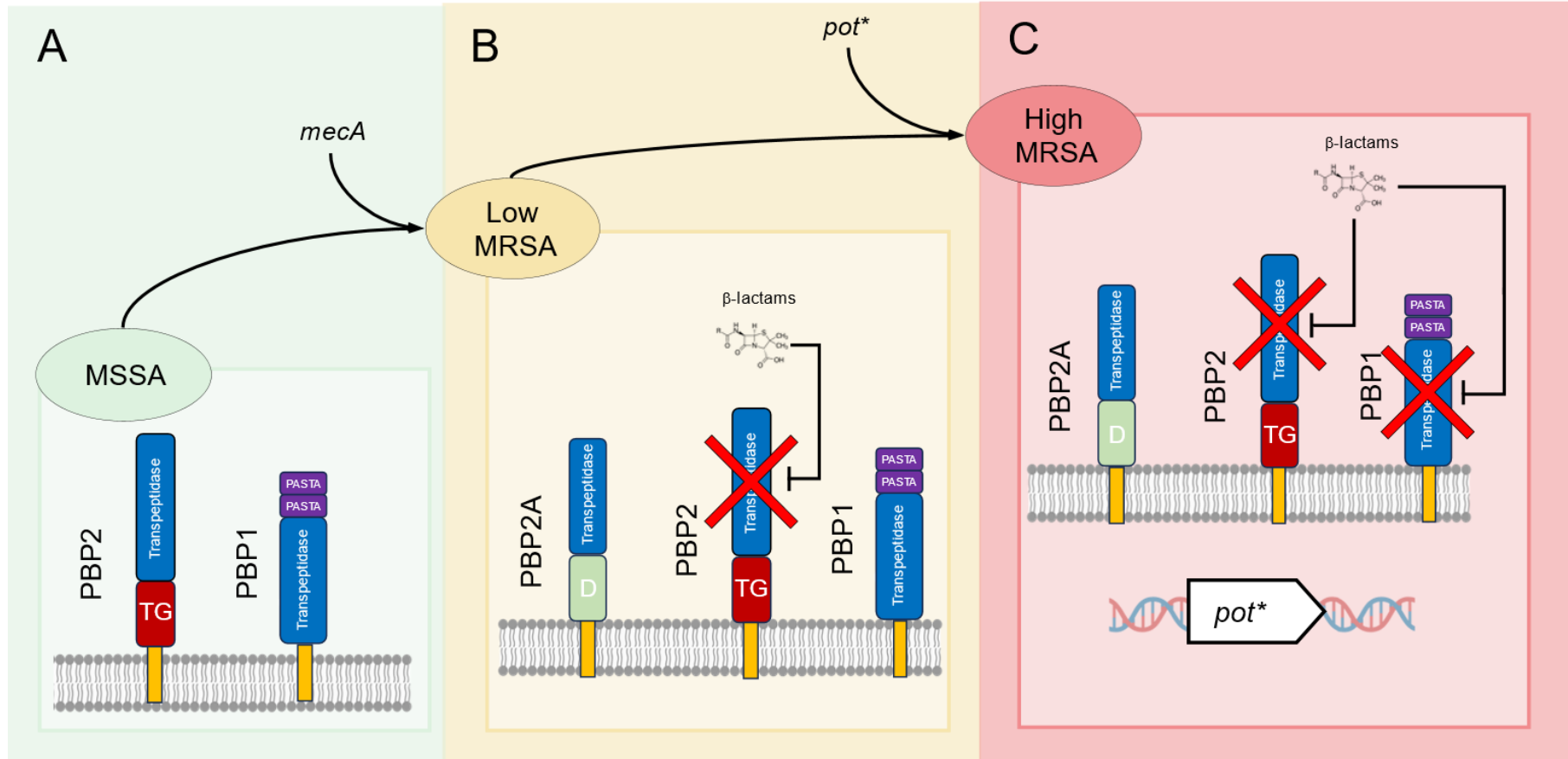
### 6.3 The basis of high-level resistance in MRSA

My study adds to the complex set of data that provides mechanistic insight into the development, and maintenance, of resistance in MRSA. As a prerequisite, cells must acquire *mecA* either naturally on *SCCmec* or in the lab. Mutations in *pot* genes then lead to a leap in resistance to the very high-levels seen clinically with the switch from heterogeneous to homogeneous resistance. Many of the *pot* genes converge around nucleotide signalling and somehow allow PBP2A to function optimally. My study has shown, that in the high-level resistant strain that already has a *rpoB\** mutation (that potentiates resistance), cells can become insensitive to the effects of resensitising compounds such as ECg by further mutations in genes all associated with nucleotide signalling pathways. Current work in our lab has shown that our high-level resistant strain (with *rpoB\**) has increased levels of the nucleotide ppGpp (Adedeji-Olulana Unpublished and Wacnik, 2024). This suggests that nucleotide signalling is a key potentiator mechanism and that this can be perhaps tuned, as my screen identified that mutations in signalling pathways could lead to loss of activity of resensitising compounds. This sets up a puzzle as to how the *pot\** mutations can lead to such a huge increase in resistance? A direct effect on PBP2A levels has been ruled out as there is no direct correlation between protein amount and resistance (Bæk et al., 2014; Panchal et al., 2020; Parvez et al., 2008) To find the solution to this question it is important to determine what PBP2A is actually required to do? *S. aureus* only has two essential PBPs that are able to carry out all the transpeptidase reactions necessary for both growth and division (Fishovitz et al., 2014; Reed et al., 2011) PBP1 has roles in cell division (Wacnik et al., 2022) and PBP2 is involved throughout the cell cycle (Łęski and Tomasz, 2005; Pinho et al., 2001). In MRSA, PBP2A must be able to carry out all the transpeptidase activity in the cell as the other enzymes are inactivated by binding to  $\beta$ -lactams. Until very recently our assumption was that the *pot* mutations somehow allowed PBP2A to assume this role. However, we have discovered an important facet of the development of high-level resistance that gives a mechanistic understanding.

PBP2A has previously been shown to be able to compensate for the loss of activity of PBP2 (Pinho et al., 2001) and we have verified this. Surprisingly, using a series of *pbp1* conditional lethal constructs (Wacnik et al., 2022) in our engineered MRSA background, we have found that PBP2A cannot compensate for the lack of PBP1 transpeptidase activity (Adedeji-Olulana Unpublished and Wacnik, 2024). So how can high-level MRSA grow in the presence of antibiotics? It transpires that it is the single point mutation in *rpoB\** that gives high-level

resistance in MRSA also allows the cells to divide without PBP1 activity. This means there are two co-dependent mechanisms that are required for high-level resistance in MRSA. Firstly, *mecA* acquisition that allows for the loss of PBP2 transpeptidase activity (Fig. 6.1). Secondly, *rpoB*\* (or another *pot* mutation) that allows division without PBP1 transpeptidase activity. We have been able to separate these two mechanisms genetically and have found that the resensitising agents effect one or both pathways (Adedeji-Olulana Unpublished and Wacnik, 2024). Now we are beginning to understand that there are two mechanisms required for resistance, allowing us to not only investigate how these are manifested but also to use the resensitising agents as probes to give mechanistic details and to determine their mode of action.





**Figure 6.1 Development of resistance in MRSA**

In MSSA, PBP1 and PBP2 are inhibited by antibiotics, leading to cessation of growth and subsequent death of the cells (A). The acquisition of *mecA* leads to Low MRSA with an intermediate MIC (B). Only after a *pot* mutation does High MRSA occur with a large increase in MIC (C). It is hypothesised that PBP2A compensates for the loss of PBP2 transpeptidase activity and the *pot* mutations allow for the inhibition of PBP1 transpeptidase activity (C). TG transglycosylase; D, Dimerisation domain. Adapted from (Adedeji-Olulana Unpublished and Wacnik, 2024).

## 6.4 Future Perspectives

My work, set within wider studies in the lab is making real inroads into understanding how high-level resistance in MRSA develops and is maintained. In doing so it gives insight into this complex mechanism but also creates important new avenues for research including:

**How does PBP2A work?** My study suggests that PBP2A may act directly with PBP2 in the presence of antibiotics. Using a combination of *in vitro* protein studies and genetic approaches one can begin to unravel this complex interplay and how together they allow PG synthesis. This can be coupled with our high-resolution AFM analysis to determine their roles in PG architecture determination during the cell cycle (Pasquina-Lemonche et al., 2020).

**How are *pot* mutations able to allow high-level MRSA?** The revelation that the *pot* mutations allow the cells to divide without the otherwise essential PBP1 activity, gives access to a whole new set of studies to determine how this is manifested. This work is underway using a range of cell biology and biochemical analyses. There is the mechanistic question as to how division occurs but also the conundrum as to the link between nucleotide signalling and this mode of cell division without PBP1 activity?

**What is the mode of action of the resensitising agents, such as ECg?** Our new finding of two pathways to resistance has allowed the onset of studies to sort the resensitising compounds into where they manifest their activity. We now have more defined assays as to whether they are affecting the PBP2/2A or the PBP1/Pot pathway. Mode of action studies using a range of approaches including investigation of the action of inhibitors using mutated PBPs can now be conducted (Adedeji-Olulana et al., 2024).

**Can resensitising agents be developed as part of adjunct therapy to combat MRSA?** The ultimate goal is to exploit weaknesses of MRSA such as resensitising agents, to reduce the burden of AMR around the world. Mechanistic understanding gives us a platform on which to rationally develop new control regimes, to beat MRSA.

## References

- Abraham, E.P., Chain, E., 1940. An enzyme from bacteria able to destroy penicillin [1]. *Nature*.  
<https://doi.org/10.1038/146837a0>
- Acar, J.F., Goldstein, F.W., 1997. Trends in bacterial resistance to fluoroquinolones. *Clinical Infectious Diseases* 24, 67–73. [https://doi.org/10.1093/clinids/24.supplement\\_1.s67](https://doi.org/10.1093/clinids/24.supplement_1.s67)
- Adedeji-Olulana, A. F., Wacnik, K., Lafage, L., Pasquina-Lemonche, L., Tinajero-Trejo, M., Sutton, J. A. F., Bilyk, B., Irving, S. E., Portman Ross, C. J., Meacock, O. J., Randerson, S. A., Beattie, E., Owen, D. S., Florence, J., Durham, W. M., Hornby, D. P., Corrigan, R. M., Green, J., Hobbs, J. K., & Foster, S. J. (2024). Two codependent routes lead to high-level MRSA. *Science*, 386(6721), 573–580. <https://doi.org/10.1126/SCIENCE.ADN1369>
- Aedo, S., Tomasz, A., 2016. Role of the stringent stress response in the antibiotic resistance phenotype of methicillin-resistant *Staphylococcus aureus*. *Antimicrob Agents Chemother* 60, 2311–2317. <https://doi.org/10.1128/AAC.02697-15/ASSET/5F45B914-EF54-4BCB-9287-B46059A35178/ASSETS/GRAPHIC/ZAC0041650370005.JPEG>
- Aiba, Y., Katayama, Y., Hishinuma, T., Murakami-Kuroda, H., Cui, L., Hiramatsu, K., 2013. Mutation of RNA polymerase  $\beta$ -subunit gene promotes heterogeneous-to-homogeneous conversion of  $\beta$ -lactam resistance in methicillin-resistant *Staphylococcus aureus*. *Antimicrob Agents Chemother* 57, 4861–4871. <https://doi.org/10.1128/AAC.00720-13>
- Aires de Sousa, M., Lencastre, H., 2004. Bridges from hospitals to the laboratory: genetic portraits of methicillin-resistant *Staphylococcus aureus* clones. *FEMS Immunol Med Microbiol* 40, 101–111. [https://doi.org/10.1016/S0928-8244\(03\)00370-5](https://doi.org/10.1016/S0928-8244(03)00370-5)
- Alborn, W.E., Allen, N.E., Preston, D.A., 1991. Daptomycin disrupts membrane potential in growing *Staphylococcus aureus*. *Antimicrob Agents Chemother* 35, 2282–2287. <https://doi.org/10.1128/AAC.35.11.2282>
- Al-Mebairik, N.F., El-Kersh, T.A., Al-Sheikh, Y.A., Marie, M.A.M., 2016. A review of virulence factors, pathogenesis, and antibiotic resistance in *Staphylococcus aureus*. *Reviews in Medical Microbiology*. <https://doi.org/10.1097/MRM.0000000000000067>
- Atkinson, G.C., Tenson, T., Hauryliuk, V., 2011. The RelA/SpoT Homolog (RSH) Superfamily: Distribution and Functional Evolution of ppGpp Synthetases and Hydrolases across the Tree of Life. *PLoS One* 6, e23479. <https://doi.org/10.1371/JOURNAL.PONE.0023479>

- Ba, X., Harrison, E.M., Lovering, A.L., Gleadall, N., Zadoks, R., Parkhill, J., Peacock, S.J., Holden, M.T.G., Paterson, G.K., Holmes, M.A., 2015. Old drugs to treat resistant bugs: Methicillin-resistant *Staphylococcus aureus* isolates with *mecC* are susceptible to a combination of penicillin and clavulanic acid. *Antimicrob Agents Chemother* 59, 7396–7404. [https://doi.org/10.1128/AAC.01469-15/SUPPL\\_FILE/ZAC012154619S01.PDF](https://doi.org/10.1128/AAC.01469-15/SUPPL_FILE/ZAC012154619S01.PDF)
- Bæk, K.T., Gründling, A., Mogensen, R.G., Thøgersen, L., Petersen, A., Paulander, W., Frees, D., 2014.  $\beta$ -lactam resistance in methicillin-resistant *Staphylococcus aureus* USA300 is increased by inactivation of the ClpXP protease. *Antimicrob Agents Chemother* 58, 4593–4603. <https://doi.org/10.1128/AAC.02802-14/ASSET/35532DA1-A525-4430-AFE5-92D31CB0CAC7/ASSETS/GRAPHIC/ZAC0081431280005.JPEG>
- Baker, T.A., Sauer, R.T., 2012. ClpXP, an ATP-powered unfolding and protein-degradation machine. *Biochim Biophys Acta* 1823, 15–28. <https://doi.org/10.1016/J.BBAMCR.2011.06.007>
- Banerjee, R., Gretes, M., Harlem, C., Basuino, L., Chambers, H.F., 2010. A *mecA*-negative strain of methicillin-resistant *Staphylococcus aureus* with high-level  $\beta$ -lactam resistance contains mutations in three genes. *Antimicrob Agents Chemother* 54, 4900–4902. <https://doi.org/10.1128/AAC.00594-10>
- Barna, J.C.J., Williams, D.H., 1984. The Structure and Mode of Action of Glycopeptide Antibiotics of the Vancomycin Group. *Annu Rev Microbiol* 38, 339–357. <https://doi.org/10.1146/annurev.mi.38.100184.002011>
- Battesti, A., Bouveret, E., 2012. The bacterial two-hybrid system based on adenylate cyclase reconstitution in *Escherichia coli*. *Methods*. <https://doi.org/10.1016/j.ymeth.2012.07.018>
- Bayer, A.S., Prasad, R., Chandra, J., Koul, A., Smriti, M., Varma, A., Skurray, R.A., Firth, N., Brown, M.H., Koo, S.U.P., Yeaman, M.R., 2000. In vitro resistance of *Staphylococcus aureus* to thrombin-induced platelet microbicidal protein is associated with alterations in cytoplasmic membrane fluidity. *Infect Immun* 68, 3548–3553. <https://doi.org/10.1128/IAI.68.6.3548-3553.2000>
- Becker, S., Frankel, M.B., Schneewind, O., Missiakas, D., 2014. Release of protein A from the cell wall of *Staphylococcus aureus*. *Proc Natl Acad Sci U S A* 111, 1574–1579. [https://doi.org/10.1073/PNAS.1317181111/SUPPL\\_FILE/PNAS.201317181SI.PDF](https://doi.org/10.1073/PNAS.1317181111/SUPPL_FILE/PNAS.201317181SI.PDF)
- Bernal, P., Lemaire, S., Pinho, M.G., Mobashery, S., Hinds, J., Taylor, P.W., 2010. Insertion of Epicatechin Gallate into the Cytoplasmic Membrane of Methicillin-resistant *Staphylococcus aureus* Disrupts Penicillin-binding Protein (PBP) 2a-mediated  $\beta$ -Lactam

- Resistance by Delocalizing PBP2. *J Biol Chem* 285, 24055. <https://doi.org/10.1074/JBC.M110.114793>
- Bi, E., Lutkenhaus, J., 1991. FtsZ ring structure associated with division in *Escherichia coli*. *Nature* 354, 161–164. <https://doi.org/10.1038/354161A0>
- Bilyk, B.L., Panchal, V. V., Tinajero-Trejo, M., Hobbs, J.K., Foster, S.J., 2022. An Interplay of Multiple Positive and Negative Factors Governs Methicillin Resistance in *Staphylococcus aureus*. *Microbiology and Molecular Biology Reviews*. <https://doi.org/10.1128/membr.00159-21>
- Bisson-Filho, A.W., Hsu, Y.P., Squyres, G.R., Kuru, E., Wu, F., Jukes, C., Sun, Y., Dekker, C., Holden, S., VanNieuwenhze, M.S., Brun, Y. V., Garner, E.C., 2017. Treadmilling by FtsZ filaments drives peptidoglycan synthesis and bacterial cell division. *Science* (1979) 355, 739–743. <https://doi.org/10.1126/science.aak9973>
- Bojer, M.S., Wacnik, K., Kjelgaard, P., Gallay, C., Bottomley, A.L., Cohn, M.T., Lindahl, G., Frees, D., Veening, J.W., Foster, S.J., Ingmer, H., 2019. *SosA* inhibits cell division in *Staphylococcus aureus* in response to DNA damage. *Mol Microbiol* 112, 1116–1130. <https://doi.org/10.1111/MMI.14350>
- Boonsiri, T., Watanabe, S., Tan, X.E., Thitiananpakorn, K., Narimatsu, R., Sasaki, K., Takenouchi, R., Sato'o, Y., Aiba, Y., Kiga, K., Sasahara, T., Taki, Y., Li, F.Y., Zhang, Y., Azam, A.H., Kawaguchi, T., Cui, L., 2020. Identification and characterization of mutations responsible for the  $\beta$ -lactam resistance in oxacillin-susceptible *mecA*-positive *Staphylococcus aureus*. *Scientific Reports* 2020 10:1 10, 1–22. <https://doi.org/10.1038/s41598-020-73796-5>
- Bottomley, A.L., 2011. Identification and characterisation of the cell division machinery in *Staphylococcus aureus* 288.
- Bottomley, A.L., Liew, A.T.F., Kusuma, K.D., Peterson, E., Seidel, L., Foster, S.J., Harry, E.J., 2017. Coordination of chromosome segregation and cell division in *Staphylococcus aureus*. *Front Microbiol* 8. <https://doi.org/10.3389/FMICB.2017.01575>
- Bowman, L., Zeden, M.S., Schuster, C.F., Kaeffer, V., Gründling, A., 2016. New Insights into the Cyclic Di-adenosine Monophosphate (c-di-AMP) Degradation Pathway and the Requirement of the Cyclic Dinucleotide for Acid Stress Resistance in *Staphylococcus aureus*. *J Biol Chem* 291, 26970–26986. <https://doi.org/10.1074/JBC.M116.747709>
- Boyle-Vavra, S., Yin, S., Jo, D.S., Montgomery, C.P., Daum, R.S., 2013. *VraT/YvqF* is required for methicillin resistance and activation of the *VraSR* regulon in *Staphylococcus aureus*.

- Antimicrob Agents Chemother 57, 83–95. [https://doi.org/10.1128/AAC.01651-12/SUPPL\\_FILE/ZAC999101453SO1.PDF](https://doi.org/10.1128/AAC.01651-12/SUPPL_FILE/ZAC999101453SO1.PDF)
- Brignoli, T., Douglas, E., Duggan, S., Fagunloye, O.G., Adhikari, R., Aman, M.J., Massey, R.C., 2022. Wall Teichoic Acids Facilitate the Release of Toxins from the Surface of *Staphylococcus aureus*. *Microbiol Spectr* 10. <https://doi.org/10.1128/SPECTRUM.01011-22>
- Brock, T.D., Madigan, M.T., Martinko, J.M., Parker, J., 2003. Brock biology of microorganisms. Upper Saddle River (NJ): Prentice-Hall, 2003.
- Brown, D.F.J., Reynolds, P.E., 1980. Intrinsic resistance to  $\beta$ -lactam antibiotics in *Staphylococcus aureus*. *FEBS Lett* 122, 275–278. [https://doi.org/10.1016/0014-5793\(80\)80455-8](https://doi.org/10.1016/0014-5793(80)80455-8)
- Brown, S., Xia, G., Luhachack, L.G., Campbell, J., Meredith, T.C., Chen, C., Winstel, V., Gekeler, C., Irazoqui, J.E., Peschel, A., Walker, S., 2012. Methicillin resistance in *Staphylococcus aureus* requires glycosylated wall teichoic acids. *Proc Natl Acad Sci U S A* 109, 18909–18914. <https://doi.org/10.1073/PNAS.1209126109>
- Brückner, A., Polge, C., Lentze, N., Auerbach, D., Schlattner, U., 2009. Yeast Two-Hybrid, a Powerful Tool for Systems Biology. *Int J Mol Sci* 10, 2763. <https://doi.org/10.3390/IJMS10062763>
- Bryson, V., Szybalski, W., 1952. Microbial selection. *Science* (1979) 116, 45–51.
- Bush, K., 2015. Antibiotics: Synergistic MRSA combinations. *Nat Chem Biol*. <https://doi.org/10.1038/nchembio.1935>
- Cameron, D.R., Jiang, J.H., Kostoulas, X., Foxwell, D.J., Peleg, A.Y., 2016. Vancomycin susceptibility in methicillin-resistant *Staphylococcus aureus* is mediated by YycH activation of the WalRK essential two-component regulatory system. *Sci Rep* 6. <https://doi.org/10.1038/srep30823>
- Campbell, E.A., Korzheva, N., Mustaev, A., Murakami, K., Nair, S., Goldfarb, A., Darst, S.A., 2001. Structural mechanism for rifampicin inhibition of bacterial RNA polymerase. *Cell* 104, 901–912. [https://doi.org/10.1016/S0092-8674\(01\)00286-0](https://doi.org/10.1016/S0092-8674(01)00286-0)
- Campbell, J., Singh, A.K., Santa Maria, J.P., Kim, Y., Brown, S., Swoboda, J.G., Mylonakis, E., Wilkinson, B.J., Walker, S., 2011. Synthetic lethal compound combinations reveal a fundamental connection between wall teichoic acid and peptidoglycan biosyntheses in *Staphylococcus aureus*. *ACS Chem Biol* 6, 106–116. [https://doi.org/10.1021/CB100269F/SUPPL\\_FILE/CB100269F\\_SI\\_001.PDF](https://doi.org/10.1021/CB100269F/SUPPL_FILE/CB100269F_SI_001.PDF)

- Carter, A.P., Clemons, W.M., Brodersen, D.E., Morgan-Warren, R.J., Wimberly, B.T., Ramakrishnan, V., 2000. Functional insights from the structure of the 30S ribosomal subunit and its interactions with antibiotics. *Nature* 2000 407:6802 407, 340–348. <https://doi.org/10.1038/35030019>
- Chambers, H.F., 2001. The changing epidemiology of *Staphylococcus aureus*, in: Emerging Infectious Diseases. Centers for Disease Control and Prevention (CDC), pp. 178–182. <https://doi.org/10.3201/eid0702.010204>
- Chambers, H.F., 1997. Methicillin resistance in staphylococci: Molecular and biochemical basis and clinical implications. *Clin Microbiol Rev.* <https://doi.org/10.1128/cmr.10.4.781>
- Chambers, H.F., DeLeo, F.R., 2009. Waves of resistance: *Staphylococcus aureus* in the antibiotic era. *Nat Rev Microbiol* 7, 629–641. <https://doi.org/10.1038/NRMICRO2200>
- Chambers, H.F., Hartman, B.J., Tomasz, A., 1985. Increased amounts of a novel penicillin-binding protein in a strain of methicillin-resistant *Staphylococcus aureus* exposed to nafcillin. *J Clin Invest* 76, 325–331. <https://doi.org/10.1172/JCI11965>
- Champney, W.S., Burdine, R., 1995. Macrolide antibiotics inhibit 50S ribosomal subunit assembly in *Bacillus subtilis* and *Staphylococcus aureus*. *Antimicrob Agents Chemother* 39, 2141. <https://doi.org/10.1128/AAC.39.9.2141>
- Chaudhuri, R.R., Allen, A.G., Owen, P.J., Shalom, G., Stone, K., Harrison, M., Burgis, T.A., Lockyer, M., Garcia-Lara, J., Foster, S.J., Pleasance, S.J., Peters, S.E., Maskell, D.J., Charles, I.G., 2009. Comprehensive identification of essential *Staphylococcus aureus* genes using Transposon-Mediated Differential Hybridisation (TMDH). *BMC Genomics* 10. <https://doi.org/10.1186/1471-2164-10-291>
- Cherkasov, A., Hsing, M., Zoraghi, R., Foster, L.J., See, R.H., Stoyanov, N., Jiang, J., Kaur, S., Lian, T., Jackson, L., Gong, H., Swayze, R., Amandoron, E., Hormozdiari, F., Dao, P., Sahinalp, C., Santos-Filho, O., Axerio-Cillies, P., Byler, K., McMaster, W.R., Brunham, R.C., Finlay, B.B., Reiner, N.E., 2011. Mapping the protein interaction network in methicillin-resistant *Staphylococcus aureus*. *J Proteome Res* 10, 1139–1150. <https://doi.org/10.1021/pr100918u>
- Claessen, D., Emmins, R., Hamoen, L.W., Daniel, R.A., Errington, J., Edwards, D.H., 2008. Control of the cell elongation-division cycle by shuttling of PBP1 protein in *Bacillus subtilis*. *Mol Microbiol* 68, 1029–1046. <https://doi.org/10.1111/J.1365-2958.2008.06210.X>
- Cleverley, R.M., Rutter, Z.J., Rismondo, J., Corona, F., Tsui, H.C.T., Alatawi, F.A., Daniel, R.A., Halbedel, S., Massidda, O., Winkler, M.E., Lewis, R.J., 2019. The cell cycle regulator GpsB

- functions as cytosolic adaptor for multiple cell wall enzymes. *Nature Communications* 2019 10:1 10, 1–17. <https://doi.org/10.1038/s41467-018-08056-2>
- Contreras-Martel, C., Martins, A., Ecobichon, C., Trindade, D.M., Mattei, P.J., Hicham, S., Hardouin, P., Ghachi, M. El, Boneca, I.G., Dessen, A., 2017. Molecular architecture of the PBP2-MreC core bacterial cell wall synthesis complex. *Nat Commun* 8. <https://doi.org/10.1038/s41467-017-00783-2>
- Corrigan, R.M., Abbott, J.C., Burhenne, H., Kaefer, V., Gründling, A., 2011. c-di-AMP is a new second messenger in *Staphylococcus aureus* with a role in controlling cell size and envelope stress. *PLoS Pathog* 7. <https://doi.org/10.1371/JOURNAL.PPAT.1002217>
- Corrigan, R.M., Bellows, L.E., Wood, A., Gründling, A., 2016. ppGpp negatively impacts ribosome assembly affecting growth and antimicrobial tolerance in Gram-positive bacteria. *Proc Natl Acad Sci U S A* 113, E1710–E1719. <https://doi.org/10.1073/PNAS.1522179113>
- Corrigan, R.M., Bowman, L., Willis, A.R., Kaefer, V., Gründling, A., 2015. Cross-talk between two nucleotide-signaling pathways in *Staphylococcus aureus*. *Journal of Biological Chemistry* 290, 5826–5839. <https://doi.org/10.1074/JBC.M114.598300>
- Corrigan, R.M., Gründling, A., 2013. Cyclic di-AMP: another second messenger enters the fray. *Nat Rev Microbiol* 11, 513–524. <https://doi.org/10.1038/NRMICRO3069>
- Cuirolo, A., Plata, K., Rosato, A.E., 2009. Development of homogeneous expression of resistance in methicillin-resistant *Staphylococcus aureus* clinical strains is functionally associated with a beta-lactam-mediated SOS response. *J Antimicrob Chemother* 64, 37–45. <https://doi.org/10.1093/JAC/DKP164>
- da Costa, T.M., de Oliveira, C.R., Chambers, H.F., Chatterjee, S.S., 2018. Pbp4: A new perspective on *Staphylococcus aureus*  $\beta$ -lactam resistance. *Microorganisms* 6. <https://doi.org/10.3390/MICROORGANISMS6030057>
- Daniel, R.A., Noirot-Gros, M.F., Noirot, P., Errington, J., 2006. Multiple interactions between the transmembrane division proteins of *Bacillus subtilis* and the role of FtsL instability in divisome assembly. *J Bacteriol* 188, 7396–7404. <https://doi.org/10.1128/JB.01031-06/ASSET/528B427E-45CE-4840-804F-7BD72A59A2DF/ASSETS/GRAPHIC/ZJB0210661860005.JPEG>
- De Lencastre, H., Jonge, B.L.M.D., Matthews, P.R., Tomasz, A., 1994. Molecular aspects of methicillin resistance in *Staphylococcus aureus*. *Journal of Antimicrobial Chemotherapy*. <https://doi.org/10.1093/jac/33.1.7>



- Delmar, J.A., Yu, E.W., 2016. The AbgT family: A novel class of antimetabolite transporters. *Protein Science*. <https://doi.org/10.1002/pro.2820>
- Dengler, V., McCallum, N., Kiefer, P., Christen, P., Patrignani, A., Vorholt, J.A., Berger-Bächi, B., Senn, M.M., 2013. Mutation in the C-di-AMP cyclase *dacA* affects fitness and resistance of methicillin resistant *Staphylococcus aureus*. *PLoS One* 8. <https://doi.org/10.1371/JOURNAL.PONE.0073512>
- Do, T., Page, J.E., Walker, S., 2020. Uncovering the activities, biological roles, and regulation of bacterial cell wall hydrolases and tailoring enzymes. *Journal of Biological Chemistry* 295, 3347–3361. <https://doi.org/10.1074/JBC.REV119.010155>
- Egan, A.J.F., Cleverley, R.M., Peters, K., Lewis, R.J., Vollmer, W., 2017. Regulation of bacterial cell wall growth. *FEBS J* 284, 851–867. <https://doi.org/10.1111/FEBS.13959>
- Eisenstein, B.I., Oleson, F.B., Baltz, R.H., 2010. Daptomycin: From the Mountain to the Clinic, with Essential Help from Francis Tally, MD. *Clinical Infectious Diseases* 50, S10–S15. <https://doi.org/10.1086/647938>
- Endl, J., Seidl, H.P., Fiedler, F., Schleider, K.H., 1983. Chemical composition and structure of cell wall teichoic acids of staphylococci. *Arch Microbiol* 135, 215–223. <https://doi.org/10.1007/BF00414483/METRICS>
- Eswara, P.J., Brzozowski, R.S., Viola, M.G., Graham, G., Spanoudis, C., Trebino, C., Jha, J., Aubee, J.I., Thompson, K.M., Camberg, J.L., Ramamurthi, K.S., 2018. An essential *Staphylococcus aureus* cell division protein directly regulates *ftsZ* dynamics. *Elife* 7. <https://doi.org/10.7554/ELIFE.38856>
- Farha, M.A., Czarny, T.L., Myers, C.L., Worrall, L.J., French, S., Conrady, D.G., Wang, Y., Oldfield, E., Strynadka, N.C.J., Brown, E.D., 2015. Antagonism screen for inhibitors of bacterial cell wall biogenesis uncovers an inhibitor of undecaprenyl diphosphate synthase. *Proc Natl Acad Sci U S A* 112, 11048–11053. [https://doi.org/10.1073/PNAS.1511751112/SUPPL\\_FILE/PNAS.1511751112.SAPP.PDF](https://doi.org/10.1073/PNAS.1511751112/SUPPL_FILE/PNAS.1511751112.SAPP.PDF)
- Farha, M.A., Leung, A., Sewell, E.W., D'Elia, M.A., Allison, S.E., Ejim, L., Pereira, P.M., Pinho, M.G., Wright, G.D., Brown, E.D., 2013. Inhibition of WTA synthesis blocks the cooperative action of pbps and sensitizes MRSA to  $\beta$ -lactams. *ACS Chem Biol* 8, 226–233. <https://doi.org/10.1021/CB300413M>
- Fedtke, I., Mader, D., Kohler, T., Moll, H., Nicholson, G., Biswas, R., Henseler, K., Götz, F., Zähringer, U., Peschel, A., 2007. A *Staphylococcus aureus* *ypfP* mutant with strongly

reduced lipoteichoic acid (LTA) content: LTA governs bacterial surface properties and autolysin activity. *Mol Microbiol* 65, 1078–1091. <https://doi.org/10.1111/J.1365-2958.2007.05854.X>

Feng, J., Michalik, S., Varming, A.N., Andersen, J.H., Albrecht, D., Jelsbak, L., Krieger, S., Ohlsen, K., Hecker, M., Gerth, U., Ingmer, H., Frees, D., 2013. Trapping and proteomic identification of cellular substrates of the ClpP protease in *Staphylococcus aureus*. *J Proteome Res* 12, 547–558. <https://doi.org/10.1021/PR300394R>

Figueiredo, T.A., Sobral, R.G., Ludovice, A.M., de Almeida, J.M.F., Bui, N.K., Vollmer, W., de Lencastre, H., Tomasz, A., 2012. Identification of genetic determinants and enzymes involved with the amidation of glutamic acid residues in the peptidoglycan of *Staphylococcus aureus*. *PLoS Pathog* 8. <https://doi.org/10.1371/JOURNAL.PPAT.1002508>

Finan, J.E., Rosato, A.E., Dickinson, T.M., Ko, D., Archer, G.L., 2002. Conversion of oxacillin-resistant staphylococci from heterotypic to homotypic resistance expression. *Antimicrob Agents Chemother* 46, 24–30. <https://doi.org/10.1128/AAC.46.1.24-30.2002>

Fischer, W., Mannsfeld, T., Hagen, G., 2011. On the basic structure of poly (glycerophosphate) lipoteichoic acids. <https://doi.org/10.1139/o90-005> 68, 33–43. <https://doi.org/10.1139/O90-005>

Fishovitz, J., Hermoso, J.A., Chang, M., Mobashery, S., 2014. Penicillin-binding protein 2a of methicillin-resistant *Staphylococcus aureus*. *IUBMB Life*. <https://doi.org/10.1002/iub.1289>

Fleming, A., 1929. On the antibacterial action of cultures of a penicillium, with special reference to their use in the isolation of *B. influenzae*. *Br J Exp Pathol* 10, 226.

Frankel, M.B., Hendrickx, A.P.A., Missiakas, D.M., Schneewind, O., 2011. LytN, a murein hydrolase in the cross-wall compartment of *Staphylococcus aureus*, is involved in proper bacterial growth and envelope assembly. *Journal of Biological Chemistry* 286, 32593–32605. <https://doi.org/10.1074/JBC.M111.258863/ATTACHMENT/27B34AF3-D769-4C82-B36D-E20A7F50B57F/MMC1.PDF>

Frei, C.R., Miller, M.L., Lewis, J.S., Lawson, K.A., Hunter, J.M., Oramasionwu, C.U., Talbert, R.L., 2010. Trimethoprim-Sulfamethoxazole or Clindamycin for Community-Associated MRSA (CA-MRSA) Skin Infections. *The Journal of the American Board of Family Medicine* 23, 714–719. <https://doi.org/10.3122/JABFM.2010.06.090270>

- French, G.L., Cheng, A.F.B., Ling, J.M.L., Mo, P., Donnan, S., 1990. Hong Kong strains of methicillin-resistant and methicillin-sensitive *Staphylococcus aureus* have similar virulence. *Journal of Hospital Infection* 15, 117–125. [https://doi.org/10.1016/0195-6701\(90\)90120-D](https://doi.org/10.1016/0195-6701(90)90120-D)
- Fuda, C., Suvorov, M., Vakulenko, S.B., Mobashery, S., 2004. The basis for resistance to  $\beta$ -lactam antibiotics by penicillin-binding protein 2a of methicillin-resistant *Staphylococcus aureus*. *Journal of Biological Chemistry* 279, 40802–40806. <https://doi.org/10.1074/jbc.M403589200>
- Fujimura, T., Murakami, K., 2008. *Staphylococcus aureus* clinical isolate with high-level methicillin resistance with an *lytH* mutation caused by IS1182 insertion. *Antimicrob Agents Chemother* 52, 643–647. <https://doi.org/10.1128/AAC.00395-07>
- Fujimura, T., Murakami, K., 1997. Increase of methicillin resistance in *Staphylococcus aureus* caused by deletion of a gene whose product is homologous to lytic enzymes. *J Bacteriol* 179, 6294–6301. <https://doi.org/10.1128/JB.179.20.6294-6301.1997>
- Fuller, A.T., Mellows, G., Woolford, M., Banks, G.T., Barrow, K.D., Chain, E.B., 1971. Pseudomonic acid: An antibiotic produced by *Pseudomonas fluorescens* [13]. *Nature* 234, 416–417. <https://doi.org/10.1038/234416a0>
- Gallagher, L.A., Shears, R.K., Fingleton, C., Alvarez, L., Waters, E.M., Clarke, J., Bricio-Moreno, L., Campbell, C., Yadav, A.K., Razvi, F., O'Neill, E., O'Neill, A.J., Cava, F., Fey, P.D., Kadioglu, A., O'Gara, J.P., 2020. Impaired Alanine Transport or Exposure to d-Cycloserine Increases the Susceptibility of MRSA to  $\beta$ -lactam Antibiotics. *Journal of Infectious Diseases* 221, 1006–1016. <https://doi.org/10.1093/INFDIS/JIZ542>
- García-Fernández, E., Koch, G., Wagner, R.M., Fekete, A., Stengel, S.T., Schneider, J., Mielich-Süss, B., Geibel, S., Markert, S.M., Stigloher, C., Lopez, D., 2017. Membrane Microdomain Disassembly Inhibits MRSA Antibiotic Resistance. *Cell* 171, 1354-1367.e20. <https://doi.org/10.1016/j.cell.2017.10.012>
- García-Lara, J., Weihs, F., Ma, X., Walker, L., Chaudhuri, R.R., Kasturiarachchi, J., Crossley, H., Golestanian, R., Foster, S.J., 2015. Supramolecular structure in the membrane of *Staphylococcus aureus*. *Proc Natl Acad Sci U S A* 112, 15725–15730. <https://doi.org/10.1073/PNAS.1509557112>
- Gardete, S., Wu, S.W., Gill, S., Tomasz, A., 2006. Role of *VraSR* in antibiotic resistance and antibiotic-induced stress response in *Staphylococcus aureus*. *Antimicrob Agents*

- Chemother 50, 3424–3434. <https://doi.org/10.1128/AAC.00356-06/ASSET/A2D27574-226C-4EFF-A15B-30E0D5CC2348/ASSETS/GRAPHIC/ZAC0100660700006.JPEG>
- Geigenmuller, U., Nierhaus, Knud H, Wittmann, A., Nierhaus, K H, 1986. Tetracycline can inhibit tRNA binding to the ribosomal P site as well as to the A site. Eur J Biochem 161, 723–726. <https://doi.org/10.1111/J.1432-1033.1986.TB10499.X>
- Geiger, T., Francois, P., Liebeke, M., Fraunholz, M., Goerke, C., Krismer, B., Schrenzel, J., Lalk, M., Wolz, C., 2012. The Stringent Response of *Staphylococcus aureus* and Its Impact on Survival after Phagocytosis through the Induction of Intracellular PSMs Expression. PLoS Pathog 8, e1003016. <https://doi.org/10.1371/JOURNAL.PPAT.1003016>
- Gentry, D., Li, T., Rosenberg, M., McDevitt, D., 2000. The rel gene is essential for in vitro growth of *Staphylococcus aureus*. J Bacteriol 182, 4995–4997. <https://doi.org/10.1128/JB.182.17.4995-4997.2000>
- Georgopapadakou, N.H., Dix, B.A., Mauriz, Y.R., 1986. Possible physiological functions of penicillin-binding proteins in *Staphylococcus aureus*. Antimicrob Agents Chemother 29, 333–336. <https://doi.org/10.1128/AAC.29.2.333>
- Ghuysen, J.M., 1968. Use of bacteriolytic enzymes in determination of wall structure and their role in cell metabolism. Bacteriol Rev 32, 425–464. [https://doi.org/10.1128/mnbr.32.4\\_pt\\_2.425-464.1968](https://doi.org/10.1128/mnbr.32.4_pt_2.425-464.1968)
- Gleckman, R., Blagg, N., Joubert, D.W., 1981. Trimethoprim: mechanisms of action, antimicrobial activity, bacterial resistance, pharmacokinetics, adverse reactions, and therapeutic indications. Pharmacotherapy 1, 14–19. <https://doi.org/10.1002/J.1875-9114.1981.TB03548.X>
- Goffin, C., Ghuysen, J.-M., 1998. Multimodular Penicillin-Binding Proteins: An Enigmatic Family of Orthologs and Paralogs. Microbiology and Molecular Biology Reviews 62, 1079–1093. <https://doi.org/10.1128/mnbr.62.4.1079-1093.1998>
- Goncheva, M.I., Flannagan, R.S., Sterling, B.E., Laakso, H.A., Friedrich, N.C., Kaiser, J.C., Watson, D.W., Wilson, C.H., Sheldon, J.R., McGavin, M.J., Kiser, P.K., Heinrichs, D.E., 2019. Stress-induced inactivation of the *Staphylococcus aureus* purine biosynthesis repressor leads to hypervirulence. Nat Commun 10, 1–14. <https://doi.org/10.1038/s41467-019-08724-x>
- Götze, M., Iacobucci, C., Ihling, C.H., Sinz, A., 2019. A Simple Cross-Linking/Mass Spectrometry Workflow for Studying System-wide Protein Interactions. Anal Chem 91, 10236–10244.

[https://doi.org/10.1021/ACS.ANALCHEM.9B02372/SUPPL\\_FILE/AC9B02372\\_SI\\_002.XLS](https://doi.org/10.1021/ACS.ANALCHEM.9B02372/SUPPL_FILE/AC9B02372_SI_002.XLS)

X

Graffunder, E.M., 2002. Risk factors associated with nosocomial methicillin-resistant *Staphylococcus aureus* (MRSA) infection including previous use of antimicrobials. *Journal of Antimicrobial Chemotherapy* 49, 999–1005. <https://doi.org/10.1093/jac/dkf009>

Gratani, F.L., Horvatek, P., Geiger, T., Borisova, M., Mayer, C., Grin, I., Wagner, S., Steinchen, W., Bange, G., Velic, A., Maček, B., Wolz, C., 2018. Regulation of the opposing (p)ppGpp synthetase and hydrolase activities in a bifunctional RelA/SpoT homologue from *Staphylococcus aureus*. *PLoS Genet* 14, e1007514. <https://doi.org/10.1371/JOURNAL.PGEN.1007514>

Griffiths, J.M., O'Neill, A.J., 2012. Loss of function of the gdpP protein leads to joint  $\beta$ -lactam/glycopeptide tolerance in *Staphylococcus aureus*. *Antimicrob Agents Chemother* 56, 579–581. <https://doi.org/10.1128/AAC.05148-11>

Halbedel, S., Lewis, R.J., 2019. Structural basis for interaction of DivIVA/GpsB proteins with their ligands. *Mol Microbiol* 111, 1404–1415. <https://doi.org/10.1111/MMI.14244>

Hammond, L.R., Sacco, M.D., Khan, S.J., Spanoudis, C., Hough-Neidig, A., Chen, Y., Eswara, P.J., 2022. GpsB Coordinates Cell Division and Cell Surface Decoration by Wall Teichoic Acids in *Staphylococcus aureus*. *Microbiol Spectr* 10. <https://doi.org/10.1128/SPECTRUM.01413-22>

Harbarth, S., von Dach, E., Pagani, L., Macedo-Vinas, M., Huttner, B., Olearo, F., Emonet, S., Uçkay, I., 2015. Randomized non-inferiority trial to compare trimethoprim/sulfamethoxazole plus rifampicin versus linezolid for the treatment of MRSA infection. *Journal of Antimicrobial Chemotherapy* 70, 264–272. <https://doi.org/10.1093/JAC/DKU352>

Hartman, B.J., Tomasz, A., 1986. Expression of methicillin resistance in heterogeneous strains of *Staphylococcus aureus*. *Antimicrob Agents Chemother* 29, 85–92. <https://doi.org/10.1128/AAC.29.1.85>

Hartman, B.J., Tomasz, A., 1984. Low-affinity penicillin-binding protein associated with  $\beta$ -lactam resistance in *Staphylococcus aureus*. *J Bacteriol* 158, 513–516. <https://doi.org/10.1128/JB.158.2.513-516.1984>

Heijenoort, J. v., 2001. Formation of the glycan chains in the synthesis of bacterial peptidoglycan. *Glycobiology* 11, 25R-36R. <https://doi.org/10.1093/GLYCOB/11.3.25R>

- Hesser, A.R., Matano, L.M., Vickery, C.R., Wood, B.M., Santiago, A.G., Morris, H.G., Do, T., Losick, R., Walker, S., 2020. The Length of Lipoteichoic Acid Polymers Controls *Staphylococcus aureus* Cell Size and Envelope Integrity. *J Bacteriol* 202, 10.1128/jb.00149-20. <https://doi.org/10.1128/jb.00149-20>
- Homburg, R., 2005. Clomiphene citrate—end of an era? a mini-review. *Human Reproduction* 20, 2043–2051. <https://doi.org/10.1093/HUMREP/DEI042>
- Hooper, D.C., 2000. Mechanisms of action and resistance of older and newer fluoroquinolones, in: *Clinical Infectious Diseases*. <https://doi.org/10.1086/314056>
- Horiuchi, K., Asakura, T., Bessho, Y., Saito, F., 2019. Infectious tenosynovitis of the long head of the biceps caused by methicillin-resistant *Staphylococcus aureus* in a patient with diabetes and small cell lung cancer. *BMJ Case Rep* 12. <https://doi.org/10.1136/bcr-2018-229040>
- Horsburgh, M.J., Aish, J.L., White, I.J., Shaw, L., Lithgow, J.K., Foster, S.J., 2002. sigmaB modulates virulence determinant expression and stress resistance: characterization of a functional rsbU strain derived from *Staphylococcus aureus* 8325-4. *J Bacteriol* 184, 5457–5467. <https://doi.org/10.1128/JB.184.19.5457-5467.2002>
- Huang, H.W., 2020. DAPTOMYCIN, its membrane-active mechanism vs. that of other antimicrobial peptides. *Biochimica et Biophysica Acta (BBA) - Biomembranes* 1862, 183395. <https://doi.org/10.1016/J.BBAMEM.2020.183395>
- Iqbal, H., Akins, D.R., Kenedy, M.R., 2018. Co-immunoprecipitation for Identifying Protein-Protein Interactions in *Borrelia burgdorferi*. *Methods Mol Biol* 1690, 47. [https://doi.org/10.1007/978-1-4939-7383-5\\_4](https://doi.org/10.1007/978-1-4939-7383-5_4)
- Irving, S.E., Choudhury, N.R., Corrigan, R.M., 2020. The stringent response and physiological roles of (pp)pGpp in bacteria. *Nature Reviews Microbiology* 2020 19:4 19, 256–271. <https://doi.org/10.1038/s41579-020-00470-y>
- Ito, T., Hiramatsu, K., Oliveira, D.C., De Lencastre, H., Zhang, K., Westh, H., O'Brien, F., Giffard, P.M., Coleman, D., Tenover, F.C., Boyle-Vavra, S., Skov, R.L., Enright, M.C., Kreiswirth, B., Kwan, S.K., Grundmann, H., Laurent, F., Sollid, J.E., Kearns, A.M., Goering, R., John, J.F., Daum, R., Soderquist, B., 2009. Classification of staphylococcal cassette chromosome mec (SCCmec): Guidelines for reporting novel SCCmec elements. *Antimicrob Agents Chemother* 53, 4961–4967. <https://doi.org/10.1128/AAC.00579-09>

- Ito, T., Katayama, Y., Asada, K., Mori, N., Tsutsumimoto, K., Tiensasitorn, C., Hiramatsu, K., 2001. Structural comparison of three types of staphylococcal cassette chromosome mec integrated in the chromosome in methicillin-resistant *Staphylococcus aureus*. *Antimicrob Agents Chemother* 45, 1323–1336. <https://doi.org/10.1128/AAC.45.5.1323-1336.2001/ASSET/38C1AD3A-C530-4442-A2E2-9CEE3FE1B4C9/ASSETS/GRAPHIC/AC0510810004.JPEG>
- Ito, T., Katayama, Y., Hiramatsu, K., 1999. Cloning and nucleotide sequence determination of the entire mec DNA of pre-methicillin-resistant *Staphylococcus aureus* N315. *Antimicrob Agents Chemother* 43, 1449–1458. <https://doi.org/10.1128/AAC.43.6.1449/ASSET/3520CCDA-92B2-41C4-BE57-D7A4A9FA51F4/ASSETS/GRAPHIC/AC0690028004.JPEG>
- Jensen, C., Bæk, K.T., Gallay, C., Thalsø-Madsen, I., Xu, L., Jouselin, A., Torrubia, F.R., Paulander, W., Pereira, A.R., Veening, J.W., Pinho, M.G., Frees, D., 2019. The ClpX chaperone controls autolytic splitting of *Staphylococcus aureus* daughter cells, but is bypassed by  $\beta$ -lactam antibiotics or inhibitors of WTA biosynthesis. *PLoS Pathog* 15, e1008044. <https://doi.org/10.1371/JOURNAL.PPAT.1008044>
- Jenul, C., Horswill, A.R., 2018. Regulation of *Staphylococcus aureus* Virulence. *Microbiol Spectr* 6. <https://doi.org/10.1128/microbiolspec.gpp3-0031-2018>
- Jouselin, A., Manzano, C., Biette, A., Reed, P., Pinho, M.G., Rosato, A.E., Kelley, W.L., Renzoni, A., 2016. The *Staphylococcus aureus* chaperone PrsA is a new auxiliary factor of oxacillin resistance affecting penicillin-binding protein 2A. *Antimicrob Agents Chemother* 60, 1656–1666. [https://doi.org/10.1128/AAC.02333-15/SUPPL\\_FILE/ZAC003164926S01.PDF](https://doi.org/10.1128/AAC.02333-15/SUPPL_FILE/ZAC003164926S01.PDF)
- Kaatz, G.W., Seo, S.M., Ruble, C.A., 1993. Efflux-mediated fluoroquinolone resistance in *Staphylococcus aureus*. *Antimicrob Agents Chemother* 37, 1086–1094. <https://doi.org/10.1128/AAC.37.5.1086>
- Kadonaga, J.T., Tjian, R., 1986. Affinity purification of sequence-specific DNA binding proteins. *Proceedings of the National Academy of Sciences* 83, 5889–5893. <https://doi.org/10.1073/PNAS.83.16.5889>
- Karimova, G., Dautin, N., Ladant, D., 2005. Interaction network among *Escherichia coli* membrane proteins involved in cell division as revealed by bacterial two-hybrid analysis. *J Bacteriol* 187, 2233–2243. <https://doi.org/10.1128/JB.187.7.2233-2243.2005/ASSET/A140C241-E9BC-405D-B1E6-FEA83A4907AF/ASSETS/GRAPHIC/ZJB0070545880005.JPEG>

- Karimova, G., Gauliard, E., Davi, M., Ouellette, S.P., Ladant, D., 2017. Protein–protein interaction: Bacterial two-hybrid, in: *Methods in Molecular Biology*. Humana Press Inc., pp. 159–176. [https://doi.org/10.1007/978-1-4939-7033-9\\_13](https://doi.org/10.1007/978-1-4939-7033-9_13)
- Karimova, G., Pidoux, J., Ullmann, A., Ladant, D., 1998. A bacterial two-hybrid system based on a reconstituted signal transduction pathway. *Proc Natl Acad Sci U S A* 95, 5752–5756. <https://doi.org/10.1073/pnas.95.10.5752>
- Karimova, G., Ullmann, A., Ladant, D., 2000. A bacterial two-hybrid system that exploits a cAMP signaling cascade in *Escherichia coli*. *Methods Enzymol* 328, 59–73. [https://doi.org/10.1016/s0076-6879\(00\)28390-0](https://doi.org/10.1016/s0076-6879(00)28390-0)
- Karinou, E., Schuster, C.F., Pazos, M., Vollmer, W., Gründling, A., 2019. Inactivation of the monofunctional peptidoglycan glycosyltransferase sgtb allows *Staphylococcus aureus* to survive in the absence of lipoteichoic acid. *J Bacteriol* 201. <https://doi.org/10.1128/JB.00574-18/ASSET/56283D2A-900E-4B1F-8D16-E785D3E47BA8/ASSETS/GRAPHIC/JB.00574-18-F0007.JPEG>
- Katayama, Y., Ito, T., Hiramatsu, K., 2001. Genetic organization of the chromosome region surrounding *mecA* in clinical staphylococcal strains: Role of IS431-mediated *mecI* deletion in expression of resistance in *mecA*-carrying, low-level methicillin-resistant *Staphylococcus haemolyticus*. *Antimicrob Agents Chemother* 45, 1955–1963. <https://doi.org/10.1128/AAC.45.7.1955-1963.2001/ASSET/9BE68097-E732-4412-A519-62F0BB0EC6E6/ASSETS/GRAPHIC/AC0710755005.JPEG>
- Katayama, Y., Ito, T., Hiramatsu, K., 2000. A new class of genetic element, staphylococcus cassette chromosome *mec*, encodes methicillin resistance in *Staphylococcus aureus*. *Antimicrob Agents Chemother* 44, 1549–1555. <https://doi.org/10.1128/AAC.44.6.1549-1555.2000/ASSET/F398BECA-6797-4400-AF61-ED3FBC6BA3D8/ASSETS/GRAPHIC/AC0601017004.JPEG>
- Keinhörster, D., George, S.E., Weidenmaier, C., Wolz, C., 2019. Function and regulation of *Staphylococcus aureus* wall teichoic acids and capsular polysaccharides. *Int J Med Microbiol* 309. <https://doi.org/10.1016/j.ijmm.2019.151333>
- Kent, V., 2013. Cell wall architecture and the role of wall teichoic acid in *Staphylococcus aureus* 242.
- Kim, C., Mwangi, M., Chung, M., Milheirco, C., De Lencastre, H., Tomasz, A., 2013. The Mechanism of Heterogeneous Beta-Lactam Resistance in MRSA: Key Role of the Stringent Stress Response. *PLoS One* 8, e82814. <https://doi.org/10.1371/JOURNAL.PONE.0082814>



- Kim, C., Mwangi, M., Chung, M., Milheirco, C., De Lencastre, H., Tomasz, A., 2013. The mechanism of heterogeneous beta-lactam resistance in MRSA: Key role of the stringent stress response. *PLoS One* 8. <https://doi.org/10.1371/JOURNAL.PONE.0082814>
- Kim, C.K., Milheirço, C., De Lencastre, H., Tomasz, A., 2017. Antibiotic resistance as a stress response: Recovery of high-level oxacillin resistance in methicillin-resistant *Staphylococcus aureus* “auxiliary” (fem) mutants by induction of the stringent stress response. *Antimicrob Agents Chemother* 61. [https://doi.org/10.1128/AAC.00313-17/SUPPL\\_FILE/ZAC008176440S1.PDF](https://doi.org/10.1128/AAC.00313-17/SUPPL_FILE/ZAC008176440S1.PDF)
- Kiriukhin, M.Y., Debabov, D. V., Shinabarger, D.L., Neuhaus, F.C., 2001. Biosynthesis of the glycolipid anchor in lipoteichoic acid of *Staphylococcus aureus* RN4220: Role of YpfP, the diglucoxyldiacylglycerol synthase. *J Bacteriol* 183, 3506–3514. <https://doi.org/10.1128/JB.183.11.3506-3514.2001/ASSET/6BB63D62-3389-47C4-BDBE-451BD9FAFA41/ASSETS/GRAPHIC/JB1111617008.JPEG>
- Kisgen, J.J., Mansour, H., Unger, N.R., Childs, L.M., 2014. Tedizolid: A new oxazolidinone antimicrobial. *American Journal of Health-System Pharmacy* 71, 621–633. <https://doi.org/10.2146/AJHP130482>
- Komatsuzawa, H., Sugai, M., Nakashima, S., Yamada, S., Matsumoto, A., Oshida, T., Suginaka, H., 1997. Subcellular Localization of the Major Autolysin, ATL and Its Processed Proteins in *Staphylococcus aureus*. *Microbiol Immunol* 41, 469–479. <https://doi.org/10.1111/J.1348-0421.1997.TB01880.X>
- Koo, S.P., Bayer, A.S., Sahl, H.G., Proctor, R.A., Yeaman, M.R., 1996. Staphylocidal action of thrombin-induced platelet microbicidal protein is not solely dependent on transmembrane potential. *Infect Immun* 64, 1070–1074. <https://doi.org/10.1128/IAI.64.3.1070-1074.1996>
- Kouidmi, I., Levesque, R.C., Paradis-Bleau, C., 2014. The biology of Mur ligases as an antibacterial target. *Mol Microbiol* 94, 242–253. <https://doi.org/10.1111/MMI.12758>
- Kreiswirth, B.N., Löfdahl, S., Betley, M.J., O’reilly, M., Schlievert, P.M., Bergdoll, M.S., Novick, R.P., 1983. The toxic shock syndrome exotoxin structural gene is not detectably transmitted by a prophage. *Nature* 305, 709–712. <https://doi.org/10.1038/305709A0>
- Kuroda, M., Kuroda, H., Oshima, T., Takeuchi, F., Mori, H., Hiramatsu, K., 2003. Two-component system VraSR positively modulates the regulation of cell-wall biosynthesis pathway in *Staphylococcus aureus*. *Mol Microbiol* 49, 807–821. <https://doi.org/10.1046/J.1365-2958.2003.03599.X>

- Kuwahara-Arai, K., Kondo, N., Hori, S., Tateda-Suzuki, E., Hiramatsu, K., 1996. Suppression of methicillin resistance in a *mecA*-containing pre-methicillin-resistant *Staphylococcus aureus* strain is caused by the *mecI*-mediated repression of PBP 2' production. *Antimicrob Agents Chemother* 40, 2680–2685. <https://doi.org/10.1128/AAC.40.12.2680>
- Lade, H., Kim, J.S., 2021. Bacterial Targets of Antibiotics in Methicillin-Resistant *Staphylococcus aureus*. *Antibiotics* 2021, Vol. 10, Page 398 10, 398. <https://doi.org/10.3390/ANTIBIOTICS10040398>
- Lakhundi, S., Zhang, K., 2018. Methicillin-Resistant *Staphylococcus aureus*: Molecular Characterization, Evolution, and Epidemiology. *Clin Microbiol Rev* 31. <https://doi.org/10.1128/CMR.00020-18>
- Lakhundi, S., Zhang, K., 2018. Methicillin-Resistant *Staphylococcus aureus*: Molecular Characterization, Evolution, and Epidemiology. *Clin Microbiol Rev*. <https://doi.org/10.1128/CMR.00020-18>
- Larsen, J., Raisen, C.L., Ba, X., Sadgrove, N.J., Padilla-González, G.F., Simmonds, M.S.J., Loncaric, I., Kerschner, H., Apfalter, P., Hartl, R., Deplano, A., Vandendriessche, S., Černá Bolfíková, B., Hulva, P., Arendrup, M.C., Hare, R.K., Barnadas, C., Stegger, M., Sieber, R.N., Skov, R.L., Petersen, A., Angen, Ø., Rasmussen, S.L., Espinosa-Gongora, C., Aarestrup, F.M., Lindholm, L.J., Nykäsenoja, S.M., Laurent, F., Becker, K., Walther, B., Kehrenberg, C., Cuny, C., Layer, F., Werner, G., Witte, W., Stamm, I., Moroni, P., Jørgensen, H.J., de Lencastre, H., Cercenado, E., García-Garrote, F., Börjesson, S., Hæggman, S., Perreten, V., Teale, C.J., Waller, A.S., Pichon, B., Curran, M.D., Ellington, M.J., Welch, J.J., Peacock, S.J., Seilly, D.J., Morgan, F.J.E., Parkhill, J., Hadjirin, N.F., Lindsay, J.A., Holden, M.T.G., Edwards, G.F., Foster, G., Paterson, G.K., Didelot, X., Holmes, M.A., Harrison, E.M., Larsen, A.R., 2022. Emergence of methicillin resistance predates the clinical use of antibiotics. *Nature* 2022 602:7895 602, 135–141. <https://doi.org/10.1038/s41586-021-04265-w>
- Le, K.Y., Otto, M., 2015. Quorum-sensing regulation in staphylococci-an overview. *Front Microbiol*. <https://doi.org/10.3389/fmicb.2015.01174>
- Le Loir, Y., Baron, F., Gautier, M., 2003. *Staphylococcus aureus* and food poisoning. *Genet Mol Res* 2, 63–76.
- Ledger, E.V.K., Sabnis, A., Edwards, A.M., 2022. Polymyxin and lipopeptide antibiotics: membrane-targeting drugs of last resort. *Microbiology (N Y)* 168, 001136.

- Lee, Y.H., Nam, K.H., Helmann, J.D., 2013. A mutation of the RNA polymerase  $\beta'$  subunit (*rpoC*) confers cephalosporin resistance in *Bacillus subtilis*. *Antimicrob Agents Chemother* 57, 56–65. <https://doi.org/10.1128/AAC.01449-12>
- Leitner, A., Faini, M., Stengel, F., Aebersold, R., 2016. Crosslinking and Mass Spectrometry: An Integrated Technology to Understand the Structure and Function of Molecular Machines. *Trends Biochem Sci* 41, 20–32. <https://doi.org/10.1016/J.TIBS.2015.10.008>
- Łęski, T.A., Tomasz, A., 2005. Role of penicillin-binding protein 2 (PBP2) in the antibiotic susceptibility and cell wall cross-linking of *Staphylococcus aureus*: Evidence for the cooperative functioning of PBP2, PBP4, and PBP2A. *J Bacteriol* 187, 1815–1824. <https://doi.org/10.1128/JB.187.5.1815-1824.2005>
- Levine, D.P., 2006. Vancomycin: A History. *Clinical Infectious Diseases* 42, S5–S12. <https://doi.org/10.1086/491709>
- Li, Z., Deguchi, T., Yasuda, M., Kawamura, T., Kanematsu, E., Nishino, Y., Ishihara, S., Kawada, Y., 1998. Alteration in the GyrA subunit of DNA gyrase and the ParC subunit of DNA topoisomerase IV in quinolone-resistant clinical isolates of *Staphylococcus epidermidis*. *Antimicrob Agents Chemother* 42, 3293–3295. <https://doi.org/10.1128/AAC.42.12.3293/ASSET/61EBA0DD-594E-4E1C-BBB7-9DB448863042/ASSETS/GRAPHIC/AC1280506001.JPEG>
- Licitra, E.J., Liu, J.O., 1996. A three-hybrid system for detecting small ligand-protein receptor interactions. *Proc Natl Acad Sci U S A* 93, 12817–12821. <https://doi.org/10.1073/PNAS.93.23.12817>
- Lim, D., Strynadka, N.C.J., 2002. Structural basis for the  $\beta$ -lactam resistance of PBP2a from methicillin-resistant *Staphylococcus aureus*. *Nat Struct Biol* 9, 870–876. <https://doi.org/10.1038/nsb858>
- Lim, D., Strynadka, N.C.J., 2002. Structural basis for the  $\beta$ -lactam resistance of PBP2a from methicillin-resistant *Staphylococcus aureus*. *Nat Struct Biol* 9, 870–876. <https://doi.org/10.1038/nsb858>
- Lim, D., Strynadka, N.C.J., 2002. Structural basis for the  $\beta$  lactam resistance of PBP2a from methicillin-resistant *Staphylococcus aureus*. *Nature Structural Biology* 2002 9:11 9, 870–876. <https://doi.org/10.1038/nsb858>
- Liu, J., Chen, D., Peters, B.M., Li, L., Li, B., Xu, Z., Shirliff, M.E., 2016. Staphylococcal chromosomal cassettes *mec* (SCC*mec*): A mobile genetic element in methicillin-resistant

*Staphylococcus aureus*. Microb Pathog 101, 56–67.  
<https://doi.org/10.1016/J.MICPATH.2016.10.028>

Liu, X., Pai, P.J., Zhang, W., Hu, Y., Dong, X., Qian, P.Y., Chen, D., Lam, H., 2016. Proteomic response of methicillin-resistant *S. aureus* to a synergistic antibacterial drug combination: a novel erythromycin derivative and oxacillin. *Scientific Reports* 2016 6:1 6, 1–12.  
<https://doi.org/10.1038/srep19841>

Livermore, D.M., 1995. beta-Lactamases in laboratory and clinical resistance. *Clin Microbiol Rev* 8, 557–584. <https://doi.org/10.1128/cmr.8.4.557>

Llarrull, L.I., Fisher, J.F., Mobashery, S., 2009. Molecular basis and phenotype of methicillin resistance in *Staphylococcus aureus* and insights into new  $\beta$ -lactams that meet the challenge. *Antimicrob Agents Chemother*. <https://doi.org/10.1128/AAC.00084-09>

Loskill, P., Pereira, P.M., Jung, P., Bischoff, M., Herrmann, M., Pinho, M.G., Jacobs, K., 2014. Reduction of the peptidoglycan crosslinking causes a decrease in stiffness of the *Staphylococcus aureus* cell envelope. *Biophys J* 107, 1082–1089.  
<https://doi.org/10.1016/j.bpj.2014.07.029>

Lovering, A.L., De Castro, L.H., Lim, D., Strynadka, N.C.J., 2007. Structural insight into the transglycosylation step of bacterial cell-wall biosynthesis. *Science* (1979) 315, 1402–1405.  
<https://doi.org/10.1126/science.1136611>

Lovering, A.L., de Castro, L.H., Lim, D., Strynadka, N.C.J., 2007. Structural insight into the transglycosylation step of bacterial cell-wall biosynthesis. *Science* (1979) 315, 1402–1405.  
<https://doi.org/10.1126/science.1136611>

Lowy, F.D., 1998. Medical progress: *Staphylococcus aureus* infections. *New England Journal of Medicine*. <https://doi.org/10.1056/NEJM199808203390806>

Lund, V.A., Wacnik, K., Turner, R.D., Cotterell, B.E., Walther, C.G., Fenn, S.J., Grein, F., Wollman, A.J.M., Leake, M.C., Olivier, N., Cadby, A., Mesnage, S., Jones, S., Foster, S.J., 2018. Molecular coordination of *Staphylococcus aureus* cell division. *Elife* 7.  
<https://doi.org/10.7554/ELIFE.32057>

Lund, V.A., Wacnik, K., Turner, R.D., Cotterell, B.E., Walther, C.G., Fenn, S.J., Grein, F., Wollman, A.J.M., Leake, M.C., Olivier, N., Cadby, A., Mesnage, S., Jones, S., Foster, S.J., 2018. Molecular coordination of *Staphylococcus aureus* cell division. *Elife* 7.  
<https://doi.org/10.7554/ELIFE.32057>

- Macheboeuf, P., Contreras-Martel, C., Job, V., Dideberg, O., Dessen, A., 2006. Penicillin binding proteins: Key players in bacterial cell cycle and drug resistance processes. *FEMS Microbiol Rev.* <https://doi.org/10.1111/j.1574-6976.2006.00024.x>
- Macheboeuf, P., Contreras-Martel, C., Job, V., Dideberg, O., Dessen, A., 2006. Penicillin binding proteins: Key players in bacterial cell cycle and drug resistance processes. *FEMS Microbiol Rev.* <https://doi.org/10.1111/j.1574-6976.2006.00024.x>
- Magnet, S., Blanchard, J.S., 2005. Molecular insights into aminoglycoside action and resistance. *Chem Rev* 105, 477–497. <https://doi.org/10.1021/CR0301088/ASSET/IMAGES/LARGE/CR0301088F00018.JPEG>
- Mahasenan, K. V., Molina, R., Bouley, R., Batuecas, M.T., Fisher, J.F., Hermoso, J.A., Chang, M., Mobashery, S., 2017. Conformational dynamics in penicillin-binding protein 2a of methicillin-resistant *Staphylococcus aureus*, allosteric communication network and enablement of catalysis. *J Am Chem Soc* 139, 2102–2110. <https://doi.org/10.1021/jacs.6b12565>
- Maki, H., Yamaguchi, T., Murakami, K., 1994. Cloning and characterization of a gene affecting the methicillin resistance level and the autolysis rate in *Staphylococcus aureus*. *J Bacteriol* 176, 4993–5000. <https://doi.org/10.1128/JB.176.16.4993-5000.1994>
- Matias, V.R.F., Beveridge, T.J., 2007. Cryo-electron microscopy of cell division in *Staphylococcus aureus* reveals a mid-zone between nascent cross walls. *Mol Microbiol* 64, 195–206. <https://doi.org/10.1111/J.1365-2958.2007.05634.X>
- Maya-Martinez, R., Alexander, J.A.N., Otten, C.F., Ayala, I., Vollmer, D., Gray, J., Bougault, C.M., Burt, A., Laguri, C., Fonvielle, M., Arthur, M., Strynadka, N.C.J., Vollmer, W., Simorre, J.P., 2019. Recognition of peptidoglycan fragments by the transpeptidase PBP4 from *Staphylococcus aureus*. *Front Microbiol* 10, 426432. <https://doi.org/10.3389/FMICB.2018.03223/BIBTEX>
- McCallum, N., Berger-Bächi, B., Senn, M.M., 2010. Regulation of antibiotic resistance in *Staphylococcus aureus*. *International Journal of Medical Microbiology.* <https://doi.org/10.1016/j.ijmm.2009.08.015>
- McCarthy, H., Waters, E.M., Bose, J.L., Foster, S., Bayles, K.W., O'Neill, E., Fey, P.D., O'Gara, J.P., 2016. The major autolysin is redundant for *Staphylococcus aureus* USA300 LAC JE2 virulence in a murine device-related infection model. *FEMS Microbiol Lett* 363. <https://doi.org/10.1093/FEMSLE/FNW087>

- McCausland, J.W., Yang, X., Lyu, Z., Söderström, B.W., Xiao, J., Liu, J., 2019. Treadmilling FtsZ polymers drive the directional movement of sPG-synthesis enzymes via a Brownian ratchet mechanism. *bioRxiv* 857813. <https://doi.org/10.1101/857813>
- Memmi, G., Filipe, S.R., Pinho, M.G., Fu, Z., Cheung, A., 2008. *Staphylococcus aureus* PBP4 is essential for  $\beta$ -lactam resistance in community-acquired methicillin-resistant strains. *Antimicrob Agents Chemother* 52, 3955–3966. <https://doi.org/10.1128/AAC.00049-08>
- Memmi, G., Filipe, S.R., Pinho, M.G., Fu, Z., Cheung, A., 2008. *Staphylococcus aureus* PBP4 is essential for  $\beta$ -lactam resistance in community-acquired methicillin-resistant strains. *Antimicrob Agents Chemother* 52, 3955–3966. <https://doi.org/10.1128/AAC.00049-08>
- Mikkelsen, K., Sirisarn, W., Alharbi, O., Alharbi, M., Liu, H., Nøhr-Meldgaard, K., Mayer, K., Vestergaard, M., Gallagher, L.A., Derrick, J.P., McBain, A.J., Biboy, J., Vollmer, W., O’Gara, J.P., Grunert, T., Ingmer, H., Xia, G., 2021. The Novel Membrane-Associated Auxiliary Factors AuxA and AuxB Modulate  $\beta$ -lactam Resistance in MRSA by stabilizing Lipoteichoic Acids. *Int J Antimicrob Agents* 57. <https://doi.org/10.1016/J.IJANTIMICAG.2021.106283>
- Miragaia, M., 2018. Factors contributing to the evolution of Meca-mediated  $\beta$ -lactam resistance in staphylococci: Update and new insights from whole genome sequencing (WGS). *Front Microbiol* 9, 396897. <https://doi.org/10.3389/FMICB.2018.02723/BIBTEX>
- Monteiro, J.M., Fernandes, P.B., Vaz, F., Pereira, A.R., Tavares, A.C., Ferreira, M.T., Pereira, P.M., Veiga, H., Kuru, E., Vannieuwenhze, M.S., Brun, Y. V., Filipe, S.R., Pinho, M.G., 2015. Cell shape dynamics during the staphylococcal cell cycle. *Nature Communications* 2015 6:1 6, 1–12. <https://doi.org/10.1038/ncomms9055>
- Monteiro, J.M., Pereira, A.R., Reichmann, N.T., Saraiva, B.M., Fernandes, P.B., Veiga, H., Tavares, A.C., Santos, M., Ferreira, M.T., Macário, V., VanNieuwenhze, M.S., Filipe, S.R., Pinho, M.G., 2018. Peptidoglycan synthesis drives an FtsZ-treadmilling-independent step of cytokinesis. *Nature* 554, 528–532. <https://doi.org/10.1038/nature25506>
- Morton, T.M., Johnston, J.L., Patterson, J., Archer, G.L., 1995. Characterization of a conjugative staphylococcal mupirocin resistance plasmid. *Antimicrob Agents Chemother* 39, 1272–1280. <https://doi.org/10.1128/AAC.39.6.1272>
- Müller, A., Wenzel, M., Strahl, H., Grein, F., Saaki, T.N.V., Kohl, B., Siersma, T., Bandow, J.E., Sahl, H.G., Schneider, T., Hamoen, L.W., 2016. Daptomycin inhibits cell envelope synthesis by interfering with fluid membrane microdomains. *Proc Natl Acad Sci U S A* 113, E7077–E7086. [https://doi.org/10.1073/PNAS.1611173113/SUPPL\\_FILE/PNAS.1611173113.SAPP.PDF](https://doi.org/10.1073/PNAS.1611173113/SUPPL_FILE/PNAS.1611173113.SAPP.PDF)

Murray, C.J., Ikuta, K.S., Sharara, F., Swetschinski, L., Robles Aguilar, G., Gray, A., Han, C., Bisignano, C., Rao, P., Wool, E., Johnson, S.C., Browne, A.J., Chipeta, M.G., Fell, F., Hackett, S., Haines-Woodhouse, G., Kashef Hamadani, B.H., Kumaran, E.A.P., McManigal, B., Agarwal, R., Akech, S., Albertson, S., Amuasi, J., Andrews, J., Aravkin, A., Ashley, E., Bailey, F., Baker, S., Basnyat, B., Bekker, A., Bender, R., Bethou, A., Bielicki, J., Boonkasidecha, S., Bukosia, J., Carvalheiro, C., Castañeda-Orjuela, C., Chansamouth, V., Chaurasia, S., Chiurchiù, S., Chowdhury, F., Cook, A.J., Cooper, B., Cressey, T.R., Criollo-Mora, E., Cunningham, M., Darboe, S., Day, N.P.J., De Luca, M., Dokova, K., Dramowski, A., Dunachie, S.J., Eckmanns, T., Eibach, D., Emami, A., Feasey, N., Fisher-Pearson, N., Forrest, K., Garrett, D., Gastmeier, P., Giref, A.Z., Greer, R.C., Gupta, V., Haller, S., Haselbeck, A., Hay, S.I., Holm, M., Hopkins, S., Iregbu, K.C., Jacobs, J., Jarovsky, D., Javanmardi, F., Khorana, M., Kisson, N., Kobeissi, E., Kostyanov, T., Krapp, F., Krumkamp, R., Kumar, A., Kyu, H.H., Lim, C., Limmathurotsakul, D., Loftus, M.J., Lunn, M., Ma, J., Mturi, N., Munera-Huertas, T., Musicha, P., Mussi-Pinhata, M.M., Nakamura, T., Nanavati, R., Nangia, S., Newton, P., Ngoun, C., Novotney, A., Nwakanma, D., Obiero, C.W., Olivas-Martinez, A., Olliaro, P., Ooko, E., Ortiz-Brizuela, E., Peleg, A.Y., Perrone, C., Plakkal, N., Ponce-de-Leon, A., Raad, M., Ramdin, T., Riddell, A., Roberts, T., Robotham, J.V., Roca, A., Rudd, K.E., Russell, N., Schnall, J., Scott, J.A.G., Shivamallappa, M., Sifuentes-Osornio, J., Steenkeste, N., Stewardson, A.J., Stoeva, T., Tasak, N., Thaiprakong, A., Thwaites, G., Turner, C., Turner, P., van Doorn, H.R., Velaphi, S., Vongpradith, A., Vu, H., Walsh, T., Waner, S., Wangrangsimakul, T., Wozniak, T., Zheng, P., Sartorius, B., Lopez, A.D., Stergachis, A., Moore, C., Dolecek, C., Naghavi, M., 2022. Global burden of bacterial antimicrobial resistance in 2019: a systematic analysis. *The Lancet* 399, 629–655. [https://doi.org/10.1016/S0140-6736\(21\)02724-0](https://doi.org/10.1016/S0140-6736(21)02724-0)

Mwangi, M.M., Kim, C., Chung, M., Tsai, J., Vijayadamodar, G., Benitez, M., Jarvie, T.P., Du, L., Tomasz, A., 2013. Whole-genome sequencing reveals a link between  $\beta$ -lactam resistance and synthetases of the alarmone (p)ppGpp in *Staphylococcus aureus*. *Microbial Drug Resistance* 19, 153–159. <https://doi.org/10.1089/MDR.2013.0053>

Nakao, A., Imai, S. ichiro, Takano, T., 2000. Transposon-mediated insertional mutagenesis of the D-alanyl-lipoteichoic acid (dlt) operon raises methicillin resistance in *Staphylococcus aureus*. *Res Microbiol* 151, 823–829. [https://doi.org/10.1016/S0923-2508\(00\)01148-7](https://doi.org/10.1016/S0923-2508(00)01148-7)

Nemeth, J., Oesch, G., Kuster, S.P., 2015. Bacteriostatic versus bactericidal antibiotics for patients with serious bacterial infections: systematic review and meta-analysis. *Journal of Antimicrobial Chemotherapy* 70, 382–395. <https://doi.org/10.1093/JAC/DKU379>

- Neu, H.C., 1985. Contribution of beta-lactamases to bacterial resistance and mechanisms to inhibit beta-lactamases. *Am J Med* 79, 2–12. [https://doi.org/10.1016/0002-9343\(85\)90123-8](https://doi.org/10.1016/0002-9343(85)90123-8)
- Neu, H.C., Fu, K.P., 1978. Clavulanic Acid, a Novel Inhibitor of  $\beta$ -Lactamases. *Antimicrob Agents Chemother* 14, 650–655. <https://doi.org/10.1128/AAC.14.5.650>
- Neuhaus, F.C., Baddiley, J., 2003. A continuum of anionic charge: structures and functions of D-alanyl-teichoic acids in gram-positive bacteria. *Microbiol Mol Biol Rev* 67, 686–723. <https://doi.org/10.1128/MMBR.67.4.686-723.2003>
- Olle, H., 1986. Putrescine, Spermidine, and Spermine. <https://doi.org/10.1152/physiologyonline.1986.1.1.12> 1, 12–15. <https://doi.org/10.1152/PHYSIOLOGYONLINE.1986.1.1.12>
- O'Neill, J., 2018. Tackling drug-resistant infections globally: Final report and recommendations. 2016. HM Government and Wellcome Trust: UK.
- Osaka, N., Kanasaki, Y., Watanabe, M., Watanabe, S., Chibazakura, T., Takada, H., Yoshikawa, H., Asai, K., 2020. Novel (p)ppGpp 0 suppressor mutations reveal an unexpected link between methionine catabolism and GTP synthesis in *Bacillus subtilis*. *Mol Microbiol* 113, 1155–1169. <https://doi.org/10.1111/MMI.14484>
- Otero, L.H., Rojas-Altuve, A., Llarrull, L.I., Carrasco-López, C., Kumarasiri, M., Lastochkin, E., Fishovitz, J., Dawley, M., Heseck, D., Lee, M., Johnson, J.W., Fisher, J.F., Chang, M., Mobashery, S., Hermoso, J.A., 2013. How allosteric control of *Staphylococcus aureus* penicillin binding protein 2a enables methicillin resistance and physiological function. *Proc Natl Acad Sci U S A* 110, 16808–16813. <https://doi.org/10.1073/pnas.1300118110>
- Ovung, A., Bhattacharyya, J., 2021. Sulfonamide drugs: structure, antibacterial property, toxicity, and biophysical interactions. *Biophys Rev* 13, 259. <https://doi.org/10.1007/S12551-021-00795-9>
- Palacios, L., Rosado, H., Micol, V., Rosato, A.E., Bernal, P., Arroyo, R., Grounds, H., Anderson, J.C., Stabler, R.A., Taylor, P.W., 2014. Staphylococcal Phenotypes Induced by Naturally Occurring and Synthetic Membrane-Interactive Polyphenolic  $\beta$ -Lactam Resistance Modifiers. *PLoS One* 9, e93830. <https://doi.org/10.1371/JOURNAL.PONE.0093830>
- Panchal, V. V., Griffiths, C., Mosaei, H., Bilyk, B., Sutton, J.A.F., Carnell, O.T., Hornby, D.P., Green, J., Hobbs, J.K., Kelley, W.L., Zenkin, N., Foster, S.J., 2020. Evolving MRSA: High-level  $\beta$ -lactam resistance in *Staphylococcus aureus* is associated with RNA polymerase alterations and



fine tuning of gene expression. PLoS Pathog 16.  
<https://doi.org/10.1371/JOURNAL.PPAT.1008672>

Panchal, V.V., 2018. The molecular basis of high-level methicillin resistance in *Staphylococcus aureus*. The University of Sheffield.

Pareek, A., Rani, P., Kishore, D., 2013. A SHORT REVIEW ON: SULPHONAMIDES. Int J Pharma Bio Sci.

Parenti, M.A., Hatfield, S.M., Leyden, J.J., 1987. Mupirocin: A topical antibiotic with a unique structure and mechanism of action. Clin Pharm.

Parvez, M.A.K., Shibata, H., Nakano, T., Niimi, S., Fujii, N., Arakaki, N., Higuti, T., 2008. No relationship exists between PBP 2a amounts expressed in different MRSA strains obtained clinically and their  $\beta$ -lactam MIC values. The Journal of Medical Investigation 55, 246–253. <https://doi.org/10.2152/JMI.55.246>

Pasquina-Lemonche, L., Burns, J., Turner, R.D., Kumar, S., Tank, R., Mullin, N., Wilson, J.S., Chakrabarti, B., Bullough, P.A., Foster, S.J., Hobbs, J.K., 2020. The architecture of the Gram-positive bacterial cell wall. Nature 1–4. <https://doi.org/10.1038/s41586-020-2236-6>

Paulander, W., Varming, A.N., Bojer, M.S., Friberg, C., Bæk, K., Ingmer, H., 2018. The agr quorum sensing system in *Staphylococcus aureus* cells mediates death of sub-population. BMC Res Notes 11, 503. <https://doi.org/10.1186/S13104-018-3600-6>

Pawar, S., Yao, X., Lu, C.D., 2019. Spermine and oxacillin stress response on the cell wall synthesis and the global gene expression analysis in Methicillin-resistance *Staphylococcus aureus*. Genes Genomics 41, 43–59. <https://doi.org/10.1007/S13258-018-0735-8>

Pereira, A.R.R., 2018. Cell Division and morphogenesis in *Staphylococcus aureus*.

Pereira, Sandro F. F., Henriques, A.O., Pinho, M.G., de Lencastre, H., Tomasz, A., 2009. Evidence for a dual role of PBP1 in the cell division and cell separation of *Staphylococcus aureus*. Mol Microbiol 72, 895–904. <https://doi.org/10.1111/j.1365-2958.2009.06687.x>

Pereira, Sandro F.F., Henriques, A.O., Pinho, M.G., De Lencastre, H., Tomasz, A., 2009. Evidence for a dual role of PBP1 in the cell division and cell separation of *Staphylococcus aureus*. Mol Microbiol 72, 895–904. <https://doi.org/10.1111/J.1365-2958.2009.06687.X>

Pereira, Sandro F. F., Henriques, A.O., Pinho, M.G., de Lencastre, H., Tomasz, A., 2009. Evidence for a dual role of PBP1 in the cell division and cell separation of *Staphylococcus aureus*. Mol Microbiol 72, 895–904. <https://doi.org/10.1111/j.1365-2958.2009.06687.x>

- Petrotchenko, E. V., Borchers, C.H., 2010. Crosslinking combined with mass spectrometry for structural proteomics. *Mass Spectrom Rev* 29, 862–876. <https://doi.org/10.1002/MAS.20293>
- Pinho, M., De Lencastre, H., Tomasz, A., 2001. An acquired and a native penicillin-binding protein cooperate in building the cell wall of drug-resistant staphylococci. *Proc Natl Acad Sci U S A* 98, 10886–10891. <https://doi.org/10.1073/PNAS.191260798>
- Pinho, Mariana G., De Lencastre, H., Tomasz, A., 2001. An acquired and a native penicillin-binding protein cooperate in building the cell wall of drug-resistant staphylococci. *Proc Natl Acad Sci U S A* 98, 10886–10891. <https://doi.org/10.1073/pnas.191260798>
- Pinho, Mariana G., De Lencastre, H., Tomasz, A., 2001. An acquired and a native penicillin-binding protein cooperate in building the cell wall of drug-resistant staphylococci. *Proc Natl Acad Sci U S A* 98, 10886–10891. <https://doi.org/10.1073/pnas.191260798>
- Pinho, M.G., Errington, J., 2005. Recruitment of penicillin-binding protein PBP2 to the division site of *Staphylococcus aureus* is dependent on its transpeptidation substrates. *Mol Microbiol* 55, 799–807. <https://doi.org/10.1111/J.1365-2958.2004.04420.X>
- Pinho, M.G., Errington, J., 2004. Recruitment of penicillin-binding protein PBP2 to the division site of *Staphylococcus aureus* is dependent on its transpeptidation substrates. *Mol Microbiol* 55, 799–807. <https://doi.org/10.1111/j.1365-2958.2004.04420.x>
- Pinho, M.G., Filipe, S.R., De Lencastre, H., Tomasz, A., 2001. Complementation of the essential peptidoglycan transpeptidase function of penicillin-binding protein 2 (PBP2) by the drug resistance protein PBP2A in *Staphylococcus aureus*. *J Bacteriol* 183, 6525–6531. <https://doi.org/10.1128/JB.183.22.6525-6531.2001>
- Pinho, M.G., Filipe, S.R., De Lencastre, H., Tomasz, A., 2001. Complementation of the essential peptidoglycan transpeptidase function of penicillin-binding protein 2 (PBP2) by the drug resistance protein PBP2A in *Staphylococcus aureus*. *J Bacteriol* 183, 6525–6531. <https://doi.org/10.1128/JB.183.22.6525-6531.2001>
- Pinho, M.G., Filipe, S.R., de Lencastre, H., Tomasz, A., 2001. Complementation of the essential peptidoglycan transpeptidase function of penicillin-binding protein 2 (PBP2) by the drug resistance protein PBP2A in *Staphylococcus aureus*. *J Bacteriol* 183, 6525–6531. <https://doi.org/10.1128/JB.183.22.6525-6531.2001>
- Pinho, M.G., Filipe, S.R., De Lencastre, H., Tomasz, A., 2001. Complementation of the essential peptidoglycan transpeptidase function of penicillin-binding protein 2 (PBP2) by the drug

- resistance protein PBP2A in *Staphylococcus aureus*. *J Bacteriol* 183, 6525–6531. <https://doi.org/10.1128/JB.183.22.6525-6531.2001>
- Pinho, M.G., Kjos, M., Veening, J.W., 2013. How to get (a)round: mechanisms controlling growth and division of coccoid bacteria. *Nature Reviews Microbiology* 2013 11:9 11, 601–614. <https://doi.org/10.1038/nrmicro3088>
- Pinho, M.G., Ludovice, A.M., Wu, S., De Lencastre, H., 2009. Massive Reduction in Methicillin Resistance by Transposon Inactivation of the Normal PBP2 in a Methicillin-Resistant Strain of *Staphylococcus aureus*. <https://home.liebertpub.com/mdr> 3, 409–413. <https://doi.org/10.1089/MDR.1997.3.409>
- Plata, K.B., Rosato, R.R., Rosato, A.E., 2011. Fate of mutation rate depends on agr locus expression during oxacillin-mediated heterogeneous-homogeneous selection in methicillin-resistant *Staphylococcus aureus* clinical strains. *Antimicrob Agents Chemother* 55, 3176–3186. <https://doi.org/10.1128/AAC.01119-09>
- Pogliano, J., Pogliano, N., Silverman, J.A., 2012. Daptomycin-Mediated Reorganization of Membrane Architecture Causes Mislocalization of Essential Cell Division Proteins. *J Bacteriol* 194, 4494. <https://doi.org/10.1128/JB.00011-12>
- Porfirio, S., Carlson, R.W., Azadi, P., 2019. Elucidating Peptidoglycan Structure: An Analytical Toolset. *Trends Microbiol* 27, 607–622. <https://doi.org/10.1016/J.TIM.2019.01.009>
- Pozzi, C., Waters, E.M., Rudkin, J.K., Schaeffer, C.R., Lohan, A.J., Tong, P., Loftus, B.J., Pier, G.B., Fey, P.D., Massey, R.C., O’Gara, J.P., 2012. Methicillin resistance alters the biofilm phenotype and attenuates virulence in *Staphylococcus aureus* device-associated infections. *PLoS Pathog* 8. <https://doi.org/10.1371/JOURNAL.PPAT.1002626>
- Puig, O., Caspary, F., Rigaut, G., Rutz, B., Bouveret, E., Bragado-Nilsson, E., Wilm, M., Séraphin, B., 2001. The Tandem Affinity Purification (TAP) Method: A General Procedure of Protein Complex Purification. *Methods* 24, 218–229. <https://doi.org/10.1006/METH.2001.1183>
- Reading, C., Cole, M., 1977. Clavulanic Acid: a Beta-Lactamase-Inhibiting Beta-Lactam from *Streptomyces clavuligerus*. *Antimicrob Agents Chemother* 11, 852–857. <https://doi.org/10.1128/AAC.11.5.852>
- Reed, P., Atilano, M.L., Alves, R., Hoiczkyk, E., Sher, X., Reichmann, N.T., Pereira, P.M., Roemer, T., Filipe, S.R., Pereira-Leal, J.B., Ligoxygakis, P., Pinho, M.G., 2015. *Staphylococcus aureus* Survives with a Minimal Peptidoglycan Synthesis Machine but Sacrifices Virulence and Antibiotic Resistance. *PLoS Pathog* 11. <https://doi.org/10.1371/JOURNAL.PPAT.1004891>

- Reed, P., Veiga, H., Jorge, A.M., Terrak, M., Pinho, M.G., 2011. Monofunctional transglycosylases are not essential for *Staphylococcus aureus* cell wall synthesis. *J Bacteriol* 193, 2549–2556. <https://doi.org/10.1128/JB.01474-10/ASSET/2707ECAAF-0142-46B7-81D4-53D83853B004/ASSETS/GRAPHIC/ZJB9990903670004.JPEG>
- Reichmann, N.T., Piçarra Cassona, C., Monteiro, J.M., Bottomley, A.L., Corrigan, R.M., Foster, S.J., Pinho, M.G., Gründling, A., 2014. Differential localization of LTA synthesis proteins and their interaction with the cell division machinery in *Staphylococcus aureus*. *Mol Microbiol* 92, 273–286. <https://doi.org/10.1111/mmi.12551>
- Reichmann, N.T., Tavares, A.C., Saraiva, B.M., Jouselin, A., Reed, P., Pereira, A.R., Monteiro, J.M., Sobral, R.G., VanNieuwenhze, M.S., Fernandes, F., Pinho, M.G., 2019. SEDS–bPBP pairs direct lateral and septal peptidoglycan synthesis in *Staphylococcus aureus*. *Nature Microbiology* 2019 4:8 4, 1368–1377. <https://doi.org/10.1038/s41564-019-0437-2>
- Reyes, D.Y., Zuber, P., 2008. Activation of transcription initiation by Spx: Formation of transcription complex and identification of a Cis-acting element required for transcriptional activation. *Mol Microbiol* 69, 765–779. <https://doi.org/10.1111/j.1365-2958.2008.06330.x>
- Reygaert, W.C., 2018. An overview of the antimicrobial resistance mechanisms of bacteria. *AIMS Microbiol* 4, 482. <https://doi.org/10.3934/MICROBIOL.2018.3.482>
- Riedel, C.U., Monk, I.R., Casey, P.G., Waidmann, M.S., Gahan, C.G.M., Hill, C., 2009. AgrD-dependent quorum sensing affects biofilm formation, invasion, virulence and global gene expression profiles in *Listeria monocytogenes*. *Mol Microbiol* 71, 1177–1189. <https://doi.org/10.1111/J.1365-2958.2008.06589.X>
- Roch, M., Lelong, E., Panasenko, O.O., Sierra, R., Renzoni, A., Kelley, W.L., 2019. Thermosensitive PBP2a requires extracellular folding factors PrsA and HtrA1 for *Staphylococcus aureus* MRSA  $\beta$ -lactam resistance. *Commun Biol* 2, 1–11. <https://doi.org/10.1038/s42003-019-0667-0>
- Roch, M., Lelong, E., Panasenko, O.O., Sierra, R., Renzoni, A., Kelley, W.L., 2019. Thermosensitive PBP2a requires extracellular folding factors PrsA and HtrA1 for *Staphylococcus aureus* MRSA  $\beta$ -lactam resistance. *Commun Biol* 2, 1–11. <https://doi.org/10.1038/s42003-019-0667-0>
- Roch, M., Lelong, E., Panasenko, O.O., Sierra, R., Renzoni, A., Kelley, W.L., 2019. Thermosensitive PBP2a requires extracellular folding factors PrsA and HtrA1 for *Staphylococcus aureus* MRSA  $\beta$ -lactam resistance. *Communications Biology* 2019 2:1 2, 1–11. <https://doi.org/10.1038/s42003-019-0667-0>

- Roemer, T., Schneider, T., Pinho, M.G., 2013. Auxiliary factors: a chink in the armor of MRSA resistance to  $\beta$ -lactam antibiotics. *Curr Opin Microbiol* 16, 538–548. <https://doi.org/10.1016/J.MIB.2013.06.012>
- Rohmer, M., Bouvier, P., Ourisson, G., 1979. Molecular evolution of biomembranes: structural equivalents and phylogenetic precursors of sterols. *Proc Natl Acad Sci U S A* 76, 847–851. <https://doi.org/10.1073/PNAS.76.2.847>
- Rohrer, S., Berger-Bächi, B., 2003. Application of a bacterial two-hybrid system for the analysis of protein-protein interactions between FemABX family proteins. *Microbiology (N Y)* 149, 2733–2738. <https://doi.org/10.1099/MIC.0.26315-0/CITE/REFWORKS>
- Rolo, J., Worning, P., Nielsen, J.B., Bowden, R., Bouchami, O., Damborg, P., Guardabassi, L., Perreten, V., Tomasz, A., Westh, H., De Lencastre, H., Miragaia, M., 2017. Evolutionary origin of the staphylococcal cassette chromosome mec (SCCmec). *Antimicrob Agents Chemother* 61. <https://doi.org/10.1128/AAC.02302-16>
- Rosado, H., Turner, R.D., Foster, S.J., Taylor, P.W., 2015. Impact of the  $\beta$ -Lactam Resistance Modifier (-)-Epicatechin Gallate on the Non-Random Distribution of Phospholipids across the Cytoplasmic Membrane of *Staphylococcus aureus*. *Int J Mol Sci* 16, 16710–16727. <https://doi.org/10.3390/IJMS160816710>
- Ross, J.I., Eady, E.A., Cove, J.H., Cunliffe, W.J., 1998. 16S rRNA Mutation Associated with Tetracycline Resistance in a Gram-Positive Bacterium. *Antimicrob Agents Chemother* 42, 1702. <https://doi.org/10.1128/AAC.42.7.1702>
- Rudilla, H., Pérez-Guillén, I., Rabanal, F., Sierra, J.M., Vinuesa, T., Viñas, M., 2018. Novel synthetic polymyxins kill Gram-positive bacteria. *Journal of Antimicrobial Chemotherapy* 73, 3385–3390. <https://doi.org/10.1093/JAC/DKY366>
- Rudkin, J.K., Edwards, A.M., Bowden, M.G., Brown, E.L., Pozzi, C., Waters, E.M., Chan, W.C., Williams, P., O’Gara, J.P., Massey, R.C., 2012. Methicillin resistance reduces the virulence of healthcare-associated methicillin-resistant *Staphylococcus aureus* by interfering with the agr quorum sensing system. *J Infect Dis* 205, 798–806. <https://doi.org/10.1093/INFDIS/JIR845>
- Ruiz, N., 2008. Bioinformatics identification of MurJ (MviN) as the peptidoglycan lipid II flippase in *Escherichia coli*. *Proc Natl Acad Sci U S A* 105, 15553–15557. [https://doi.org/10.1073/PNAS.0808352105/SUPPL\\_FILE/0808352105SI.PDF](https://doi.org/10.1073/PNAS.0808352105/SUPPL_FILE/0808352105SI.PDF)

- Sabath, L.D., 1982. Mechanisms of resistance to beta-lactam antibiotics in strains of *Staphylococcus aureus*. *Ann Intern Med* 97, 339–344. <https://doi.org/10.7326/0003-4819-97-3-339>
- Sacco, M.D., Hammond, L.R., Noor, R.E., Bhattacharya, D., Madsen, J.J., Zhang, X., Butler, S.G., Kemp, M.T., Jaskolka-Brown, A.C., Khan, S.J., Gelis, I., Eswara, P.J., Chen, Y., 2022. *Staphylococcus aureus* FtsZ and PBP4 bind to the conformationally dynamic N-terminal domain of GpsB. *bioRxiv* 2022.10.25.513704. <https://doi.org/10.1101/2022.10.25.513704>
- Salamaga, B., Kong, L., Pasquina-Lemonche, L., Lafage, L., Von Und Zur Muhlen, M., Gibson, J.F., Grybchuk, D., Tooke, A.K., Panchal, V., Culp, E.J., Tatham, E., O’Kane, M.E., Catley, T.E., Renshaw, S.A., Wright, G.D., Plevka, P., Bullough, P.A., Han, A., Hobbs, J.K., Foster, S.J., 2021. Demonstration of the role of cell wall homeostasis in *Staphylococcus aureus* growth and the action of bactericidal antibiotics. *Proc Natl Acad Sci U S A* 118, e2106022118. [https://doi.org/10.1073/PNAS.2106022118/SUPPL\\_FILE/PNAS.2106022118.SM05.MOV](https://doi.org/10.1073/PNAS.2106022118/SUPPL_FILE/PNAS.2106022118.SM05.MOV)
- Salamaga, B., Kong, L., Pasquina-Lemonche, L., Lafage, L., von Und Zur Muhlen, M., Gibson, J.F., Grybchuk, D., Tooke, A.K., Panchal, V., Culp, E.J., Tatham, E., O’Kane, M.E., Catley, T.E., Renshaw, S.A., Wright, G.D., Plevka, P., Bullough, P.A., Han, A., Hobbs, J.K., Foster, S.J., 2021. Demonstration of the role of cell wall homeostasis in *Staphylococcus aureus* growth and the action of bactericidal antibiotics. *Proc Natl Acad Sci U S A* 118. <https://doi.org/10.1073/PNAS.2106022118/-/DCSUPPLEMENTAL>
- Sauvage, E., Kerff, F., Terrak, M., Ayala, J.A., Charlier, P., 2008. The penicillin-binding proteins: Structure and role in peptidoglycan biosynthesis. *FEMS Microbiol Rev.* <https://doi.org/10.1111/j.1574-6976.2008.00105.x>
- Sauvage, E., Kerff, F., Terrak, M., Ayala, J.A., Charlier, P., 2008. The penicillin-binding proteins: Structure and role in peptidoglycan biosynthesis. *FEMS Microbiol Rev.* <https://doi.org/10.1111/j.1574-6976.2008.00105.x>
- Schindelin, J., Arganda-Carreras, I., Frise, E., Kaynig, V., Longair, M., Pietzsch, T., Preibisch, S., Rueden, C., Saalfeld, S., Schmid, B., Tinevez, J.Y., White, D.J., Hartenstein, V., Eliceiri, K., Tomancak, P., Cardona, A., 2012. Fiji: an open-source platform for biological-image analysis. *Nature Methods* 2012 9:7 9, 676–682. <https://doi.org/10.1038/nmeth.2019>
- Schlesier, T., Siegmund, A., Rescher, U., Heilmann, C., 2020. Characterization of the Atl-mediated staphylococcal internalization mechanism. *Int J Med Microbiol* 310. <https://doi.org/10.1016/J.IJMM.2020.151463>

- Schmitt, J., Hess, H., Stunnenberg, H.G., 1993. Affinity purification of histidine-tagged proteins. *Mol Biol Rep* 18, 223–230. <https://doi.org/10.1007/BF01674434/METRICS>
- Schneewind, O., Missiakas, D.M., 2019. Staphylococcal Protein Secretion and Envelope Assembly. *Microbiol Spectr* 7. <https://doi.org/10.1128/microbiolspec.gpp3-0070-2019>
- Schneewind, O., Missiakas, D.M., 2012. Protein secretion and surface display in Gram-positive bacteria. *Philos Trans R Soc Lond B Biol Sci* 367, 1123–1139. <https://doi.org/10.1098/RSTB.2011.0210>
- Shajari, G., Khorshidi, A., Moosavi, G., 2017. Vancomycin resistance in *Staphylococcus aureus* strains. *Arch Razi Inst* 90, 107–110.
- Sham, L.T., Butler, E.K., Lebar, M.D., Kahne, D., Bernhardt, T.G., Ruiz, N., 2014. MurJ is the flippase of lipid-linked precursors for peptidoglycan biogenesis. *Science* (1979) 345, 220–222. [https://doi.org/10.1126/SCIENCE.1254522/SUPPL\\_FILE/SHAM-SM.PDF](https://doi.org/10.1126/SCIENCE.1254522/SUPPL_FILE/SHAM-SM.PDF)
- Shannon, P., Markiel, A., Ozier, O., Baliga, N.S., Wang, J.T., Ramage, D., Amin, N., Schwikowski, B., Ideker, T., 2003. Cytoscape: A Software Environment for Integrated Models of Biomolecular Interaction Networks. *Genome Res* 13, 2498–2504. <https://doi.org/10.1101/GR.1239303>
- Sharma, A.D., Gutheil, W.G., 2023. Synergistic Combinations of FDA-Approved Drugs with Ceftobiprole against Methicillin-Resistant *Staphylococcus aureus*. *Microbiol Spectr* 11. <https://doi.org/10.1128/SPECTRUM.03726-22/ASSET/934496B1-F939-4B85-B85F-B8E5AA3ADEA6/ASSETS/IMAGES/MEDIUM/SPECTRUM.03726-22-F002.GIF>
- Silverman, J.A., Perlmutter, N.G., Shapiro, H.M., 2003. Correlation of Daptomycin Bactericidal Activity and Membrane Depolarization in *Staphylococcus aureus*. *Antimicrob Agents Chemother* 47, 2538. <https://doi.org/10.1128/AAC.47.8.2538-2544.2003>
- Singh, V.K., Syring, M., Singh, A., Singhal, K., Dalecki, A., Johansson, T., 2012. An insight into the significance of the DnaK heat shock system in *Staphylococcus aureus*. *Int J Med Microbiol* 302, 242–252. <https://doi.org/10.1016/J.IJMM.2012.05.001>
- Smale, S.T., 2010. Luciferase Assay. *Cold Spring Harb Protoc* 2010, pdb.prot5421. <https://doi.org/10.1101/PDB.PROT5421>
- Snowden, M.A., Perkins, H.R., 1990. Peptidoglycan cross-linking in *Staphylococcus aureus*. *Eur J Biochem* 191, 373–377. <https://doi.org/10.1111/J.1432-1033.1990.TB19132.X>
- Song, H.S., Choi, T.R., Han, Y.H., Park, Y.L., Park, J.Y., Yang, S.Y., Bhatia, S.K., Gurav, R., Kim, Y.G., Kim, J.S., Joo, H.S., Yang, Y.H., 2020. Increased resistance of a methicillin-resistant

- Staphylococcus aureus* Δagr mutant with modified control in fatty acid metabolism. *AMB Express* 10. <https://doi.org/10.1186/S13568-020-01000-Y>
- Stahlhut, S.G., Alqarzaee, A.A., Jensen, C., Fisker, N.S., Pereira, A.R., Pinho, M.G., Thomas, V.C., Frees, D., 2017. The ClpXP protease is dispensable for degradation of unfolded proteins in *Staphylococcus aureus*. *Sci Rep* 7. <https://doi.org/10.1038/S41598-017-12122-Y>
- Stapleton, P.D., Shah, S., Ehlert, K., Hara, Y., Taylor, P.W., 2007. The β-lactam-resistance modifier (-)-epicatechin gallate alters the architecture of the cell wall of *Staphylococcus aureus*. *Microbiology (Reading)* 153, 2093. <https://doi.org/10.1099/MIC.0.2007/007807-0>
- Stapleton, P.D., Shah, S., Ehlert, K., Hara, Y., Taylor, P.W., 2007. The β-lactam-resistance modifier (-)-epicatechin gallate alters the architecture of the cell wall of *Staphylococcus aureus*. *Microbiology (N Y)* 153, 2093–2103. <https://doi.org/10.1099/MIC.0.2007/007807-0>
- Stapleton, P.D., Taylor, P.W., 2002. Methicillin resistance in *Staphylococcus aureus*: mechanisms and modulation. *Sci Prog*. <https://doi.org/10.3184/003685002783238870>
- Steele, V.R., Bottomley, A.L., Garcia-Lara, J., Kasturiarachchi, J., Foster, S.J., 2011. Multiple essential roles for EzrA in cell division of *Staphylococcus aureus*. *Mol Microbiol* 80, 542–555. <https://doi.org/10.1111/J.1365-2958.2011.07591.X>
- Steele, V.R., Bottomley, A.L., Garcia-Lara, J., Kasturiarachchi, J., Foster, S.J., 2011. Multiple essential roles for EzrA in cell division of *Staphylococcus aureus*. *Mol Microbiol* 80, 542–555. <https://doi.org/10.1111/J.1365-2958.2011.07591.X>
- Steele, V.R., Bottomley, A.L., Garcia-Lara, J., Kasturiarachchi, J., Foster, S.J., 2011. Multiple essential roles for EzrA in cell division of *Staphylococcus aureus*. *Mol Microbiol* 80, 542–555. <https://doi.org/10.1111/J.1365-2958.2011.07591.X>
- Sutton, J.A.F., Carnell, O.T., Lafage, L., Gray, J., Biboy, J., Gibson, J.F., Pollitt, E.J.G., Tazoll, S.C., Turnbull, W., Hajdamowicz, N.H., Salamaga, B., Pidwill, G.R., Condliffe, A.M., Renshaw, S.A., Vollmer, W., Foster, S.J., 2021. *Staphylococcus aureus* cell wall structure and dynamics during host-pathogen interaction. *PLoS Pathog* 17. <https://doi.org/10.1371/JOURNAL.PPAT.1009468>
- Sutton, J.A.F., Cooke, M., Tinajero-Trejo, M., Wacnik, K., Salamaga, B., Portman Ross, C., Lund, V.A., Hobbs, J.K., Foster, S.J., 2023. The roles of GpsB and DivIVA in *Staphylococcus aureus* growth and division. *Front Microbiol* 14, 1241249. <https://doi.org/10.3389/FMICB.2023.1241249>



- Szklarczyk, D., Kirsch, R., Koutrouli, M., Nastou, K., Mehryary, F., Hachilif, R., Gable, A.L., Fang, T., Doncheva, N.T., Pyysalo, S., Bork, P., Jensen, L.J., Von Mering, C., 2023. The STRING database in 2023: protein-protein association networks and functional enrichment analyses for any sequenced genome of interest. *Nucleic Acids Res* 51, D638–D646. <https://doi.org/10.1093/NAR/GKAC1000>
- Taguchi, A., Welsh, M.A., Marmont, L.S., Lee, W., Sjodt, M., Kruse, A.C., Kahne, D., Bernhardt, T.G., Walker, S., 2019. FtsW is a peptidoglycan polymerase that is functional only in complex with its cognate penicillin-binding protein. *Nat Microbiol* 4, 587–594. <https://doi.org/10.1038/s41564-018-0345-x>
- Tamang, M.D., Bae, J., Park, M., Jeon, B., 2022. Potentiation of  $\beta$ -Lactams against Methicillin-Resistant *Staphylococcus aureus* (MRSA) Using Octyl Gallate, a Food-Grade Antioxidant. *Antibiotics* 11. <https://doi.org/10.3390/ANTIBIOTICS11020266>
- Tan, C.M., Therien, A.G., Lu, J., Lee, S.H., Caron, A., Gill, C.J., Lebeau-Jacob, C., Benton-Perdomo, L., Monteiro, J.M., Pereira, P.M., Elsen, N.L., Wu, J., Deschamps, K., Petcu, M., Wong, S., Daigneault, E., Kramer, S., Liang, L., Maxwell, E., Claveau, D., Vaillancourt, J., Skorey, K., Tam, J., Wang, H., Meredith, T.C., Sillaots, S., Wang-Jarantow, L., Ramtohul, Y., Langlois, E., Landry, F., Reid, J.C., Parthasarathy, G., Sharma, S., Baryshnikova, A., Lumb, K.J., Pinho, M.G., Soisson, S.M., Roemer, T., 2012. Restoring methicillin-resistant *Staphylococcus aureus* susceptibility to  $\beta$ -lactam antibiotics. *Sci Transl Med* 4. <https://doi.org/10.1126/SCITRANSLMED.3003592>
- Tavares, A.C., Fernandes, P.B., Carballido-López, R., Pinho, M.G., 2015. MreC and MreD Proteins Are Not Required for Growth of *Staphylococcus aureus*. *PLoS One* 10, e0140523. <https://doi.org/10.1371/JOURNAL.PONE.0140523>
- Thalsø-Madsen, I., Torrubia, F.R., Xu, L., Petersen, A., Jensen, C., Frees, D., 2019. The Sle1 Cell Wall Amidase is essential for  $\beta$ -Lactam Resistance in Community Acquired Methicillin Resistant *Staphylococcus aureus* USA300. *Antimicrob Agents Chemother*. <https://doi.org/10.1128/AAC.01931-19>
- Tinajero-Trejo, M., Carnell, O., Kabli, A.F., Pasquina-Lemonche, L., Lafage, L., Han, A., Hobbs, J.K., Foster, S.J., 2022. The *Staphylococcus aureus* cell division protein, DivIC, interacts with the cell wall and controls its biosynthesis. *Commun Biol* 5. <https://doi.org/10.1038/s42003-022-04161-7>

- Tong, S.Y.C., Davis, J.S., Eichenberger, E., Holland, T.L., Fowler, V.G., 2015. *Staphylococcus aureus* infections: Epidemiology, pathophysiology, clinical manifestations, and management. *Clin Microbiol Rev* 28, 603–661. <https://doi.org/10.1128/CMR.00134-14>
- Traxler, M.F., Summers, S.M., Nguyen, H.T., Zacharia, V.M., Hightower, G.A., Smith, J.T., Conway, T., 2008. The global, ppGpp-mediated stringent response to amino acid starvation in *Escherichia coli*. *Mol Microbiol* 68, 1128–1148. <https://doi.org/10.1111/J.1365-2958.2008.06229.X>
- Trucksis, M., Hooper, D.C., Wolfson, J.S., 1991. Emerging resistance to fluoroquinolones in staphylococci: An alert. *Ann Intern Med*. <https://doi.org/10.7326/0003-4819-114-5-424>
- Tsubakishita, S., Kuwahara-Arai, K., Sasaki, T., Hiramatsu, K., 2010. Origin and molecular evolution of the determinant of methicillin resistance in staphylococci. *Antimicrob Agents Chemother* 54, 4352–4359. <https://doi.org/10.1128/AAC.00356-10>
- Turlej, A., Hryniewicz, W., Empel, J., 2011. Staphylococcal Cassette Chromosome mec (SCCmec) classification and typing methods: An overview. *Pol J Microbiol* 60, 95–103. <https://doi.org/10.33073/PJM-2011-013>
- Turner, R.D., Ratcliffe, E.C., Wheeler, R., Golestanian, R., Hobbs, J.K., Foster, S.J., 2010. Peptidoglycan architecture can specify division planes in *Staphylococcus aureus*. *Nature Communications* 2010 1:1 1, 1–9. <https://doi.org/10.1038/ncomms1025>
- Typas, A., Banzhaf, M., Gross, C.A., Vollmer, W., 2012. From the regulation of peptidoglycan synthesis to bacterial growth and morphology. *Nat Rev Microbiol*. <https://doi.org/10.1038/nrmicro2677>
- Uehara, T., Bernhardt, T.G., 2011. More than just lysins: peptidoglycan hydrolases tailor the cell wall. *Curr Opin Microbiol* 14, 698–703. <https://doi.org/10.1016/J.MIB.2011.10.003>
- Uehara, Y., 2022. Current Status of Staphylococcal Cassette Chromosome mec (SCCmec). *Antibiotics* 2022, Vol. 11, Page 86 11, 86. <https://doi.org/10.3390/ANTIBIOTICS11010086>
- Utsui, Y., Yokota, T., 1985. Role of an altered penicillin-binding protein in methicillin- and cephem-resistant *Staphylococcus aureus*. *Antimicrob Agents Chemother* 28, 397–403. <https://doi.org/10.1128/AAC.28.3.397>
- van Heijenoort, J., 2007. Lipid Intermediates in the Biosynthesis of Bacterial Peptidoglycan. *Microbiology and Molecular Biology Reviews* 71, 620–635. <https://doi.org/10.1128/MMBR.00016-07>

- Van Sorge, N.M., Beasley, F.C., Gusarov, I., Gonzalez, D.J., Von Köckritz-Blickwede, M., Anik, S., Borkowski, A.W., Dorrestein, P.C., Nudler, E., Nizet, V., 2013. Methicillin-resistant *Staphylococcus aureus* bacterial nitric-oxide synthase affects antibiotic sensitivity and skin abscess development. *Journal of Biological Chemistry* 288, 6417–6426. <https://doi.org/10.1074/jbc.M112.448738>
- Veiga, H., Jousselin, A., Schäper, S., Saraiva, B.M., Marques, L.B., Reed, P., Wilton, J., Pereira, P.M., Filipe, S.R., Pinho, M.G., 2023. Cell division protein FtsK coordinates bacterial chromosome segregation and daughter cell separation in *Staphylococcus aureus*. *EMBO J* 42. [https://doi.org/10.15252/EMBJ.2022112140/SUPPL\\_FILE/EMBJ2022112140-SUP-0001-APPENDIX.PDF](https://doi.org/10.15252/EMBJ.2022112140/SUPPL_FILE/EMBJ2022112140-SUP-0001-APPENDIX.PDF)
- Vermassen, A., Leroy, S., Talon, R., Provot, C., Popowska, M., Desvaux, M., 2019. Cell wall hydrolases in bacteria: Insight on the diversity of cell wall amidases, glycosidases and peptidases toward peptidoglycan. *Front Microbiol* 10, 418687. <https://doi.org/10.3389/FMICB.2019.00331/BIBTEX>
- Villanueva, M., Jousselin, A., Baek, K.T., Prados, J., Andrey, D.O., Renzoni, A., Ingmer, H., Frees, D., Kelley, W.L., 2016. Rifampin Resistance *rpoB* Alleles or Multicopy Thioredoxin/Thioredoxin Reductase Suppresses the Lethality of Disruption of the Global Stress Regulator *spx* in *Staphylococcus aureus*. *J Bacteriol* 198, 2719–2731. <https://doi.org/10.1128/JB.00261-16>
- Vollmer, W., Blanot, D., De Pedro, M.A., 2008. Peptidoglycan structure and architecture. *FEMS Microbiol Rev* 32, 149–167. <https://doi.org/10.1111/J.1574-6976.2007.00094.X>
- Vollmer, W., Joris, B., Charlier, P., Foster, S., 2008. Bacterial peptidoglycan (murein) hydrolases. *FEMS Microbiol Rev* 32, 259–286. <https://doi.org/10.1111/J.1574-6976.2007.00099.X>
- Vos, F.J., Kullberg, B.J., Sturm, P.D., Krabbe, P.F.M., van Dijk, A.P.J., Wanten, G.J.A., Oyen, W.J.G., Bleeker-Rovers, C.P., 2012. Metastatic Infectious Disease and Clinical Outcome in *Staphylococcus aureus* and *Streptococcus* species Bacteremia. *Medicine* 91, 86–94. <https://doi.org/10.1097/MD.0b013e31824d7ed2>
- Vuong, C., Götz, F., Otto, M., 2000. Construction and characterization of an *agr* deletion mutant of *Staphylococcus epidermidis*. *Infect Immun* 68, 1048–1053. <https://doi.org/10.1128/IAI.68.3.1048-1053.2000>
- Wacnik, K., Rao, V.A., Chen, X., Lafage, L., Pazos, M., Booth, S., Vollmer, W., Hobbs, J.K., Lewis, R.J., Foster, S.J., 2022. Penicillin-Binding Protein 1 (PBP1) of *Staphylococcus aureus* Has Multiple Essential Functions in Cell Division. *mBio* 13. <https://doi.org/10.1128/MBIO.00669-22>

22/ASSET/C0C99CE1-5308-48E8-976C-

7941C4B321A6/ASSETS/IMAGES/MEDIUM/MBIO.00669-22-F006.GIF

- Wang, H., Gill, C.J., Lee, S.H., Mann, P., Zuck, P., Meredith, T.C., Murgolo, N., She, X., Kales, S., Liang, L., Liu, J., Wu, J., Santa Maria, J., Su, J., Pan, J., Hailey, J., McGuinness, D., Tan, C.M., Flattery, A., Walker, S., Black, T., Roemer, T., 2013. Discovery of wall teichoic acid inhibitors as potential anti-MRSA  $\beta$ -lactam combination agents. *Chem Biol* 20, 272–284. <https://doi.org/10.1016/J.CHEMBIOL.2012.11.013>
- Wang, M., Buist, G., van Dijl, J.M., 2022. *Staphylococcus aureus* cell wall maintenance – the multifaceted roles of peptidoglycan hydrolases in bacterial growth, fitness, and virulence. *FEMS Microbiol Rev* 46. <https://doi.org/10.1093/FEMSRE/FUAC025>
- Wang, P. zhi, Projan, S.J., Novick, R.P., 1991. Nucleotide sequence of  $\beta$ -lactamase regulatory genes from staphylococcal plasmid p1258. *Nucleic Acids Res* 19, 4000. <https://doi.org/10.1093/nar/19.14.4000>
- Wang, X., Song, K.S., Guo, Q.X., Tian, W.X., 2003. The galloyl moiety of green tea catechins is the critical structural feature to inhibit fatty-acid synthase. *Biochem Pharmacol* 66, 2039–2047. [https://doi.org/10.1016/S0006-2952\(03\)00585-9](https://doi.org/10.1016/S0006-2952(03)00585-9)
- Wanner, S., Schade, J., Keinhörster, D., Weller, N., George, S.E., Kull, L., Bauer, J., Grau, T., Winstel, V., Stoy, H., Kretschmer, D., Kolata, J., Wolz, C., Bröker, B.M., Weidenmaier, C., 2017. Wall teichoic acids mediate increased virulence in *Staphylococcus aureus*. *Nat Microbiol* 2. <https://doi.org/10.1038/NMICROBIOL.2016.257>
- Weber, S.G., Gold, H.S., Hooper, D.C., Karchmer, A.W., Carmeli, Y., 2003. Fluoroquinolones and the Risk for Methicillin-resistant *Staphylococcus aureus* in Hospitalized Patients, in: *Emerging Infectious Diseases*. Centers for Disease Control and Prevention (CDC), pp. 1415–1422. <https://doi.org/10.3201/eid0911.030284>
- Weihs, F., Wacnik, K., Turner, R.D., Culley, S., Henriques, R., Foster, S.J., 2018. Heterogeneous localisation of membrane proteins in *Staphylococcus aureus*. *Scientific Reports* 2018 8:1 8, 1–11. <https://doi.org/10.1038/s41598-018-21750-x>
- Wertheim, H.F.L., Melles, D.C., Vos, M.C., Van Leeuwen, W., Van Belkum, A., Verbrugh, H.A., Nouwen, J.L., 2005. The role of nasal carriage in *Staphylococcus aureus* infections. *Lancet Infectious Diseases*. [https://doi.org/10.1016/S1473-3099\(05\)70295-4](https://doi.org/10.1016/S1473-3099(05)70295-4)
- Wheeler, R., 2012. Peptidoglycan architecture and dynamics in Gram-positive bacteria. University of Sheffield.

- Wheeler, R., Turner, R.D., Bailey, R.G., Salamaga, B., Mesnage, S., Mohamad, S.A.S., Hayhurst, E.J., Horsburgh, M., Hobbs, J.K., Foster, S.J., 2015. Bacterial cell enlargement requires control of cell wall stiffness mediated by peptidoglycan hydrolases. *mBio* 6. [https://doi.org/10.1128/MBIO.00660-15/SUPPL\\_FILE/MBO003152389S1.PDF](https://doi.org/10.1128/MBIO.00660-15/SUPPL_FILE/MBO003152389S1.PDF)
- White, M.L., Eswara, P.J., 2021. ylm has more than a (Z Anchor) ring to it! *J Bacteriol* 203. [https://doi.org/10.1128/JB.00460-20/SUPPL\\_FILE/JB.00460-20-S0001.PDF](https://doi.org/10.1128/JB.00460-20/SUPPL_FILE/JB.00460-20-S0001.PDF)
- WHO, W.H.O., 2015. WHO Library Cataloguing-in-Publication Data Global Action Plan on Antimicrobial Resistance.
- Wood, A., Irving, S.E., Bennison, D.J., Corrigan, R.M., 2019. The (p)ppGpp-binding GTPase era promotes rRNA processing and cold adaptation in *Staphylococcus aureus*. *PLoS Genet* 15, e1008346. <https://doi.org/10.1371/journal.pgen.1008346>
- Wood, W.B., Austrian, R., 1942. STUDIES ON THE ANTIBACTERIAL ACTION OF THE SULFONAMIDE DRUGS : II. THE POSSIBLE RELATION OF DRUG ACTIVITY TO SUBSTANCES OTHER THAN p-AMINOBENZOIC ACID. *J Exp Med* 75, 383–394. <https://doi.org/10.1084/JEM.75.4.383>
- Wu, S., De Lencastre, H., Tomasz, A., 1996. Sigma-B, a putative operon encoding alternate sigma factor of *Staphylococcus aureus* RNA polymerase: molecular cloning and DNA sequencing. *J Bacteriol* 178, 6036–6042. <https://doi.org/10.1128/JB.178.20.6036-6042.1996>
- WYKE, A.W., WARD, J.B., HAYES, M. V., CURTIS, N.A.C., 1981. A Role in vivo for Penicillin-Binding Protein-4 of *Staphylococcus aureus*. *Eur J Biochem* 119, 389–393. <https://doi.org/10.1111/J.1432-1033.1981.TB05620.X>
- Xiong, Y.Q., Mukhopadhyay, K., Yeaman, M.R., Adler-Moore, J., Bayer, A.S., 2005. Functional interrelationships between cell membrane and cell wall in antimicrobial peptide-mediated killing of *Staphylococcus aureus*. *Antimicrob Agents Chemother* 49, 3114–3121. <https://doi.org/10.1128/AAC.49.8.3114-3121.2005/ASSET/D870CD8C-0B06-449C-8F9C-9F71D37F5431/ASSETS/GRAPHIC/ZAC0080551280004.JPEG>
- Yansura, D.G., Henner, D.J., 1984. Use of the *Escherichia coli* lac repressor and operator to control gene expression in *Bacillus subtilis*. *Proc Natl Acad Sci U S A* 81, 439–443. <https://doi.org/10.1073/PNAS.81.2.439>
- Yao, X., Lu, C.-D., 2012. A PBP 2 Mutant Devoid of the Transpeptidase Domain Abolishes Spermine- $\beta$ -Lactam Synergy in *Staphylococcus aureus* Mu50. *Antimicrob Agents Chemother* 56, 83. <https://doi.org/10.1128/AAC.05415-11>

- Yeaman, M.R., Bayer, A.S., Koo, S.P., Foss, W., Sullam, P.M., 1998. Platelet microbicidal proteins and neutrophil defensin disrupt the *Staphylococcus aureus* cytoplasmic membrane by distinct mechanisms of action. *J Clin Invest* 101, 178–187. <https://doi.org/10.1172/JCI562>
- Yeaman, M.R., Yount, N.Y., 2003. Mechanisms of antimicrobial peptide action and resistance. *Pharmacol Rev* 55, 27–55. <https://doi.org/10.1124/PR.55.1.2>
- Yoshii, Y., Okuda, K.I., Yamada, S., Nagakura, M., Sugimoto, S., Nagano, T., Okabe, T., Kojima, H., Iwamoto, T., Kuwano, K., Mizunoe, Y., 2017. Norgestimate inhibits staphylococcal biofilm formation and resensitizes methicillin-resistant *Staphylococcus aureus* to  $\beta$ -lactam antibiotics. *NPJ Biofilms Microbiomes* 3, 18. <https://doi.org/10.1038/S41522-017-0026-1>
- Yu, C., Huang, L., 2018. Cross-Linking Mass Spectrometry (XL-MS): an Emerging Technology for Interactomics and Structural Biology. *Anal Chem* 90, 144. <https://doi.org/10.1021/ACS.ANALCHEM.7B04431>
- Zapun, A., Contreras-Martel, C., Vernet, T., 2008. Penicillin-binding proteins and beta-lactam resistance. *FEMS Microbiol Rev* 32, 361–385. <https://doi.org/10.1111/J.1574-6976.2007.00095.X>
- Zessel, K., Mohring, S., Hamscher, G., Kietzmann, M., Stahl, J., 2014. Biocompatibility and antibacterial activity of photolytic products of sulfonamides. *Chemosphere* 100, 167–174. <https://doi.org/10.1016/J.CHEMOSPHERE.2013.11.038>
- Zhanel, G.G., Love, R., Adam, H., Golden, A., Zelenitsky, S., Schweizer, F., Gorityala, B., Lagacé-Wiens, P.R.S., Rubinstein, E., Walkty, A., Gin, A.S., Gilmour, M., Hoban, D.J., Lynch, J.P., Karlowsky, J.A., 2015. Tedizolid: A novel oxazolidinone with potent activity against multidrug-resistant gram-positive pathogens. *Drugs* 75, 253–270. <https://doi.org/10.1007/S40265-015-0352-7/TABLES/6>
- Zhang, R., Shebes, M.A., Kho, K., Scaffidi, S.J., Meredith, T.C., Yu, W., 2021. Spatial regulation of protein A in *Staphylococcus aureus*. *Mol Microbiol* 116, 589–605. <https://doi.org/10.1111/MMI.14734>
- Zhang, S., Qu, X., Tang, H., Wang, Y., Yang, H., Yuan, W., Yue, B., 2021. Diclofenac Resensitizes Methicillin-Resistant *Staphylococcus aureus* to  $\beta$ -Lactams and Prevents Implant Infections. *Advanced Science* 8, 2100681. <https://doi.org/10.1002/ADVS.202100681>
- Zhong, W., Tang, M., Xie, Y., Huang, X., Liu, Y., 2023. Tea Polyphenols Inhibit the Activity and Toxicity of *Staphylococcus aureus* by Destroying Cell Membranes and Accumulating

Reactive Oxygen Species. <https://home.liebertpub.com/fpd> 20, 294–302.  
<https://doi.org/10.1089/FPD.2022.0085>

Zhou, X., Halladin, D.K., Rojas, E.R., Koslover, E.F., Lee, T.K., Huang, K.C., Theriot, J.A., 2015. Mechanical crack propagation drives millisecond daughter cell separation in *Staphylococcus aureus*. *Science* (1979) 348, 574–578.  
[https://doi.org/10.1126/SCIENCE.AAA1511/SUPPL\\_FILE/ZHOU-SM.PDF](https://doi.org/10.1126/SCIENCE.AAA1511/SUPPL_FILE/ZHOU-SM.PDF)

Zhou, X., Halladin, D.K., Rojas, E.R., Koslover, E.F., Lee, T.K., Huang, K.C., Theriot, J.A., 2015. Mechanical crack propagation drives millisecond daughter cell separation in *Staphylococcus aureus*. *Science* (1979) 348, 574–578.  
[https://doi.org/10.1126/SCIENCE.AAA1511/SUPPL\\_FILE/ZHOU-SM.PDF](https://doi.org/10.1126/SCIENCE.AAA1511/SUPPL_FILE/ZHOU-SM.PDF)

Zuber, P., 2004. Spx-RNA Polymerase Interaction and Global Transcriptional Control during Oxidative Stress. *J Bacteriol.* <https://doi.org/10.1128/JB.186.7.1911-1918.2004>

Zygmunt, D.J., Stratton, C.W., Kernodle, D.S., 1992. Characterization of four  $\beta$ -lactamases produced by *Staphylococcus aureus*. *Antimicrob Agents Chemother* 36, 440–445.  
<https://doi.org/10.1128/AAC.36.2.440>

## Appendices

### Appendix 1 Loci nearest T18 Reporter Gene

Hits of nearest locus to the T18 Library reporter identified in bacterial two hybrid screening. For each insert the number of calls are shown, either false positive: no fusion, or In frame fusion: greater than 10 amino acids in frame with two hybrid reporter or LSQ low sequence quality.


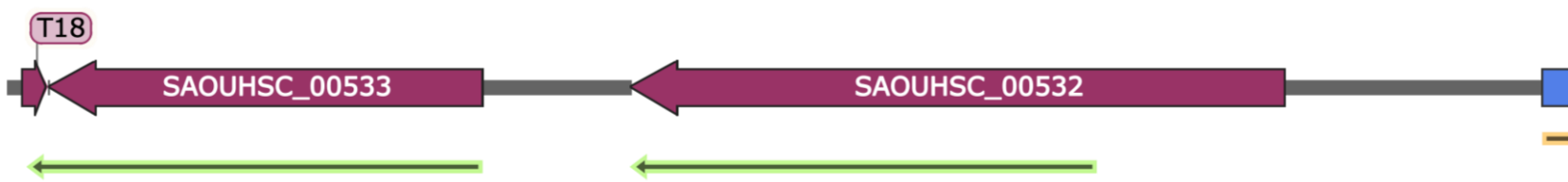
Count of Nearest locus to T18	Column Labels		
	False positive	In Frame Fusion	Grand Total
0.5-1kB T18C	49	5	55
PBP1 T25	46	4	51
SAOUHSC_pyrB	1		1
SAOUHSC_00092	1		1
SAOUHSC_00122	1		1
SAOUHSC_00160	2		2
SAOUHSC_00262	1		1
SAOUHSC_00534		1	1
SAOUHSC_00717	7		7
SAOUHSC_00886	5		5
SAOUHSC_01178	2		2
SAOUHSC_01272	1		1
SAOUHSC_01475	5		5
SAOUHSC_01916	2		2
SAOUHSC_01949	1		1
SAOUHSC_02138		2	2
SAOUHSC_02648	1		1
SAOUHSC_02713	1		1
SAOUHSC_02790	1		1
SAOUHSC_02798	1		1
SAOUHSC_02856	8		8
SAOUHSC_02953	4		4
SAOUHSC_03002	1		1
SAOUHSC_hypothetical protein BIT38_13765		1	1
<i>Staphylococcus aureus</i> strain RJ1267 chromosome, complete genome			1



PBP2 T25	2	1	3
SAOUHSC_00833		1	1
SAOUHSC_02671	2		2
PBP2a C T25	1		1
SAOUHSC_00086	1		1
0.5-1kB T18N	2	10	13
PBP1 T25	2	1	4
SAOUHSC_00197			1
SAOUHSC_00338	1		1
SAOUHSC_00559	1		1
SAOUHSC_00835		1	1
(blank)			
PBP2a C T25		9	9
SAOUHSC_00435		9	9
1-3kB T18C	1		1
PBP1 T25	1		1
SAOUHSC_02317	1		1
1-3kB T18N	5	29	34
PBP1 T25	4	3	7
LSQ OOF	1		1
SAOUHSC_00206	1		1
SAOUHSC_00531		1	1
SAOUHSC_01102	1		1
SAOUHSC_02134		2	2
SAOUHSC_02750	1		1
PBP2a C T25	1	17	18
SAOUHSC_01561	1		1
SAOUHSC_01868		1	1
SAOUHSC_02773		15	15
SAOUHSC_02912		1	1
PBP2a N T25		9	9
SAOUHSC_02333		1	1
SAOUHSC_02773		7	7
SOAUHSC_03015		1	1
Grand Total	57	44	103

## Appendix 2 Summary of in frame fusions of proteins identified by bacterial two hybrid library screen.

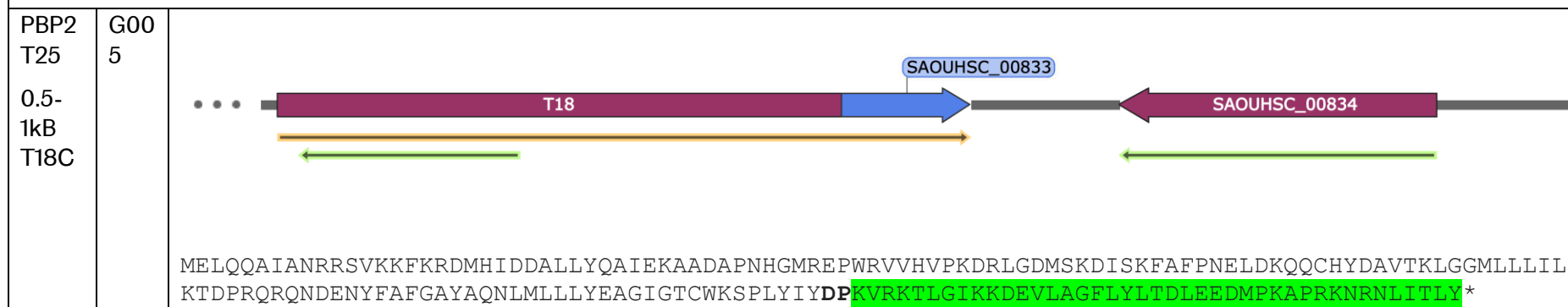
Verified in frame fusions were sequenced, identifying the protein fused to the reporter gene and in silico assemblies into the bacterial two hybrid vectors were generate Translated fusion region highlighted in green. Stop codons denoted by \*

Details	Sample(s)	Assembly
SAOUHSC_02134 Nitric oxide synthase oxygenase		
PBP1 T25 1-3kB T18N	AD.014  AD.020	 <p>MLFKEAQAFIENMYKECHYETQIINKRLHDIELEIKETGTYHTEELIYGAKMAWRNSNRCIGRLFWDLSLNVIDADVDVTDEASFLSSITYHI TQATNEGKLPYITIIYAPKDGPKIFNNQLIRYAGYDNCQDPAEKEVTRLANHLGWKGGTDFDVLPLIYQLPNEVSVKFFYEYPTSLIKEVPIEH NHYPKLRKLNKWKYAVPIISNMDLKIIGGIVYPTAPFNGWYMVTEIGVRNFIDYRYNLLKVVADAFEFDTLKNNSFNKDRALVELNYAVYHSF KKEGVSIVDHLTAAKQFELFERNEAQQGRQVTGKWSWLAPPLSPTLTSNYHHGYDNTVKDPNFFYKKKESNANQCPFHH</p>
SAOUHSC_00531 Hypothetical protein; homology to MULTISPECIES: amidohydrolase		
PBP1 T25 1-3kB T18N	AD.028	 <p>MHACGHDGHTAILLTVAEILDEHKHLLLEGNVVLIFQYGEEIMPGGSQEMIDAGCLENVDRIYGTHLWSGYPTGTIHSRAGAIMASPDEFVSVE KGRGGHGAKPHETIDPIVIMAEFILSAQKIISRTIDPVKQAVLSFGMIQAGTTDSVIPDQAFCKGTVRTFDSDIQNHVMDKMDKLLQGLAIAN DINYDLNYIKGYLPVHNNEKAYQVIKEATNDLHVRFNESDLMMIGEDFSHYLKVVRPGAFFLTGCGNESKGI TAPHHNPKFDI DEKSLKYAVAV FLKIIELEQVFKTN*</p>
SAOUHSC_00835 Arsenate reductase		

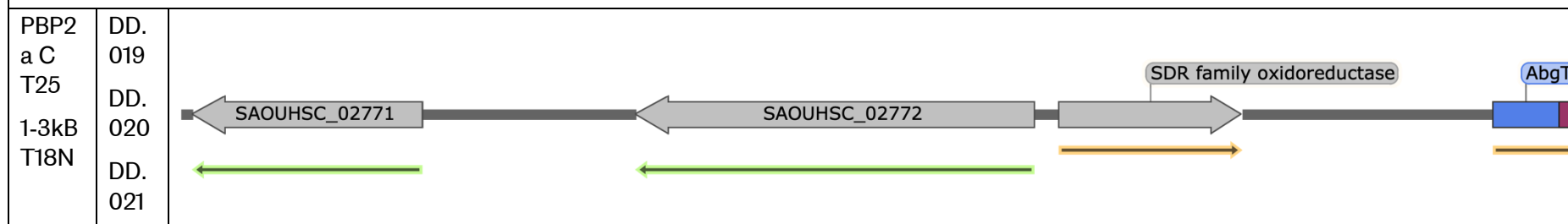
PBP1 T25 0.5- 1kB T18N	AC. 007	<p>SAOUHSC_00833 SAOUHSC_00834 SAOUHSC_00835</p> <p>MIKFYQYKNCTTCKKAAKFLDEYGVSYEPIDIVQHTPTINEFKTIIANTGVEINKLFNTHGAKYRELDLKNKLQTLSDDEKLELLSSDGMLVK RPLAVMGDKITLGFKEDQYKETWLA*</p>
SAOUHSC_02912 Unknown Protein, Homology to glyoxalase/bleomycin resistance/extradiol dioxygenase family protein		
PBP2 a C T25 1-3kB T18N	DD. 042	<p>SAOUHSC_02911 SAOUHSC_02912</p> <p>MTALFPYIAFENSKEALAYEEVFGATDVKRLEVGEEOASHFGMTKEEAQEATMHAEFVVLGKVLCSDFSFRADKINNGISLLIDYDVNNKE DADKVEAFYEQIKDHSSEIEIELPFADQFWGGKMGVFTDKYGVRWMLHGQDYTAIQQ*</p>
SAOUHSC_00435 Glutamate Synthase, Large Subunit		
PBP2 a C T25 0.5- 1kB T18N	DC. 011 DC. 016 DC. 020 DC. 028	<p>SAOUHSC_00435 SAOUHSC_00432</p> <p>MHNEKLIKGLYDREEHDACGIGFYANMDNKRSHDIIDKSLEMLRRLDHRGGVGADGITGDGAGIMTEIPFAFFKQHVTDFDIPGEGEYAVGL FFSKERILGSEHEVVFKKYFEGEGLSILGYRNPVNKDAIAKHVADTMPVIQQVFIDIRDIEDVEKRLFLARKQLEFYSTQCDLELYFTSLSR KTIVYKGLRSDQIKKLYTDLSDDLYQSKLGLVHSRFSSTNTPFSWKRAHPNRMLMHNGEINTIKGNVNWMRARQHKLIETLFGEDQHKVFQIV DEDGSDSAIVDNALEFLSLAMEPEKAAMLLIPEPWLYNEANDANVRAFYEYFYSYLMPEWDGPTMISFCNGDKLGALTDRNGLRPGRYTITKDN FIVFSSEVGVVDVPESNVAFKQLNPGKLLLVDKQNKVIENNDLKGA IAGELPYKAWIDNHKVDFFENIQYQDSQWKDETFLKLRQFAYT</p>

	DC. 032	KEEIHKYIQELVEGKKDPIGAMGYDAPIAVLNERPESLFNYFKQLFAQVTNPPIDAYREKIVTSELSYLGEGNLLAPDETVLDRIQLKRPVL
	DC. 033	NESHLAAIDQEHFKLTYLSTVYEGDLEDALEALGREAVNAVQGAQILVLDSDGLVDSNGFAMPMLLAI SHVHQLLIKADLRMSTSLVAKSGE
	DC. 034	TREVHHVACLLAYGANAI VPYLAQRTVEQLTTLTEGLQGTVDNVKTYTDVLSEGVIKVMAKMGISTVQSYQGAQIFEAI GLSHDVIDRYFTGT
	DC. 036	QSKLSGISIDQIDAENKARQQSDDNYLASGSTFQWRQQQHAFNPESIFLLQHACKENDYAQFKAYSEAVNKNRTDHIRHLLLEFKACTPIDI
	DC. 040	DQVEPVSDIVKRFNTGAMS YGSI SAEAHETLAQAMNQLGGKSNSGEGGEDAKRYEVQVDGSNKVS AIKQVASGRFGVTS DYLQHAKEIQIKVA
		QGAKPGEQQLPGTKVYPWIAKTRGSTPGIGLISPPPHHDIYSIEDLAQLIHDLKNANKDADI AVKLVSKTGVGTIASGVAKAFADKIVISGY
		DGGTGASPKTSIQHAGVPWEIGLAETHQTLKLNLDLRSRVKLET DGKLLTGKDVAYACALGAE EFGFATAPLVVLGCIMMRVCHKDTC PVG VAT
		QNKDLRALYRGKAHHVVNFMHFIAQELREILASLGLKRVEDLVGR TDLLQRSSTLKANSKAASIDVEKLLCPFDGPNTKEIQQNHNL EHGFDL
		TNLYEVTKPYIAEGRRYTGSFTVNNEQRDVG VITGSEISKQYGEAGLPENTINVTNGHAGQSLAAYAPKGLMIHHTGDANDYV GKGLSGGTV
		IVKAPFEERQNEIIAGNVSFYGATSGKAFINGSAGERFCIRNSGVDVVVEGIGDHGLE YMTGGHVINLGDVGNFQGMSSGAIAYVIPS DVEA
		FVENNQD L T L S F T K I K H Q E E K A F I K Q M L E E H V S H T N S T R A I H V L K H F D R I E D V V V K V I P K D Y Q L M M Q K I H L H K S L H D N E D E A M L A A F Y D D S K T
		IDAKHKPAVVY*

SAOUHSC\_00833 Conserved hypothetical protein, Nitroreductase family



SAOUHSC\_02773 Putative Transporter, Homology to AbgT putative transporter family



And/or retransformed with PBP2 a N T25 1-3kB T18N	DD. 022	MTSKHQKGSIVNRFLNSVEKIGNKLEDP SVLFFLMCVGLAIMTWVISLFNVSVKHPGTHQTIYIKNII SHDGFTMIMNDTIKNFSEFPALGL VLAVMIGIGVAEKTGYFDKLMISVVRAPRFLILPTIILIGILG STAGDAATIILPPLAAMLFIKIGYHPIAGLTMAYASAVGGFAANIVVGM
	DD. 024	QDALVYSFTEPATRIVSDSIKTNVAMNWFIAASVVVLLPTILLVTTKLIIPRLGKYDDSLMHDDHEETSSHITDKEAHALKWANISFIVTII LLIITAIPEHSFLRNAKTGSLDDAPLINGVGLIILVVFLVPGLVYGILSKEIKNTKDLGKMFGDAVGSMTFIVIVFFAAQLLAYLKWSNLG IIAAVKGAKLLEHQNGIVLILGIIVLSAMVNMLIGSASAKWGILGPIFVPMILILIGFHPAFTQVIYRVGDSITNPITPMPYLP LLLLTYAQYDKRMKLGALLSSLMPYSIALSIVWTVFVIIWFLLGIPVGGPIFVK*
	DD. 029	
	DD. 032	
	CD. 004	
	DD. 034	
	DD. 036	
	DD. 037	
	CD. 005	
	DD. 044	
	DD. 045	
	DD. 046	
	CD. 001	

	CD. 003 CD. 006 CD. 007 CD. 009 DD. 033 DD. 039	
Hypothetical protein B1T38_13765		
PBP1 T25 0.5- 1kB T18C	AA.1 38	<p>MLGPRQLALSVGIGD <b>PISLCCGPTSIEKTCYKLIFI*</b></p>
SAOUHSC_03015 HisZ, ATP phosphoribosyltransferase regulatory subunit		
PBP2 a N T25 1-3kB T18N	CD. 012	

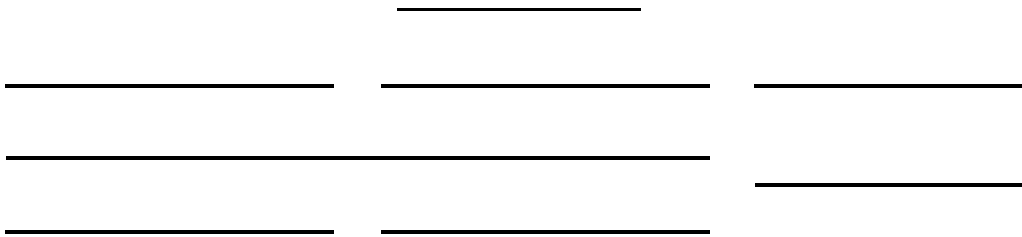
		<p>MGERNFWQEHQIYALRNDFTQLLRYYSMYPTAATKVAYTGLIIRNNEAAVQVGLENYAPSLANVQQLKLFIQFIQQQLRDNVHFVVLGHYQ LLDALLDKSLQTPDILSMIEERNLSGLVTYLSTEHPIVQILKENTQQQLNVLEHYIPNDHPALVELKIWERWLHKQGYKDIHLDITAQPPRSY YTGLFIQCHFAENESRVLTGGYYKGSIEGFGLGLTL*</p>
SAOUHSC_01868      Dipeptidase pepV; Homology to Mn(2+)-dependent dipeptidase Sapep		
PBP2 a C T25 1-3kB T18N	DD. 026	<p>MWKEKVQQYEQIINDLKGLLAIESVRDDAKASEDAPVGGPGRKALDYMYEIAHRDGFTHDVDHIAGRIEAGKGNVDVLGILCHVDVVPAGDGW DSNPFEPVVTEDAI IARGTLDDKGPTIAAYYAIKILEDMNVDWKKRIHMI IGTDEESDWKCTDRYFKTEEMPTLGFAPDAEFPCIHGEKGIT T FDLVQNKLTEDQDEPDYELITFKSGERYNMVPDHAEARVLVKENMTDVIQDFEYFLEQNHMQGDSTVDSGILVLTVEGKAVHGMDPSIGVNAG LYLLKFLASLNLNNAQAFVAFSNRYLFNSDFGEKMGKMFHTDVMGDVTTNIGVITYDNENAGLFGINLRYPEGFEFEKAMDRFANEIQQYGF EVKLGKVQPPHYVDKNDPFVQKLVTA YRNQTNDMTEPYTIGGGTYARNLDKGVAFGAMFSDSEDLMHQNEYITKKQLFNATSIYLEAIYSLC VEE*</p>

# Appendix 3 B2H Constructs; Genewiz order reference 40-541290844



**GENEWIZ LLC**  
 115 Corporate Boulevard  
 South Plainfield, NJ 07080  
 p (877) GENEWIZ (436-3949)  
 f (908) 333-4511  
 www.genewiz.com

III

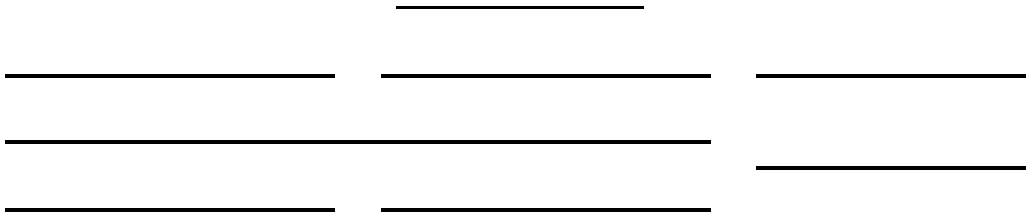


		√ Pass
		√ Pass
		√ Pass
		√ Pass
	<	
		√ Pass
		√ Pass

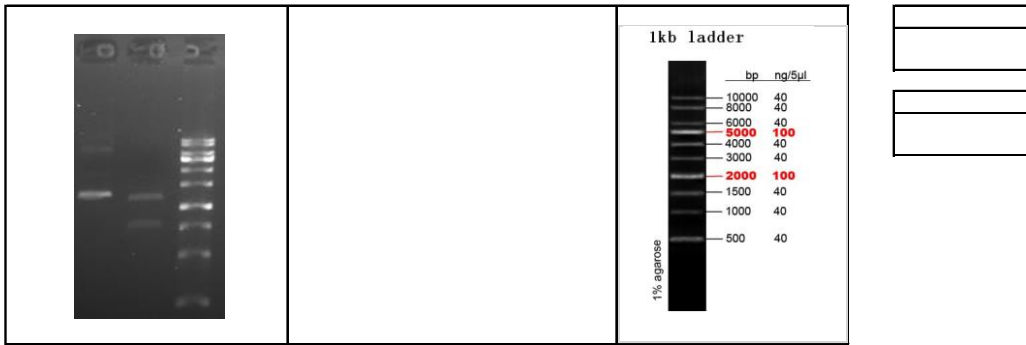
		<p><b>1kb ladder</b></p> <table border="1"> <thead> <tr> <th>bp</th> <th>ng/5µl</th> </tr> </thead> <tbody> <tr><td>10000</td><td>40</td></tr> <tr><td>8000</td><td>40</td></tr> <tr><td>6000</td><td>40</td></tr> <tr><td>5000</td><td>100</td></tr> <tr><td>4000</td><td>40</td></tr> <tr><td>3000</td><td>40</td></tr> <tr><td>2000</td><td>100</td></tr> <tr><td>1500</td><td>40</td></tr> <tr><td>1000</td><td>40</td></tr> <tr><td>500</td><td>40</td></tr> </tbody> </table>	bp	ng/5µl	10000	40	8000	40	6000	40	5000	100	4000	40	3000	40	2000	100	1500	40	1000	40	500	40	
			bp	ng/5µl																					
10000	40																								
8000	40																								
6000	40																								
5000	100																								
4000	40																								
3000	40																								
2000	100																								
1500	40																								
1000	40																								
500	40																								



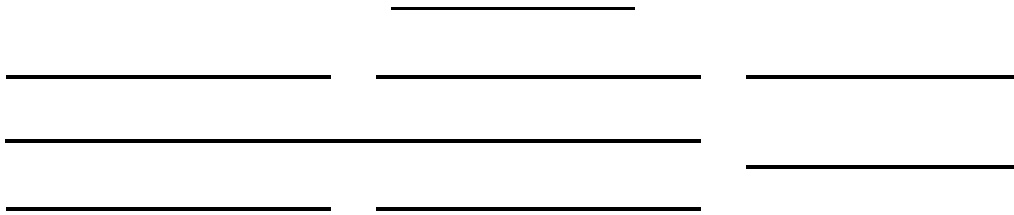
III



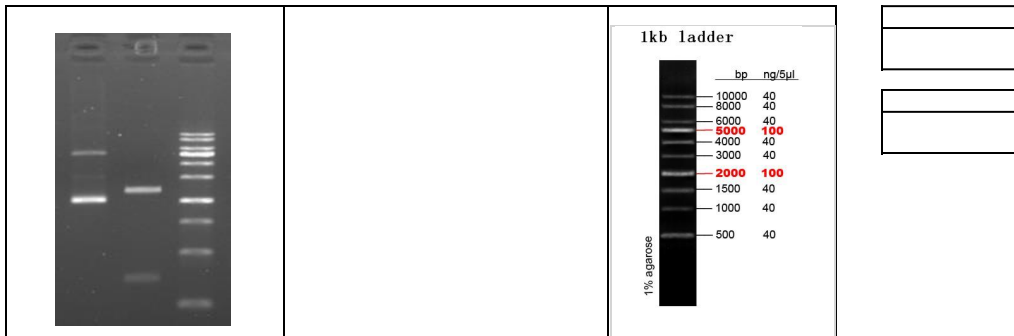
		√ Pass
		√ Pass
		√ Pass
		√ Pass
	<	
		√ Pass
		√ Pass



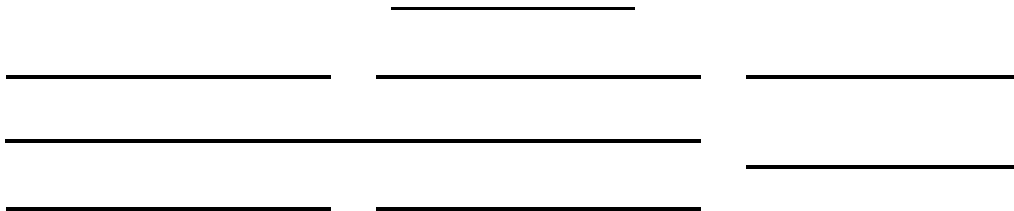
III



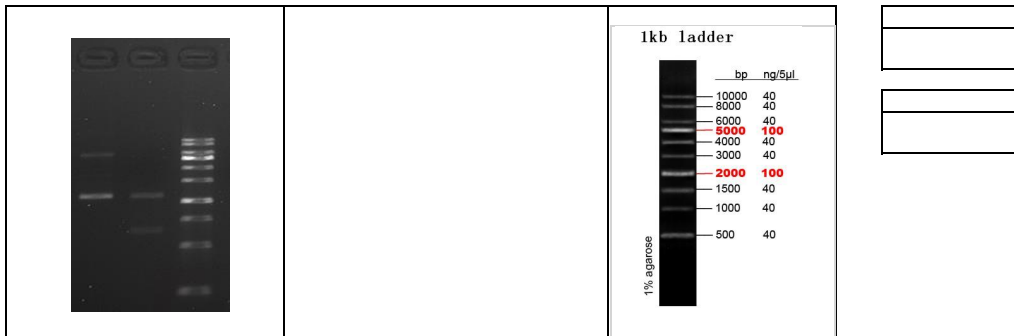
		√ Pass
		√ Pass
		√ Pass
		√ Pass
	<	
		√ Pass
		√ Pass



III



		√ Pass
		√ Pass
		√ Pass
		√ Pass
		√ Pass
		√ Pass

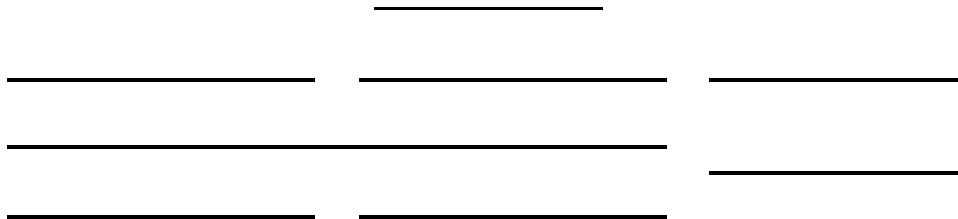


# Appendix 4 LytN and LytH Constructs; Genewiz order reference 40-541290844

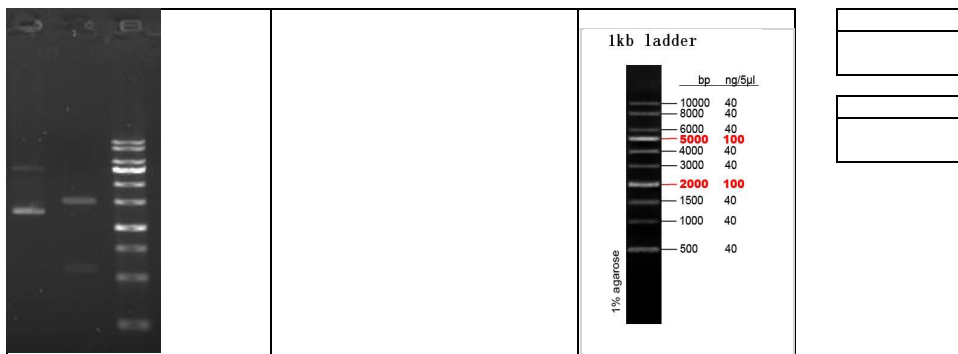


**GENEWIZ LLC**  
 115 Corporate Boulevard  
 South Plainfield, NJ 07080  
 p (877) GENEWIZ (436-3949)  
 f (908) 333-4511  
 www.genewiz.com

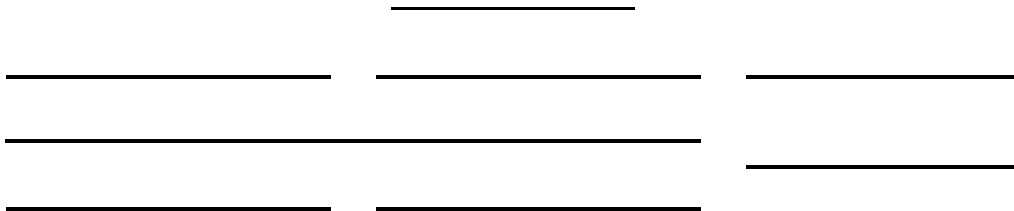
III



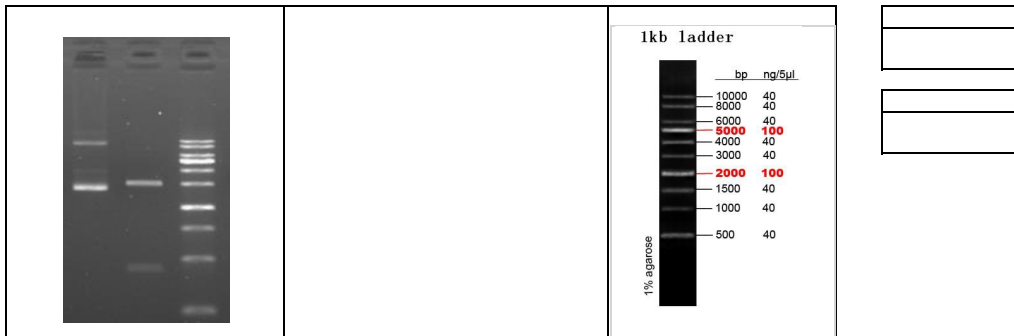
		√ Pass
		√ Pass
		√ Pass
		√ Pass
	<	
		√ Pass
		√ Pass



III



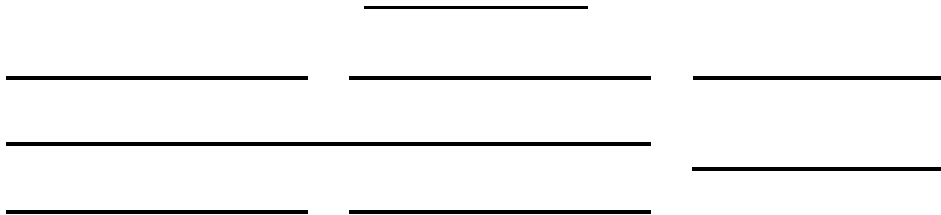
		√ Pass
		√ Pass
		√ Pass
		√ Pass
	<	√ Pass
		√ Pass



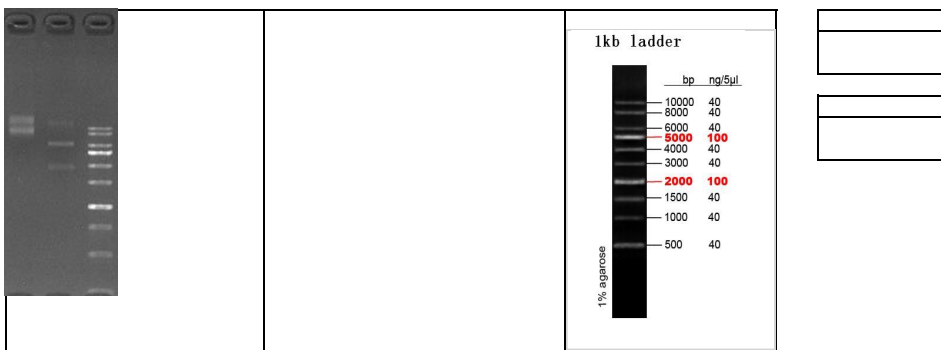
# Appendix 5 PBP2A GFP Constructs; Genewiz order reference 40-760878046



Q-03-DR01-01



		√ Pass
		√ Pass
		√ Pass
		√ Pass
	<	
		√ Pass
		√ Pass






---



---



---



---

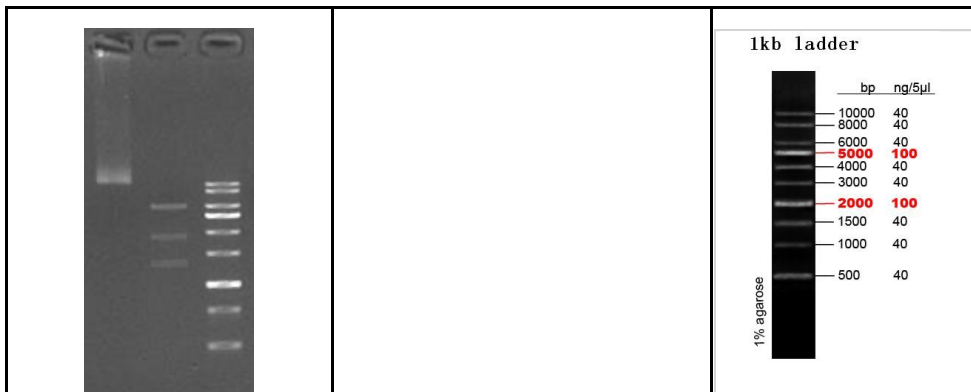


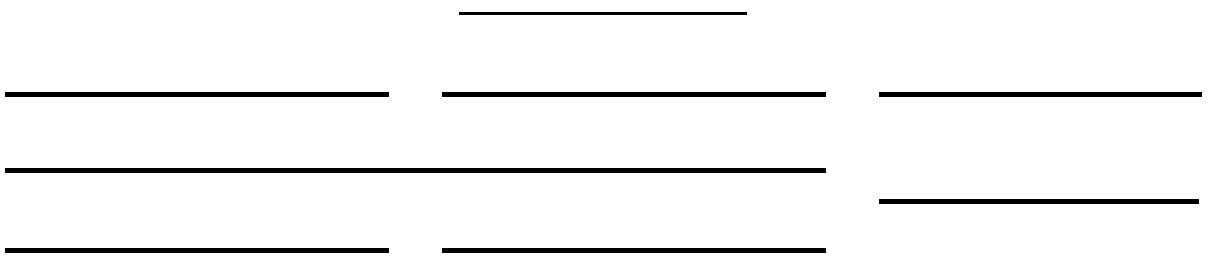
---



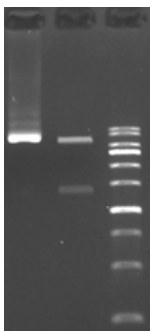
---

		√ Pass
		√ Pass
		√ Pass
		√ Pass
	<	
		√ Pass
		√ Pass



		√ Pass
		√ Pass
		√ Pass
		√ Pass
	<	
		√ Pass
		√ Pass

		<p><b>1kb ladder</b></p> <table border="1"> <thead> <tr> <th>bp</th> <th>ng/5μL</th> </tr> </thead> <tbody> <tr><td>10000</td><td>40</td></tr> <tr><td>8000</td><td>40</td></tr> <tr><td>6000</td><td>40</td></tr> <tr><td>5000</td><td>100</td></tr> <tr><td>4000</td><td>40</td></tr> <tr><td>3000</td><td>40</td></tr> <tr><td>2000</td><td>100</td></tr> <tr><td>1500</td><td>40</td></tr> <tr><td>1000</td><td>40</td></tr> <tr><td>500</td><td>40</td></tr> </tbody> </table> <p>1% agarose</p>	bp	ng/5μL	10000	40	8000	40	6000	40	5000	100	4000	40	3000	40	2000	100	1500	40	1000	40	500	40	<table border="1"> <tr><td></td></tr> <tr><td></td></tr> <tr><td></td></tr> </table>			
bp	ng/5μL																											
10000	40																											
8000	40																											
6000	40																											
5000	100																											
4000	40																											
3000	40																											
2000	100																											
1500	40																											
1000	40																											
500	40																											





## Appendix 7 PCR analysis of transposon insertions

